TUM School of Engineering and Design
Technische Universität München

Traffic Noise Modeling in Agent-Based Land Use/Transport Models

Nico Kühnel

Vollständiger Abdruck der von der TUM School of Engineering and Design der Technischen Universität München zur Erlangung des akademischen Grades eines

Doktors der Ingenieurwissenschaften (Dr.-Ing.)

genehmigten Dissertation.

Vorsitzender:

Prof. Dr.-Ing. Constantinos Antoniou

Prüfende der Dissertation:

1. Prof. Dr.-Ing. Rolf Moeckel
2. Prof. Dr.-Ing. Kay W. Axhausen,
   Eidgenössische Technische Hochschule Zürich / Schweiz
3. Prof. Dr.-Ing. Klaus Bogenberger

Die Dissertation wurde am 11.05.2021 bei der Technischen Universität München eingereicht und durch die TUM School of Engineering and Design am 09.11.2021 angenommen.

Acknowledgement

This dissertation is dedicated to the memory of my mother and father, who are deeply missed.

I would like to express my sincere gratitude to Rolf Moeckel, who made it possible for me to conduct the research presented here and always provided me with assistance and guidance as well as generously granted freedom in my endeavors. Similarly, I would like to thank my teammates Alona, Ana, Carlos, Cat, Karin, Qin, and Wei-Chieh for their fruitful and great collaboration. Additional thanks go to collaborators and project partners that I met and worked with in the last years, especially Dominik, Felix, Lennart, Raoul and Vishal.

Furthermore, I would like to thank Kai Nagel, Kay Axhausen, and the many people at VSP Berlin for working with me and keeping the MATSim community going.

Last but not least, I am grateful for the constant support, patience and encouragement from Stephanie, my family Daniel, Nadine, Dagmar, Lutz and Cord, the 'Wednesday group' and my friends Maximilian, Linh, Florian, Simon and Eduard.

Abstract

Contemporary traffic models use agent-based approaches that microscopically represent individuals, including their characteristics and behaviors. This work examines use cases of agent-based models with respect to traffic noise modeling with a focus on scenarios for which an individual representation of actors is necessary. In particular, mutual interactions between land use, traffic and noise as well as equity aspects are investigated.

Building upon an existing noise model of an agent-based transport simulation, multiple use cases are addressed. One use case deals with the feasibility of modeling an interaction between transport, land use and noise that introduces sensitivity to traffic noise for individual residents and their location decisions. As a prerequisite for this, the negative influence of noise on rental prices is estimated, whereby earlier findings in the literature are confirmed. Another scenario presents an extended analysis of environmental equity by not only evaluating individual noise exposure but also individual causation. Thereby it is shown that causation is even more unequally distributed than the exposure of noise. The last use case presents possible implications of the introduction of large-scale automated and electric ride-pooling services on traffic noise. It is shown that these services can reduce noise, especially with an efficient service design and accompanying policies.

The extensions of the applied noise model as well as the implemented feedback loop in the integrated land use/transport model are available as part of open-source libraries and may further be applied and developed in future endeavors.

Zusammenfassung

Zeitgenössische Verkehrsmodelle nutzen agentenbasierte Ansätze, mit denen Individuen inklusive ihrer Merkmale und Verhaltensweisen mikroskopisch dargestellt werden. Diese Arbeit untersucht Anwendungsfälle agentenbasierter Modelle im Hinblick auf Verkehrslärmmodellierung mit einem Fokus auf Szenarien, für die eine individuelle Darstellung von AkteurInnen notwendig ist. Insbesondere werden Wechselwirkungen zwischen Flächennutzung, Verkehr und Lärm sowie Gerechtigkeitsaspekte untersucht.

Aufbauend auf einem bestehenden Lärmmodell einer agentenbasierten Verkehrssimulation werden mehrere Anwendungsfälle adressiert. Ein Anwendungsfall befasst sich mit der Möglichkeit, eine Wechselwirkung zwischen Verkehr, Lärm und Flächennutzung zu modellieren, die eine Empfindlichkeit gegenüber Verkehrslärm für einzelne BewohnerInnen und deren Standortentscheidungen einführt. Als Voraussetzung dafür wird der negative Einfluss von Lärm auf Mietpreise geschätzt, wobei frühere Erkenntnisse aus der Literatur bestätigt werden. Ein weiteres Szenario stellt eine erweiterte Analyse der Umweltgerechtigkeit dar, indem nicht nur die individuelle Lärmbelastung, sondern auch die individuelle Verursachung derselben bewertet wird. Dabei wird gezeigt, dass die Lärmverursachung noch ungleicher verteilt ist als die Lärmbelastung. Der letzte Anwendungsfall stellt mögliche Auswirkungen der Einführung von großflächigen automatisierten und elektrischen Mitfahrdiensten auf den Verkehrslärm dar. Es zeigt sich, dass mögliche Lärmminderungen stark von der Gestaltung der Dienste und begleitender Maßnahmen abhängen.

Die Erweiterungen des angewandten Lärmmodells sowie die implementierte Rückkopplungsschleife im integrierten Flächennutzungs-/Verkehrsmodell sind als Teil von Open-Source-Bibliotheken verfügbar und können in zukünftigen Arbeiten weiter verwendet und entwickelt werden.

Contents

List of Figures

List of Tables

Acronyms

L_{DEN}	Energy Equivalent Continuous Sound Level.
AIC	Akaike Information Criterion.
AMoD	Autonomous Mobility on-Demand.
BBSR	Bundesinstitut für Bau-, Stadt- und Raumforschung.
BEA	Bavarian Environmental Agency.
CN	Condition Numbers.
CNOSSOS-EU	Common Noise Assessment Methods in Europe.
DRT	Demand Responsive Transit.
EV	Electric Vehicles.
FABILUT	Flexible, Agent-Based Integrated Land Use/Transport.
GHG	Greenhouse Gas Emissions.
GIS	Geographical Information System.
GNS	General Nesting Spatial.
GWR	Geographically Weighted Regression.
ICEV	Internal Combustion Engine Vehicles.
IDW	Inverse Distance Weights.
ILUT	Integrated Land Use/Transport.
L_{DEN}	Day-Evening-Night Level.
LCR GW	Locally Compensated Ridge Geographically Weighted Regression.
LTE	Land Use/Transport/Environment.
MATSim	Multi-Agent Transport Simulation.
MAUP	Modifiable Areal Unit Problem.
MITO	Microscopic Transportation Orchestrator.

NSDI	Noise Sensitivity Depreciation Index.
OLS	Ordinary Least Squares.
OSM	OpenStreetMap.
RLS-19	Richtlinien für den Lärmschutz an Straßen 2019.
RLS-90	Richtlinien für den Lärmschutz an Straßen 1990.
SAR	Spatial Auto-Regressive Model.
SaV	Shared autonomous Vehicles.
SDM	Spatial Durbin Model.
SEM	Spatial Error Model.
SILO	Simple, Integrated Land use Orchestrator.
SLX	Spatially Lagged X Model.
VDP	Variance Decomposition Proportions.
VGI	Volunteered Geographic Information.
VIF	Variance Inflation Factor.
VKT	Vehicle Kilometers Traveled.
WHO	World Health Organization.

1 Introduction

> The day will come when man will have to fight noise as inexorably as cholera and the plague
>
> Robert Koch

Even in the digital age, with all its possibilities of teleworking, telecommunication, online services and on-demand entertainment, the necessity for the transportation of goods and persons remains high. It is expected to grow, especially around metropolitan areas (Mendez et al., 2017). As persons and goods move throughout space, their actions impact their surroundings and environment. There are many examples of how transportation (and its required facilities and services) interacts with the environment, including society, nature and climate. Infrastructure such as roads and railways consume large amounts of space, as do additional transport-dedicated facilities such as parking lots and train stations. In addition, infrastructure may separate areas from each other, which can lead to social segregation. Other impacts of transportation on the environment are air pollutants and greenhouse gas emissions and **traffic noise**. Some of those impacts have in common that those responsible for causing them are not held accountable for their actions. The economic literature refers to those as 'transport externalities'. In contrast to, e.g., odorless gases, traffic noise is one of the externalities which is most often actively perceived by residents.

Traffic noise is a common nuisance in the urban environment and is primarily driven by road traffic. The growth and densification of cities lead to higher traffic volumes and noise levels and more people being exposed to these levels. According to the World Health Organization (WHO), more than 43 % of the urban population in Europe is exposed to road noise levels greater than 55 dB(A) (WHO, 2009). Noise can impair the health of affected people and can lead to sleep disturbances, tinnitus and cardiovascular diseases. In addition, it can affect residential location choices as residents derive lower satisfaction from living at exposed locations (Maloir et al., 2009).

A modern definition of transportation is that of derived demand. Persons (or goods) need to travel because they usually need to reach a location at which they can perform an activity which they cannot perform at their current location. This in turn means that the allocation of activity locations affects travel demand and, thus, transportation. In this way, shaping land use also shapes transportation. However, in free markets, where dwellers and employers are somewhat free to choose where to settle, transportation also shapes land use. This is typically known as the land use/transport interaction cycle. An

even more complex view acknowledges that the transport-related environmental impacts such as noise can have a feedback impact on land use, as people can be annoyed by noise and instead choose to live in quiet neighborhoods. A fascinating historic example for an interaction of traffic noise and land use is the ancient Roman emperor Trajan, who is said to have cut down on public building activity as a consequence of the traffic noise that was generated by the wagon traffic that delivered building materials to the construction sites (Brians, 1996). A recent example is the Elbtower, a planned 64-story building in Hamburg (Germany), which will not host any apartments due to traffic noise (Stanek, 2021).

Typically, traffic noise is assessed by physical measurements and noise prediction models. Recently, Kaddoura et al. (2017) presented an integrated approach in which an agent-based transport simulation was coupled with an official noise prediction model. Agent-based simulations use synthetic agents to represent individual persons or groups and analyze complex systems and phenomena that emerge as an outcome of simple individual interactions ('emergence'). This new approach has multiple advantages. On the one hand, the agent-based simulation allows assessing noise emissions and immissions at a fine spatial and temporal resolution. In addition, transport scenarios implemented in the simulation can easily be analyzed in terms of noise. This is useful for recent scenarios that require simulating individuals explicitly, for example ride-hailing and -pooling. However, the real power of this agent-based approach is that it allows modeling traffic noise as an emergent phenomenon. Noise exposure can be analyzed at the person level since individual locations are known. Similarly, individual contribution to traffic noise can be represented as each individual can be traced throughout the transport network. As both exposure and contribution per agent are known, issues of environmental equity can be addressed in more detail.

This dissertation builds upon the initial work by Kaddoura et al. (2017) and addresses new possibilities that arise from the usage of an agent-based simulation in the context of road traffic noise. In a first step, some existing limitations of the work by Kaddoura et al. (2017) will be analyzed and resolved. In a next step, multiple use cases that benefit from an agent-based simulation of traffic noise will be presented.

A first use case will implement an environmental feedback loop in an agent-based integrated land use/transport simulation that models the interaction between land use and transport. Thereby, individual agents whose locations and activities are determined by the land use component will lead to travel patterns in the transport simulation, which, in turn, leads to resulting noise immissions. Eventually, these noise immissions will then affect the housing and relocation decisions of individual agents with different preferences. Similarly, the environmental noise will lead to reduced property prices in the land-use model. The aim is to let residents react to their environment and, as such, improve understanding of relocation patterns and issues of environmental equity.

The second use case will look deeper into the equity aspects of traffic noise. Given the detailed microscopic resolution of an agent-based model, exposure and - as a novel approach - causation of individual agents will be analyzed and compared.

Lastly, a use case that applies the agent-based transport simulation to model ride-pooling as a modern transport service will be presented to understand impacts on traffic noise. Like for the other use cases, an agent-based approach is crucial to microscopically model the behavior of ride-pooling passengers and providers and individual residents exposed to the resulting traffic noise.

The thesis continues with a literature review and definitions of traffic noise, its negative effects and existing noise models in chapter 2. Existing studies related to the given use cases of an integrated land use/transportation/environmental model, equity issues, and ride-pooling are presented to build a background from which specific research questions are developed. The research questions then lead to the actual structure of the thesis.

2 Literature Review and Research Questions

This chapter serves as a basis for the introduced use cases in the introduction. Based on definitions and existing literature, the actual research questions of this thesis will be developed.

2.1 Traffic Noise

2.1.1 Definitions and Indicators

The presence of noise is usually quantified by noise levels. Noise or *sound levels* are determined by measurements or model estimates and are expressed in decibels (dB). The unit Bel is an auxiliary quantity that converts the wide range of values of sound pressure p perceptible by the human ear into a simpler scale. The human ear can perceive average sound pressures between 0.00002 (hearing threshold) and 20 Pa (pain threshold). The sound level L is defined as:

$$L = 20 \cdot \log_{10}\left(\frac{p}{p_0}\right) \quad [\text{dB}], \tag{2.1}$$

where p is the sound pressure and p_0 is the reference sound pressure of the hearing threshold ($p_0 = 0.00002$ Pa). Due to this correlation, a doubling of the sound pressure does not lead to a doubling of the sound level. A doubling of the sound pressure corresponds to an increase of the level by 6 dB. In general, it can be said that an increase of the level by 10 dB corresponds to a perceived doubling of the volume. This, in turn, corresponds to a tenfold increase of the sound pressure. The sound level can also be defined by the sound energy W for which the relationship is $W \sim p^2$ and, thus:

$$L = 10 \cdot \log_{10}\left(\frac{W}{W_0}\right) \quad [\text{dB}], \tag{2.2}$$

here, the reference value is $W_0 = 10^{-12}\ J$.

The human ear is not equally sensitive to all sound frequencies. In general, lower frequencies are perceived as less loud when compared to higher frequencies of the same pressure. To account for this, filters have been developed to represent the sensitivity of the human ear better. The most common filter is the A-filter, which attenuates bass and treble. As such, sound levels represented with an A filter better reproduce human sensations. To indicate the A-filter, the unit is given as [dB(A)]. In general, all of the

subsequent levels in this dissertation will refer to A-filtered decibels.

Because of the logarithmic level scale, one cannot obtain a resulting level by simple addition when adding up sound levels of multiple sources. One has to add up the underlying sound energy values and use 2.2 to transform it to a level:

$$\begin{aligned} L_{\text{sum}} &= \sum_i W_i \quad [\text{J}] \\ &= 10 \cdot \log_{10}\Big[\sum_i \frac{W_i}{W_0}\Big] \quad [\text{dB}] \\ &= 10 \cdot \log_{10}\Big[\sum_i 10^{\frac{L_i}{10}}\Big] \quad [\text{dB}] \end{aligned}$$

Since sound is a strongly fluctuating quantity over time, averaging levels are used to measure sound effects over a longer period of time. Since it is not meaningful to average the logarithmic level scale, the sound energies are averaged instead:

$$L_{\text{eq}} = \frac{1}{T} \sum_i t_i \cdot W_i \quad [\text{J}], \tag{2.3}$$

where T is the total measurement duration and t_i is the duration of measurement i of the sound energy W_i. Again this can be turned into a level:

$$\begin{aligned} L_{\text{eq}} &= 10 \cdot \log_{10}\left[\frac{\frac{1}{T}\sum_i t_i \cdot W_i}{W_0}\right] \quad [\text{dB}] \\ &= 10 \cdot \log_{10}\Big[\frac{1}{T}\sum_i t_i \cdot 10^{\frac{L_i}{10}}\Big] \quad [\text{dB}] \end{aligned}$$

L_{eq} is called energy equivalent continuous sound level. If T covers one hour, the indicator is called **hourly energy equivalent sound level**.

Often noise is assessed for whole day periods. Therefore an aggregated measure is commonly employed that adds up hourly noise levels and gives extra penalties to evening and night time values:

$$L_{\text{DEN}} = 10 \cdot \log_{10}\left[\frac{1}{24}\left(\sum_{t=0}^{23} 10^{0.1 \cdot (L_{\text{eq},t} + \tau(t))}\right)\right], \text{ with} \tag{2.4}$$

$$\tau(t) = \begin{cases} 0\,\text{dB(A)}, & 6 \le t < 18 \\ 5\,\text{dB(A)}, & 18 \le t \le 22 \\ 10\,\text{dB(A)}, & \text{else.} \end{cases} \tag{2.5}$$

which is the Day-Evening-Night Level (L_{DEN}) and $\tau(t)$ is the penalty given to hour t. $L_{eq,t}$ is the hourly energy equivalent sound level over the period of hour t. The L_{DEN} is the most common indicator used around the world and is used in many different applications (Word Health Organization, 2018). It is usually reported for outside exposure at the most exposed facade of a building.

Road traffic noise from passing vehicles comprises multiple factors. The two most important components are propulsion and rolling noise. As shown in figure 2.1, the propulsion noise is dominant at low speeds. However, at around 30 km/h the rolling noise becomes the dominant source of the total noise. The figure also shows the logarithmic relationship between vehicle speed and noise.

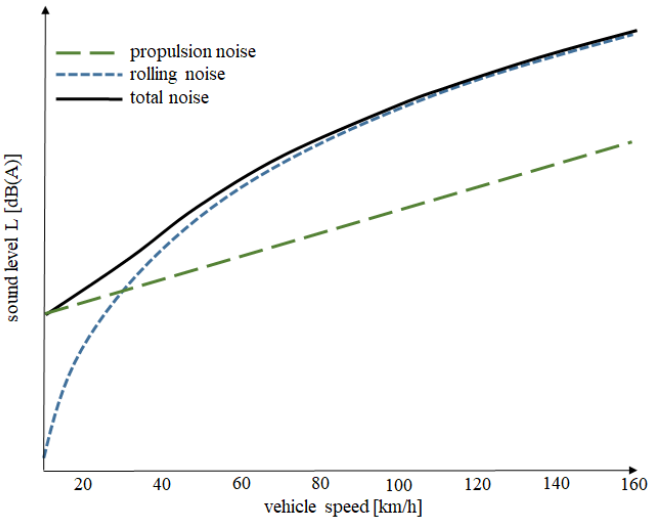

Figure 2.1: Components of vehicular noise for a passenger car. Based on van Blokland and Peeters (2007).

A comparison of different transport-related noise levels is shown in figure 2.2.

2.1.2 Noise as a negative Traffic Externality

2.1.2.1 Health Impacts

Reviews compiled for the WHO indicate that noise can reduce residents' well-being and quality of life, leading to stress and stress-related diseases such as poor mental health (Clark and Paunovic, 2018). Bluhm et al. (2004) reported positive correlations between noise exposure and sleep disturbances. Tobías et al. (2015) find evidence for an association between noise levels and cardiovascular as well as respiratory mortality and compare the impact of reducing noise by 1 dB(A) to being similar with a reduction of 10μg of $PM_{2.5}$ (particulate matter). Another study by Leon Bluhm et al. (2007) found an odds ratio of 1.38% for hypertension per 5 dB(A) of noise increase. Similarly, Babisch et al. (2005) found an odds ratio of 1.3% for myocardial infarction. The two latter studies both

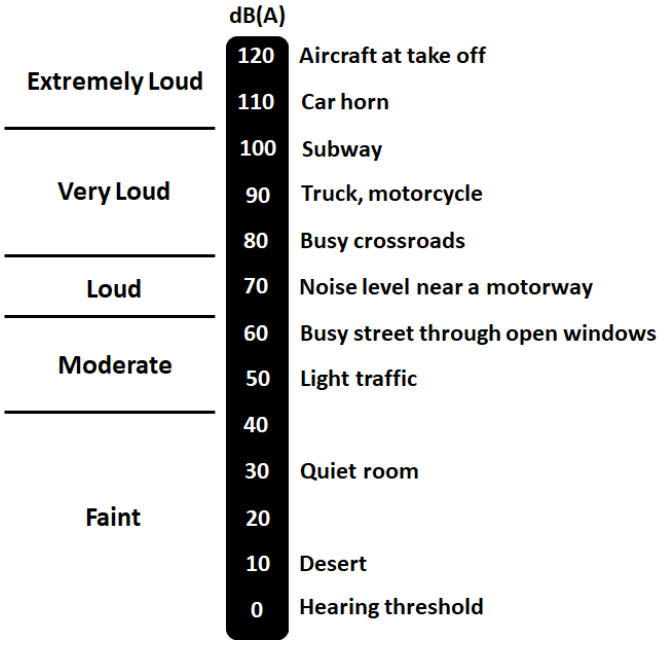

Figure 2.2: Comparison of transport-related noise levels. Based on Rodrigue (nd).

found that the odds increased even higher when the person lived at the exposed location for a long time. A meta-analysis of multiple studies by Babisch (2008) concluded a dose-response relationship between noise exposure and cardiovascular risk for noise levels above 60 dB(A). A more recent meta-analysis of the same author found a 20% higher risk of coronary heart diseases for people exposed to high levels of noise (Babisch, 2014). de Kluizenaar et al. (2009) found significant increases in morning tiredness for night time road noise exposure above 35 dB(A). Traffic noise can also disturb local neighborhood quality and impair recreation capacities. Hartig (2007) reports that residents going for a walk in noisy areas even showed increased stress levels during the first half of the walk.

One study to be highlighted is the LARES report on noise effects and morbidity (Niemann and Maschke, 2004). The LARES (Large Analysis and Review of European housing and health Status) was conducted across eight European cities. The report analyzes the relationship between several diseases diagnosed by physicians and noise pollution and sleep disorders caused by noise. While controlling for possible confounders, multiple significant increased odds ratios have been found. The results were differentiated for children, adults and older people. Figure 2.3 shows the significantly increased odd ratios for adults.

In contrast, other studies have found less clear or no relationship between noise and health. Fyhri and Aasvang (2010) report that, although they found significant relationships between noise, annoyance and sleeping problems, they did not find a relationship

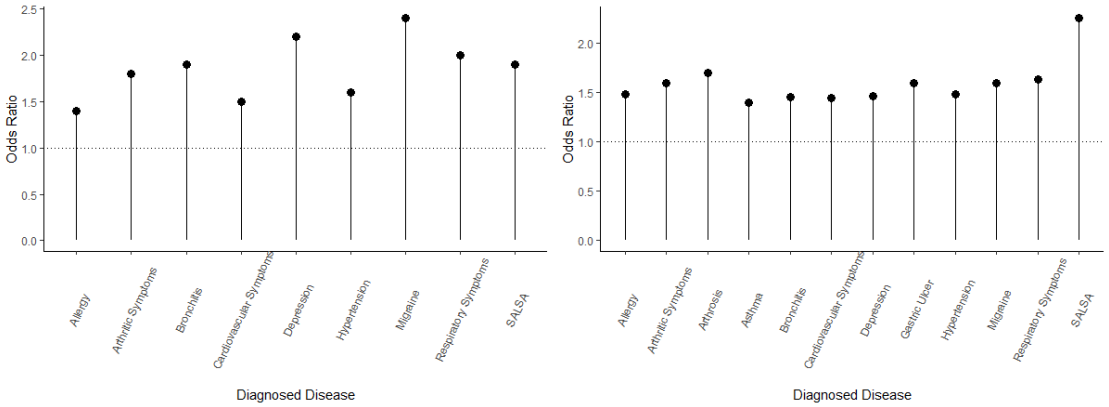

Figure 2.3: Significantly increased odds ratios for diagnosed diseases in relationship with a) strong traffic noise annoyance (left) and b) reported noise induced sleep disturbances (right). Values taken from the LARES report.

between noise and cardiovascular problems. Another study found a 'positive, but not statistically significant association between noise exposure and symptoms of distress' (Sygna et al., 2014, p. 17). Fyhri and Klæboe (2009) investigated the relationship between noise exposure, noise complaints as well as noise sensitivity and self reported hypertension and heart problems with a structured equations modeling approach. They find an association between noise sensitivity and heart problems but no relationship between noise exposure and reported health problems.

2.1.2.2 Impacts on Residential Satisfaction and Relocation

The German environmental agency calls traffic noise 'the bane of many Germans' lives' (Umweltbundesamt, 2012). According to a survey on environmental consciousness, 55% of the German population are disturbed by road traffic noise (Rückert-John et al., 2013). In addition, 34% and 23% of the population report disturbance caused by train and aircraft noise, respectively (see table 2.1).

Table 2.1: Percentage of respondents who have felt disturbed by several noise sources in the last 12 months. Values taken from (Rückert-John et al., 2013).

Source	extremely disturbed	strongly disturbed	moderately disturbed	somewhat disturbed	not disturbed at all
Railyway	0	2	7	13	78
Road	2	9	16	28	45
Industry	1	2	9	16	72
Aviation	1	3	7	18	71
Neighbors	1	4	7	25	63

Among all sources of transport noise, road traffic noise is consistently being reported as the one that annoys the most people. A review by Guski et al. (2017) confirmed that

there is a significant relationship between (road) traffic noise levels and the percentage of the population that feels highly annoyed. Ouis (2001) pointed out that '[...] decades of research on this topic have permitted lately the establishment of a more or less quantitative relationship between the objective quantities characterizing road traffic noise and the human subjective reaction to it as expressed by annoyance.' (Ouis, 2001, p. 101), see also (Lambert et al., 1984; Osada, 1991; Fields, 1993).

Other studies confirmed that noise can be a crucial factor that affects the willingness to move, relocation choice and satisfaction with housing (Bradley and Jonah, 1979). For example, (Źróbek et al., 2015) identified that 'quiet neighborhoods' ranked second after 'affordable price' and before other common location factors, such as 'proximity to workplace' or 'proximity to kindergarten' when asking respondents for neighborhood characteristics of residential properties. In their study 'What Makes People Dissatisfied with their Neighborhoods?' Parkes et al. (2002) find significant relationships between noise and neighborhood appraisal. Al-harthy and Tamura (1999) present results of a survey in Muscat city (Oman) in which 'quietness' ranked first among respondents' dissatisfaction with their neighborhood. Wardman and Bristow (2004) showed that reducing noise levels is among the top three priorities for improvement in residential satisfaction. A similar result has been found by Hanák et al. (2015) when evaluating the perception of the residential environment. Shepherd et al. (2013) found a negative relationship between noise and self-reported quality of life, health and well-being. Osada et al. (1997) used path analysis to identify that noise significantly increases the willingness to move, which can be explained directly by noise levels and other indirect consequences, including noise annoyance. Lercher and Kofler (1996) show that households who experience noise levels above 55 dB(A) are 2.45 times as likely to express a willingness to move. The odds increase to 6.8 for households that express a moderate or strong noise annoyance. In a study carried out by Bendtsen et al. (2000), 'road traffic noise' was the second most common answer expressed by 25% of the people who plan to move when asked for the three main reasons for moving. Furthermore, in a survey on livable public space in the German cities Ravensburg and Heidelberg presented by Görgen and Fisch (2013), 15% to 19% of the respondents who expressed a willing to move mentioned noise as one of the main motivations for relocating. A similar finding has been reported by Bauer-Wolf et al. (2003), who present that 28% of the people moving from the city of Wien to the suburbs state noise as their main reason to move.

The impact of noise on residential locations is a complex topic as it not only depends on noise levels alone but also on its perception, sensitivity and even awareness of adverse health impacts of noise (Han et al., 2015). Not every person is equally sensitive to noise. While biological responses to noise exposure appear to be very similar across the population, the psychological response can differ considerably. A study by Matsumura and Rylander (1991) confirmed that noise annoyance is strongly linked to noise sensitivity, which is a personal trait that relates to other socioeconomic attributes. In this particular study, approximately 25% of the studied population was found to be 'noise sensitive'. Noise sensitivity as a mediator of noise annoyance can explain up to 9% of the variation

in human responses to noise (Miedema and Vos, 2003). Miedema and Vos (1998) report that the difference in noise annoyance between least and most sensitive persons had the same impact as a difference of 11 dB(A) change of actual noise exposure. Figure 2.4 shows an illustrative visualization of the impact of sensitivity on annoyance.

This can also lead to the phenomenon of residential self-selection, where people who are less sensitive to noise will benefit from more affordable property prices and are more willing to move to more noisy areas (Weinhold, 2008). Van Wee (2007) discusses that this can lead to underestimating the negative impacts of transport on noise when assessing new infrastructure in quiet areas, as these possibly accommodate higher shares of noise-sensitive residents. However, a study by Nijland et al. (2009) did not find evidence for the existence of a residential self-selection phenomenon due to noise. If the effect exists, it is not easy to detect it. It should be mentioned that the existence of person-/household-dependent noise sensitivities encourages the use of agent-based models in which each agent can be represented with individual traits.

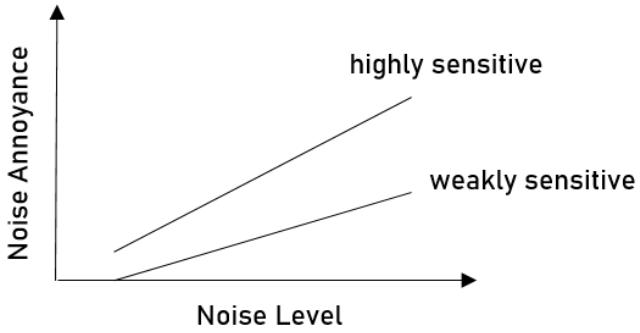

Figure 2.4: Illustrative presentation of the relationship between noise exposure and annoyance for highly and weakly noise-sensitive persons. Based on Miedema and Vos (2003).

Maloir et al. (2009) discuss how the impact of transport infrastructure on land use has to be valued with a trade-off between positive effects such as increased accessibility in the surroundings and negative effects such as air pollution, noise and landscape destruction. The negative effects are typically predominant adjacent to the source, while accessibilities usually have a wider spatial impact. The strong local nature of negative impacts often leads to 'not in my backyard' oppositions of households that live close to newly planned infrastructure and oppose construction plans. The strength of the impacts thus largely depends on the actual distance between roads and home locations. Maloir et al. therefore argue for carefully assessing the positive and negative impacts on a local scale. In addition, they point out that detrimental road infrastructure impacts can be twofold - by harming the well-being of residents who consequently derive lower values from living at exposed locations and, in addition, by a possible subsequent reduction in property prices. Similarly, Schirmer et al. (2014) find that transport facilities are valued by peo-

ple depending on them while at the same time noise and pollution make them undesirable.

Even though it is sometimes argued that people will eventually come to peace with or get used to the noise, studies found evidence against this claim. Weinstein (1982) present a study that concluded that there was no evidence of adaptation in self-reported annoyance and other noise effects and respondents even got more pessimistic about adapting over time. Here, adaptation only meant responding less negatively to noise and did not include other actions such as improving sound insulation or even moving away.

2.1.2.3 Impacts on Property Values

The negative impact of road traffic nuisances on housing is twofold – noise reduces the housing satisfaction of residents and, in some cases, can lead to a reduction in property values (Maloir et al., 2009). A typical link between land use and traffic noise is the impact of noise on real estate prices which has extensively been reviewed in previous studies. In general, a significant negative relationship can be found (Bateman et al., 2001). A typical indicator is the Noise Sensitivity Depreciation Index (NSDI) which is the percentage change in housing prices caused by an increase of dB(A) in noise level exposure:

$$\text{NSDI} = \frac{\text{percentage change of housing price}}{\text{increase of noise}} \tag{2.6}$$

In an overview of previous studies, Bateman et al. (2001) report NSDI values between 0.08% and 2.22%, with an average of 0.4%. Nelson (1982) found NSDI values between 0.17% and 0.63%, with 0.4% being the average. Two basic approaches for evaluating noise impacts on real estate prices can be identified. Surveys and stated preferences can be used to identify willingness-to-pay for a reduction in noise (Theebe, 2004). An advantage of this method is the low amount of required data. However, survey data may be biased and might not reflect true valuations paid on the market. The more common approach is to use the hedonic pricing method, which allows to estimate the impact of different goods on prices based on observed transactions by employing a regression model. The downside of observed transactions is that in very tight housing markets, in which people have to take what they can get, the costs might reflect compromises that underestimate true valuations.

Most studies in the literature focus on the total price of buying a house or an apartment. Theebe (2004) estimated NSDI values between 0.3% and 0.5% with the help of hedonic pricing applied on a rich data set in the Netherlands. In his estimation, he included accessibility values to control for positive aspects of infrastructure and to prevent underestimation of noise impacts. However, he did not use noise as a continuous variable but ranges of noise as dummy variables to allow for a nonlinear relationship between noise and price. Noise impacts varied across sub-markets and did not significantly change throughout different years. Szczepańska et al. (2014) conducted a study on traffic noise impacts on urban apartment prices. The data consisted of 215 apartments in multi-

family houses in the city of Olsztyn in Poland. They found NSDI values between 0.74% and 0.83%. Another study by Allen et al. (2015) used distance to highway as a proxy for traffic noise in a spatial regression. Based on a sample of 1,025 single-family detached house transactions in Orange County, California, they found a price discount of 4% for houses adjacent to highways, while also controlling for accessibility impacts. Wilhelmsson (2000) conducted a study on the impact of noise on the values of single-family houses in Sweden using the hedonic pricing approach. Loud properties sold with a discount of up to 30% compared to more quiet houses. Using a double-log form regression, Kim et al. (2007) found a relation in which a 1% increase in traffic noise leads to a decrease of 1.3% in land price per square meter in an urban area. In a cost-benefit analysis by Becker and Lavee (2002) in Israel, the reported NSDI values are 1.2% and 2.2% for urban and rural areas, respectively. The application of hedonic pricing on property prices in Sweden by Andersson et al. (2010) included a concave function to reflect noise impact on prices and was compared to a traditional semi-log regression model. While the traditional model resulted in NSDI values between 1.15% and 1.17%, the concave specification resulted in values between 1.35% and 2.9%, depending on the base noise level. When comparing NSDI between traditional Ordinary Least Squares (OLS) regression and a spatial lag model, the difference was negligible. Baranzini and Ramirez (2005) studied the impact of multiple noise sources on rent prices in Geneva and found an NSDI of 0.7% when looking at all noise sources.

2.1.2.4 Issues of Environmental Equity

The spatial nature of exposure to transportation-related environmental stressors such as noise and air pollutants as well as different capabilities of coping (e.g. affordability of sound insulation or relocation) can raise questions about environmental justice. Rodrigue (2016) gives the example that, on a local level, 'a community may be affected by noise levels well over its own contribution (notably those near major highways), while another (in the suburbs) may be affected in a very marginal way and still significantly contribute to noise elsewhere during commuting' (Rodrigue, 2016, p. 261). In this comparison, inequality is compared solely based on various spatial conditions. However, inequality can also be identified when comparing socio-demographic attributes of the causers and the affected. As discussed in the sections above, dwelling prices can be affected by environmental conditions, and as such, qualities like 'quietness' become a matter of affordability. In a free market without regulation, environmental outcomes 'are mainly left up to market forces' (Kruize et al., 2007, p. 578). For example, Herridge and Low-Beer (1973) report on the development of 'noise ghettos' because persons with high incomes can afford to move into quieter neighborhoods, while low-income persons must stay or move into noisy but inexpensive areas.

Greenberg and Cidon (1997) present two common definitions of environmental (in-) equity:

Process inequity occurs when individuals (groups) are not fairly involved in the decision-making process that can lead to environmental impacts (such as the decision on

where to put a waste plant). In this definition, unequal distribution of burdens would be acceptable as long as the decision-making process is fair.

Outcome inequity occurs when the environmental burden itself is unequally distributed among (groups of) individuals.

Most existing studies that address transport-related environmental equity issues focus on outcome inequity and report how environmental burdens are distributed. Carrier et al. (2016) show that areas with a higher share of low-income individuals and minorities have a higher probability of being exposed to higher road traffic noise levels when compared to the rest of the population. Another study by Potvin et al. (2019) finds that low-income persons and minorities in Montreal live more often close to major roads. Remarkably, the study also revealed that among those who live close to major roads, low-income persons were less likely to be protected by noise barriers. Different authors find similar findings for Montreal, reporting associations between noise exposure and multiple socioeconomic factors (Dale et al., 2015). For the Twin Cities, USA, Nega et al. (2013) demonstrate an association between noise levels and household income and percentage of non-white residents, among others. A review of studies on noise and environmental equity for the European region concludes that there is a trend that confirms a positive association between noise exposure and lower socioeconomic position (Dreger et al., 2019). This is also supported by a report compiled for the European Commission (for Environment Policy, 2016). However, this report also acknowledges that the relationships are less clear in European cities. Here, the city centers are often very attractive and inhabited by affluent persons, but they are also noisy. The report underlines that analyses of inequities should also take into account the concept of vulnerability. Affluent households or persons are more likely to cope better with high exposure (e.g. because of healthier lifestyles or affordability of counter-measures) and, thus, are often less vulnerable than households with a lower socioeconomic status. Laußmann et al. (2013) present another study that analyzed the inequity of noise exposure in Germany. One of the interesting findings is that the city classification ('large city', 'medium city', 'small town' and 'rural area', Bundesamt für Bauwesen und Raumordnung, 2020) showed different frequencies of extreme noise exposure, with residents in large cities reporting twice as likely to be highly annoyed by road traffic noise.

Some studies also report evidence against environmental inequity or opposite findings. For example, Havard et al. (2011) identified a positive association between noise exposure and advantaged neighborhoods in Paris. The existence of inequity related to socioeconomic variables seems to be highly case-specific.

For the city of Munich, which is the focus area of this dissertation, Kistler et al. (2017) found that poor households were twice as likely to be annoyed by noise than more affluent households. An official report published by the city administration of Munich showed that districts that are exposed to more than 55 dB(A) are also more likely to be considered as districts that face sociodemographic challenges such as higher rates of unemployment or a

larger share of households with a foreign background (Landeshauptstadt München, 2015).

Some studies used the Gini index as a formal measure of inequality (Millimet and Slottje, 2002; Maguire and Sheriff, 2011; Wu and Heberling, 2013). The Gini index G tries to reduce distributions of a certain good (e.g. income or costs) to a single indicator. It can be defined by:

$$G = \frac{\sum_{a=1}^{n} \sum_{b=1}^{n} |x_a - x_b|}{2n^2 \overline{x}} \tag{2.7}$$

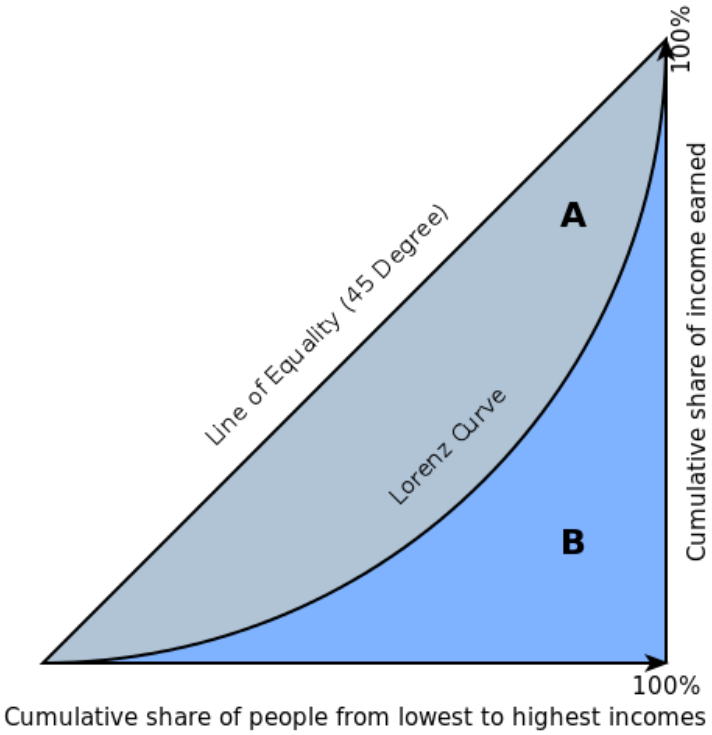

Figure 2.5: A typical Lorenz curve and its relation to the Gini index.

Here, n is the total population (or the number of agents) and x_a/x_b is the number of units of the studied good assigned to an individual a or b. This way, the G can be understood as half of the relative mean absolute difference between observations (Sen et al., 1973). A more intuitive explanation makes use of the underlying concept of the Lorenz curve. A typical Lorenz curve is shown in figure 2.5. In a Lorenz curve, the population is sorted by their respective amount of the studied good in ascending order. The curve then shows for a certain percentage of the population (x-axis) how much of the total amount of the studied good they are attributed to (y-axis). If the distribution of a good is perfectly equal, the curve is represented by the line of equality, as shown in figure 2.5. The more unequal a good is distributed, the larger the area between the line of equality and the Lorenz curve will become (area A in figure 2.5). If B is the area under the Lorenz

curve, the Gini index can also be defined as $G = \frac{A}{A+B}$, i.e. as the ratio of A over the total area $A+B$. G usually takes values from 0 (perfect equality) to 1 (perfect inequality).

The majority of studies have only looked at the distribution of environmental burdens. However, as discussed above with the example of quiet suburbs with residents commuting into the city, the contribution to noise exposure may be an additional factor to look at when assessing environmental equity. This opens up another use case of agent-based simulations coupled with an environmental model. Kaddoura (2019) already presented an approach to attribute noise exposure contribution to individual agents by monetizing the external cost. As such, agent-based models can be used to analyze and compare both individual exposure and individual contribution to noise (or air pollutants) per agent at a fine spatio-temporal resolution. Like flocks of birds or traffic jams, environmental inequity can be understood as an emergent phenomenon that is not deliberately induced by a single actor but results from the interplay of many microscopic interactions. Therefore, agent-based models are particularly suited for this type of research (Campbell et al., 2015).

Another aspect in the analyses of environmental equity is that the analyses can be subject to the 'ecological fallacy'. Ecological fallacy can arise when the spatial scale of an analysis is too coarse and thereby blurs the distribution of pollutants and exposed individuals and their traits (Banzhaf et al., 2019). In a review of 110 environmental justice studies, Baden et al. (2007) find that evidence of inequity becomes stronger when smaller spatial units are used. This underlines that microscopic models may be more suitable for addressing these issues.

2.2 Traffic Noise Models

To analyze the impact of noise, one has to obtain data on sound levels. One possible approach to retrieve the data is to measure noise physically. As a more flexible and less expensive alternative, noise can be modeled by using traffic noise models, of which many have been developed over the years. The first models go back into the 1950s and modeled the 50th percentile of traffic noise based on distances and traffic volume (Quartieri et al., 2009). Later models also included the mean speed of vehicles and the share of heavy vehicles. Reviews and comparisons of official traffic noise models are given by Quartieri et al. (2009), Steele (2001), de Lisle (2016) and Garg and Maji (2014).

An overview of official traffic noise models and their main location of application is given in table 2.2. Even though official noise prediction models have different formulations for noise prediction, Quartieri et al. (2009) show that the resulting noise levels are similar. In principle, most models rely on empirically estimated equations that usually postulate a logarithmic functional relationship between traffic volume and noise. The estimations may be subject to 'site bias', leading to errors in the predictions at different sites (Guarnaccia et al., 2011). A special case is the CNOSSOS-EU model, as it aims to

Table 2.2: Overview of Official Traffic Noise Prediction Models

Traffic Noise Model	Offical model or most commonly applied in	Reference
MPB-Routes 2008 (Nouvelle Methode de Prevision de Bruit)	France	(Dutilleux et al., 2010)
CNR (Consiglio Nazionale delle Ricerche)	Italy	(Cannelli et al., 1983)
RLS-19	Germany	(FGSV, 2019)
CoRTN procedure (Calculation of Road Traffic Noise)	United Kingdom, Australia, Hong Kong, New Zealand	(United Kingdom Department of the Environment, 1988)
FHWA TNM (Federal Highway Administration Traffic Noise Model)	United States, Canada, Mexico	(US Federal Highway Administration, 2004)
ASJ RTN Model (Acoustical Society of Japan Road Traffic Noise)	Japan	(Sakamoto, 2015)
Son Road	Switzerland	(Heutschi, 2004)
Nord 2000	Norway, Denmark, Sweden, Finland	(Jonasson and Storeheier, 2001)
CNOSSOS-EU	European Union	(Kephalopoulos et al., 2012)

harmonize the different national prediction methods in the European Union. The goal is to make results comparable and to allow for common standards for strategic noise mapping. Khan et al. (2020) report that prediction results are comparable with previous official models (correlation between CNOSSOS-EU and Nord 2000: R=0.96).

In Germany, the standard for modeling traffic noise for prevention and remediation is defined in the Richtlinien für den Richtlinien für den Lärmschutz an Straßen 1990 (RLS-90) which was updated in 2019 (RLS-19) (FGSV, 2019). The standard takes into account various variables, such as noise propagation and reflection, sound barriers, traffic flow, road dimension and geometry, among others. The base of the calculation is a function that takes into account vehicles per hour and the percentage of heavy vehicles and their speeds. Based on this, various correction terms are added, such as corrections for road surfaces, gradients and absorption characteristics of buildings. Although similar, the RLS is not fully compliant with the harmonized CNOSSOS-EU model and leads to minor differences in predictions (Müller, 2014). For strategic noise mapping an additional standard, the 'Berechnungsmethode für den Umgebungslärm von bodennahen Quellen' implements the CNOSSOS-EU for Germany (Arbeitsring Lärm der Deutschen Gesellschaft für Akustik (ALD), 2020).

Besides official guidelines, other approaches for noise modeling can be found in the literature. Gulliver et al. (2015) present TRANEX, an open-source noise model for assessing

noise exposure embedded in a Geographical Information System (GIS). Golmohammadi et al. (2009) estimated a noise model based on multiple linear regression, including 12 explanatory variables, which account for road dimensions, traffic flows and traffic speeds. The model was estimated and applied to Iranian cities and showed a good model fit ($R^2 = 0.901$). A different approach is taken by Cammarata et al. (1995); Mansourkhaki et al. (2018) and studies reviewed by Kumar et al. (2011) where artificial neural networks are utilized to predict noise levels. While some of the studies showed remarkably low estimation errors (average error: 0.76 dB, Genaro et al., 2010), it is acknowledged that these models are hard to interpret and work like black-box models. In addition, the models are highly data-driven and might not easily be transferable to different study regions. Similarly, Caponetto et al. (1997) present a fuzzy-logic approach combined with a genetic algorithm to estimate noise levels. Again, the interpretability of the method is limited and the results are highly dependent on the training data set. Guarnaccia et al. (2017) combine time series analysis for predicting noise over multiple days of the week and use an artificial neural network to correct for the residuals produced by the prediction.

Since noise prediction models require the local traffic conditions such as traffic volumes and speeds as an input, it is a natural step to connect noise prediction models with transport models, as highlighted by Can (2019, also see for a comprehensive overview) and done for e.g. VISUM (Rickborn, 2012), VISSIM (Estévez-Mauriz and Forssén, 2018) and AIMSUN (De Coensel et al., 2016).

Kaddoura et al. (2017); Kaddoura (2019) present an implementation of the RLS-90 for the Multi-Agent Transport Simulation (MATSim) which will be explained in more detail in chapter 3. An advantage of using a (microscopic) transport model is that actual time and location-dependent (albeit simulated) speed levels can be taken into account and the prediction does not need to rely on speed limits only. More recent 'dynamic' noise prediction models such as the RLS-19 are reported to result in better fits when compared to purely statistical models that do not account for speed (Guarnaccia et al., 2018). The analysis of population exposures to noise may benefit from a microscopic and time-dependent model resolution as given in agent-based models. Agent-based models provide insights into population groups and person-specific exposures. They allow to include residential locations and activities such as being at home and other sensitive sites like schools, offices, and hospitals. In addition, a time-dependent model allows to account for the time of day (e.g. day vs. night) and exposure duration (e.g. short-term vs. long-term).

2.3 Integrated Land-Use/Transport Models

The explicit interaction between land use and transport is often studied in Integrated Land Use/Transport (ILUT) models. These models usually build upon the idea of the land-use transport feedback cycle (Wegener and Fürst, 1999, see figure 2.6) and typically run for multiple years or decades into the future. The land use component of the model

deals with the representation of synthetic dwellers (and firms) and their (residential) location choices in space. In agent-based ILUT models, a synthetic population represents individuals who age, relocate, die or give birth, among others. In addition, there is usually a representation of the built environment, including sub-models for construction, deterioration and renovation. Land use decisions such as relocations or construction of buildings are explicitly influenced by locational characteristics, which, in turn, account for transport-related conditions, often in the form of **accessibility**. On the other side, the location of dwellers and firms results in a given spatial arrangement of **activities**.

In the modern understanding of transport as derived demand in which people and goods have to travel because they cannot perform the desired activity at their current given location, the location of activities defines resulting travel demand. As such, the activities link the land use and the transport component. The transport model simulates the traffic at a given resolution (i.e. micro-/meso or macroscopic) and, thus, estimates travel times, costs and distances between locations. Based on these travel **impedances**, accessibilities can be calculated. The provision of accessibilities by the transport model closes the loop back to the land use component. ILUT models can differ significantly in their level of detail (microscopic vs. macroscopic), spatial resolution (large zones vs. fine grid cells or micro-locations), level of (software) integration (file-based vs. tightly coupled in the same programming language) and level of operation (Moeckel et al., 2018). ILUT models have been developed and applied for multiple decades with many theoretical and computational advancements since the first models going back to Lowry's model of Metropolis (Lowry, 1964). Good overviews of ILUT models, as well as current applications and research directions, are given in Moeckel et al. (2018); Acheampong and Silva (2015); Wegener (2021); Hunt et al. (2005).

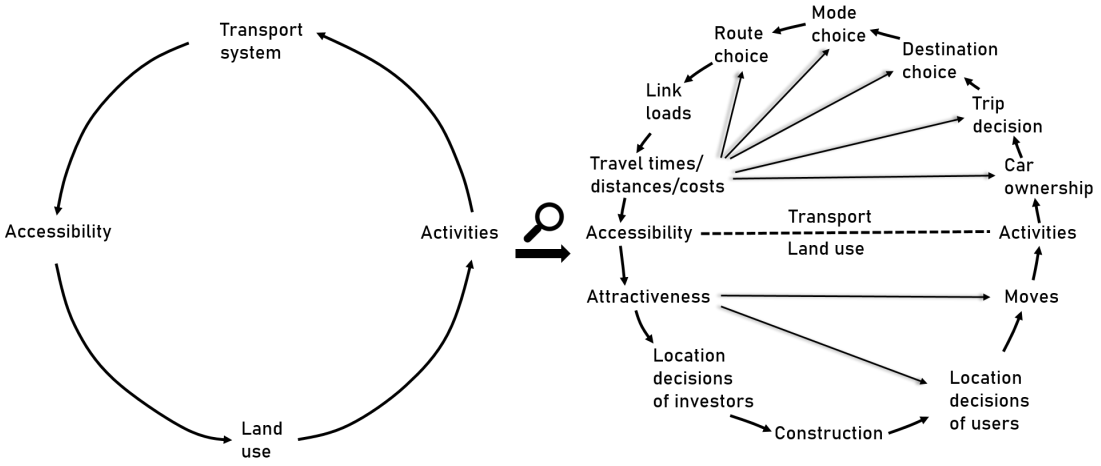

Figure 2.6: Land-use/transport feedback cycle. Based on Wegener and Fürst (1999).

In their paper 'Environmental Feedback in Urban Models' from 2008, Spiekermann and Wegener (2008) expressed that environmental and ecological aspects have long been ignored in ILUT models. While some models have been extended by environmental submodules to become Land Use/Transport/Environment (LTE) models, Spiekermann and Wegener highlight that most models only account for the effects of land use and transportation on the environment, ignoring the opposite direction. As the environment may affect the quality of neighborhoods, noise may also have an impact on land use and – indirectly – travel patterns. Spiekermann and Wegener identified the need for a high spatial resolution as a key requirement for implementing environmental feedback. Among others, they argue that noise is one of the key environmental factors for which a feedback to land use can be observed in reality. While almost every environmental indicator is affected by land use and transportation, only few of the indicators have a feedback impact on land use. For transport, none of the environmental indicators seem to have a *direct* impact (one example, that the author of this thesis can think of, is a policy reaction to noise by implementing (nocturnal) speed limits, which may affect traffic flow). Spiekermann and Wegener conclude that, as a minimum, the feedback from the environment to land use by affecting household relocation decisions should be implemented in LTE models. Acheampong and Silva (2015) confirm that integrated models should better account for environmental issues in future applications. In their overview of contemporary land use/transport/environment models, Gu et al. (2015) state that the environmental component has long been ignored and only recently gained attention. Their review of recent models concluded that 'most model[s] contain only a minimum of environmental indicators which are generated from the model as outputs, the feedback on land use are not considered.' (Gu et al., 2015, p. 11). Similar to the traditional ILUT cycle, figure 2.7 illustrates how the different interactions in LTE models may be modeled.

The CityPlan model presented by Gu and Young (1998) accounts for environmental impacts such as noise and air pollution in an ILUT model but analyzes them as an output only. However, while they claim that reactions to environmental conditions tend to be slow, they acknowledge that 'with the increasing concerns regarding urban traffic congestion, air pollution emissions from road vehicles and traffic noise problems, this feedback will be getting stronger and needs to be incorporated into the model in the future.' (Gu and Young, 1998, p. 184).

The DELTA integrated land use/transport model incorporates environmental indicators such as noise and air pollutants based on outputs of the transport model (Simmonds, 1999, 2010). In this model, the indicators have either been calculated as zonal values per indicator or as a single traffic-density measure as a proxy for environmental impacts. The authors recognize that meaningful zonal values might be problematic and that 'some effects such as noise are highly localized and hence difficult to represent except in models representing individual properties' (Feldman and Simmonds, 2007, Transport-DELTA interfaces and accessibility calculations section). In the DELTA model, the environmental impact on relocation is represented by an environmental quality variable which consists of multiple components, including noise and pollutants. The weight of the impact is

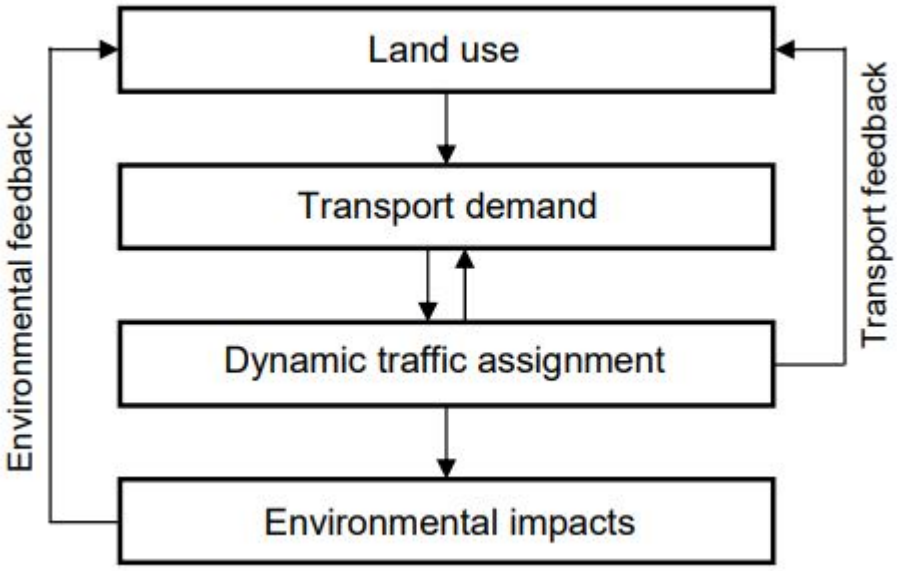

Figure 2.7: Feedback in LTE models (taken from Moeckel et al. (2003)).

based on willingness-to-pay values for a reduction in these environmental stressors. As such, environmental disutility is expressed in monetary terms.

Another example of an LTE model is the ILUMASS (Integrated Land-Use Modelling and Transportation System Simulation) project which aimed at microscopically linking transport and land-use models. It was also intended to feed back environmental impacts to the land-use model (Beckmann et al., 2007). The study area Dortmund was divided into 352,000 grid cells of 100x100 m size to be able to generate meaningful emission values. However, due to the complexity of the project, very long model run times and a file-based data transfer, the ambitious goals were not met (Wagner and Wegener, 2012). While the environmental sub-module was working for a small test scenario, it never became operational for the entire integrated model.

There were no studies found for other contemporary ILUT models such as ILUTE, PECAS or UrbanSim that present a linkage between environment and land-use/transport.

As pointed out by multiple studies above, a fine spatial resolution is key to obtain reasonable sensitivities to local decision factors such as travel times, accessibility or noise. Many models use zone systems to keep computational costs low at the cost of spatial aggregation.

The problem of spatial aggregation has been widely discussed and is referred to as the Modifiable Areal Unit Problem (MAUP) as described by Openshaw (1977), which

states that results of spatial analyses are influenced by the chosen zone size (scale effect) and the criteria used to form spatial units (aggregation effect) (Viegas et al., 2009). While the aggregation effect is reported to be hardly solvable (Fotheringham and Wong, 1991), Openshaw (1984) proposes four ways of dealing with the scale effect: ignore it, use individual data, use an 'appropriate' scale or use spatial units that the results produce a predicted outcome. According to Stępniak and Jacobs-Crisioni (2017), methods to reduce the MAUP have been proposed for location-allocation problems. However, the problem has not yet been resolved in spatial interaction models (such as in ILUT models). They present an approach that uses interaction-weighted travel times based on population density to reduce errors in aggregated zone-to-zone travel times. The impact of MAUP on spatial interaction models, which was also analyzed by Putman and Chung (1989) and Zhang and Zhou (2018), does not exist if individual (=non-aggregated) data are used (Fotheringham, 1989).

While the problem of spatial biases is well known, 'the effects of spatial biases on LUTI models remain largely unexplored and underestimated' (Thomas et al., 2015, p. 55). In a review of existing ILUT studies, Badoe and Miller (2000) identified several studies that 'have worked with zonal-aggregate variables for gross spatial units [...] thus clouding the effects [...]' (Badoe and Miller, 2000, p. 260). The MAUP affects the true representation of spatial attributes such as travel times (Homer and Murray, 2002). Rosenbaum and Koenig (1997) report that zone-based land-use models may be limited in their ability to assess policies that aim at influencing development at small spatial scales, such as areas near a transit stop. Jones (2016) presented sensitivity analyses for spatial biases in ILUT models caused by the *spatial resolution* (i.e. size, number and shape of areal units/zones) and the *spatial extent* (i.e. size and boundaries of the study area) of the model input. Results indicate that both resolution and extent significantly impact model outputs. New scenarios that address equity issues, pricing scenarios and environmental impacts may require more detail, as 'for such scenarios, the traditional feedback from land use to transport with aggregate accessibilities may not be sufficient' (Moeckel et al., 2018, p. 466).

Integrated models that aim to represent environmental feedback should therefore work with a detailed spatial representation. Preferably, the representation should be detailed for *all* locational attributes. Otherwise, it is hard to argue that a locational factor such as noise is modeled at a very microscopic scale while other (even more important) influential factors such as travel times are only coarsely represented.

2.4 New Mobility Concepts in the Context of Traffic Noise Modeling

2.4.1 Ridepooling

Recently, agent-based simulations have been extended and employed to analyze emerging mobility options such as demand-responsive transportation, including ride-hailing and -pooling. There have been multiple simulation studies in the field of (pooled) Autonomous Mobility on-Demand (AMoD), often also described as Shared autonomous Vehicles (SaV) applications. In the real world, several app-based dynamic ride-pooling services such as UberPool [1], GrabShare [2], Clevershuttle [3] or MOIA [4] were introduced in recent years and promise to reduce traffic volumes and resources consumed in urban areas, as several car trips can be bundled and replaced by a single pooled trip.

Previous studies have shown the potential of pooled on-demand mobility to reduce traffic and vehicle fleets in urban areas (Martinez and Viegas, 2017; Alonso-Mora et al., 2017) and suggested that ride-pooling can significantly reduce air pollutants and Greenhouse Gas Emissions (GHG) (Greenblatt and Saxena, 2015). However, the positive effects are not only achieved through the introduction of these new services but must be accompanied by urban policies that make car travel less attractive and prevent a modal shift away from public transport (Naumov et al., 2020).

Pernestål and Kristoffersson (2019) and Jing et al. (2020) reviewed 26 and 44 simulation studies that investigate the effects of autonomous vehicles, respectively. While each study has a slightly different focus, most focus on driverless taxi applications in urban areas without pooling passengers. Results indicate that the introduction of unpooled fleets causes an increase in Vehicle Kilometers Traveled (VKT) between 5 % and 35 % compared to the existing system, mainly due to empty kilometers to pick up customers and to reallocate vehicles. At the same time, it is stated by Pernestål and Kristoffersson (2019) that in most studies, one autonomous vehicle replaces between 6 and 14 conventional cars. If rides are pooled, system efficiency generally increases and VKT can be reduced if penetration rate and request density are large enough.

Out of the 44 agent-based simulation studies of autonomous vehicles that Jing et al. (2020) reviewed, almost half (20) made use of the simulation framework MATSim (Horni et al., 2016). However, there have been extensive investigations in other frameworks that need to be considered. Martinez and Viegas (2017) replaced all private car, bus and taxi trips in Lisbon (approximately 565,000 inhabitants) with a ride-pooling fleet, serving all requests with a maximum time loss of 15 minutes. They found an overall VKT reduction of 25 %, a CO_2 reduction of 32 % and that only 4.8 % of the city's current car fleet size

[1] https://www.uber.com/de/de/ride/uberpool/
[2] https://www.grab.com/sg/transport/share/
[3] https://www.clevershuttle.de/
[4] https://www.moia.io/

is necessary to serve the demand.

Alonso-Mora et al. (2017) introduced an anytime optimal ride-pooling algorithm and served all taxi rides (up to 460,700 daily) in Manhattan with a pooled fleet. They found that the vehicle fleet may be drastically reduced from 13,000 single-occupied vehicles to only 3,000 vehicles with a capacity of 4. Service levels are kept at a reasonable level with an average waiting time of fewer than 3 minutes and an average trip delay of 3.5 minutes. Engelhardt et al. (2019) based their investigation of a ride-pooling service on the same algorithm and replaced between 1 % and 15 % of all car trips in Munich. Their results show that with adoption rates below 5 %, total VKT increase, whereas higher adoption rates lead to decreased VKT due to pooling. Vehicle flow volumes were mainly reduced on major roads.

Ruch et al. (2020) implemented four previously developed ride-pooling policies (Alonso-Mora et al., 2017; Ma et al., 2013; Fagnant and Kockelman, 2018; Bischoff and Maciejewski, 2016) in the framework AMoDeus (Ruch et al., 2018) that is based on the mobility simulation of MATSim. They applied those four algorithms to an urban scenario with 16,400 requests and a rural scenario with 1,000 requests. Although VKT and fleet sizes can be decreased through pooling compared to an un-pooled system, the efficiency gain may not be sufficient to compensate for privacy loss and decreased service levels to attract customers. Pernestål and Kristoffersson (2019) draw the same conclusion from their reviewed papers and propose incentives or public policies to achieve a higher penetration rate of pooled service to accomplish major VKT reductions through on-demand mobility systems.

Bischoff et al. (2017) introduced another ride-pooling extension within MATSim called Demand Responsive Transit (DRT). They applied a ride-pooling fleet to 27,336 taxi requests that occurred on one day in Berlin. It is shown that VKT could be reduced by 15 % to 20 % compared to the existing taxi system if rides were pooled while average waiting times are below 5 minutes. High pooling rates occur in the city center and in the area of the airport where request density is highest.
The DRT extension is used in numerous simulation studies (Wang et al., 2018; Vosooghi et al., 2019; Bischoff et al., 2018; Bischoff and Maciejewski, 2020; Leich and Bischoff, 2019).

In contrast to air pollutants and GHG, much less focus has been put on the impact of ride-pooling and shared mobility on traffic noise. Kaddoura et al. (2020) analyzed noise impacts in the context of an un-pooled autonomous taxi fleet and find decreasing levels of air pollution and slightly increasing noise levels in the inner-city area of Berlin. However, the impacts of a **pooled** system on traffic noise have not yet been investigated systematically. As one of the few studies that look at noise in conjunction with ride-pooling, Bistaffa et al. (2021) include noise (costs) as a component in their analysis of environmental benefits of ride-sharing services but do not report detailed results for impacts on noise emissions or immissions. In addition, noise is only based on differences in

travel distances and does not account for actual traffic and the individual time-dependent exposure.

As it has been shown that interventions implemented to reduce noise exposure can be linked to positive health outcomes (Brown and Van Kamp, 2017), it is important to study potential noise reductions of policies such as the implementation of ride-pooling services. The implications that the introduction of a new mobility system has on an existing mobility system are versatile and complex. While car traffic noise depends on the traffic flow volume, the relationship is non-linear and follows a logarithmic curve. In addition, resulting noise immissions depend on vehicle speeds, road geometries and the built environment, among others. Therefore, one cannot infer noise impacts by looking at changes in VKT and traffic volumes alone, which is why the impact of ride-pooling on noise has to be studied explicitly.

2.4.2 Electric Vehicles and Noise

Another reduction could be expected from fleets of fully Electric Vehicles (EV) when compared to Internal Combustion Engine Vehicles (ICEV). This has also been identified as one of the possible extensions to the initial noise model presented by Kaddoura (2019). However, for constant driving speeds above 30 km/h, the main contribution to car traffic noise emerges from the tires rolling on the surface (also compare with figure 2.1), which reduces the potential of reducing noise with EVs (Bekke et al., 2013). Similarly, the European Environmental Agency states that while electric cars contribute to lower noise levels at low speeds, a recent regulation will require the installation of artificial sound generators in all electric and hybrid vehicles by 2021 to improve pedestrian safety, which may further reduce potential reductions in noise (European Environment Agency, 2018). In a recent study, (Campello-Vicente et al., 2017) showed that EVs equipped with an acoustic vehicle alerting system still emit lower levels of noise than conventional ICEV (1 dB(A) less at 30 km/h, compared to EVs without alerting system: 2 dB(A)). The reductions diminish for higher shares of heavy vehicles and lower shares of EVs in the fleet. In the same study, the authors adapted the official French noise prediction model to correct emission values for electric fleets. In a simulation case study, they showed that replacing ICEV with EVs leads to an improvement for 6 % to 10 % of the population in terms of noise exposure.

In a state-of-the-art survey by (Iversen et al., 2013), the authors presented an overview of studies dealing with possible noise reduction due to EVs. They reported mixed findings, with reductions ranging between 1 and 15 dB(A) at different speeds. Most references indicate that the difference in noise levels vanishes between 30 and 50 km/h. They stressed that these results include a high level of uncertainty and depend on how the comparisons were carried out in detail. Jabben et al. (2012) presented a comparison of noise measurements between ICEV and EV in a drive-by scenario and reported reductions between 11 dB(A) at very low speeds and 3 dB(A) at 50 km/h. The same authors

implemented a noise prediction model with correction terms for fully electric fleets (Verheijen and Jabben, 2010). The presented correction terms can be distinguished by vehicle types and respective speeds. In an application, they found reductions of 3 to 4 dB(A) in noise exposure, on average. Similarly, (Estévez-Mauriz and Forssén, 2018) report a mean reduction of 4.5 dB(A) for an all-electric scenario compared to internal combustion engine vehicles in a simulation study on the noise level at intersections.

2.5 Research Questions and Structure of the Thesis

Based on the literature review and starting from the work of Kaddoura et al. (2017), multiple research questions have been defined to study new applications of traffic noise modeling in agent-based simulations.

The initial noise model by Kaddoura et al. (2017) points to future improvements regarding the implementation of shielding, reflection and corrections for EV. Meanwhile, the underlying official guideline RLS-90 has been updated to the RLS-19. Therefore, as a first step, the existing noise model will be presented, analyzed and then updated to the latest guideline. In addition, correction terms missing in the initial implementation of the RLS-90 as well as a correction term for EV will be implemented. As the correction for shielding was identified to be one of the most important missing terms, the shielding correction is presented in more detail. In addition, the following research questions will be addressed:

1. How high is the impact of neglecting shielding corrections in noise modeling in dense urban environments?

2. Does the broad usage of EV lead to considerably lower noise immissions?

Building upon the updated noise model, this thesis concentrates on three basic use cases of agent-based simulations. First, the gap in the literature identified in section 2.3, which is to incorporate environmental impacts in ILUT models, will be addressed for the example of road traffic noise. Hereby, with a focus on traffic noise, an approach similar to the study by Löchl and Axhausen (2010) will be applied. They present a hedonic pricing study that compared ordinary regression against spatial modeling techniques to estimate rent prices in Zurich with the aim of building a model for the UrbanSim ILUT modeling framework. Consequently, this part of the thesis is split into two subsequent parts that deal with the following questions:

3. Can simulated noise values coming out of an agent-based transport model explain price variations of rent prices in observed data? If yes, how high is the estimated impact?

4. Does the inclusion of model reactions to noise in agent-based ILUT models lead to different outcomes in relocation patterns of households? How high is the impact?

The subsequent use case presents how an agent-based model can be used to analyze environmental equity issues at a more detailed level by tracing back exposure and causation to individuals. The application looks at two questions:

5. Is the causation of noise more unequally distributed than the exposure thereof?
6. Is there a spatial pattern of noise contributors when looking at a larger metropolitan area?

Lastly, the third use case uses recent capabilities of agent-based models to simulate ride-pooling to analyze potential impacts in potential large-scale scenarios. As such, this use case addresses the following questions:

7. Does a large-scale implementation of a ride-pooling service in a large city lead to reduced noise immissions among residents?
8. How do penetration rate and service design influence potential changes in noise immissions?

Based on these questions, the thesis is structured as follows:

- Chapter 3 presents the agent-based modeling framework, which will be used throughout this thesis.
- Chapter 4 describes the two study areas in which the use cases will be carried out.
- Chapter 5 shows the implementation of the updates to the noise model prior to the application of the following use cases. This chapter addresses question 1.
- Chapter 6 estimates noise impacts on rent prices of observed data. As such, it deals with question 3.
- Chapter 7 builds upon chapter 6 and implements noise as a feedback to the existing ILUT model with the goal of answering question 4.
- Chapter 8 analyzes environmental equity issues of traffic noise in a spatial context and targets research questions 5 and 6.
- Chapter 9 answers questions 2, 7 and 8 by presenting the results of large-scale (electric) ride-pooling scenarios and their impacts on traffic noise.
- Chapter 10 concludes the thesis and points to limitations and future work.

Figure 2.8 shows the structure of the main chapters of the thesis.

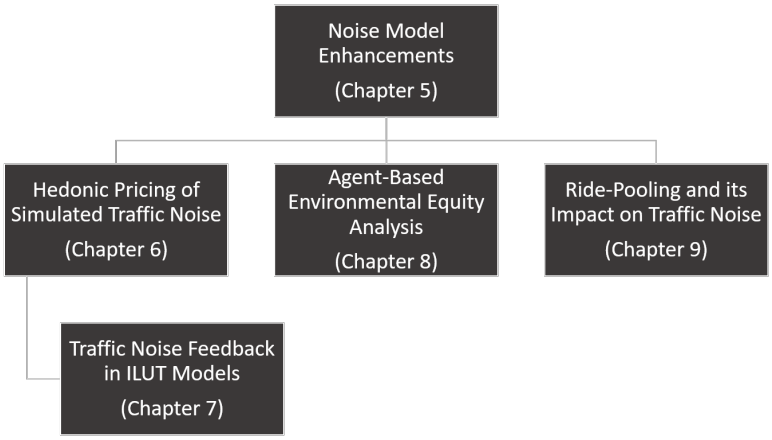

Figure 2.8: Structure and chapters of the scenarios presented in this thesis.

3 The FABILUT Modeling Suite

The Flexible, Agent-Based Integrated Land Use/Transport (FABILUT) modeling suite consists of the Simple, Integrated Land use Orchestrator (SILO)[1] (Moeckel, 2016) and the transport simulation model MATSim[2] (Horni et al., 2016). For travel demand generation, the Microscopic Transportation Orchestrator (MITO)[3] (Moeckel et al., 2020) is used in this study. All three models are open source and written in Java, which allows for a tight integration without the need for file-based communication. The FABILUT modeling suite can also be run with SILO and MATSim only, which e.g. allows simulating the commute segment of traffic (Ziemke et al., 2016).

The three main components used in this thesis will be presented in the following sections.

3.1 SILO

SILO is a zone-based microscopic land-use model currently developed at the Technical University of Munich. SILO models long- and short-term decisions based on a synthetic population over multiple years in a one-year time-step resolution. The population consists of households and their members. Each household lives in a synthesized dwelling and persons can take individual jobs. The spatial level of resolution of dwellings and jobs are either zones or microscopic coordinates, depending on implementation. Spatial decisions like relocation and dwelling development are modeled with Logit models (Domencich and McFadden, 1975). Markov models with applied transition probabilities simulate other decisions like marriage, dwelling renovation and giving birth (Moeckel, 2016). Currently, demographic changes, household relocation and real estate changes are covered within SILO. The model has been successfully implemented and integrated for Maryland and Austin (USA), Munich (Germany), Kagawa (Japan) and Bangkok (Thailand). SILO can optionally run with a transport model to update travel times and, thus, accessibilities, which in turn influence location choices. The model incrementally updates an initial synthetic population in which each dwelling, household, person and job is represented individually. The typical process of generating a synthetic population for SILO is described in Moreno and Moeckel (2018).

[1] https://github.com/msmobility/silo
[2] https://github.com/matsim-org/matsim-libs/
[3] https://github.com/msmobility/mito

3.2 MITO

MITO is a microscopic travel demand model which can be defined as a hybrid between classical trip-based models and activity-based models. It overcomes some of the former and is less complex than the latter (Moeckel et al., 2020). Similar to SILO, MITO takes a microscopic synthetic population of households, persons, jobs and dwellings as an input and generates disaggregated trips for each household/person. Most of the model has been estimated with the help of the German travel survey MiD (Mobilität in Deutschland, eng.: mobility in Germany, (Infas and DLR, 2010)). In the default setup, MITO distinguishes between the purposes home-based work (HBW), home-based education (HBE), home-based shopping (HBS), home-based other (HBO), non-home-based work (NHBW) and non-home-based other (NHBO). Home-based means that a trip starts and ends at the home location of a person's household, i.e. it resembles a round-trip. Non-home-based trips start or end at work locations (NHBW) or any other destination that is not the home of the trip maker (NHBO). The result of MITO is a set of microscopic trips for each person in the synthetic population with an assigned purpose, destination, mode and time of day. However, since MITO is not a full activity-based model, the trips are independent of each other and do not represent a person's full activity schedule. In fact, each of the trips is assigned with a separate agent in the assignment.

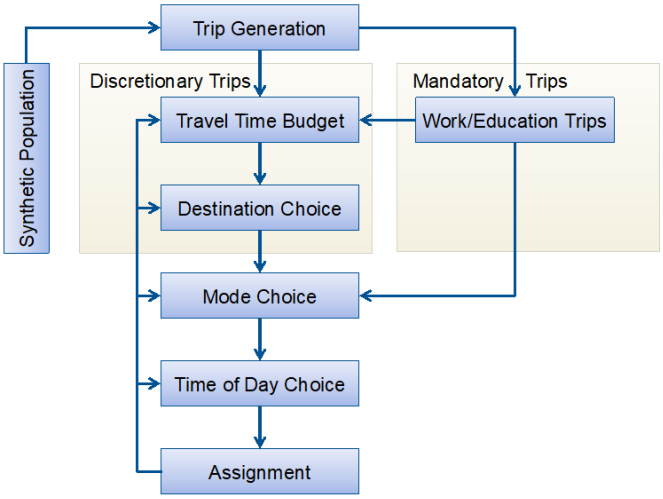

Figure 3.1: Overview of the MITO model.

MITO is defined by the following subsequent steps (see also figure 3.1):

1. Trip Generation. In the trip generation step, MITO classifies the synthetic households into pre-defined types and copies trips from similar households in the travel time survey diary.

2. Travel Time Budget Calculation. MITO follows the notion of constant travel time budgets as described by Zahavi (1974). The idea is that, on average, the time spent

traveling remains rather constant throughout the years. In MITO, travel time budgets are calculated for each household to influence destination choice (Moreno and Moeckel, 2016).

3. Destination Choice. Destinations are chosen as microscopic x/y coordinates. For work and education trips, the locations are pre-defined in the synthetic population. For the remaining purposes, MITO uses a random utility model to choose from a set of given locations. The utilities take into account purpose-dependent zonal attraction and travel times and are also influenced by the calculated travel time budgets.

4. Mode Choice. Mode choice is processed with the help of a nested multinomial logit model that can be estimated with travel survey data. By default, MITO distinguishes between seven modes (auto driver, auto passenger, bicycle, bus, train, tram/metro and walk). The existing model used in this thesis is shown in figure 3.2 and is described in more detail in Rayaprolu et al. (2018).

5. Time of Day Choice. The time of day choice is based on reported arrival times in the travel survey. Probability distributions have been derived for each purpose. For each trip, the time of day is randomly chosen from those distributions.

6. Assignment. MITO produces a list of individual trips with all the chosen characteristics such as mode, destination and time of day. In theory, MITO can be coupled with any dynamic traffic assignment model to simulate traffic. By default, MATSim is used to serve this purpose whereby each MITO trip is converted into a separate MATSim agent.

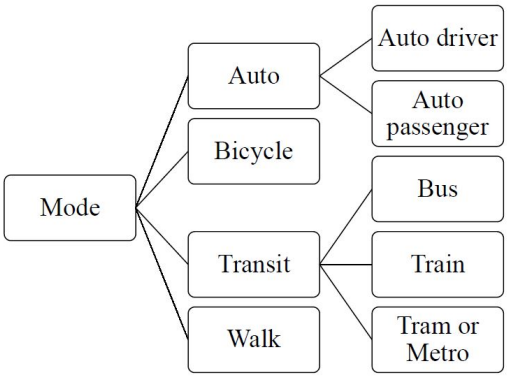

Figure 3.2: Nested Structure of the Mode Choice Model

3.3 MATSim

MATSim (Horni et al., 2016) is a microscopic, agent-based framework for transport simulation and analysis. In contrast to aggregated trip-based approaches, travel demand in MATSim is derived from activities that agents perform throughout their simulated day. To obtain a state of equilibrium, MATSim utilizes a co-evolutionary approach in which each agent tries to maximize their score (i.e. utility) individually by adapting to current transport situations. Agents increase their plan's score when spending time on scheduled activities. Time spent traveling or waiting leads to negative scores. MATSim uses an iterative approach that is shown in figure 3.3 and is further explained in the following subsections.

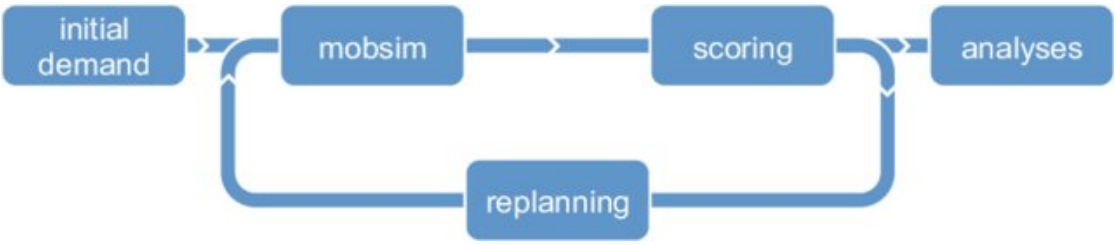

Figure 3.3: Overview of the MATSim cycle. Taken from (Horni et al., 2016).

3.3.1 Initial Demand

MATSim requires initial demand as an input to the simulation. Demand is treated as a set of individual agents, including their scheduled activities throughout the day, so-called plans. Typically, the demand has to be created prior to the simulation for which various solutions exist. As a minimum, every agent should have one plan that includes durations and locations of activities.

3.3.2 Assignment

In the assignment step, every agent carries out its currently selected plan and the resulting demand is loaded onto the network. For explicitly simulated modes, MATSim uses a queue-based traffic flow simulation by default. Links are represented as point-queues with a spatial limit, meaning that the simulation keeps track of the number of vehicles currently waiting on a link and limits the resulting amount according to the capacity of the respective link. If the storage capacity is exceeded, congestion spill-backs can be observed for upstream links. The queue-based approach allows to efficiently simulate a large number of agents in reasonable computation times. However, detailed intersection logic or car-following behavior cannot be captured.

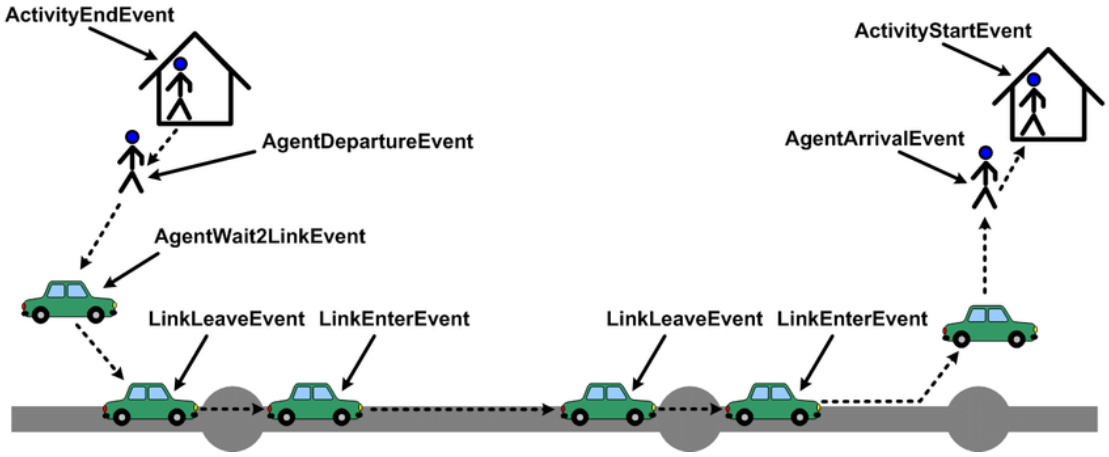

Figure 3.4: The standard MATSim events. Taken from (Horni et al., 2016).

3.3.3 Scoring

After each iteration, agents score their executed plan. Thereby agents receive positive scores for performing activities and negative scores for time spent traveling or coming late to an activity. Score accumulation usually follows a logarithmic pattern with diminishing marginal score increases as the actual performed time approaches the usual time spent for the type of activity. MATSim assumes that the simulation captures a whole 24 hour day and requires that the first and last activity are the same for proper scoring (usually 'being at home'). Through this 'wrap-around' assumption, MATSim introduces as an implicit utility of travel time savings as the limited time available can be spent on more activity performing instead of traveling. If an agent travels less, it does not only reduce the negative penalty in scores for traveling; it also is able to spend more time performing an activity such as being at work which additionally increases the score.

3.3.4 Re-Planning

At the end of each iteration, a certain share of agents is allowed to re-plan or re-schedule their daily activities. MATSim offers multiple individual strategies to allow agents to adapt. Among others, these include re-routing according to the latest traffic conditions, changing the mode of (sub-)trips or changing the departure time. The remaining agents choose from existing plans such that the plans that reached the highest score are the most likely to be chosen in the next iteration. Through this iterative approach and adaptation, the simulation usually converges towards a stochastic user equilibrium in which agents cannot improve their plan by unilaterally changing it.

3.3.5 Analysis

At the end of a MATSim simulation, a detailed analysis can be carried out since all the important steps are written out in an events file that contains detailed information on

the time, place and agent of e.g. a vehicle entering or leaving a link. The standard MATSim events are shown in figure 3.4. Apart from travel and delay times, this also allows imputing additional information, such as air pollutants or noise emissions (see also 3.4).

3.4 Noise Extension

The noise extension of MATSim has been described by (Kaddoura et al., 2017). The extension allows computing noise emissions, immissions and resulting damages at a fine spatial and temporal resolution. Based on the events thrown during a MATSim simulation, the analysis can be carried out online (during the simulation, registered to 'listen' to events) or offline (after the simulation, using the output events file). The approach is based on the German guideline for noise protection at streets (FGSV, 1990) and uses a set of assumptions for simplifications. The essential steps of MATSim's noise analysis are described in the following subsections.

3.4.1 Noise Emissions

First, emission levels per link have to be calculated, which are mainly driven by the traffic volumes in the simulation. Resulting average emission levels $L_{j,t}$ in dB(A) are calculated per link j and time bin t using the following general formula:

$$L_{j,t} = L^{25}_{j,t} + D^{v}_{j}, \tag{3.1}$$

where $L^{25}_{j,t}$ is the average noise emission level in dB(A) for a set of assumptions: a fixed distance of 25 meters from the emitter, a height of 2.25 meters, a maximum speed level of 100 km/h on a smooth asphalt road surface and a gradient of less than 5%. This level is an hourly equivalent noise level as defined in 2.4. It is calculated as:

$$L^{25}_{j,t} = 37.3 + 10 \cdot \log_{10} \left[M_{j,t} \cdot (1 + 0.082 \cdot p_{j,t}) \right] \ , \tag{3.2}$$

where $M_{j,t}$ is the traffic volume; $p_{j,t}$ is the HGV (heavy goods vehicle) share in %. D^{v}_{j} is the speed correction term which is

$$D^{v}_{j} = L^{car}_{j} - 37.3 + 10 \cdot \log_{10} \left[\frac{100 + (10^{0.1 \cdot (L^{hgv}_{j} - L^{car}_{j})} - 1) \cdot p_{j,t}}{100 + 8.23 \cdot p_{j,t}} \right] \ , \tag{3.3}$$

with

$$L^{car}_{j} = 27.7 + 10 \cdot \log_{10} \left[1 + \left(0.02 \cdot v^{car}_{j} \right)^{3} \right] \tag{3.4}$$

$$L^{hgv}_{j} = 23.1 + 12.5 \cdot \log_{10} \left(v^{hgv}_{j} \right) \ , \tag{3.5}$$

where v^{car}_{j} denotes the maximum speed level for passenger cars in kilometers per hour; and v^{hgv}_{j} denotes the maximum speed for HGV in kilometers per hour. Further road-

related correction terms provided by the RLS-90 (FGSV, 1990) are neglected. Time bins can be defined arbitrarily but are usually set to 1 hour intervals. This allows MATSim to show the course of noise emissions throughout time. Corrections for road surface and gradients as well as reflections are ignored to keep computation and input requirements low.

3.4.2 Noise Immissions

Immission values are calculated for defined receiver points, which can be represented by a spatial grid or at other predefined coordinates such as activity locations. The immission at receiver point i per time bin t is obtained by logarithmic addition of emissions of nearby links:

$$L_{eq,i,t} = 10 \cdot \log_{10} \sum_{j} 10^{0.1 \cdot L_{i,j,t}} \quad \{L_{i,j,t} > 0\} \ , \tag{3.6}$$

$$L_{i,j,t} = L_{j,t} + D^{d}_{i,j} + D^{\alpha}_{i,j} - D^{z}_{i,j} \ , \tag{3.7}$$

where $L_{eq,i,t}$ is the total energy equivalent continuous sound immission level in dB(A) and $L_{i,j,t}$ is the immission resulting from a single road j, which is based on the emission $L_{j,t}$ as defined in 3.1. In addition, the following correction terms are defined. The correction term $D^{d}_{i,j}$ follows the RLS-90 approach for 'long, straight lanes' and is defined as

$$D^{d}_{i,j} = 15.8 - 10 \cdot \log_{10}(d_{i,j}) - 0.0142 \cdot d^{0.9}_{i,j} \ , \tag{3.8}$$

where $d_{i,j}$ is the shortest distance between the road segment j and the receiver point i in meters (minimally 5 meters). $D^{\alpha}_{i,j}$ is an angle correction which is not included in the RLS-90 but comes from the Nordic prediction method (Nielsen, 1997). It was included to account for different link lengths albeit using the 'long, straight lane approach'. It is defined as

$$D^{\alpha}_{i,j} = 10 \cdot \log_{10}\left(\frac{\alpha}{180}\right) \ , \tag{3.9}$$

where α is the angle from receiver point i to road segment j in degrees. $D^{z}_{i,j}$ is the correction term which accounts for the effect of shielding that is implemented as part of this dissertation (see chapter. 5). Besides the correction for shielding effects, other correction terms such as the correction for reflections or road gradients are also not included in the initial MATSim extension.

3.4.3 Noise Exposure and Damages

Noise damages can be calculated to estimate the economic impact of traffic noise and as a key indicator to identify actual exposure (as immission is worse the more people are actually affected). To do that, activity locations of agents are mapped to the closest receiver point. Then, a measure of exposed agents per time bin t can be defined as

$$N_{j,t} = \sum_{n} \frac{a_{n,j,t}}{T} \tag{3.10}$$

here, $N_{i,t}$ is the number of demand units exposed to noise at receiver point i in time interval t. n is an individual agent performing a considered activity of duration $a_{n,i,t}$ and T is the time bin size. Noise damage costs and monetarization approaches were defined in the German Empfehlungen für Wirtschaftlichkeitsuntersuchungen an Straßen (Forschungsgesellschaft für Straßen- und Verkehrswesen, 1997, EWS, engl.: Recommendations for profitability analyses near roads,). Following that, noise costs emerge at receiver points whose immission values exceed defined thresholds:

$$C_{i,t} = \begin{cases} c^T \cdot N_{i,t} \cdot 2^{0.1 \cdot (L_{eq,i,t} - L_t^{min})}, & L_{eq,i,t} \geq L_t^{min} \\ 0, & L_{i,t} < L_t^{min} \end{cases} \tag{3.11}$$

The resulting damage $C_{i,t}$ for each receiver point i in time interval t takes into account a monetary cost rate c^T in monetary units per dB(A) for each demand unit that is exposed for the duration of T and L_t^{min} is the threshold immission level which depends on the time of day. If not stated otherwise, the following thresholds are used for the remainder of this work (taken from Kaddoura et al. (2017)): 50 dB(A) during the day (6 a.m. to 6 p.m.); 45 dB(A) during the evening (6 p.m. to 10 p.m.) and 40 dB(A) during the night time (10 p.m. to 6. a.m.). The monetary cost rate c^T is derived by multiplying the annual cost rate c^{annual} with the time bin size T (in hours):

$$c^T = c^{annual} \cdot \frac{T}{(365 * 24)} \tag{3.12}$$

Again, the value for the annual cost rate is taken from (Kaddoura et al., 2017), which is based on the EWS and translated to an equivalent rate for 2015: $c^{annual} = 63.3\ EUR$.

3.5 Demand-Responsive Transit Extension

For research questions 7 and 8, a ride-pooling scenario will be implemented to assess noise implications of shared large-scale on-demand mobility systems. Several extensions exist in MATSim to simulate on-demand mobility systems (Maciejewski, 2016). Hörl (2017) developed an extension to simulate (pooled) autonomous taxis, which was further extended by Ruch et al. (2018, 2020) with different operational strategies and algorithms to operate (pooled) autonomous on-demand systems. The DRT extension developed by Bischoff et al. (2017) will be used in this thesis. Agents in MATSim can submit requests for rides served by a fleet of taxi agents. When a trip request with pick-up and drop-off coordinates is submitted, the algorithm searches for a vehicle that can serve the request within a defined maximum wait time and without exceeding a maximum travel time for the waiting customer and all other customers in the vehicle. The performance of the DRT system highly depends on the service parameters, as shown by Bischoff et al. (2017) and

Zwick and Axhausen (2020b).

Other pooling strategies, such as the one proposed by Alonso-Mora et al. (2017), collect all requests for a certain time frame and dispatch requests and vehicles after a certain time step, taking into account all requests and vehicles. In this way, the system gains more knowledge of all possible assignments, which may increase the efficiency in high-demand scenarios with limited fleet sizes, as shown by Zwick and Axhausen (2020a). The substantially lower computation time combined with a reasonable system performance led to the decision to apply the algorithm by Bischoff et al. (2017). The DRT extension includes a rebalancing strategy that reallocates idle vehicles to areas with a historically high demand (Bischoff and Maciejewski, 2020). Several studies have shown the beneficial effect of the rebalancing strategy on acceptance rates, travel times and wait times with the potential drawback of increased VKT and consequently more noise exposure (Bischoff and Maciejewski, 2020; Vosooghi et al., 2019; Zwick and Axhausen, 2020a). The algorithm allows to operate a door-to-door service, in which all customers are picked up and dropped off at their desired origin and destination. Alternatively, a stop-based system can be used, in which customers need to walk to and from a pre-defined stop before and after the ride-pooling trip. The stop-based ride-pooling system promises to decrease noise, especially in residential areas without stops, as pick-up and drop-off rides in these areas are avoided.

The output of DRT in MATSim allows to assess efficiency and quality of the service, including vehicles distances and rejection rates. For the noise analysis, the vehicles are treated as normal passenger cars that are considered in the total (hourly) traffic volume of a given link.

4 Study Areas and Scenarios

This chapter introduces the study areas and scenarios that will be used in the subsequent chapters. An illustrative scenario will serve as a testbed for the extensions to the existing noise model in MATSim. For most other subsequent use cases, the Munich metropolitan area will be used. An exception is the chapter on environmental equity analysis. For this, the MATSim open Berlin scenario is used.

4.1 Illustrative Scenario

For the noise model analysis and enhancements presented in chapter 5, an illustrative scenario will be used. The scenario is based on a simple network shown in figure 4.1 a), which consists of 7 nodes with multiple bi-directional links. The links are either 'suburban' or 'urban' with different attributes that influence the capacity and the speed of traveling agents. The demand for this scenario is likewise kept simple and consists of 500 agents traveling from node 0 (home) to 7 (work), i.e. from left to right in the morning and back home in the afternoon (see figure 4.1 b)). All agents depart at the same time for each leg. Since the central links have a reduced capacity, there will be some congestion. Ideally, MATSim's iterative approach should lead to a stochastic equilibrium in which roughly one half of agents use the upper and lower route each. The simple setup allows easy analyses for the subsequent extensions.

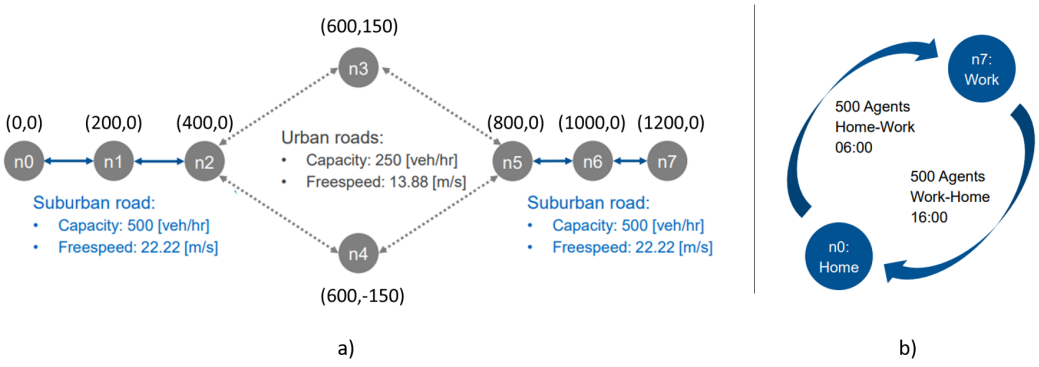

Figure 4.1: a) Network and b) demand of the illustrative scenario.

4.2 The Munich Metropolitan Area

The Munich metropolitan area will be the main study area of this thesis as it has a full implementation of the FABILUT modeling suite, including SILO, MITO and MATSim. Located in its south, Munich is Germany's third-largest city, with a population of 1.56 million (Landeshauptstadt Muenchen, 2020). Munich is surrounded by multiple larger cities for which strong commuting flows and economic interrelationships exist. Taking that into account, the study area delineation (see figure 4.2) has been chosen such that it includes the four major cities Augsburg (blue in figure 4.2, Ingolstadt (yellow), Landshut (green) and Rosenheim (orange) and additionally every municipality for which more than 25% of the population commute to Munich (purple). On the basis of these extents, the study area delineation has been smoothed and - if possible - cut along neighboring county limits. Basing study area delineation on commuter relations has been stressed to be essential to reduce spatial bias (Thomas et al., 2018).

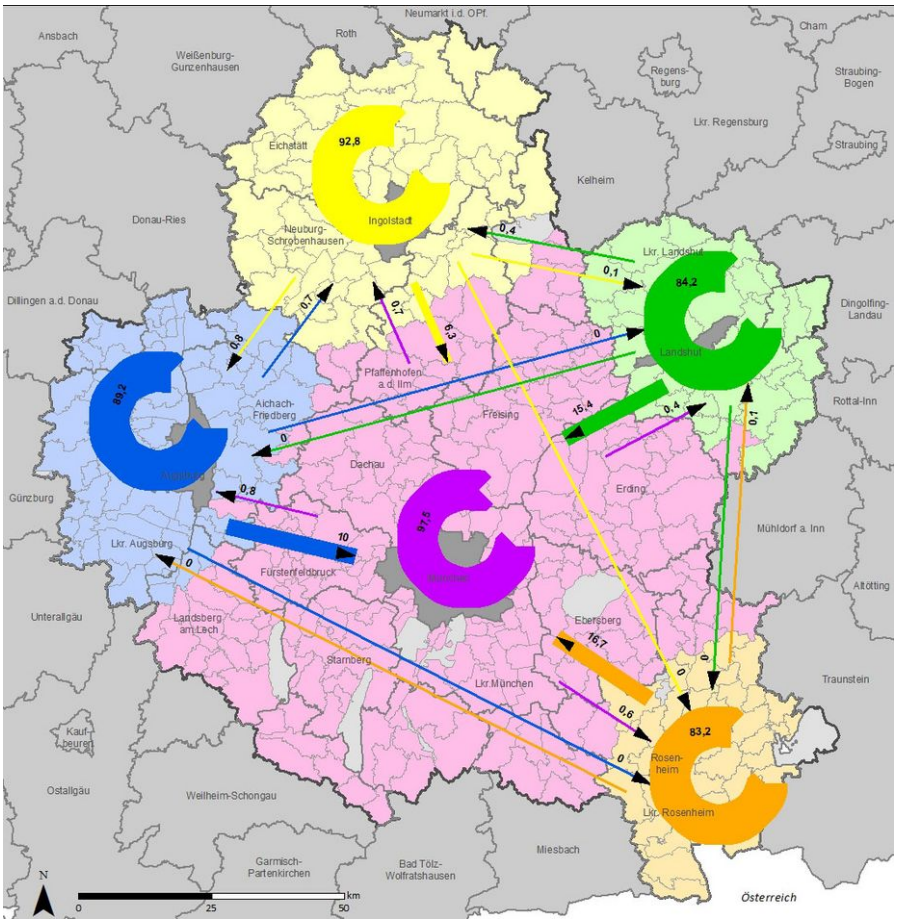

Figure 4.2: Commuting relationships in the Munich metropolitan area

The zone system for SILO and MITO has been created using an automated zoning algorithm described in Molloy and Moeckel (2017). The algorithm iteratively splits cells such that the population contained in each zone is similar and zones are small where the population is dense and large where the population is sparse. In addition, municipal boundaries have been respected to avoid having a separate zone system that does not match with jurisdictions and their available socioeconomic data. In total, the zone system consists of 4,924 zones. The zone system is presented in figure 4.3. It becomes clear that the zone sizes are smallest in the five core cities.

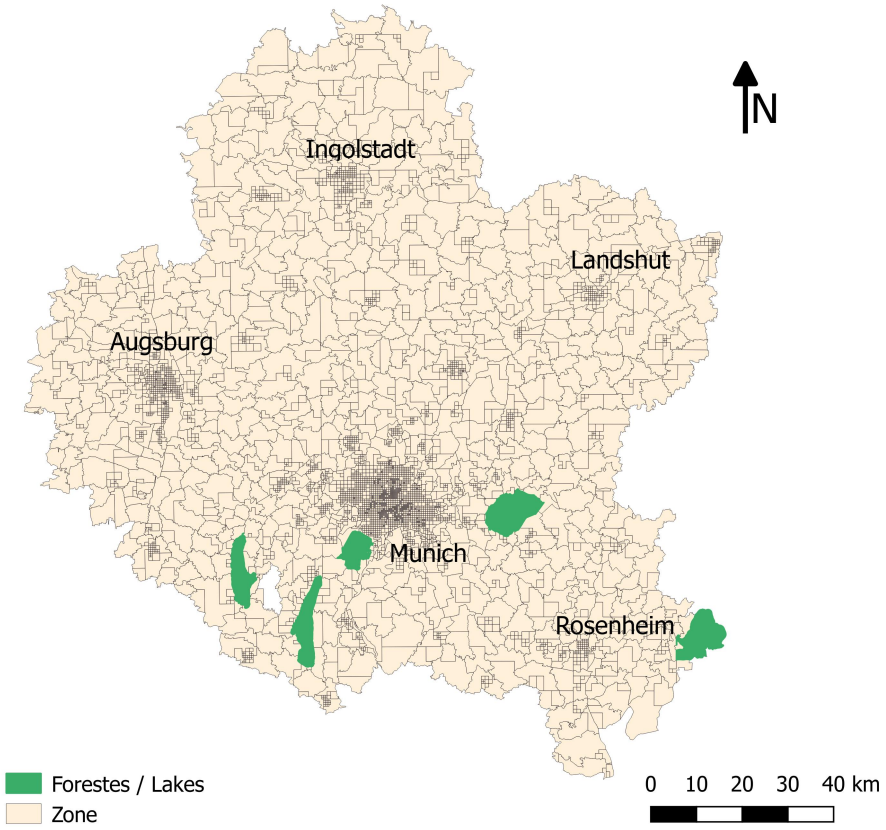

Figure 4.3: Zone system of the Munich metropolitan area.

The synthetic population has been created using an iterative proportional update approach and is presented in Moreno and Moeckel (2018). The reference year is 2011 and includes approximately 4 million persons and jobs and 2.2 million households and dwellings. Control totals at different geographical scales ensured that the synthetic population represents a valid representation of the true population.

The MATSim network for the study was derived from OpenStreetMap (OSM) (OpenStreetMap Contributors, 2018). The network consists of 504,109 links and can be con-

sidered 'dense' as it includes all roads up until the 'residential' classification of OSM[1].

4.3 The Open MATSim Scenario for Berlin and Brandenburg

For the agent-based equity analysis presented in chapter 8, complete daily activity plans of agents are required. As the Munich scenario currently comes with MITO's trip-based demand, the MATSim open Berlin scenario (Ziemke et al., 2019, `https://github.com/matsim-scenarios/matsim-berlin`) will be used for the equity part of the thesis. The scenario covers the two federal states Berlin and Brandenburg and contains full activity chains of agents, which is required to have an accurate estimate of exposure and causation throughout a typical day. The scenario is provided with input and output for a 5% sample (uncalibrated) and a 10% sample calibrated for traffic volumes, modal split and mode-specific trip distance distributions. For the subsequent analysis, the calibrated 10% sample will be used. In addition, a list of links that represent tunnels is provided and can be used for noise estimations.

Figure 4.4 shows Berlin as part of the whole study area, including the network, vehicle locations and distribution of activities of agents.

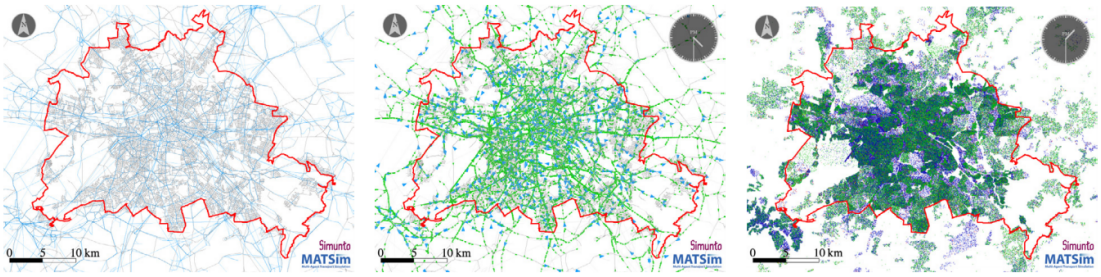

(a) Car network (grey) and public transit network (blue).

(b) Cars (green) and public transit vehicles (blue).

(c) Home (green) and work (blue) activities.

Figure 4.4: The MATSim Open Berlin Scenario: network, vehicles and activity location. Taken from (Ziemke et al., 2019).

[1] `https://wiki.openstreetmap.org/wiki/Key:highway`

5 Noise Model Enhancements in MATSim

The initial MATSim noise extension by Kaddoura et al. (2017) works well for time-dependent and spatial noise analysis on a large scale. However, some intriguing questions made it worthwhile to update and improve the initial extension. First of all, the neglect of shielding effects of larger urban structures (i.e. buildings) can lead to an overestimation of noise in dense urban settings, where large blocks of buildings between streets are common. In the outlook of his thesis, Kaddoura (2019) identified multiple future enhancements for MATSim's noise model:

- Incorporation of noise shielding effects of buildings
- Incorporation of reflection effects at building facades
- The impact of road surface and
- Consideration of different vehicle types (electric vs. combustion engines)

In addition, the simplification of always using the 'long straight lane' instead of dividing links into segments leads to artifacts when dealing with a variety of link lengths. With the release of an updated national noise guideline, the RLS-19, it seemed natural to update MATSim's noise extension as well. Here, the segmentation of links is mandatory and the 'long straight lane' approach was discontinued. Lastly, as discussed earlier, a correction for electric vehicles should be discussed and analyzed.

5.1 Discussion and Limitations of the Current Model

The current implementation of the RLS-90 always uses the 'long straight lane' approach for emission and immission calculation. However, according to the guideline, this is only applicable for links that are visible for at least a minimum length l_z to both sides from the projected closest point on the link. l_z is defined as:

$$l_z = 48 * \frac{s}{\sqrt{100 + s}}, \tag{5.1}$$

where s is the projected closest distance. This means that for a receiver point which is 25 (50) meters away from the road, the road should extend roughly 107 (196) meters to the left and right, not changing any traffic characteristics, not becoming obstructed

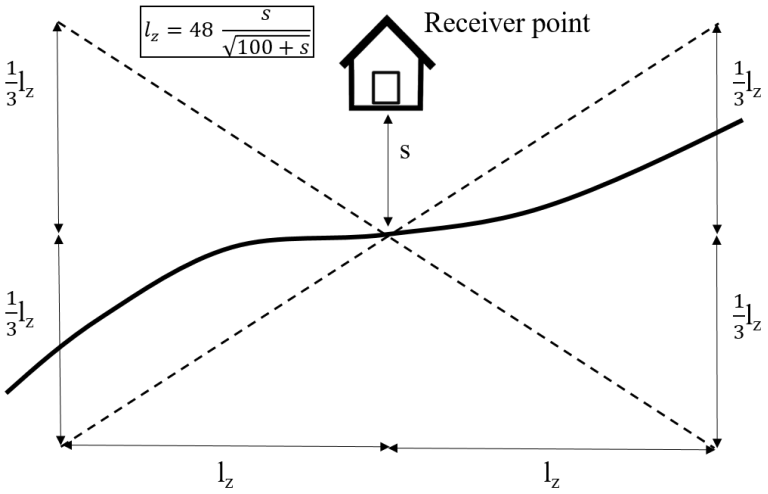

Figure 5.1: Long, straight lane approach of the RLS-90.

by a building and staying almost straight. In addition, the road has to stay inside the area defined by the dashed lines, as shown in figure 5.1. Although these conditions are seldom true for MATSim links in urban settings, the guideline was implemented with this approach only. In dense urban areas, links tend to be relatively short. Applying the 'long, straight lane' approach to links shorter than l_z results in longer links being equally as loud as short links if traffic volume is the same. Thus, the representation of roads as MATSim links would heavily influence estimated noise levels. A MATSim network generated with a higher segmentation of links into many smaller links would lead to higher levels of noise, as each of those small links would equally contribute to the sum of immissions in equation 3.7.

This is why the angle correction $D^{\alpha}_{i,j}$ was introduced. This correction term is not defined in the official RLS-90 guideline and was taken from the Nordic prediction method with questionable compatibility. The angle correction was meant to decrease noise from smaller roads and to reduce the impact on link layout on noise estimation. However, the angle does not only depend of the length on the link but also on the relative position of the receiver point to the link. This leads to the artifact that equation 3.9 goes towards negative infinity for very small angles, which is when receiver points are (almost) perpendicular to the link. This means that standing next to the end of the link would suddenly lead to a large decrease in noise. This issue can be observed in figure 5.2. Here, the noise immission yields unrealistic 'gaps' at the receiver points at the beginning/end of the links on the left and right sides of the network.

Another issue of this solution is that the angle correction also introduces an additional *implicit* distance-dependent correction, even in cases where the 'long straight lane' approach is justified and condition 5.1 holds true. If it is assumed for now that condition

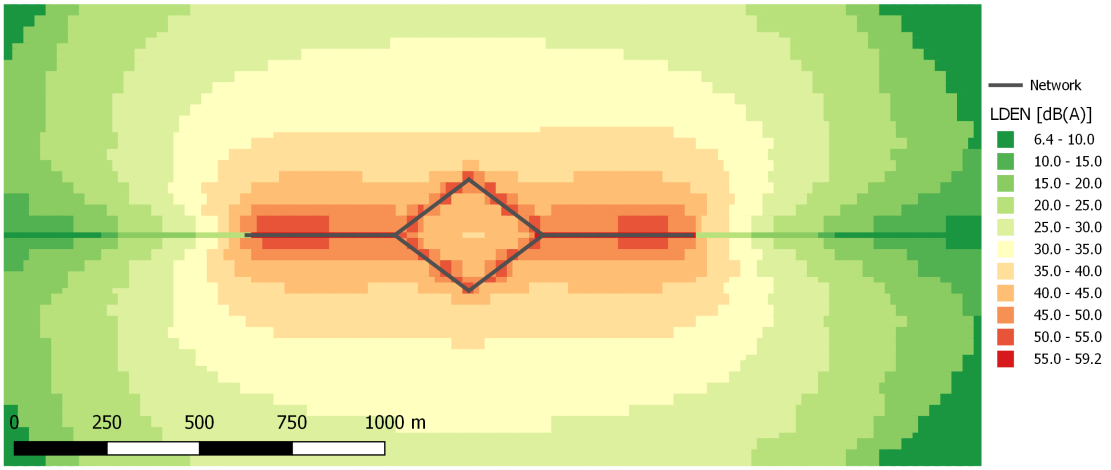

Figure 5.2: Noise immissions in the illustrative scenario with the old RLS-90 implementation.

of equation 5.1 holds exactly true and the link extends exactly l_z to both sides from the projected direct distance to the receiver point. Then one can express the angle α between the link nodes and receiver point as

$$\alpha = 2 \times tan^{-1}(\frac{l_z}{s}) \tag{5.2}$$

$$\alpha = 2 \times tan^{-1}(\frac{48 \times \frac{s}{\sqrt{100+s}}}{s}) \tag{5.3}$$

$$\alpha = 2 \times tan^{-1}(\frac{48}{\sqrt{100+s}}) \tag{5.4}$$

$$\tag{5.5}$$

With that, the angle immission D^{α} in cases where equation 5.1 holds exactly true is dependent on s:

$$D_s^{\alpha} = 10 \cdot \log_{10}\left(\frac{2 \times tan^{-1}(\frac{48}{\sqrt{100+s}})}{180}\right) \tag{5.6}$$

Figure 5.3 shows the resulting correction term in relation to s. In addition, the minimum extended distance l_z is shown. It can be seen that towards a distance s of 500 meters, which is the default maximum radius in which links are taken into account in MATSim, l_z would need to be almost 1000 meters long on either side of the projected nearest distance. In urban settings, it is improbable to have links with a length of two kilometers. Nevertheless, even in cases where the condition is met, the introduced angle correction imposes an additional *distance-dependent* correction of up to about 1.6 dB(A), regardless of the actual link length for which it originally was introduced for.

This and the fact that the angle correction was not designed to work with the RLS-90 makes its application questionable. A solution to this would be to rely on the 'segmented

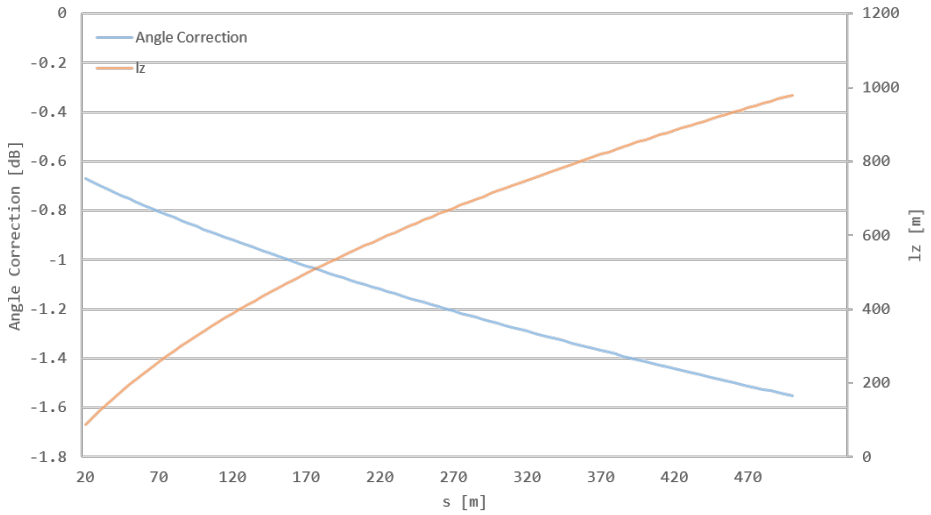

Figure 5.3: Implicit correction term introduced by the angle correction.

link' approach defined in the RLS-90. Here, links would be segmented into sublinks and the length of the actual segment would have an impact on the emission/immission calculation.

Regarding the missing shielding correction thus far, Kaddoura (2019) presents a validity analysis of MATSim's noise model by comparing noise immissions in a study area in Berlin against results from Krapf and Ibbeken (2012). While the noise estimates along major roads show good agreement among both models' results, a large share of noise estimations along side-roads were more than 6 dB(A) louder in the MATSim model results. Kaddoura acknowledges that one of the main reasons is the neglect of shielding effects.

5.2 Update to the RLS 19

Over the course of this dissertation, the three-decades-old RLS-90 guideline has been updated with the release of the new RLS-19 noise prediction guideline. The new guideline has been implemented in MATSim and was used for the presented results in this thesis. This section describes the background of the RLS-19, the differences between the RLS-90 and its implementation in MATSim.

5.2.1 Background and Comparison to RLS-90

In comparison to the RLS-90, the RLS-19 distinguishes three instead of two different vehicle types by further subdividing the truck vehicle type into a light and heavy truck

type. Motorbikes can be treated as heavy truck types. In addition, there no longer is an approach similar to the 'long straight lanes' in the RLS-90. The new guideline only allows an approach similar to the link segmenting approach in the old guideline. Here, links have to be segmented into smaller sub-segments. Another difference is that the directive also takes account of the fact that vehicle emissions have changed over the years. While passenger cars, in general, have become larger and are equipped with larger tires, leading to more noise, heavy-duty vehicles emit less noise because of advancements in technology. Overall, most changes apply to the emission calculation. However, since there are also subtle changes in the calculation of immissions, some of the equations will be presented here.

Similar to the RLS-90, the immission values for hour t are calculated as the logarithm of power sums over all emissions $L_{W,j}$ of relevant links. However, different from the 'long, straight lane' approach, the individual links j are actually subsegments of large roads. In addition, there is a correction that takes into account the length of the link to eliminate the impact of segmentation:

$$L_{\text{eq},i,t} = 10 * log_{10} \sum_{j} 10^{0.1*(L_{W,j,t}+10*log_{10}[l_j]-D_{A,j}-D_{RV1,j}-D_{RV2,j})} \tag{5.7}$$

where l_j is the length of link j, $D_{A,j}$ is a dampening correction for sound propagation from the link and shielding of buildings, and $D_{RV1,j}$ and $D_{RV2,j}$ are correction terms for the first and second order reflection, respectively. The emission $L_{W,j}$ of a single link j is calculated as

$$L_{W,j,t} = 10 * log_{10}[M_{j,t}] + 10 * log_{10}\left[\sum_{m} \lambda_{j,m,t} \times \frac{10^{0.1*L_{W,j,m,t}(v_{j,m,t})}}{v_{j,m,t}}\right] - 30, \tag{5.8}$$

where M_j is the average hourly traffic volume, $\lambda_{j,k}$ is the share of vehicles of type m, $L_{W,j,m}$ is the speed-dependant emission of a vehicle of type m and $v_{j,k}$ is the average speed of a vehicle of type m on link j. Different from the emission level $L^{25}_{j,t}$ defined in 3.2, $L_{W,j,t}$ is not based on the same assumptions of a fixed distance of 25 meters from the emitter, a height of 2.25 meters, a maximum speed level of 100 km/h on a smooth asphalt road surface and a gradient of less than 5%. The speed, road surfaces and gradients are direct parameters of $L_{W,j,t}$ and $L_{W,j,m,t}(v_{j,m,t})$. Thus, to compare both, the following transformation has to be applied (Wolfram Bartolomaeus, 2019):

$$L_{W,j,t} = L^{25}_{j,t} + 19.1 \tag{5.9}$$

The type- and speed-dependent emission is defined as:

$$L_{W,j,m,t}(v_{m,t}) = L_{\text{W0},m,t}(v_{m,t}) + D_{\text{surf},m}(v_{m,t}) + D_{\text{grad},m}(g, v_{m,t}) + D_{\text{inter}}(x) + D_{\text{refl},j}(h) \tag{5.10}$$

Here, $L_{\text{W0},m,t}(v_{m,t})$ is the base emission value of a vehicle of type m with speed $v_{m,t}$. $D_{\text{surf},m}(v_{m,t})$ is a correction for the road surface, $D_{\text{grad},m}(g, v_{m,t})$ is a correction for the

gradient g, $D_{\text{inter}}(x)$ is a correction for intersections in a distance of x and $D_{\text{refl}}(h)$ is a correction for multiple reflections for obstacles with a height h.

Figure 5.4 illustrates the differences in emissions between RLS-90 and RLS-19. Values for the RLS-90 have been estimated by using equation 5.9.

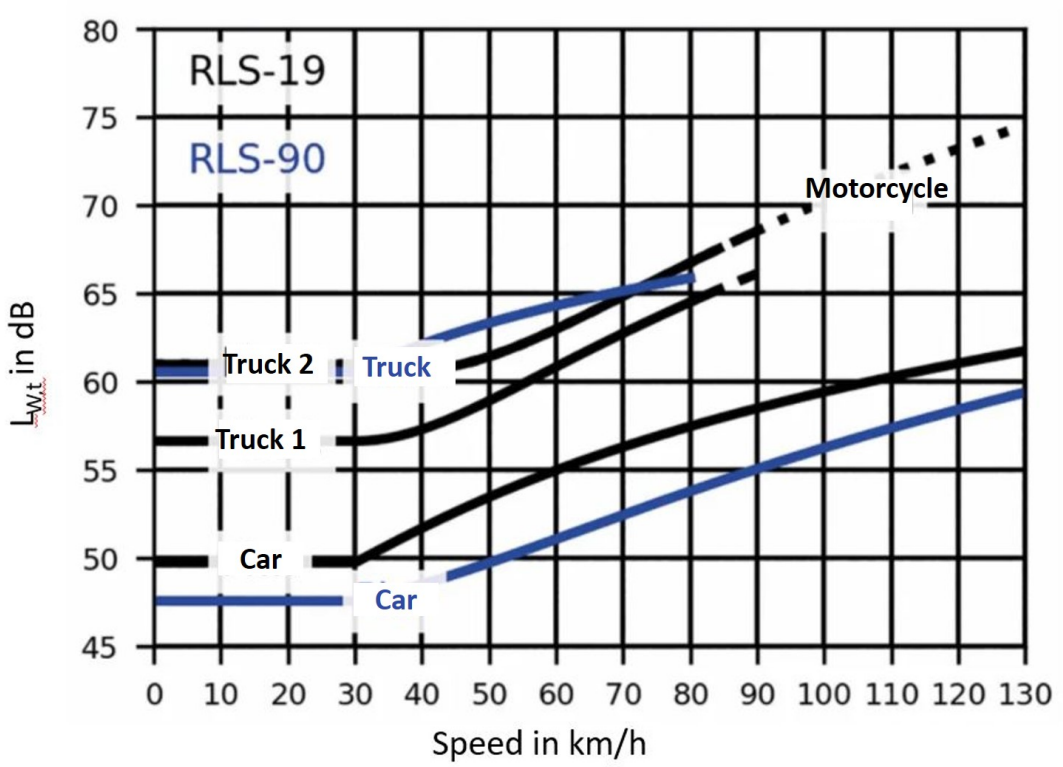

Figure 5.4: Differences in speed dependent emissions $L_{w,t}$ between RLS-90 and RLS-19 for different vehicle types. Based on Wolfram Bartolomaeus (2019)

As stated earlier, the 'long, straight lane' approach was discontinued in the RLS-19. Instead, a link segmentation approach has become mandatory. Here, the road has to be split into smaller segments so that each segment has uniform conditions along its length. In addition, the length l of a segment should not exceed half of the distance between the midpoint of the segment and the receiver s, i.e.:

$$l < \frac{s}{2}. \tag{5.11}$$

The concept of link segmentation is also shown in figure 5.5 (also compare to figure 5.1). It should be noted that the condition in equation 5.11 also means that, in general, segments closer to the receiver will be shorter. These will also be the more important

ones, as they will contribute most to a receiver's immission. With growing distance to the receiver point, segments will be longer. This ensures that accuracy is highest for the closest and more important segments.

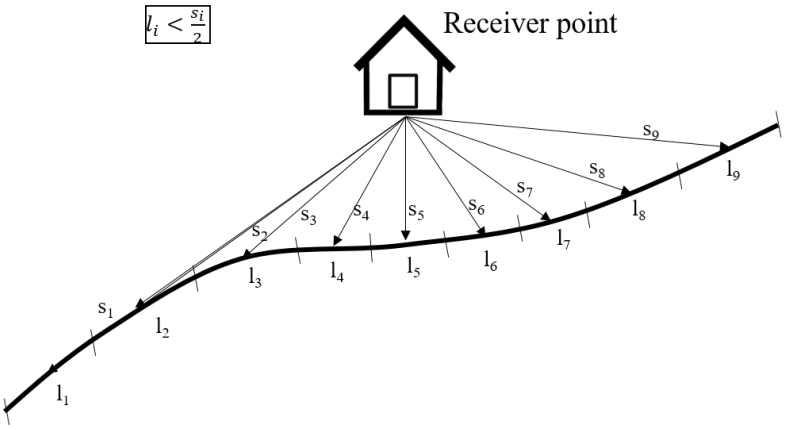

Figure 5.5: Link segmentation in the RLS-19

5.2.2 Implementation and Assessment

To comply with the new guideline and the segmented link approach, one can define link segments k_j for each link j. Equation 5.7 thus sums up over all *segments* of each link:

$$L_{\text{eq},i,t} = 10 \cdot \log_{10} \sum_{j} \sum_{k_j} 10^{0.1 \cdot (L_{\text{W},k_j,t} + 10 \cdot \log_{10}[l_{k_j}] - D_{\text{A},k_j} - D_{\text{RV1},k_j} - D_{\text{RV2},k_j})} \tag{5.12}$$

MATSim uses a mesoscopic queue-based representation of traffic flow. As such, average speeds and volumes can only be analyzed at the link level. MATSim networks are usually created from OSM ways. In OSM, it is assumed that road surface and gradient stay constant across a way. Therefore, it is assumed that traffic volumes and speeds, vehicle type shares, velocities, gradient and road surface of each link segment stay constant across the full link. Applying this assumption to equation 5.10 leads to (see Appendix for a step-by-step transformation):

$$L_{\text{eq},i,t} = 10 \cdot \log_{10} \left[\sum_{j} \left(10^{0.1 \cdot L_{\text{W},j,t}} \cdot c_j \right) \right], \text{ with} \tag{5.13}$$

$$c_j = \sum_{k_j} 10^{0.1 \cdot (D_{\text{inter}}(x_{k_j}) + 10 \cdot \log_{10}[l_{k_j}] - D_{\text{A},k_j} - D_{\text{RV1},k_j} - D_{\text{RV2},k_j})} \tag{5.14}$$

Now only $L_{\text{W},j,t}$ is dependent on t. The corrections for all segments c_j only need to be calculated once and can be stored as a single correction term during a pre-processing step. This means that no matter how detailed links are split, the memory requirement

remains the same. Since c_j is a simple sum, segments can be processed one by one by addition, which again keeps memory requirements low. The link segmentation was implemented by employing a recursive algorithm, as shown in algorithm 1. The link is treated as a single segment first. If the length of the link exceeds the maximum length condition, the link is recursively split into smaller segments. For each of the segments, correction terms are added up according to 5.14. As stated earlier, this process happens once upon initialization. For the immission calculations in the individual hours t, the emission $L_{W,j,t}$ is then multiplied by c_j.

Algorithm 1: Link Segmentation and Correction Term Calculation

foreach *receiver point* i **do**
  look up relevant link candidates in a 500 meter (configurable) buffer radius;
  foreach *relevant link* j **do**
    create segment k_j for the whole link;
    c_j = `processSegment`(i, k_j);
  end
end

Function `processSegment`$(i,\ k_j)$**:**
  Data: Receiver point i, link segment k_j with points P_0 and P_1
  Result: correction term c_j
  define $c_{k_j} = 0$;
  identify midpoint M_{k_j} of segment k_j;
  calculate distance between receiver and midpoint $d_{i,M_{k_j}}$;
  calculate max length $maxL = \frac{d_{i,M_{k_j}}}{2}$;
  calculate length l_{k_j} of segment k_j;
  if $l_{k_j} < maxL$ **then**
    $c_{k_j} +=$ `calcSegmentCorrection` (k_j);
  else
    define left point PL_{k_j} at $\frac{maxL}{2}$ to the 'left' of M_{k_j};
    define right point PR_{k_j} at $\frac{maxL}{2}$ to the 'right' of M_{k_j};
    create segment $\overline{PL_{k_j}PR_{k_j}}$;
    $c_{k_j} +=$ `calcSegmentCorrection` $(\overline{PL_{k_j}PR_{k_j}})$;
    create left segment $\overline{P0PL_{k_j}}$;
    $c_{k_j} +=$ `processSegment`$(\overline{P0PL_{k_j}})$;
    create right segment $\overline{PR_{k_j}P1}$;
    $c_{k_j} +=$ `processSegment`$(\overline{PR_{k_j}P1})$;
  end
return $c_{r,x}$

Figure 5.6 shows the differences in resulting L_{DEN} for the old and the new implementation. One can see that the RLS-19 results in slightly louder values around the road sources. In addition, while the RLS-90 implementation shows erratic behavior around the ends of links, the RLS-19 implementation produces smoother results at link ends and around the whole network. This is driven by the fact that the RLS-19 was implemented with a link segmentation approach while the RLS-90 relies on the angle correction as discussed in 5.1.

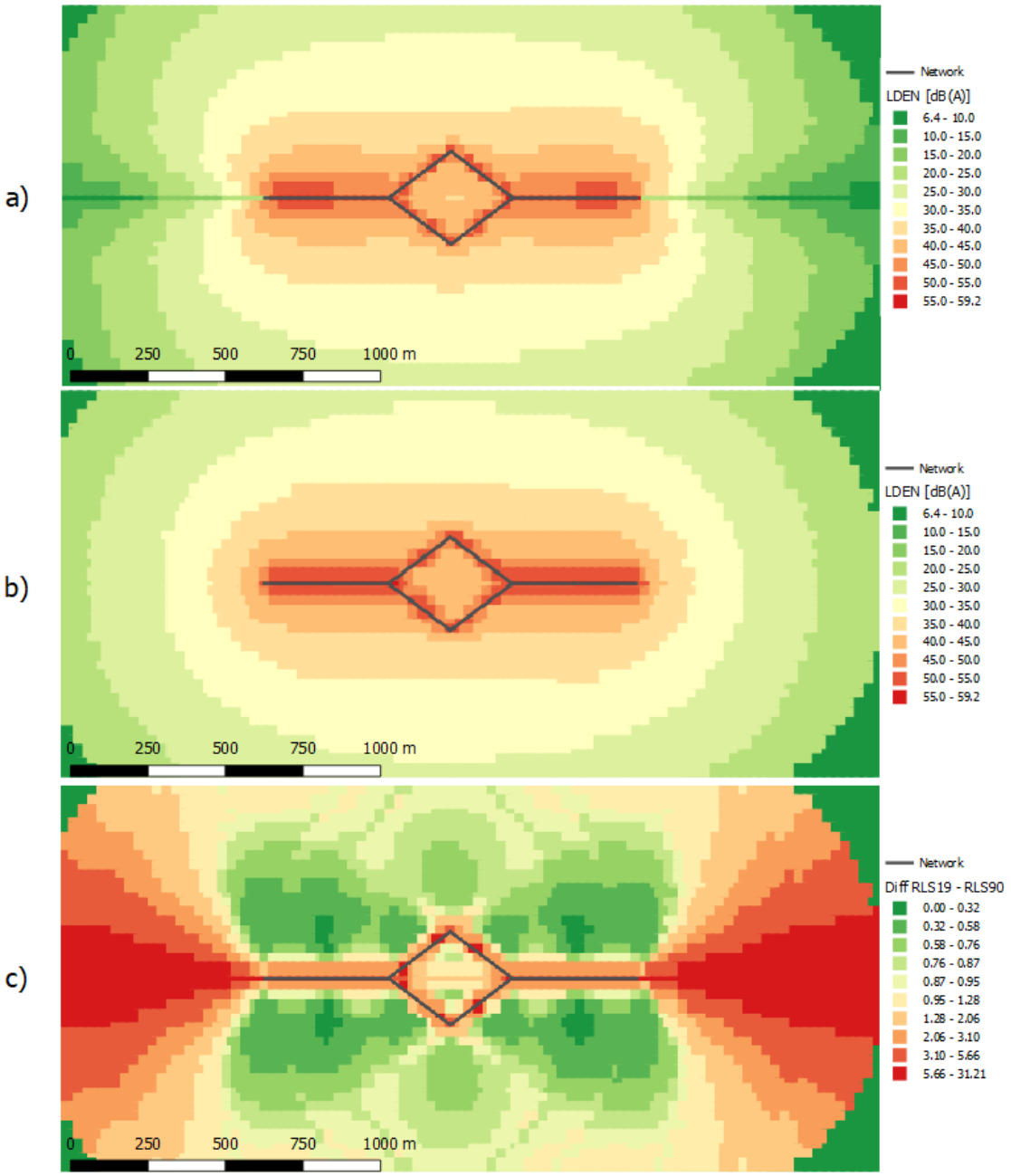

Figure 5.6: Illustrative presentation of L_{DEN} values for a) the old RLS-90 and b) the new RLS-19 implementation as well as c) their differences for the illustrative scenario. Differences based on a decile scale.

5.3 Correction for Intersections

The intersection correction $D_{\text{inter}}(x_{k_j})$ is linearly dependent on the distance x_{k_j} from the point source of the link segment k_j to the nearest intersection and is calculated as follows:

$$D_{\text{inter}}(x_{j_i}) = \kappa_\tau * max\left\{1 - \frac{x_{j_i}}{120}; 0\right\} \tag{5.15}$$

Here, κ_τ is the maximum correction term for the intersection type τ as defined in table 5.1. The table also shows the OSM tags that were used to identify the location of intersections during data preparation.

Table 5.1: Maximum correction terms κ_τ and respective OSM identifier tags.

Type τ	Correction κ_τ in dB(A)	OSM Tag
signalized intersection	3	'highway=traffic_signals'
roundabout	2	'junction=roundabout'
other	0	-

5.4 Correction for Road Surfaces

The surface correction $D_{\text{surf},m}(v_{k_j,m,t})$ is defined for different surfaces and depends on the vehicle type and its speed. Due to the lack of surface data, the differentiation of surface types was limited to the surfaces with a positive correction term (i.e. louder surfaces). These can commonly be obtained by using OSM data. Table 5.2 shows the implemented link between OSM tags and surface correction terms.

Table 5.2: Surface correction terms for different speeds and surfaces and their respective OSM identifier tags.

Surface type	$D_{\text{surf},m}(v_{k_j,m,t})$ in dB(A) for $v >= ...$			OSM Tag
	...30 km/h	...40 km/h	...50 km/h	
cobblestone with smooth surface	1	2	3	'surface=sett'
other cobblestone	5	6	7	'surface=cobblestone'

5.5 Correction for Gradients

The gradient correction $D_{\text{grad},m}(g, v_{k_j,m,t})$ depends on vehicle type $m = \{\text{car,truck1,truck2}\}$, speed $v_{k_j,m,t}$ and gradient g and is defined as follows:

$$D_{\text{grad,car}}(g, v_{k_j,\text{car},t}) = \begin{cases} \frac{g+6}{-6} \cdot \frac{90-\min(v_{k_j,\text{car},t};70)}{20}, & g < -6 \\ \frac{g-2}{10} \cdot \frac{(v_{j_i,\text{car},t}+70}{100}, & g > 2 \\ 0 & \text{else.} \end{cases} \tag{5.16}$$

$$D_{\text{grad,truck1}}(g, v_{k_j,\text{truck1},t}) = \begin{cases} \frac{g+4}{-8} \cdot \frac{v_{k_j,\text{truck1},t}-20}{10}, & g < -4 \\ \frac{g-2}{10} \cdot \frac{v_{k_j,\text{truck1},t}}{10}, & g > 2 \\ 0 & \text{else.} \end{cases} \tag{5.17}$$

$$D_{\text{grad,truck2}}(g, v_{k_j,\text{truck2},t}) = \begin{cases} \frac{g+4}{-8} \cdot \frac{v_{k_j,\text{truck2},t}}{10}, & g < -4 \\ \frac{g-2}{10} \cdot \frac{v_{k_j,\text{truck2},t}+10}{10}, & g > 2 \\ 0 & \text{else.} \end{cases} \tag{5.18}$$

The gradient can be obtained from digital elevation models. Another source can be OSM by evaluating the 'incline=...' tag. However, this tag is not widely present and sometimes only tagged as 'up' or 'down' without a detailed percentage.

Since Munich is located in the Munich gravel plain and Berlin-Brandenburg is part of the North German Plain, most parts of the study areas in this thesis are essentially flat. For example, the largest road elevation in Munich has a maximum gradient of 4% which would result in a negligible correction term. For the scenarios in this thesis, the gradient correction is therefore set to 0.

5.6 Correction for Electric Vehicles

In line with uncertain noise benefits of electric vehicles, there is no distinction between the type of engine in the official guideline. However, as discussed in section 2.4.2, some reductions in noise could emerge from fully electric fleets. For scenarios that model fleets of electric vehicles, the calculation of emissions was adapted by adding another correction term $D_{electric}(v_{j_i,k,t})$, similar to the approach of (Verheijen and Jabben, 2010). For this term, a simple interpolated speed-based reduction was implemented which is based on the reductions presented by (Campello-Vicente et al., 2017):

$$D_{\text{electric}}(v_{k_j,m,t}) = 5.59 \cdot e^{-0.031 \cdot v_{k_j,m,t}} \tag{5.19}$$

In line with the RLS-19, the lower bound is set to 30 km/h which is the minimal speed that is assumed for noise estimation. Thus, equation 3.1 becomes:

$$\begin{aligned} L_{\text{W},k_j,m,t}(v_{k_j,m,t}) = L_{\text{W0},m,t}(v_{k_j,m,t}) + D_{\text{surf},k}(v_{k_j,m,t}) + D_{\text{grad},m}(g, v_{k_j,m,t}) \\ + D_{\text{inter}}(x_{k_j}) + D_{\text{refl}}(h) + D_{\text{electric}}(v_{k_j,m,t}) \end{aligned} \tag{5.20}$$

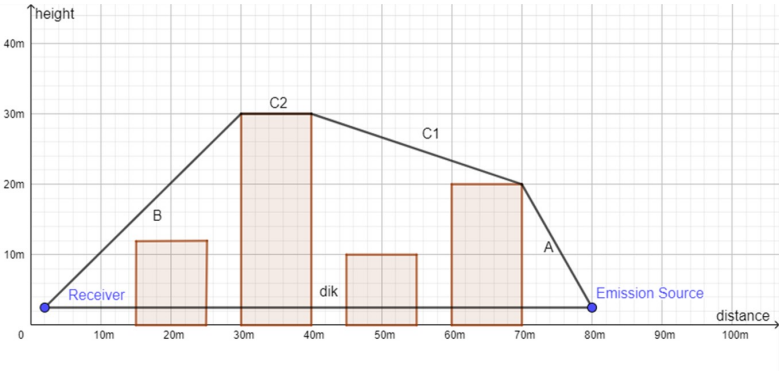

Figure 5.7: Construction of the shielding term. Sectional view on the xy-z plane.

5.7 Correction for Shielding

This section introduces noise shielding of urban structures to the MATSim noise extension. More specifically, the correction term $D^z_{k,j}$ that, according to FGSV (2019), is applied to equation 3.7 is implemented in the code. As this has been identified as one of the largest limitations of the initial implementation and is less straightforward to implement, this correction is presented in more detail. In contrast to previous versions, the new implementation takes into account the shielding of noise at building facades. The simplified approach is based on the German noise modeling guidelines.

A previous implementation for the old RLS-90 and the 'long, straight lane' approach has been described in Kuehnel et al. (2019).

5.7.1 Implementing the Shielding Correction

The correction term is calculated as follows:

$$D^z_{k_j,i} = 10 \cdot log_{10}[3 + 80 \cdot z_{k_j,i} \cdot K^w_{k_j,i}] \tag{5.21}$$

Here, $z_{k_j,i}$ is the shielding term for receiver point i in relation to link segment k_j and $K^w_{k_j,i}$ is a weather correction. The shielding term $z_{k_j,i}$ is the extra distance that sound beams have to travel because of the shielding (see figure 5.7). It is obtained by adding up the distance between the emission source and first edge of diffraction $A_{k_j,i}$, the distance between last edge of diffraction and receiver point $B_{k_j,i}$ and the sum of distances between diffraction edges $C_{k_j,i}$ between $A_{k_j,i}$ and $B_{k_j,i}$, minus the distance between receiver point and the midpoint of the segment $s_{k_j,i}$:

$$z_{k_j,i} = A_{k_j,i} + B_{k_j,i} + C_{k_j,i} - s_{k_j,i} \tag{5.22}$$

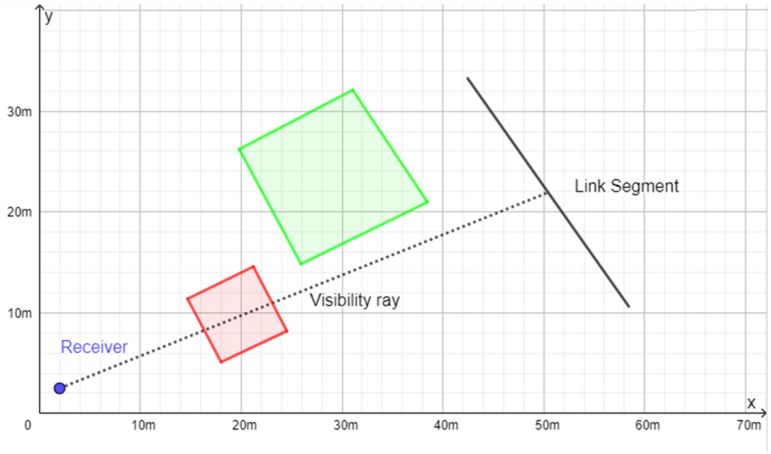

Figure 5.8: An example for an obstructing polygon (red) and a polygon not considered for shielding (green). Bird's eye view on the x-y-plane.

$K^w_{i,j}$ is a distance dependent correction:

$$K^w_{k_j,i} = exp\left(\frac{-1}{2000}\sqrt{\frac{A_{k_j,i} \cdot B_{k_j,i} \cdot s_{k_j,i}}{2 \cdot z_{k_j,i}}}\right) \tag{5.23}$$

For an obstruction to be taken into account into the shielding correction, it has to intersect the direct line of sight between emission source and receiver. Therefore, the algorithm will check whether the line of sight is obstructed (see figure 5.8).

After determining all obstacles between the receiver point and the link, the shielding value $z_{k_j,i}$ is calculated. The height of each obstacle is assumed to be given and flat roofs are assumed. The construction of the distances $A_{k_j,i}$,$B_{k_j,i}$ and $C_{k_j,i}$ is a two-dimensional shortest path problem around the obstacles. This is equivalent to finding the convex hull of the edges of sound diffraction. One way to solve it is the so-called gift wrapping algorithm (also known as Jarvis march, based on Jarvis (1973)). It is outlined in the following for the problem at hand. Starting from the receiver point, the slopes of the connections to all following edges are calculated. The edge with the highest slope is then fixed as the next considered edge of diffraction, from which the slopes to the remaining edges are determined. This process continues until the entire path between the receiver point and emission link is constructed. Finally, the lengths of the path segments are used to determine $z_{k_j,i}$ and the shielding correction term $D^z_{k_j,i}$. The process is outlined in figure 5.9.

Figure 5.9: Construction of the shortest path around the obstacles, starting from the receiver on the left. After calculating the slopes to all possible edges, the edge connected with the highest slope is fixed (thick lines). The procedure is repeated starting from the last fixed edge until the emission source is reached.

To conclude, the approach can be summarized as follows:

Algorithm 2: Shielding correction term calculation

Data: Receiver point i, link segment k_j
Result: shielding correction term $D^z_{k_j,i}$
identify midpoint M_{k_j} of segment k_j;
construct line of sight $\overline{iM_{k_j}}$;
initialize set of edge candidates S;
identify obstacle candidates Ω from spatial search tree look-up by using the bounding box of $\overline{iM_{k_j}}$ as a first intersection criteria;
foreach $o \in \Omega$ **do**
    check actual intersection: $I = \overline{iM_{k_j}} \cap o$;
    if $I \neq \emptyset$ **then**
        store intersection edges: $S = S \cup I$;
    end
end
initialize set of shortest path edges Z;
initialize last fixed edge $E_{fixed} = i$;
while $E_{fixed} \neq M_{k_j}$ **do**
    initialize max slope $a = -\infty$;
    initialize temporary edge T;
    foreach *remaining edge* $E_{curr} \in S$ **do**
        calculate slope m of $\overline{E_{fixed}E_{curr}}$;
        if $m >= a$ **then**
            $a = m$;
            $T = E_{curr}$;
        end
    end
    $E_{fixed} = T$;
    $Z = Z \cup E_{fixed}$;
    $S = S \setminus Z$;
end
determine $A_{k_j,i}$,$B_{k_j,i}$ and $C_{k_j,i}$ from edges in Z;
calculate $z_{k_j,i}$ following 5.22;
calculate $K^w_{k_j,i}$ following 5.23;
calculate $D^z_{k_j,i}$ following 5.21;

It is worth noting that the runtime for immission calculation increases significantly when the impact of shielding is included. The computationally most expensive part is checking for geometric intersection which was performed using the Java Topology Suite (JTS) library [1]. A proper spatial search tree reduces unnecessary intersection checks and was the most crucial part of keeping computation times feasible.

[1] https://github.com/locationtech/jts

5.7.2 Illustrative Shielding Example

The implemented shielding functionality is first tested in the illustrative scenario that was introduced in chapter 4. This time, two detached buildings are added on the left, as shown in figure 5.10. The two buildings have different heights (10 meters for the upper building, 20 meters for the lower building). In addition, a larger building block with an inner yard and a small gap is added on the top right. The building block has a height of 20 meters.

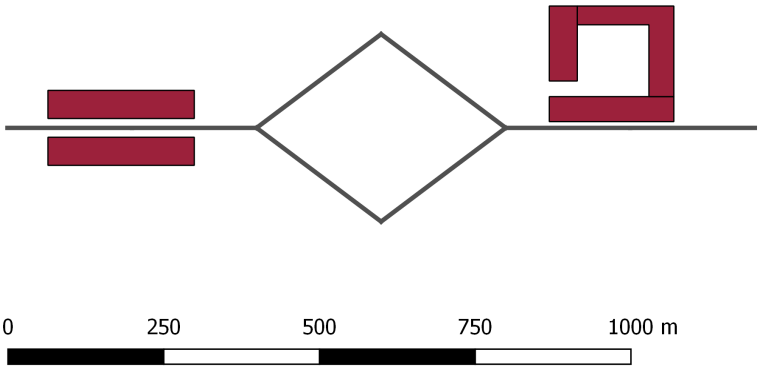

Figure 5.10: Obstacles in the illustrative scenario.

In the next step, the calculation of noise was done with and without the shielding correction. The results can be seen in figure 5.11. There are multiple noteworthy observations. First of all, the effect of shielding is clearly visible behind the defined obstacles. For the detached buildings, the shielding correctly has a slightly stronger impact behind the lower building when compared to the upper building since it is twice as high. One can see that the noise propagates in a cone shape to the left of the buildings. Lastly, it is observable that shielding is more extensive when the receiver is very close to an obstacle. Receiver points that lie further away experience larger immission values as their view on the roads is not blocked completely. For the building block, it can be observed that the inner yard correctly shows considerably lower noise immissions. The reductions are slightly lower near the gap of the building block on the left.

5.7.3 Realistic Use Case of the Shielding Implementation

Now, the shielding impact is tested in a densely urban setting in the Munich scenario. Noise damages (see section 3.4.3) are calculated to answer the first research question of this thesis which aims to assess the impact of neglecting shielding corrections in dense urban environments. The difference between noise damages obtained with and without

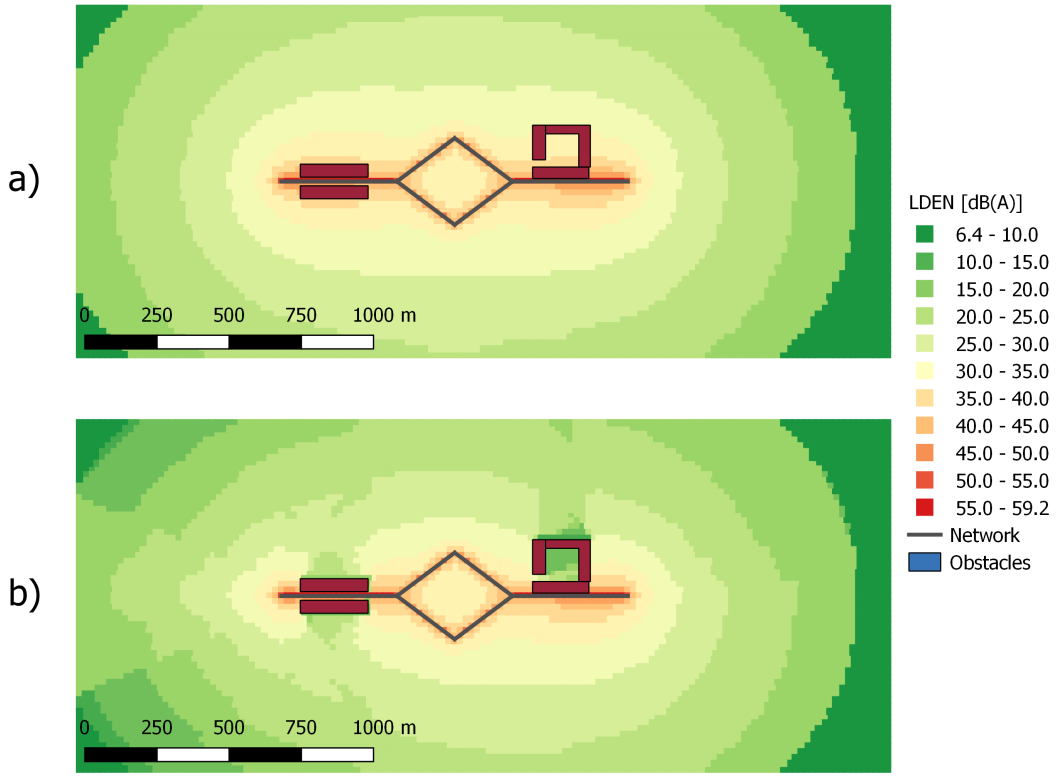

Figure 5.11: Resulting L_{DEN} values a) without and b) with the new shielding implementation.

the shielding calculation will serve as a proxy to quantify the impact.

5.7.3.1 Scenario Preparation

For the setup, travel demand is first generated by MITO and subsequently assigned in MATSim. Around 8.8 million trips with a car share of 43% were created for the whole study area. A five percent sample of the trips was converted into MATSim agents, which was identified as a reasonable tradeoff between computation time and model accuracy (Llorca and Moeckel, 2019).

The most common structures in an urban environment are buildings. It is crucial to have an accurate representation of buildings in order to estimate the impact of shielding. In general, noise levels are lowered substantially behind larger building blocks and in inner yards. Volunteered Geographic Information (VGI) like OSM contain information about building footprints. OSM data has been downloaded for the Munich metropolitan study area by cutting the Bavarian dataset provided by Geofabrik [2] to the study area de-

[2] https://download.geofabrik.de/

lineation. In a next step, all objects tagged as buildings have been extracted and saved to a geojson format which is the standard that has been used to read in obstacles in the noise shielding extension. Figure 5.12 shows a map of the distributions of buildings obtained from OSM. The five core cities Munich, Augsburg, Ingolstadt, Landshut and Rosenheim clearly stick out. Figure 5.13 shows a close-up view of buildings in Munich. While specific details on height or number of levels are sparse, the actual number and spatial extent of buildings is considered sufficiently complete. In cases where no height tag or level tag was present, an average building height of 10 meters was assumed, which is a more conservative approximation for buildings with three to four levels (Nexiga GmbH, nd).

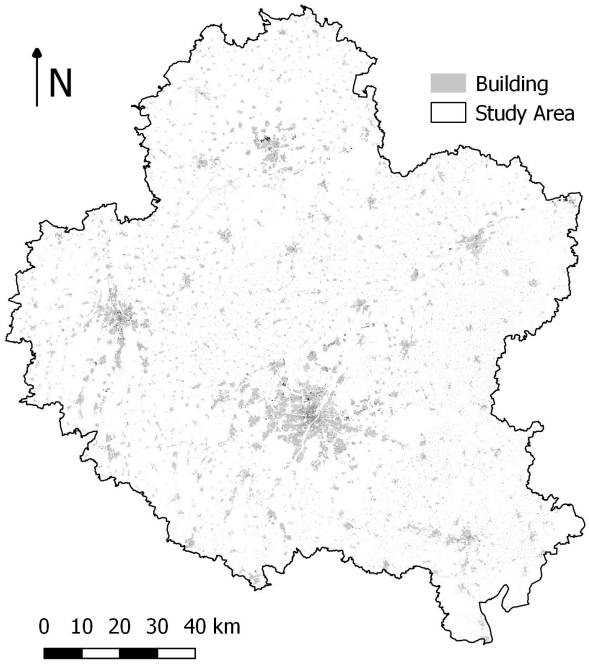

Figure 5.12: Buildings in the Munich metropolitan area.

Within Munich, 160,490 building features were obtained. Height information of buildings was partially given by the 'height' OSM tag (1,286 cases). More common, the number of levels is given in OSM where an average height of 3.5 meters per level was assumed (20,394 cases).

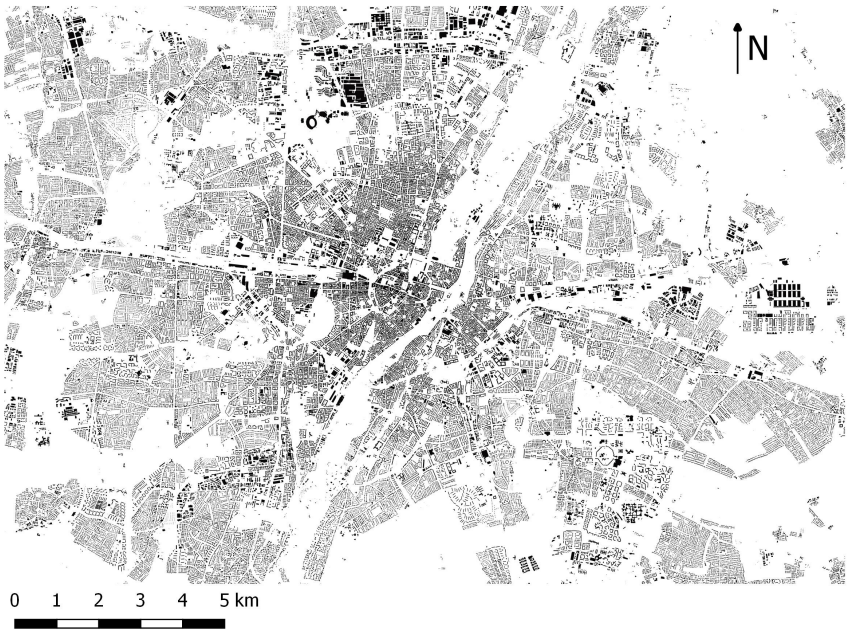

Figure 5.13: Buildings in Munich.

5.7.3.2 Resulting Shielding Impacts for Munich

The receiver point grid was defined with a spacing of roughly 15 meters in x- and y-direction. A fine grid is necessary to capture the effect of shielding in backyards. A grid covering the center of the city with a dense building structure was created. The grid is roughly 10 kilometers from East to West and 5 kilometers from North to South. In total, about 225,000 receiver points were evaluated.

Figure 5.14 shows a comparison of simulated noise immission values expressed as the L_{DEN} value (day-evening-night index) for the inner city of Munich (part of the full receiver point grid). The building polygons are visualized on top. On the left side, the immissions are shown without taking into account the shielding correction and mainly decrease with the distance to roads. On the right side, the shielding correction is included. Taking into consideration the effect of shielding yields a major reduction in noise levels in most of the backyards. In addition, larger areas behind buildings are 'shadowed' and thus show a reduction of immissions. As expected, unobstructed receiver points (e.g. close to the roads) do not seem to be affected by shielding. Overall, the results confirm the functionality of the implemented shielding correction feature.

In the next step, noise exposure costs were analyzed using equation 3.11 and adding up costs at all receiver points. The dwelling locations of residents are defined in the synthetic population. As these were mapped to OSM buildings, 'home' activities were taken into account for the exposure analysis to obtain a realistic distribution of activity

locations. Without shielding correction, daily exposure costs (or noise damages) amount to 1,945.36 EUR. When taking into account the effect of shielding, the noise damages decrease to 1,555.69 EUR. This indicates that in densely populated urban areas, a noise exposure analysis that neglects the effect of shielding may overestimate the damages by up to 20%.

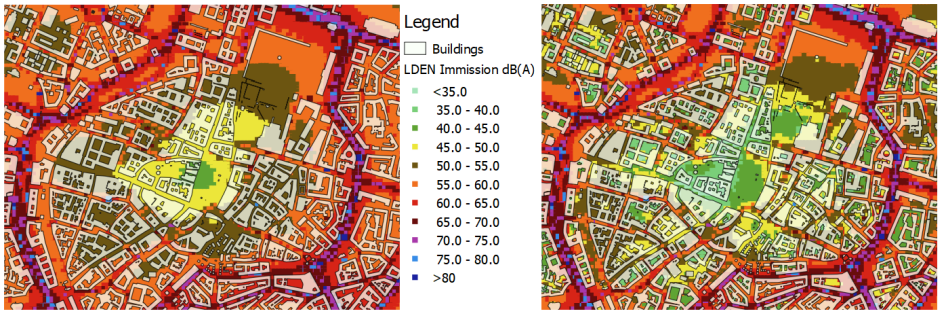

Figure 5.14: Immission L_{DEN} levels before (left) and after (right) taking shielding into account. While unprotected areas remain the same, covered areas and backyards of building blocks show a major noise reduction.

To sum up, this section answers research question 1 of this thesis, which aims to identify the impact of neglecting shielding corrections in dense urban environments. From the use case shown here, the neglection would lead to an overestimation of noise damages by up to 20%. However, it should be noted that this may be highly case-specific as it largely depends on the distribution and interplay of roads, buildings and traffic volumes and speeds.

5.8 Reflection Correction

In addition to the shielding effect, buildings and obstacles also exhibit a reflection effect. Reflection occurs when noise hits a (smooth) wall and is reflected by it. The guideline RLS-19 considers reflections in two ways:

- as part of the *emission* calculation. This is the correction term $D_{refl,j}(h)$ in equation 5.10 which only depends on the link segment.
- as part of the *immission* calculation. This includes the two correction terms $D_{\mathrm{RV1},i,j}$ and $D_{\mathrm{RV2,i,j}}$ in equation 5.7 for first and second-order reflection, respectively.

The implementation is described in the respective subsections that follow.

5.8.1 Link segment dependent reflection correction

This correction accounts for multiple reflections and is applicable if the link segment j is between two parallel walls with a distance no further than 100 m. Walls are considered

parallel if their angle difference is less than five degrees. The term is defined as:

$$D_{\text{refl},j}(h) = min\left[2 \cdot \frac{h}{w}; 1.6\right] \tag{5.24}$$

where h is the height of the walls. If the walls have different heights, the lower height is used. w is the distance of the reflecting walls in meters.

For the implementation, a simple ray-casting algorithm was used, in which a beam is projected on both sides perpendicular to the link segment. The spatial search tree that is already used for the shielding effect is then used to find possible polygons that intersect the visible beam. If a polygon intersects the view beam, the edge that intersects the beam first is taken. If there is an edge on both sides of the link, their distance from each other is less than 100 m and they are parallel according to the above definition, the correction term is applied. The conditions for multiple reflections are illustrated in figure 5.15.

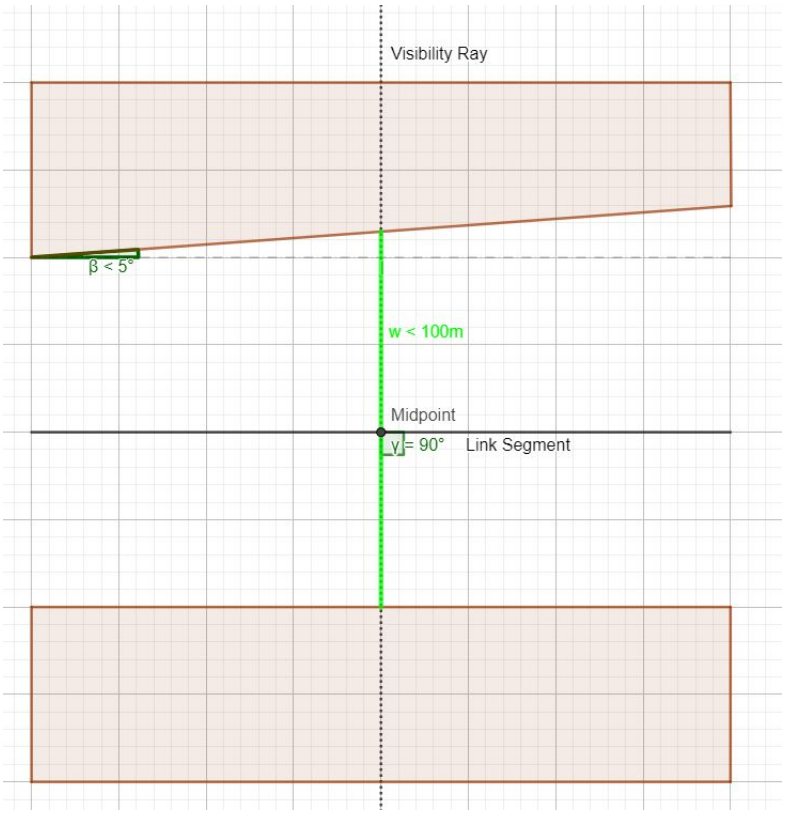

Figure 5.15: Illustrative scenario for multiple reflections. The link segment is surrounded by two obstacles with almost perpendicular walls and a distance w of less than 100 m.

Table 5.3: Reflection correction terms

Reflector type	$D_{\mathrm{RV1},i,j}$ and $D_{\mathrm{RV2,i,j}}$ in dB
Building walls and reflecting noise walls	0.5
antireflective noise walls	3.0
highly antireflective	5.0

5.8.2 Receiver dependent reflection correction

This term accounts for reflections along single walls which are directed to a specific receiver point. The RLS19 requires the consideration of reflections when the height h_{R} of the reflecting area is at least 1m. In addition, the condition $h_{\mathrm{R}} \geq 0.3 \cdot \sqrt{a_{\mathrm{R}}}$, where a_{R} is the smaller of the distances of source and reflector or reflector and receiver, must be met.
In the case of reflection, the emission link segment is mirrored on the axis of the reflecting surface, resulting in another -theoretical- emission source behind the reflecting surface. This process is shown in figure 5.16. Note that only the part of the mirrored segment, which is obscured by the reflecting area, is considered (right side of figure 5.16).

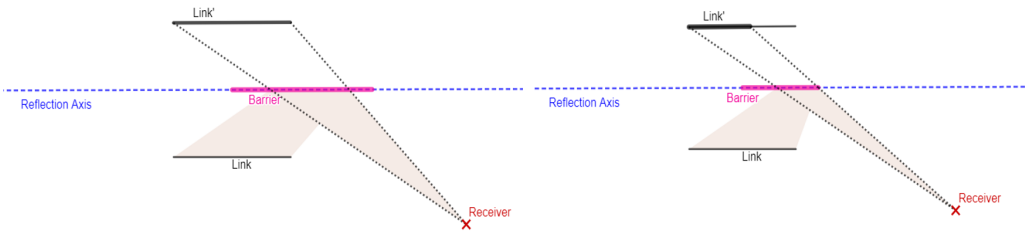

Figure 5.16: Construction of reflected links behind reflecting barriers.

To calculate the immission at the receiver, the mirror sound source is treated as a regular sound source. However, the reflection loss $D_{\mathrm{RV1},i,j}$ for the first-order reflection and, additionally, in the case of second-order reflection, $D_{\mathrm{RV2,i,j}}$ are subtracted from the immission contribution of the mirror link (see table 5.3).

Figure 5.16 showed the construction of reflected links when the reflecting area is identified. The more complicated part is to efficiently identify those walls that actually reflect a given link segment for a given receiver. For this purpose, a two-step process was implemented, which is explained in the following. Figure 5.17 shows a simple theoretical scenario with a receiver point (blue), two link segments j_1 and j_2 (black) and four polygons with edges $\overline{bcde}$, $\overline{fghi}$, $\overline{jklm}$ and $\overline{nopq}$ (apricot).

During immission calculation, the noise module iterates over all receiver points and for each of these points over all relevant links. Therefore, in the first step, all possible walls that could reflect noise from a link segment are identified for each receiver point. There-

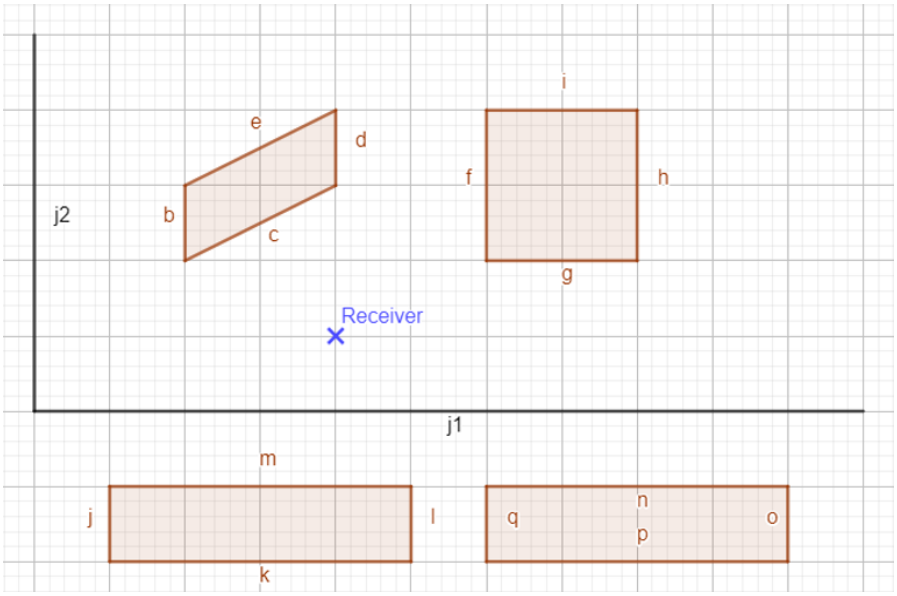

Figure 5.17: Theoretical scenario for identification of reflection facades.

fore a simplified angular sweep algorithm based on Asano (1985) was implemented. For each polygon in a configurable radius around the receiver point, the maximum possible angle between all polygon nodes is calculated. This is illustrated by the angles α, β, γ and δ in figure 5.18. This angle is divided into 10 (configurable) incremental angle steps. For each step, a visibility ray is cast and it is checked which edge intersects the visibility ray first. It is irrelevant where the intersection point is, so expensive intersection calculations can be avoided. It is only necessary to check whether the endpoints of an edge are on different sides of the visibility ray. The resulting reflection candidates are indicated in blue in figure 5.18 (c, f, g, n, q, m). Note that for simplification, only five visibility rays for each polygon are shown.

When all relevant link segments are iterated over, the second part of the algorithm identifies all edges for each segment for which there is a direct visual relationship. Thereby only edges are considered, which were identified as possible reflection candidates in the first step. To simplify, a direct vision is assumed if there is no obstacle between the midpoint of the edge and the segment's midpoint. In order to check this, a visibility ray is generated between the midpoints. All surrounding polygons around the ray are queried from the spatial search tree. For each of these polygons, it is then checked whether one of their edges intersects the visibility ray. If no polygon interrupts the ray, there may be a reflection between the edge and segment on the receiver. This part of the algorithm is illustrated in figure 5.19.

While segment j_1 (red) has no obstacles between its midpoint and possible reflection candidates, segment j_2 can only reflect on edges m, q and n, since the other edges are blocked by edges b. As such, there are edges that can reflect both segments (m, q, n - yellow) and edges that can only reflect segment j_1 (c, f, g - magenta).

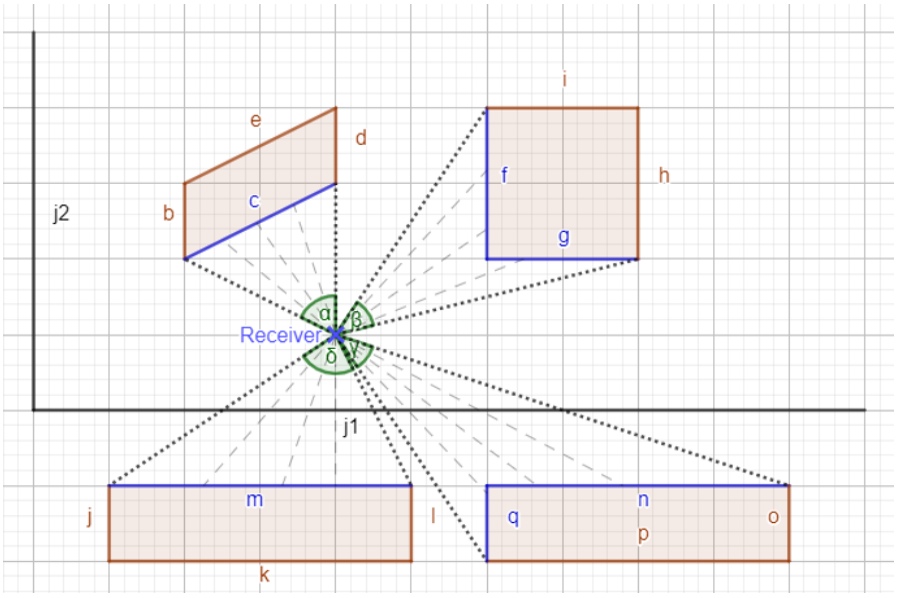

Figure 5.18: Ray casting for reflecting facade identification step 1.

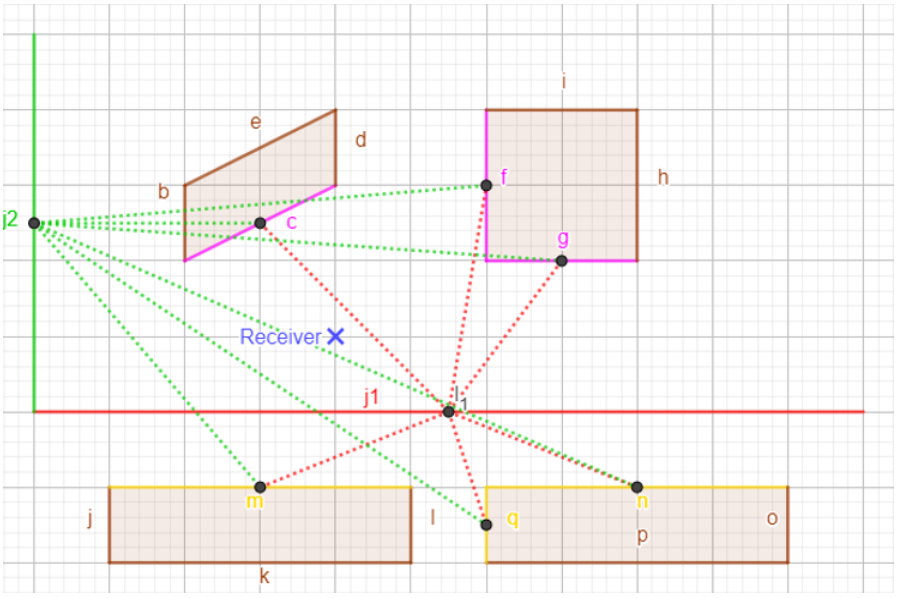

Figure 5.19: Ray casting for reflecting facade identification step 2.

Note that the identification of possible reflection edges does not necessarily mean that there actually is a reflection (for example, edge n is very unlikely to have a reflection on the receiver point). For each identified segment-edge tuple, the actual reflection has to be constructed as shown in figure 5.16.

This approach described the construction of first-order reflections. Because of the complexity of computation and comparatively small impacts of first-order reflections, the second-order reflections have not been implemented. A straightforward approach would be to extend the first step of the algorithm to mark for each possible first-order reflection edge all other edges which are visible from the first order edge candidate.

5.9 Discussion of the Noise Model Extensions

The RLS-19, including a link segmentation approach and various correction terms, were successfully added to MATSim's existing noise prediction model. It is shown that open-source building data can be used for modeling noise shielding. As expected, the improved noise computation methodology yields reduced noise levels in backyards and behind larger buildings. The comparative exposure analysis for the Munich use case reveals a significant overestimation of noise damage costs when shielding effects of buildings are neglected. As OSM data do not provide complete information about building heights, more comprehensive data sources may improve the model accuracy. The impact of shielding effects on exposure analysis may be analyzed in more detail by looking at other noise-sensitive activity types such as education or office activities. It should be noted that the shielding effects presented here do not include shielding from noise protection walls, which are commonly not included in OSM data. In addition, shielding effects can also occur at larger vegetation belts such as dense forests or hedges (Samara and Tsitsoni, 2011; Ow and Ghosh, 2017). Regardless of the difficulty of obtaining vegetation data, vegetation is not considered in the official noise prediction models such as the RLS-19. Most of the studies identified a shielding effect for bands with a width of 15 to 100 meters. Since this thesis focuses on urban environments of large cities where such large vegetation bands are relatively uncommon, these effects are not considered further. The last remaining component of the RLS-19 are second-order reflections which could still be added in the future.

The presented enhanced noise model will be applied in the following chapters and use cases. The first use case is presented in the next chapter and analyzes the impact of road traffic noise on rent prices.

6 Simulation-Based Traffic Noise Impact on Rent Prices

> The sick die here because they can't sleep,/ Though most people complain about the food / Rotting undigested in their burning guts. / For when does sleep come in rented rooms? / It costs a lot merely to sleep in this city!
>
> Juvenal, Roman poet

A goal of this thesis is to add scenario sensitivity for traffic noise in a microscopic ILUT model. Therefore, as the next step, the impact of simulated car traffic noise on real rent prices in Munich is analyzed and compared to existing studies. It is shown that modeled noise values from the transportation model are able to explain significant impacts on rent prices when using a hedonic pricing regression. When using noise as a continuous variable, price discounts of 0.46% per dB(A) are found. A discount of up to 10% for particularly loud locations is estimated when noise is used as a categorical variable. Care should be taken when controlling for measures of centrality that correlate with noise. While the usage of simulated noise values of a transport simulation together with microscopic accessibilities can be considered novel, the results are in line with results of previous studies and confirm that environmental aspects can and should be considered in integrated models.

This chapter deals with assessing whether simulation-based traffic noise is able to explain price discounts in apartment rental prices. Previous findings based on the RLS-90 implementations have been published in Kuehnel and Moeckel (2020). The results presented here follow the same basic methodology, however, the calculation of noise has been updated to the newly implemented RLS-19 guideline. In addition, the noise calculation now accounts for tunnels and more significant variables have been added to improve the estimation.

6.1 Apartments - Data Collection and Analysis

In contrast to most other studies that focus on the total value of real estate properties, the present study analyzes rent prices of individual apartments. This allows better integration with the land use model, as agents in SILO relocate based on – among other location factors – rent prices of dwellings. Data on rent prices for the city of Munich

were collected by observing advertisements on immobilienscout24.de [1], one of the largest online platforms for real estate properties in Germany. In total, the collected database contains 3,144 geocoded records of apartments from the years 2016 to mid of 2018. The mean rent per square meter over these three years was 17.27 EUR, 17.90 EUR and 18.03 EUR, respectively. For the estimation, the rent prices were scaled to the base year of 2016 to correct for this gradual increase. The locations of the objects and their respective price per square meter can be seen in figure 6.1. As expected, the price increases towards the city center. The corrected data show a mean total rent of 1,209 EUR and a mean rent per square meter of 18.04 EUR/m^2 for Munich, which is considered to be the most expensive housing market in Germany (official data for newly rented apartments: 18 EUR/m^2 (Bettina Funk, 2017)). In addition to monthly rent and size, the collected records include information on the number of rooms, construction year, level, number of accompanying parking spots, state (i.e. an indicator of how 'new' the apartment is) and quality ('Average dwelling quality', 'Superior dwelling quality' and 'Luxury dwelling quality') as reported by the property owner or real estate agent. The reported quality of an apartment is subjective. However, it is assumed that the three classes exhibit an ordinal scale and represent, on average, differences in quality levels reasonably well. The state variable has seven levels: 'First time use', 'New building' (but not rented for the first time), 'First time use after restoration', 'Restored', 'Modernized', 'Well-kept' and 'Renovated'. The three categories 'Restored', 'Modernized' and 'Renovated' are harder to interpret and are often used interchangeably. However, they can be distinguished as follows (Felix Mildner, 2019):

- 'Restored' usually means that the apartment or building was damaged or had a defect that had to be professionally repaired. Examples for this are damp basements or water damages.
- 'Modernized' means that the apartment or building is updated to current heating and/or insulation standards and also includes larger interventions.
- 'Renovated' apartments have undergone smaller or optical updates, which are not necessarily done by professionals. Examples are the installation of new floors or window blinds.

Other information, such as rent and area, is assumed to be correct, as there is no incentive to provide wrong information, as long as the advertisement is not fake. Suspicious outliers with unrealistic rent prices per m^2 (i.e. lower than 5 or higher than 50 EUR per m^2) were excluded from the final dataset.

6.2 Simulated Noise Levels of Georeferenced Apartments

Starting from 2011, the land use model has been run until the year 2016, which will serve as the reference year. Subsequently, travel demand for the whole Munich metropolitan

[1] https://www.immobilienscout24.de/

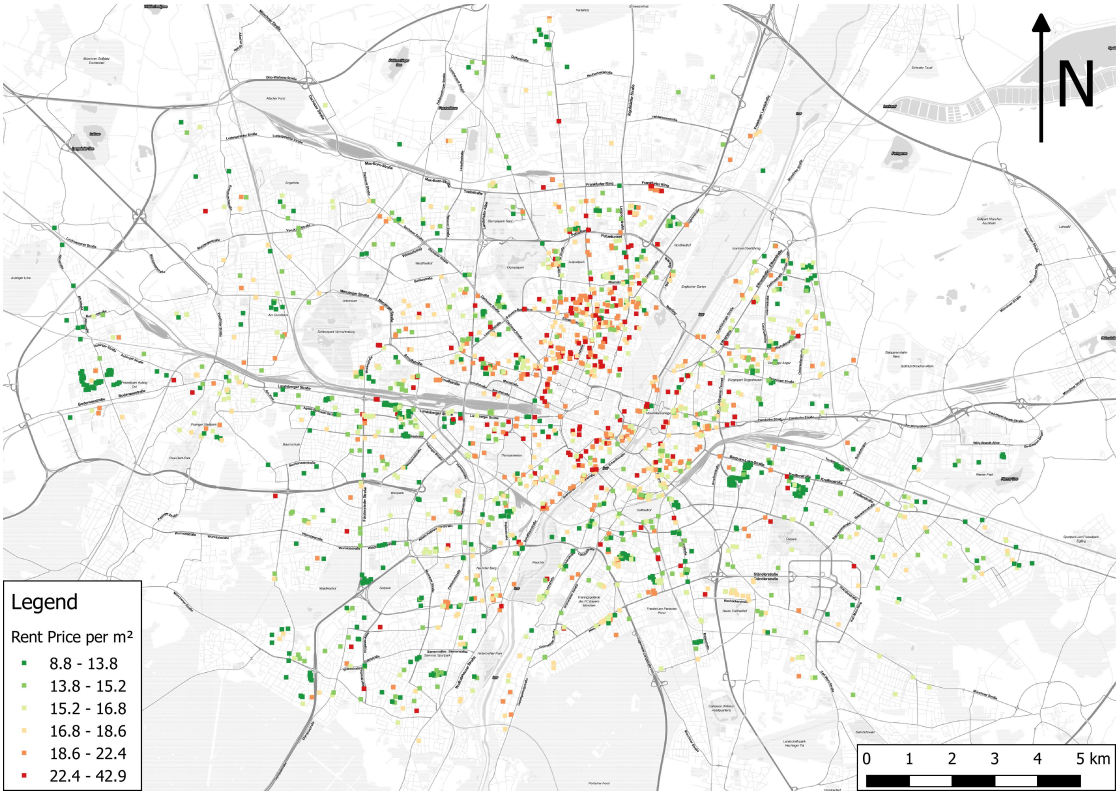

Figure 6.1: Apartment prices per square meter of the obtained records.

study area was generated using MITO. In total, around 8.8 million trips were created in MITO, of which around 3.5 million trips were made by car. A ten percent sample of all car trips was assigned in MATSim to get a trade-off between computational run time and reasonable results. The network capacities were scaled down accordingly. In total, 175,340 car trips were assigned. Since the travel demand provided by MITO is already a good starting solution that includes decisions on mode and departure time choice, only 100 iterations of MATSim were run for assignment and route choice. A previous study for the same study region confirmed the efficiency of this combination of sample size and the number of iterations (Llorca and Moeckel, 2019). Figure 6.2 shows the leg histogram for the simulated car users in the last iteration. It represents the number of agents that arrive, depart and are en route over the course of the day. One can identify a morning peak at 8 AM and an afternoon peak at around 4 PM. As it is shown, the assignment not only covers the peak hours but also gives reasonable traffic flows throughout the day, which is important for averaged daily noise levels. A simple representation of heavy-duty vehicles is included and has been disaggregated from German-wide aggregated commercial flows. For the remainder of this chapter, only the city of Munich itself will be analyzed. The simulation of the greater study area was still required to capture in- and outbound traffic. The focus on a single city for noise impact evaluation is necessary to get a more homogeneous data set, which inherits a more or less homogenous housing market. Rural

areas around Munich feature different housing markets in which the share of property owners is much higher compared to the share of tenants.

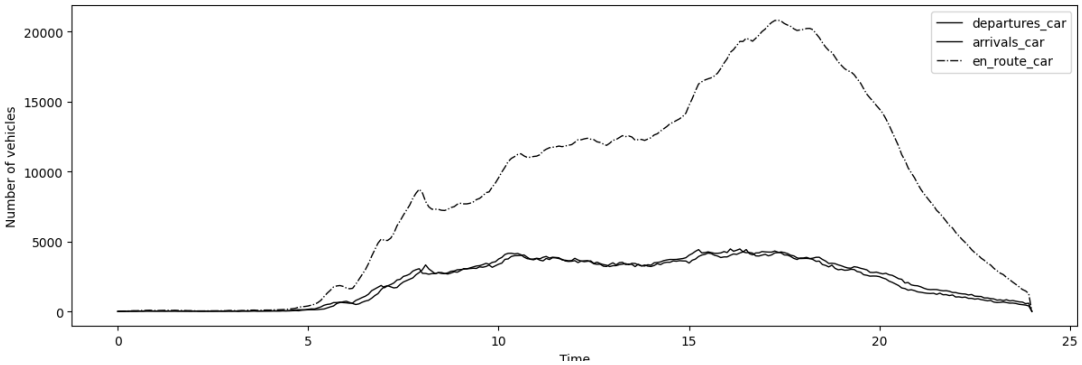

Figure 6.2: Leg histogram of the MATSim simulation

Noise levels of car traffic were obtained using the noise contribution of MATSim as described in chapter 3 with the updated RLS-19 approach and the shielding extension presented in chapter 5. Sound insulation of dwellings is hard to measure and not available in the dataset of apartments and was thus ignored. Most buildings in this area are built out of stone and have at least double-glazed windows, leading to comparable insulation levels. To get an average noise level for a whole day, immissions are expressed in weighted average L_{DEN} values as defined in equation 2.5. Figure 6.3 shows computed noise emission values for links in Munich during the eight AM peak hour. The maximum emission is 77 dB(A) and was observed on the outer motorway ring. The points in figure 6.3 represent the obtained apartment records. Their color is graduated based on L_{DEN} immission values. One can see that noise is highest along major roads and near the city center. Apartments in the outskirts show a lower L_{DEN} value.

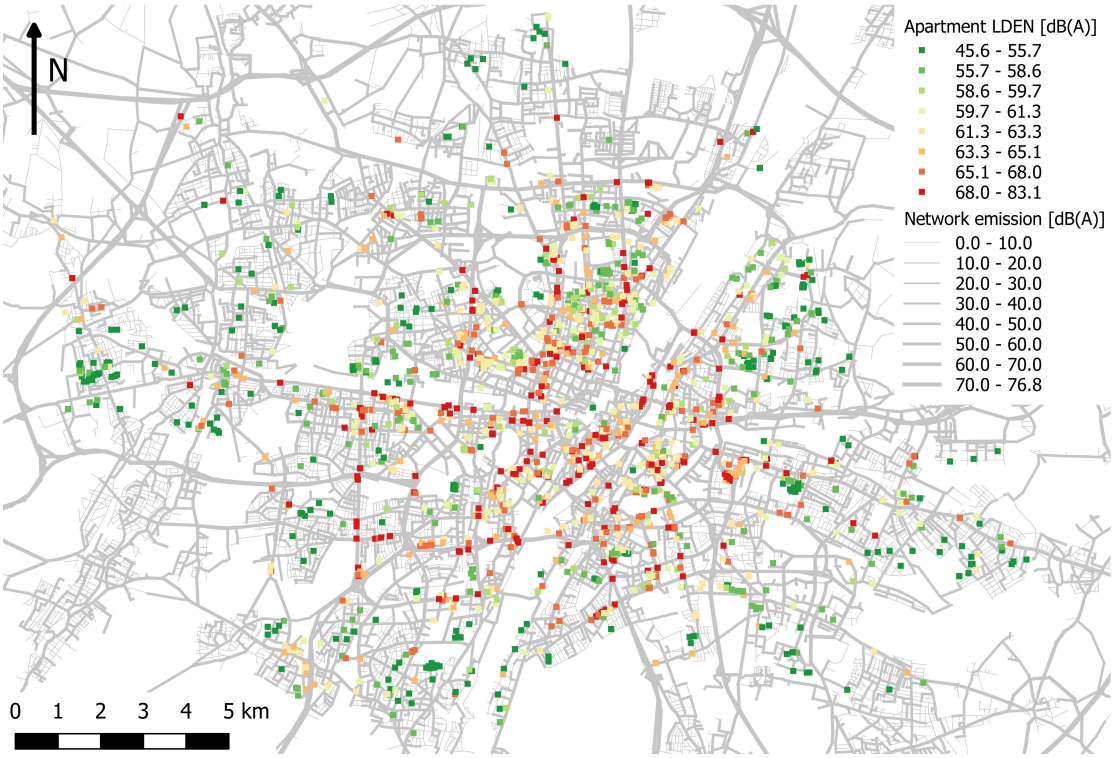

Figure 6.3: Apartment noise immission values.

6.2.1 Plausibility Analysis

So far, the presented noise model and its extensions have not been validated. Unfortunately, there are no available data from systematically measured traffic noise for Munich. However, the Bavarian Environmental Agency (BEA) publishes strategic noise maps as part of the fulfillment of the EU noise directive. Therefore, these data are used to check the simulated MATSim noise values for plausibility. The BEA data is published as a web map service (WMS)[2]. The service allows querying the underlying data via HTTP requests that include a *GetFeatureInfo* query[3]. Subsequently, all noise values at the geocoded locations of the apartments were queried one by one. This resulted in a total of 422 unique locations of apartments for which a reference value of the BEA was available.

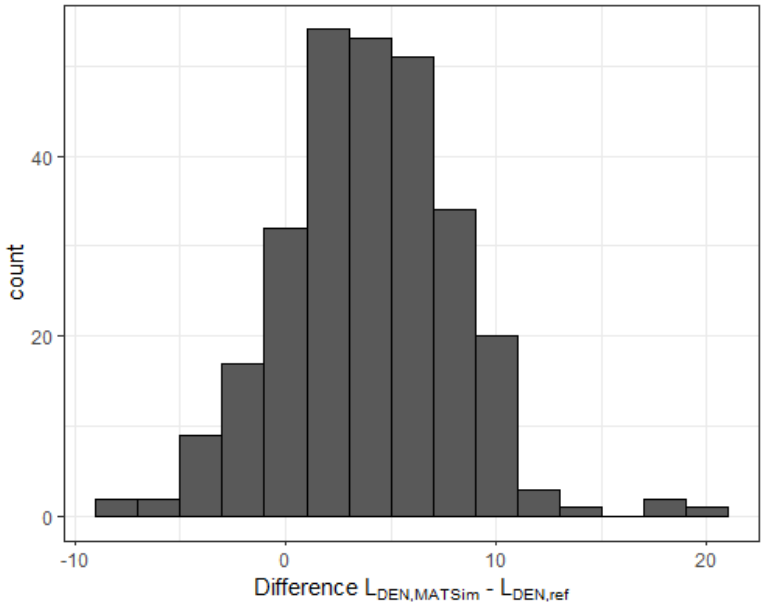

Figure 6.4: Histogram of differences of noise immission values $L_{\mathrm{DEN},MATSim} - L_{\mathrm{DEN},ref}$.

Figure 6.4 shows the distribution of differences between the simulated MATSim values $L_{\mathrm{DEN},MATSim}$ and reference values $L_{\mathrm{DEN},ref}$ from the BEA. One can see that the differences almost form an unskewed normal distribution. The mean is 3.93 dB(A) and the median is 3.65 dB(A), which suggests that the MATSim noise values on average overestimate immissions by 3 to 4 dB(A) when compared to the values obtained from the

[2] https://www.umweltatlas.bayern.de/mapapps/resources/apps/lfu_laerm_ftz/index.html?lang=de

[3] see https://geoportal.bayern.de/getcapabilities/CapabilitiesViewer?ows_url=https://www.lfu.bayern.de/gdi/wms/laerm/hauptverkehrsstrassen?&format=html&link=true for a description of available services. An example for the noise value at x=4465949 and y=5337789 would be: https://www.lfu.bayern.de/gdi/wms/laerm/hauptverkehrsstrassen?request=GetFeatureInfo&service=WMS&version=1.3.0&crs=31468&bbox=4465749,5337589,4466149,5337989&width=400&height=400&layers=mroadbylden&i=200&j=200&query_layers=mroadbylden&INFO_FORMAT=text/plain

BEA. While there seems to be a systematic offset, the general relation appears plausible, as can be seen in figure 6.5. The Pearson's correlation coefficient between both measures is $r = 0.68$, which can be considered moderately high.

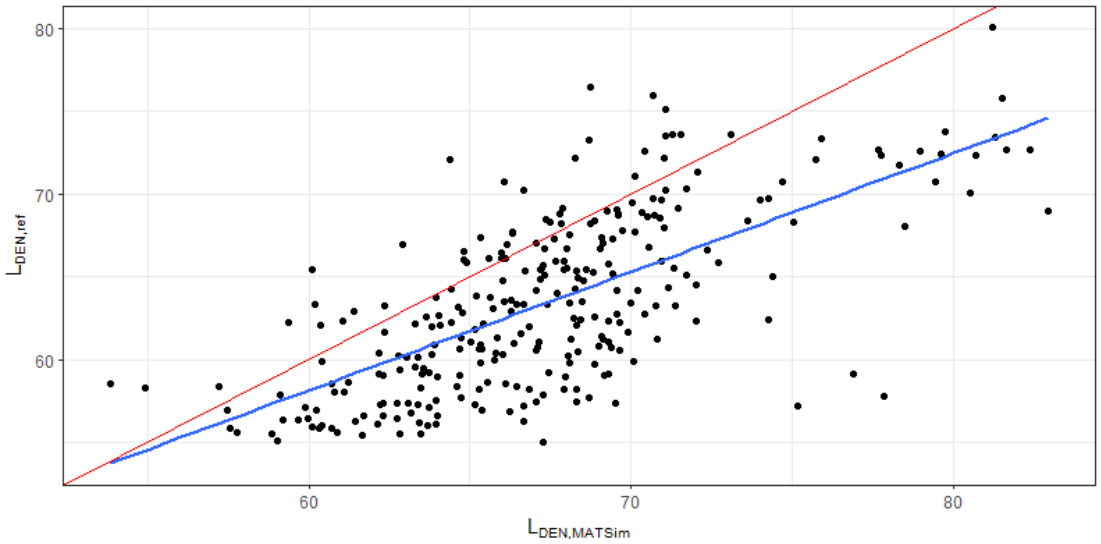

Figure 6.5: Scatter plot of $L_{\mathrm{DEN},ref}$ versus $L_{\mathrm{DEN},MATSim}$.

Figure 6.6 shows the spatial distribution of differences between $L_{\mathrm{DEN},MATSim}$ and $L_{\mathrm{DEN},ref}$. The figure does not suggest that the differences are clustered or form a specific spatial pattern at a large scale.

To put the bias in the differences in perspective, a difference of 3 dB is often seen as the lower bound of a considerable change in German law (BImSchV, 1990). Several reasons could lead to the systematic bias:

- The underlying traffic volumes and speeds are overestimated by the underlying simulation in MATSim. While the Munich model has been calibrated to represent volumes reasonably well, validation on speed was not possible as of yet.

- The BEA does not only have access to real-world traffic counts but also to better models of the built environment (i.e. buildings, noise protection walls). The OSM buildings used in the MATSim simulation often lack detail on the actual dwelling height and may systematically bias the shielding effect.

- The data from the BEA is based on the 'Vorläufige Berechnungsmethode für den Umgebungslärm an Straßen (VBUS, engl: Preliminary calculation method for environmental noise at roads)' from 2006, a preliminary guideline for the implementation of the EU environmental noise directive (see section 2.2). The VBUS is based on and similar to the RLS-90 guideline (Bartolomaeus and Schade, 2006). As discussed in section 5.2.1 and as can be seen in figure 5.4, the newly implemented RLS-19 assumes higher base emission values for cars that could explain a

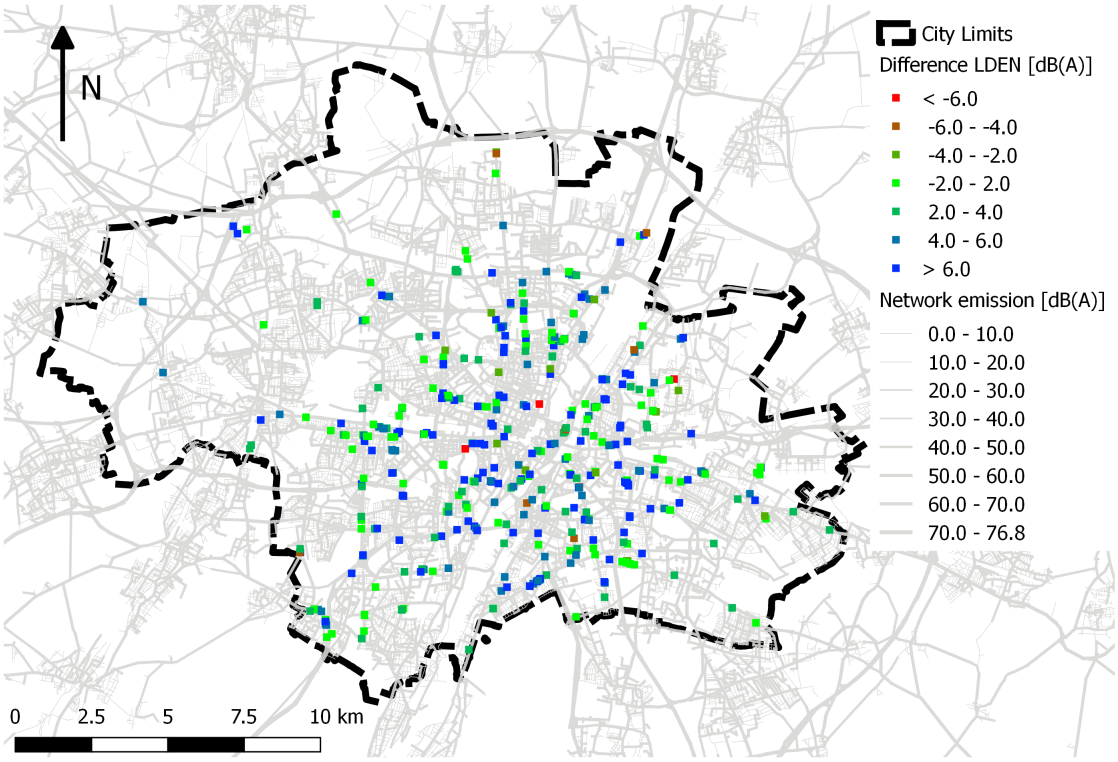

Figure 6.6: Spatial locations of differences of noise immission values $L_{\mathrm{DEN},MATSim} - L_{\mathrm{DEN},ref}$ and network noise emissions.

large share of the bias (roughly 3 dB[A] at speeds between 40-50 km/h, a common speed limit for primary roads).

- The data from the BEA only includes major roads with a volume above 8,200 vehicles per day. It is, therefore, possible that noise from roads with slightly fewer volumes is omitted (especially if the receiver point lies in a side road) and, thus, leads to a lower estimated noise value.

However, given that the mean difference is not prohibitively large, the correlation between both noise estimates is reasonably high and the data from the BEA is based on an older guideline, the simulated noise values are considered acceptable for the following analyses. It should be noted that the comparison with the BEA data cannot be seen as validation as they, too, are model outputs and no measured 'ground truth'. As emphasized by Wolde (2003) and Murphy and King (2010), differences of five decibels are not exceptional for outcomes of different calculation methods.

6.3 Microscopic Accessibility Indicators

To account for higher prices closer to the city center, accessibilities measures are commonly used (Xiao Y, 2017). Accessibility can be understood as the potential for inter-

action (Hansen, 1959). Various accessibility measures were tested, including distance to the Munich city center, zonal accessibilities and microscopic accessibilities (Ziemke et al., 2018). Based on model fit and reasonability of parameters, the latter was selected for this research. The simple distance to city center measure cannot capture the spatial structure of the city and ignores that some neighborhoods are connected better or worse than others. The microscopic accessibility measure was preferred over the zonal indicator to avoid spatial aggregation bias in larger zones. Ziemke et al. (2018) presented this microscopic accessibility measure, which is integrated into the MATSim framework and defined by the following logsum:

$$A_i = \frac{1}{\mu} \ln \sum_J e^{\mu \cdot v_{i,j}^{trav}} \tag{6.1}$$

Where A_i is the accessibility at location i, μ is a scale parameter and $v_{i,j}^{trav}$ is the (negative) utility of traveling from i to opportunity j. Note that i and j are microscopic places with x/y coordinates. The microscopic accessibility can be directly calculated within MATSim for either a grid or for defined points i. Ziemke et al. (2018) showed that opportunities j can be identified with data from OSM, which makes the accessibility measure easy to calculate and the method transferable to other study areas. Results suggest that this measure leads to intuitive patterns of accessibility. In this thesis, the microscopic accessibility indicator is used as the centrality measure. A data set of all amenities[4] that would typically be identified as activity locations (e.g. bars, shops, doctors, banks, etc.) was retrieved from OSM for the whole study area and used for the accessibility calculation in MATSim. The selection of OSM tags is shown in table 6.1. It is based on the accessibility extension by Ziemke et al. (2018) (in the version of [5]).

The resulting MATSim facilities for the accessibility calculation based on OSM amenities for the whole Munich study area are shown in figure 6.7. As expected, most amenities/facilities are located in the core cities. Facilities were collected for the whole study area to avoid boundary effects at the city limits of Munich.

Figures 6.8 and 6.9 show computed microscopic MATSim accessibilities of recorded apartments in Munich for the car and transit mode. Obviously, accessibility is the highest in the city center. However, the figure shows that accessibilities do not linearly decrease with increasing distance to the center. Although the logsum is hard to interpret, one can see that car accessibility, in general, is higher than transit accessibility, which suggests that car travel times are shorter for most relations.

[4] https://wiki.openstreetmap.org/wiki/Key:amenity

[5] https://github.com/matsim-org/matsim-libs/blob/01167ed5fc375c2802c8c8c95d0a0defa78b7380/contribs/accessibility/src/main/java/org/matsim/contrib/accessibility/utils/AccessibilityFacilityUtils.java#L301-L343

Table 6.1: OSM values for the 'amenity' tag used to identify amenities for accessibility calculations.

Group	Value
sustenance	'bar'
	'biergarten'
	'cafe'
	'drinking_water'
	'fast_food'
	'food_court'
	'ice_cream'
	'pub'
	'restaurant'
education	'college'
	'kindergarten'
	'library'
	'school'
	'university'
transportation	'charging_station'
	'fuel'
financial	'atm'
	'bank'
healthcare	'clinic'
	'doctors'
	'hospital'
	'pharmacy'
entertainment	'cinema'
	'theatre'
other	'place_of_worship'
	'police'
	'post_box'
	'post_office'
	'water_point'

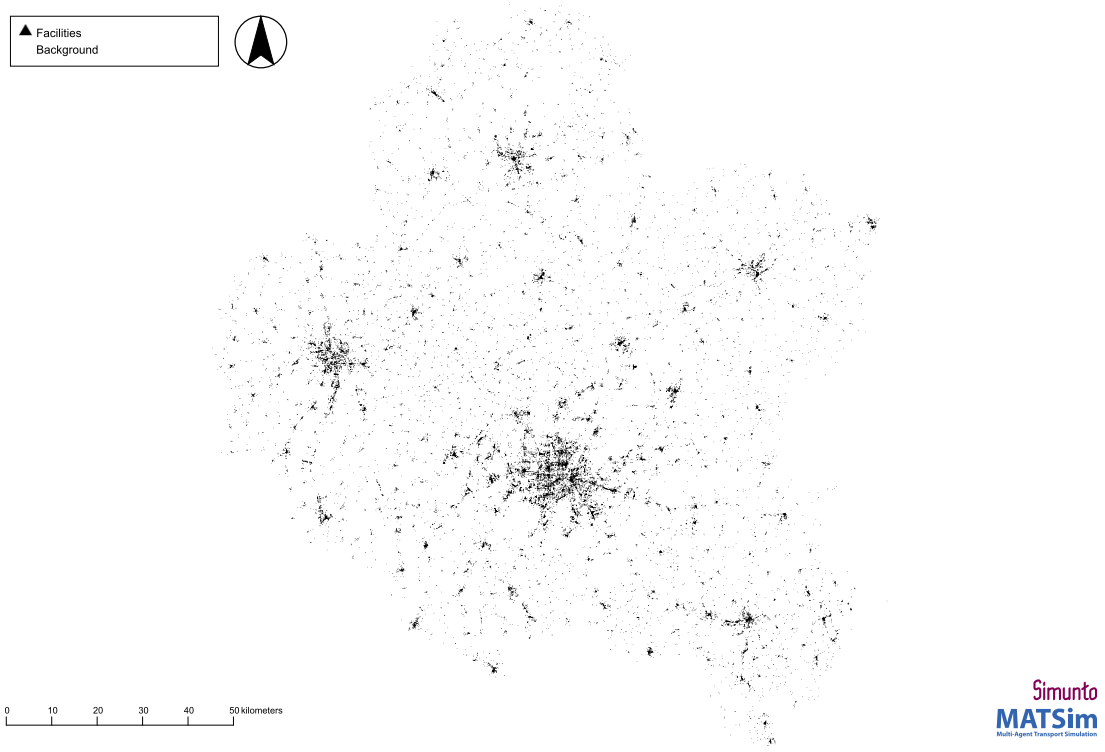

(a) Individual MATSim facilities

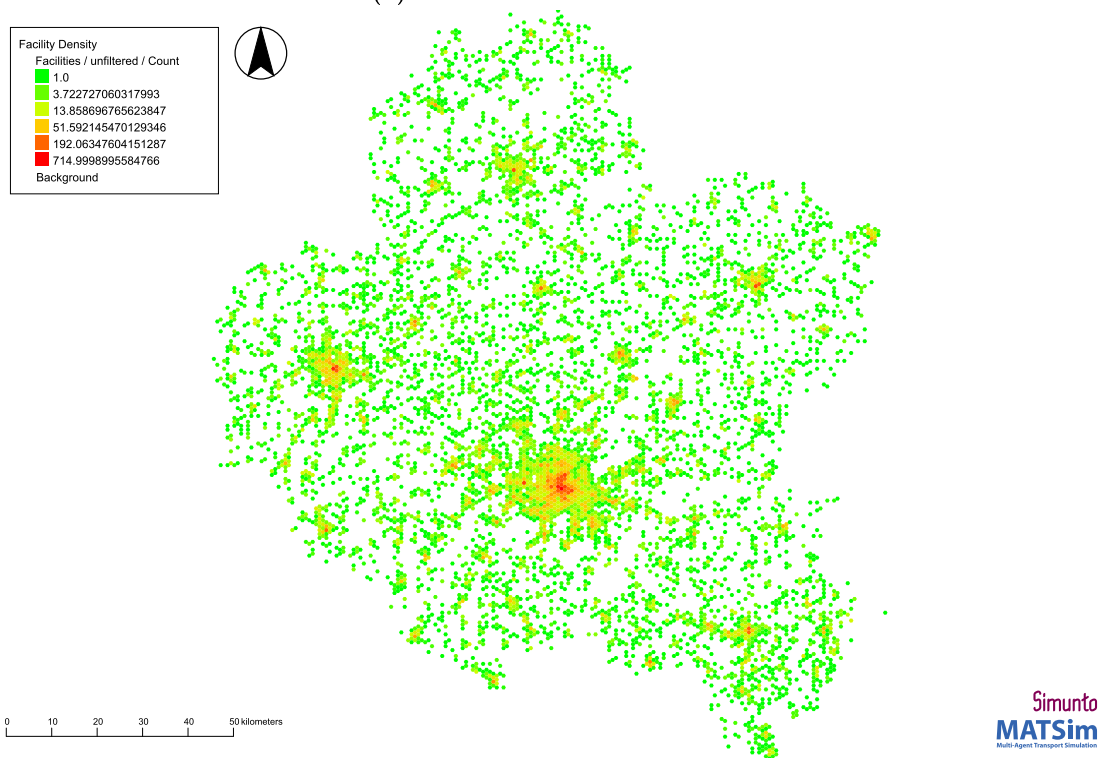

(b) Facility densities, based on logarithmic scale

Figure 6.7: MATSim faciltities converted from OSM amenities. a) individual facilities b) facility densities based on a hexagonal grid.

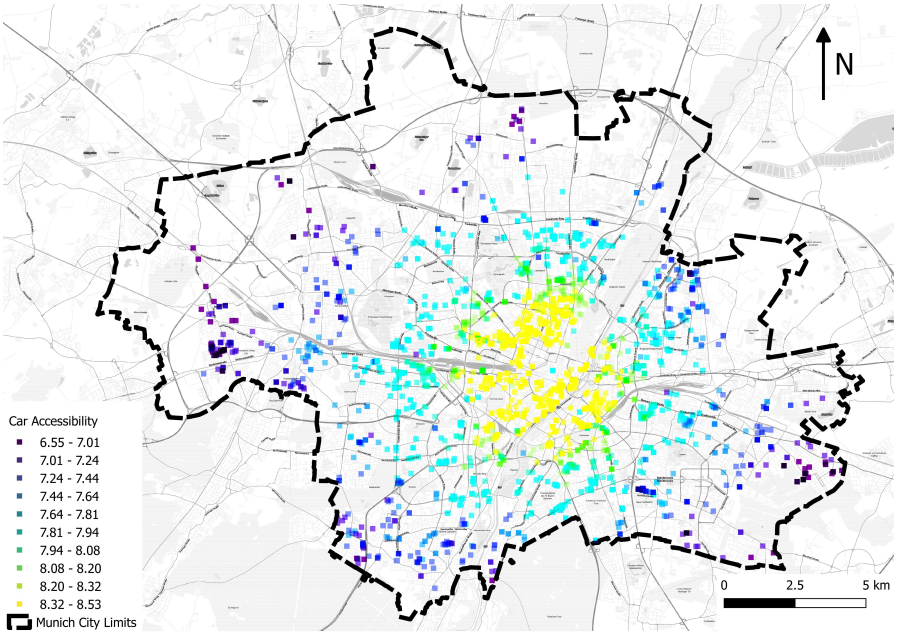

Figure 6.8: Microscopic Car accessibilities.

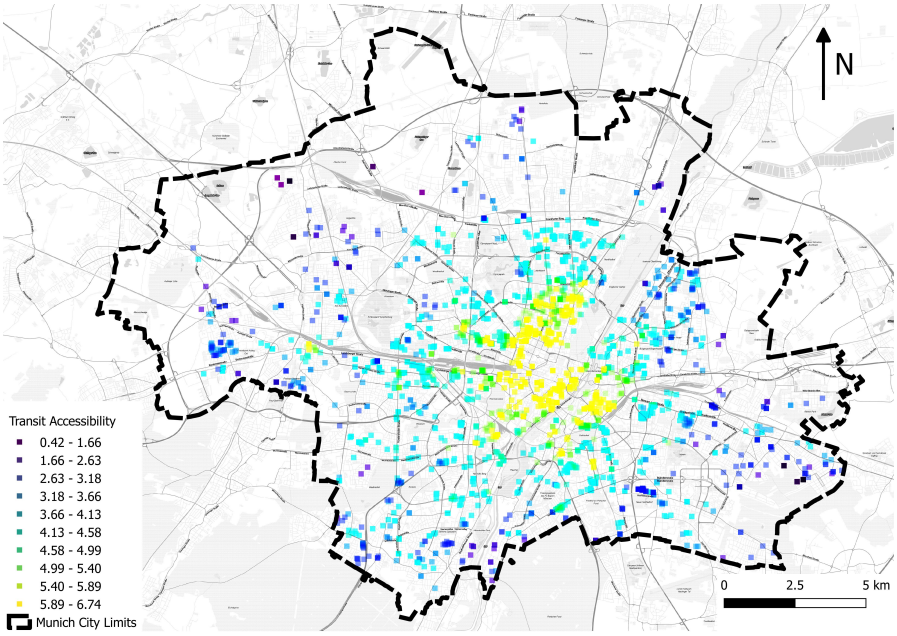

Figure 6.9: Microscopic transit accessibilities.

6.4 Hedonic Pricing of Noise Impacts on Apartment Prices

Hedonic pricing is used to estimate the impact of simulated traffic noise on rent prices. The theory was described by Rosen (1974). The idea is that in a competitive market, the value of a composite good can be decomposed such that every component can be attributed to an individual implicit value as a contribution to the total value. In the case of real estate properties, differences in price can therefore be explained by the different attributes of each property. In the overview of Bateman et al. (2001), four groups of explanatory variables are identified:

- Structural variables (level, number of rooms)
- Accessibility variables (distance to city center, travel time to various points of interest)
- Neighborhood variables (crime/ unemployment rates)
- Environmental variables (noise, pollution)

To infer the value of each component, multiple linear regression can be used:

$$y = \alpha + \beta_1 \cdot x_1 + \beta_2 \cdot x_2 + \ldots + \beta_n \cdot x_n + \epsilon \tag{6.2}$$

Where y is the response variable or composite good. The parameter α is a constant term and $\beta_{1\ldots n}$ are estimated parameters for the predictor variables $x_{1\ldots n}$. The error term ϵ accounts for variation that cannot be explained by the included predictor variables and follows an independent identically distributed normal distribution with a mean of 0. In this simple linear form, the change of one unit of x_k would lead to a change of β_k units of y, all else held constant. In cases where a simple linear relationship is not justified, transformations to either response or predictor variable can be applied. Two commonly used transformed models are the log-log-model and the semi-log model (Xiao Y, 2017). In a log-log-model, predictor and response are transformed by taking the logarithm:

$$ln(y) = \alpha + \beta_1 \cdot ln(x_1) + \beta_2 \cdot ln(x_2) + \ldots + \beta_n \cdot ln(x_n) + \epsilon \tag{6.3}$$

In a log-log formulation, the impact of a predictor can be interpreted as a (price) elasticity (von Auer, 2016):

$$\text{percentage change of response} = \beta \cdot \text{percentage change of predictor} \tag{6.4}$$

Log-log relations can only be applied to positive continuous variables. In the semi-log model, only the response variable is transformed by the logarithm:

$$ln(y) = \alpha + \beta_1 \cdot x_1 + \beta_2 \cdot x_2 + \ldots + \beta_n \cdot x_n + \epsilon \tag{6.5}$$

The semi-log model thus allows the incorporation of dummy variables. For small β, the relation between response and the predictor is a semi-elasticity (von Auer, 2016):

$$\text{percentage change of response} = \beta \cdot 100 \cdot \text{change in the predictor} \tag{6.6}$$

This makes the semi-log relation very convenient to infer the NSDI when noise is used as a continuous variable:

$$\text{NSDI} = \beta_{noise} \cdot 100 \tag{6.7}$$

Where β_{noise} is the estimated noise coefficient. In addition to using noise as a continuous variable, the impact of a categorical classification of noise was evaluated. As Theebe (2004) pointed out, a noise level of 55 dB(A) can be identified as the ambient noise level from which housing prices start to decrease. Similarly, 55 dB(A) is the level at which noise annoyance among residents is reported to rise (Ouis, 2001). This was confirmed when plotting rent prices against noise. Multiple re-classifications and re-estimations of the models based on model fit and coefficient significance led to the four noise categories low, moderate, loud and very loud noise. Low noise is used for immission values below the 55 dB(A) threshold. The moderate noise category describes values from 55 to 65 dB(A), loud noise is defined between 65 and 75 dB(A) and very loud is defined for values above 75 dB(A). The calculated accessibility measures show a moderate correlation with noise with a correlation coefficient of 0.48 and 0.37 for car and transit accessibility, respectively. While the correlation between independent variables is undesired in regression analyses, this fairly moderate correlation is accepted to represent the positive impacts of road infrastructure and to prevent introducing an omitted variable bias. However, car and transit accessibility have a high correlation of 0.85. Therefore, it was decided to drop the transit accessibility to obtain more precise estimates. The car accessibility is better suited, as the accessibility variable is meant to account for the positive impact of *road* infrastructure, which may not correlate as well with transit accessibility, which focuses on individual access points and also includes rail and subway access. When including both accessibilities into the model, the resulting coefficients did not change significantly, which is why the more parsimonious model that only includes car accessibility was preferred. The variables level and construction year turned out to be not significant. The number of rooms and the area of the apartment provided similar explanatory power and could be used interchangeably. However, those two variables were highly correlated, and the more significant variable, namely area, was chosen. Obviously, the data set does not include all variables that influence the rent price. It is assumed that those excluded variables distribute randomly across all observations, and thus, are absorbed by the error term.

Two different models are presented. Both of them include the log-transformed area, the accessibility variables and the quality and state of the apartment as dummy variables. The difference between both models is that one uses noise as a continuous variable while the other one makes use of the categorical classification. Table 6.2 shows the selected variables and their usage in the models. Area is log-transformed, while the other variables

Table 6.2: Selected variables and descriptive statistics for the hedonic pricing model.

Variable	Unit	Min	Max	Mean	n (N=3,144)	Used in model
Area	m^2	14	278	70.1		both (log transformed)
Noise (L_{DEN})	dB(A)	45.61	83.05	61.84		1
Low noise	Dummy				322	2 (baseline category)
Moderate noise	Dummy				2000	2
Loud Noise	Dummy				733	2
Very Loud Noise	Dummy				89	2
Microscopic car accessibility	-	6.54	8.52	7.91		both
Quality: Average	Dummy				1,063	both
Quality: Superior	Dummy				2,178	both (baseline category)
Quality: Luxury	Dummy				289	all
State: First time use	Dummy				434	both (baseline category)
State: New building	Dummy				764	both
State: First time use after restoration	Dummy				256	all
State: Restored	Dummy				85	both
State: Modernized	Dummy				171	both
State: Well-kept	Dummy				915	both
State: Renovated	Dummy				519	both

form a semi-log relation with the response variable. Multiple combinations by trial and error led to the decisions of which transformations were applied based on coefficient significance and model fit. The response variable in this study is the total monthly rent for an apartment.

6.5 Results of the OLS Model

The results of the two specified models are shown in table 6.3. All variables are significant at least at the 99.9% level. Robust standard errors were used to account for heteroscedasticity in higher rent price ranges. Both models show similar and reasonable estimates for area and quality. The area of an apartment has a positive impact on the total rent price. Because of the log-log relation between predictor and response variable, the estimator cannot be directly interpreted as price per square meter. Following equation 6.4 and using estimates of table 6.3, a 1% change in area is thus reflected in a change in rent price between 0.7705% and 0.7706%, depending on the selected model. This non-linear relationship means that prices per m^2 are not constant and decrease at higher area levels. This finding was verified by plotting rent price against area. The estimates for quality show expected signs for 'Luxury dwelling quality' and 'Average dwelling quality', with 'Superior dwelling quality' being the baseline. According to equation 6.5, a luxury apartment is rented for a roughly 17% higher price compared to superior apartments. Average apartments are rented for 14% less. The adjusted R^2 of both models are similarly high, with a value of about 0.86.

Microscopic car accessibility shows stable estimates across both model formulations. For each unit increase of the microscopic accessibility, prices increase by about 22%. The model that uses noise as a continuous variable shows a noise estimate of -0.0046. Equation 6.7 leads to an NSDI of 0.46. An increase of 1 dB(A) thus refers to a discount of 0.46% in rent prices. The minimum modeled noise level for an apartment is around 45 dB(A), while the maximum is 83 dB(A). The maximum implicated price difference between the loudest and the quietest apartment is (83 dB – 38 dB) * 0.46 = 21%. When noise is used as a categorical variable, a price discount of 10% for very loud apartments can be found. For loud and moderately noisy apartments, the discount is 5.8% and 3.6%, respectively.

Figure 6.10 shows a plot of predicted against actual values of the model that uses noise as a categorical variable (model 2 in table 6.3) differentiated by apartment quality. It can be seen that the linear fit matches well, although the variance of residuals increases with rent level, especially for luxury apartments with prices above 2.000 EUR. This could be explained by the fact that exclusive, high-quality apartments may feature a higher variance in rent prices, caused by unobserved (exclusive) variables such as concierge services, shared gyms or whirlpools. The model gives a reasonable linear fit for the majority of apartments with a price below 2.000 EUR.

The author tends to favor the second model, which uses noise as a categorical variable. It is more reasonable that noise levels below the 55 dB(A) threshold do not have an impact on price. Also, having noise as a continuous variable pretends an accuracy that is not reflected in the applied simulation approach. The microscopic accessibility measure is assumed to be more accurate than zonal accessibility that has been used initially for this study, especially for larger zones. In an earlier estimation, the noise estimates had a substantially higher p-value and were less significant when zonal accessibility was used. In fact, microscopic accessibility overcomes the issues that results are influenced by zone size. As the required input data is solely dependent on open source data from OSM, it is easy to transfer this approach to different study areas.

The accessibility measure can be seen as a confounding variable that avoids biases for the estimates of noise. Accessibility is positively correlated with noise and price and noise is negatively correlated with price. Omitting the accessibility measure, therefore, leads to an underestimation of the negative impact of noise. When omitting any accessibility measure from the estimation, the noise estimate yields a positive change of 0.2% in rent prices per decibel, which shows the positive bias. This is confirmed by Maslianskaïa-Pautrel and Baumont (2016), who found that accessibility prevails over noise disturbance when evaluating the impact of road infrastructure on prices. When including the confounding variable, possible issues of multicollinearity that reduce the precision of estimates need to be analyzed. A common measure for this is the Variance Inflation Factor (VIF) which can detect collinearity among predictor variables in multiple linear regression models (Belsley et al., 1980). It is calculated by running a regression on each predictor against all other predictors and should ideally have a value of 1 in the

Table 6.3: Estimation Results of the hedonic pricing model.

	Dependent variable: log(rent)	
	Model (1)	Model (2)
log(area)	0.7705*** (0.0077)	0.7706*** (0.0077)
noise	-0.0046*** (0.0006)	
low noise		0 (Base)
moderate noise		-0.0360*** (0.0103)
loud noise		-0.0583*** (0.0127)
very loud noise		-0.1005*** (0.0243)
microscopic car accessibilities	0.2272*** (0.0091)	0.2165*** (0.0091)
Parking available	0.0183 ** (0.0070)	0.0180** (0.0070)
Quality: Luxury	0.1666*** (0.0114)	0.1678*** (0.0114)
Quality: Superior	0 (Base)	0 (Base)
Quality: Average	-0.1433*** (0.0082)	-0.1430*** (0.0083)
State: First time use	0 (Base)	0 (Base)
State: New Building	-0.0340*** (0.0096)	-0.0298** (0.0097)
State: First time use after restoration	-0.0817*** (0.0122)	-0.0815*** (0.0124)
State: Restored	-0.1021*** (0.0214)	-0.1020*** (0.0215)
State: Modernized	-0.1179*** (0.0151)	-0.1171*** (0.0152)
State: Well-kept	-0.1589*** (0.0106)	-0.1580*** (0.0108)
State: Renovated	-0.1694*** (0.0114)	-0.1697*** (0.0115)
constant	2.4031*** (0.0753)	2.2390*** (0.0798)
Observations	3,145	3,145
R2	0.8597	0.8552
Adjusted R2	0.8591	0.8545
Residual Std. Error	0.1783	0.1757
F Statistic	1,213	1,124

Note:Signif. codes: '***' 0.001 '**' 0.01 '*' 0.05 '.' 0.1 ' ' 1 robust SE in (brackets)

Figure 6.10: Predicted versus actual plot of rent prices.

case of no multicollinearity. A typical cutoff point for problematic cases is a VIF greater than 5 (Craney and Surles, 2002). Table 6.4 shows VIFs for the used predictors in model 2. All values are close to 1, which suggests that multicollinearity is not a problem in the fitted model.

Table 6.4: Variance inflation factors.

Variable	VIF Model (1)	VIF Model (2)
log(area)	1.21	1.22
noise	1.35	
low noise		(Base)
moderate noise		3.42
loud noise		3.52
very loud noise		1.40
microscopic car accessibilities	1.59	1.65
Parking available	1.39	1.39
Quality: Luxury	1.14	1.14
Quality: Superior	(Base)	(Base)
Quality: Average	1.46	1.46
State: First time use	(Base)	(Base)
State: New Building	2.34	2.34
State: First time use after restoration	1.57	1.58
State: Restored	1.23	1.24
State: Modernized	1.47	1.49
State: Well-kept	2.97	3.01
State: Renovated	2.14	2.16

6.6 Spatial Considerations

Newer studies point out that studies in spatial contexts may need to account for spatial relationships explicitly. The underlying idea has become known by Tobler's first law of geography, which states that 'everything is related to everything else, but near things are more related than distant things' (Tobler, 1970, p. 236).

The process of model selection includes multiple steps. First, the results of the OLS regression are used to spatially locate the residuals of the fitted values to have a first impression of whether spatial patterns are present. Figure 6.11 reveals that while the residuals look scattered at first glance, some local clusters can be observed, which suggests that a spatial model could be applied.

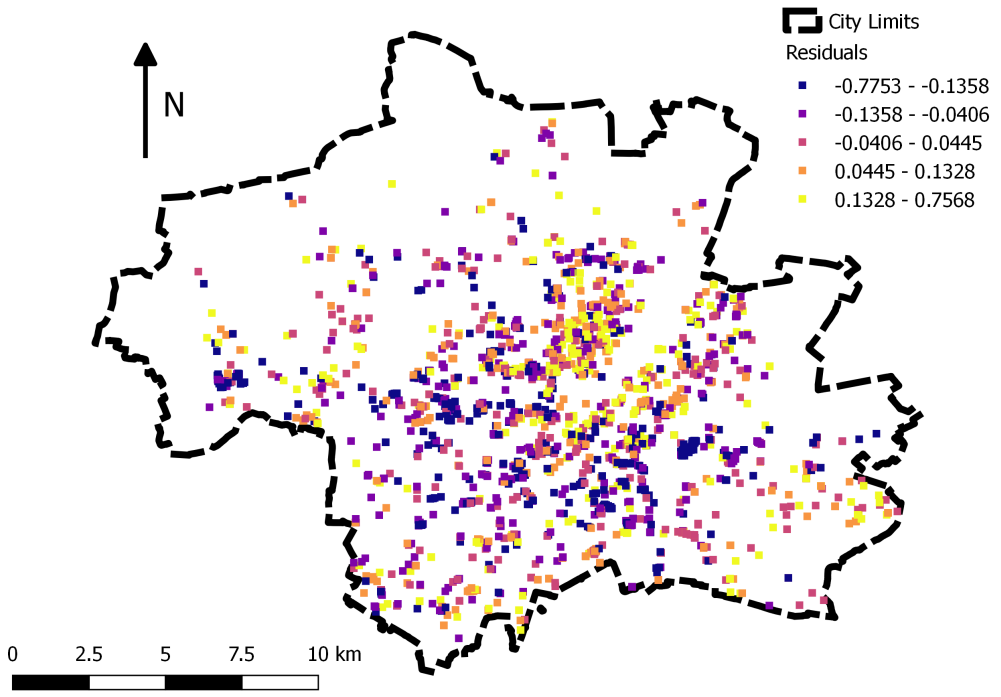

Figure 6.11: Residuals of fitted values for the OLS model with a continuous noise variable. The results when using a categorical variable are virtually the same.

Two approaches that have been applied in recent times are:

1. Geographically Weighted Regression (GWR) models allow insight into local dependencies. Here, each dependent variable will have a distribution of estimates resulting from multiple individual estimations at different locations, taking differ-

ent neighbors into account. As such, the dependent variable's impact may change and can be different across space.

2. Spatial Econometric Models aim to take into account spatial dependencies by applying interaction terms that make neighbors influence each other. These models rely on the definition of a spatial weights matrix and assume a 'global' relationship between dependent and independent variables, i.e. similar to the ordinary least squares regression, there will only be global estimates for each independent variable.

A brief introduction followed by the application will be given for both types of spatial models in the following subsections.

6.6.1 Geographically Weighted Regression

One of the first descriptions of GWR has been given by Brunsdon et al. (1996). The idea is that the coefficients of the independent variables are allowed to vary over space heterogeneously ('spatial nonstationarity'). This follows up to the observation by Fotheringham et al. (1996), who found significantly varying relationships over space that are obscured by 'global' estimates and that these variations can be quite complex, which invalidates simpler linear approaches. Therefore, for each observation, an individual regression is applied in which only the nearest observations are taken into account, each weighted by distance. The approach can be formulated as:

$$y_i = X\beta_i + \epsilon_i, \tag{6.8}$$

i.e. multiple regressions dependent on the location/observation i are defined. For estimation, the weighted least squares method is used, which gives different weights to each observation when trying to minimize the sum of squared differences between actual and predicted y_i. Whereas typical weighted regressions apply a fixed weight for each observation, the weights in the GWR model depend on the location of estimation i and usually decrease with distance. For application in the present study, the 'GWmodel'[6] (Gollini et al., 2015) R package is used. The package offers multiple 'kernel' functions that define the distance decay. In the results presented here, an exponential distance decay function of the form $w_{i,j} = e^{-\beta \cdot d_{i,j}}$ is used to determine the weights. In addition to the kernel function, a bandwidth for the selection of a subset of neighbors has to be defined. This bandwidth can either be a fixed distance in which observations are still taken into account or an adaptive number of nearest neighbors. Here, the adaptive bandwidth is chosen to ensure that every observation has enough neighboring observations. An automatic bandwidth selection was utilized to minimize the Akaike Information Criterion (AIC), which is a common indicator to compare model performance, with a lower value indicating a better fit. The selection process returns an adaptive bandwidth of 171, meaning that for each regression at an observation, the 171 nearest neighbors are taken into account. Using the exponential kernel function and an adaptive bandwidth of 171,

[6] https://cran.r-project.org/package=GWmodel

a robust version of the GWR was applied to the dataset to reduce the impact of outliers and heteroscedasticity.

The results are shown in tables 6.5 and 6.6 for the continuous noise variable model and the one using a categorical variable, respectively. Note that since the number of estimates per variable equals the number of observations, one actually obtains a distribution of estimates.

It becomes obvious that the order of magnitude of estimates stays similar to the results of the simple OLS regression, which are close to the median values in many cases. However, it has to be noted that quite a few variables vary strongly. Some of these even have unintuitive changes in sign (e.g. the categorical noise variables, the accessibility variable and the parking availability variable). The R^2 increases in both model formulations (from 0.8591 to 0.889 for the continuous noise model and from 0.8545 to 0.891 in the categorical noise model formulation), which suggests that the GWR models better explain variation in rent prices when compared to the OLS models.

The distribution of noise estimates for both models is shown in figure 6.12. While the overall trend confirms a negative association between traffic noise and rent prices, here, too, it can be seen that the estimates vary strongly. For example, the loudest noise category's estimates vary from -0.3 to 0.7, which, following the semi-elasticity, would imply price differences between -30% and +70% for very loud apartments. Similarly, the continuous noise variable estimates imply NSDI values ranging from -1% difference in rent per decibel increase to +0.4% difference in price per decibel. Similar strong changes can be seen in the accessibility variable, as is shown in tables 6.5 and 6.6.

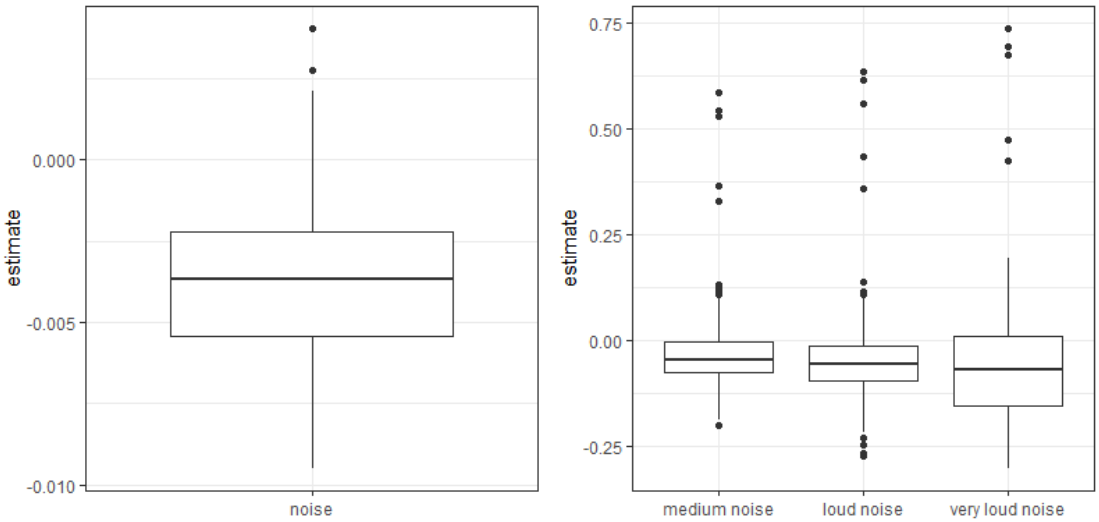

Figure 6.12: Distribution of estimates of the continuous noise variable model (left) and the categorical noise variable model (right).

Table 6.5: Estimation Results of the GWR with a continuous noise variable.

	Dependent variable: log(rent)				
	Min	1st Quantile	Median	3rd Quantile	Max
log(area)	0.5230559	0.7602276	0.7756313	0.7927283	0.8245
noise	-0.01	-0.005	-0.004	-0.002	0.004
microscopic car accessibilities	-1.167	0.201	0.232	0.274	0.444
Parking available	-0.094	-0.004	0.006	0.023	0.054
Quality: Luxury	0.126	0.165	0.176	0.188	0.367
Quality: Superior			0 (Base)		
Quality: Average	-0.305	-0.175	-0.151	-0.129	-0.003
State: First time use			0 (Base)		
State: New Building	-0.247	-0.044	-0.032	-0.018	0.059
State: First time use after restoration	-0.142	-0.1	-0.078	-0.032	0.138
State: Restored	-0.220	-0.126	-0.109	-0.087	0.005
State: Modernized	-0.373	-0.134	-0.119	-0.091	-0.033
State: Well-kept	-0.246	-0.169	-0.154	-0.130	0.007
State: Renovated	-0.291	-0.196	-0.159	-0.117	-0.0161
constant	1.038	1.880	2.209	2.551	14.847
Observations	3,145				
R2	0.895				
Adjusted R2	0.889				
AIC	-3228.928				

Table 6.6: Estimation Results of the GWR with a categorical noise variable.

	Dependent variable: log(rent)				
	Min	1st Quantile	Median	3rd Quantile	Max
log(area)	0.539	0.758	0.773	0.790	0.819
low noise			0 (Base)		
medium noise	-0.201	-0.078	-0.046	-0.004	0.584
loud noise	-0.275	-0.097	-0.058	-0.015	0.632
very loud noise	-0.304	-0.154	-0.069	0.007	0.736
microscopic car accessibilities	-1.470	0.199	0.225	0.269	0.396
Parking available	-0.094	-0.005	0.004	0.022	0.050
Quality: Luxury	0.121	0.164	0.175	0.187	0.387
Quality: Superior			0 (Base)		
Quality: Average	-0.300	-0.174	-0.151	-0.129	-0.007
State: First time use			0 (Base)		
State: New Building	-0.239	-0.039	-0.028	-0.011	0.048
State: First time use after restoration	-0.145	-0.105	-0.074	-0.041	0.069
State: Restored	-0.189	-0.127	-0.107	-0.084	0.011
State: Modernized	-0.378	-0.134	-0.115	-0.095	-0.030
State: Well-kept	-0.252	-0.170	-0.153	-0.122	0.026
State: Renovated	-0.283	-0.200	-0.166	-0.110	-0.005
constant	1.000	1.76	2.093	2.369	16.632
Observations	3,145				
R2	0.898				
Adjusted R2	0.891				
AIC	-3284.697				

While many studies find similar phenomena of strongly varying coefficients, including the flip of signs, especially for spatially correlated/ neighborhood explanatory variables (Hiebert and Allen, 2019; Dziauddin and Idris, 2017; Zhang et al., 2021; Tomal, 2020), it is often presented uncommented.

Guo et al. (2008) show that the optimal bandwidth selection based on the AIC may lead to small bandwidths, which overfit the model and lead to high coefficient variability. Similarly, Chang Chien et al. (2020) find that their applied GWR 'exacerbate[s] local collinearity between covariates, both overfitting and underfitting the model with highly varied and localized results' (Chang Chien et al., 2020, p. 1). Strong fluctuations of coefficients as a sign of overfitting have also been described by Fotheringham et al. (2002), who report that smaller bandwidths produce more tight estimators but may also result in extreme coefficients. Wheeler (2007) shows that the issue of local collinearity can lead to contradictive signs even when there is no 'global' collinearity between the explanatory variables. Another issue is that in the case of predictor variables with little local spatial variation (which is common in shared neighborhood attributes), collinearity with the intercept may be present (Gollini et al., 2015). Lastly, local collinearity may lead to the prediction of spatial patterns where they are not present in reality (Páez et al., 2011).

The problem can be intuitively visualized. For dense neighborhoods, the bandwidth may not cover a large area. Since noise (or accessibility) can also be interpreted as environmental variables, these may change slowly and gradually over space. This means that for small bandwidths, the local regression may not have much variation in these predictors in the included observation points and thus fails to attribute price variations to these variables. For example and as shown in table 6.2, only 89 out of 3,144 observations fall into the 'very loud' noise category, which means that a lot of local regression points will not assign influential weights to observations that are exposed to this noise category.

Gollini et al. (2015) and Lu et al. (2014) present multiple criteria and rule-of-thumb cutoff values that can be investigated to detect multicollinearity issues:

- local correlations between predictors should be lower than 0.8
- local VIF values should be lower than 10
- local Variance Decomposition Proportions (VDP) should be lower than 0.5
- local (design matrix) Condition Numbers (CN) should be lower than 30

Two of these are presented in figure 6.13. With the exception of very few outliers, the local VIF values do not suggest systematic collinearity issues between predictors. However, the map of local CNs shows that all local regressions largely exceed the cutoff value of 30 (median value is 134.2). As pointed out by Gollini et al. (2015), the VIF does not capture collinearity between predictors and the intercept, while the CN does. In fact, the accessibility variable and the local intercept both show very high VDP values (mean

values 0.966 and 0.977), which suggests that problematic collinearity may be present among them.

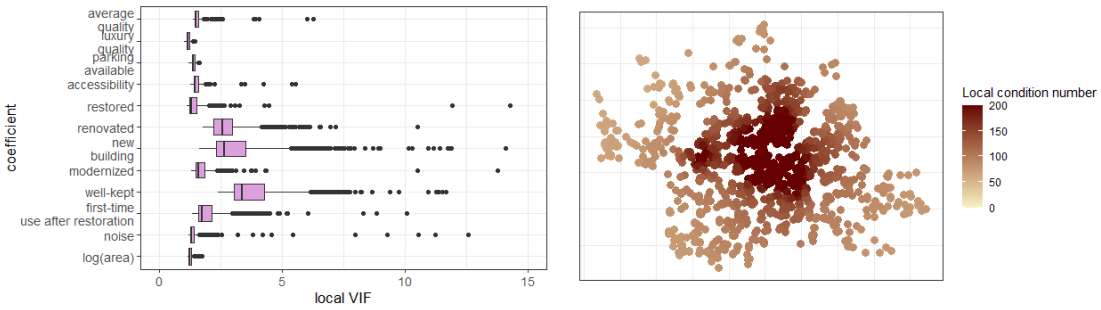

Figure 6.13: Local VIF values for each predictor (left) and local condition numbers (right) for the model using the continuous noise variable.

Multiple approaches can be considered to alleviate the issues of overfitting, local collinearity and strongly varying coefficients:

- Choose different bandwidths to avoid overfitting and 'smooth' the spatial pattern of estimates. This is also stressed by Gollini et al. (2015), who point out that the automatic bandwidth selection is based on the best model fit (i.e. best prediction of the response variable) and not on the accurate prediction of the coefficients.
- Mixed Geographically Weighted Regression (M GWR) can be used to fix certain variables for which a 'global' estimation is obtained and spatial homogeneity is assumed. Even more complex, multi-scale geographically weighted regression (MS GWR) makes use of different bandwidths for each predictor to account for the different spatial scales on which predictor coefficients may change.
- Locally Compensated Ridge Geographically Weighted Regression (LCR GW) aims to keep the coefficients more stable by adding local bias to the estimates such that high slopes are penalized. Thereby the estimates will be biased, but the standard errors are reduced and overfitting is avoided.

Monte-Carlo tests can be used to test whether parameter estimates change significantly over space, i.e. to test whether a predictor can be considered stationary or non-stationary (Lu et al., 2014). In the presented models, the test is significant for all variables, indicating that all variables show a spatial pattern of variation.

The LCR GW is a variant of ridge regression in which the ridge value λ varies locally for each regression point and is only applied when the CN is higher than 30 (or any configurable threshold). In these cases, λ is chosen such that the CN equals 30. In ridge regression, the estimation not only minimizes the residual sum of squares but in addition a penalty term $\lambda \cdot \beta^2$ is added, such that higher estimators β will receive a higher penalty.

This way, the magnitude of λ can be interpreted as a 'desensitization' parameter. If λ equals zero, the estimation yields the same results as the OLS estimation. As λ goes towards positive infinity, the estimator β goes towards zero. Details on the LCR GW estimation process are given by Gollini et al. (2015).

Results for the LCR GW regressions are presented in tables 6.7 and 6.8. While the R^2 values remain virtually the same, it becomes obvious that coefficients vary less when compared to the initial GWR results. In fact, there is no more sign flip in the accessibility variable and the extreme magnitudes of minimum and maximum estimates for noise, accessibility and intercept have considerably decreased as expected.

The reduced variance of coefficient estimates is also shown in figure 6.14. The resulting spatial pattern of noise coefficients is shown in figure 6.15 as an example for the continuous variable. Interestingly, the patterns suggest that noise estimates are higher in magnitude in the city center, from the center going north along the Isar river and east of the Isar. These are areas that are usually considered upscale residential areas [7]. Similarly, the areas with the lowest (in magnitude) noise estimates in the north fall within the lower/average residential locations. While the coefficients should still be taken with care, this could possibly hint at underlying phenomena. One hypothesis is that objects in the upscale residential locations are more exclusive and their residents may have higher expectations from their homes and therefore put higher values on quietness. Similarly, the local household and apartment structure may impact sensitivity. Whereas households of young, flexible people may put a higher value on location and accept noise and live in smaller apartments, other households such as families may be more sensitive to noise. These possible reasons were also identified by Wäscher (2018). This could be true even if there is no significant difference in noise sensitivity between more or less affluent people.

Overall the GWR models confirmed the negative relationship between traffic noise and rent price. In addition, the results suggest that the applied coefficients are non-stationary and vary across space. However, because of the presented issues of overfitting and local collinearity between coefficients, individual coefficients should be treated with caution. In addition, GWR is still considered a more exploratory tool since any hypothesis testing and interpretation of (pseudo) t-values is limited (Gollini et al., 2015). Lastly, for implementation in an ILUT model, the application is relatively complex, since local sensitivities of coefficients need to be interpolated for synthetic dwellings (especially for new development). The limited applicability of a GWR regression for an ILUT model was also acknowledged by Löchl and Axhausen (2010), who favored a spatial econometric model with global coefficients instead. The application of spatial econometric models is presented next.

[7] compare with https://2019.mietspiegel-muenchen.de/wohnlagenkarte/

Table 6.7: Estimation Results of the geographically weighted ridge regression with a continuous noise variable.

	Dependent variable: log(rent)				
	Min	1st Quantile	Median	3rd Quantile	Max
log(area)	0.652	0.768	0.782	0.797	0.826
noise	-0.014	-0.006	-0.004	-0.003	0.002
microscopic car accessibilities	0.202	0.251	0.300	0.367	0.579
Parking available	-0.052	0.005	0.013	0.027	0.057
Quality: Luxury	0.126	0.158	0.168	0.184	0.237
Quality: Superior			0 (Base)		
Quality: Average	-0.293	-0.172	-0.150	-0.129	-0.027
State: First time use			0 (Base)		
State: New Building	-0.093	-0.045	-0.033	-0.017	0.051
State: First time use after restoration	-0.138	-0.094	-0.076	-0.044	0.058
State: Restored	-0.237	-0.120	-0.104	-0.082	-0.008
State: Modernized	-0.184	-0.127	-0.111	-0.086	-0.036
State: Well-kept	-0.234	-0.166	-0.152	-0.125	-0.059
State: Renovated	-0.276	-0.190	-0.151	-0.114	-0.013
constant	0.223	1.161	1.643	2.121	2.5984
Observations	3,145				
R2	0.893				
Adjusted R2	0.886				
AIC	-2699.475				

Table 6.8: Estimation Results of the geographically weighted ridge regression with a categorical noise variable.

	Dependent variable: log(rent)				
	Min	1st Quantile	Median	3rd Quantile	Max
log(area)	0.650	0.767	0.780	0.797	0.824
low noise			0 (Base)		
medium noise	-0.209	-0.093	-0.064	-0.026	0.102
loud noise	-0.306	-0.119	-0.083	-0.044	0.083
very loud noise	-0.300	-0.188	-0.105	-0.043	0.070
microscopic car accessibilities	0.194	0.242	0.294	0.355	0.531
Parking available	-0.094	-0.005	0.004	0.022	0.050
Quality: Luxury	0.124	0.159	0.169	0.185	0.239
Quality: Superior			0 (Base)		
Quality: Average	-0.288	-0.172	-0.150	-0.128	-0.026
State: First time use			0 (Base)		
State: New Building	-0.084	-0.042	-0.030	-0.014	0.042
State: First time use after restoration	-0.140	-0.104	-0.076	-0.046	0.035
State: Restored	-0.244	-0.124	-0.103	-0.084	0.008
State: Modernized	-0.190	-0.129	-0.115	-0.096	-0.033
State: Well-kept	-0.252	-0.169	-0.153	-0.127	-0.055
State: Renovated	-0.276	-0.196	-0.155	-0.114	-0.009
constant	0.202	1.029	1.530	1.992	2.345
Observations	3,14				
R2	0.894				
Adjusted R2	0.887				
AIC	-2695.862				

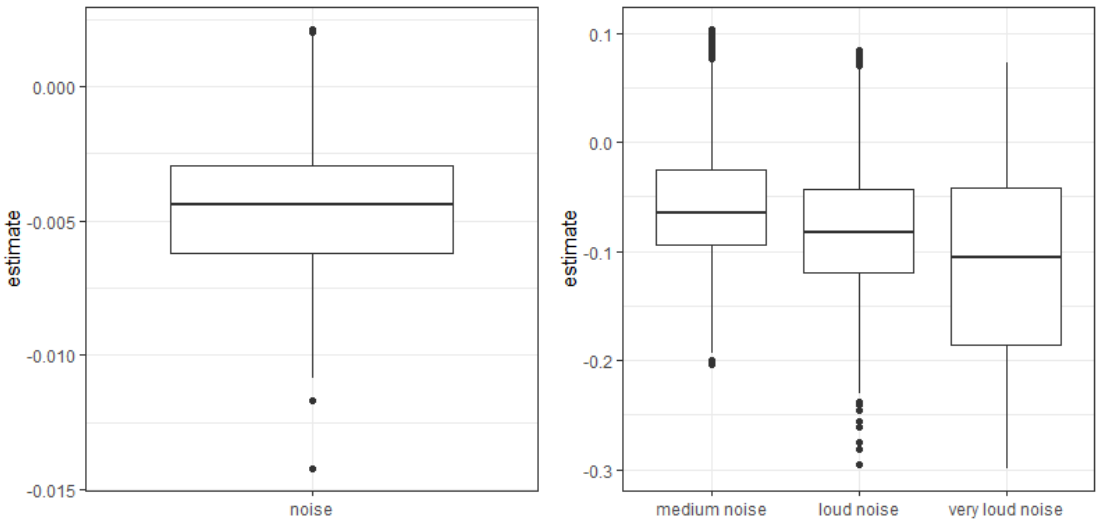

Figure 6.14: Distribution of estimates of the continuous noise variable model (left) and the categorical noise variable model (right). Results for the LCR GWR models.

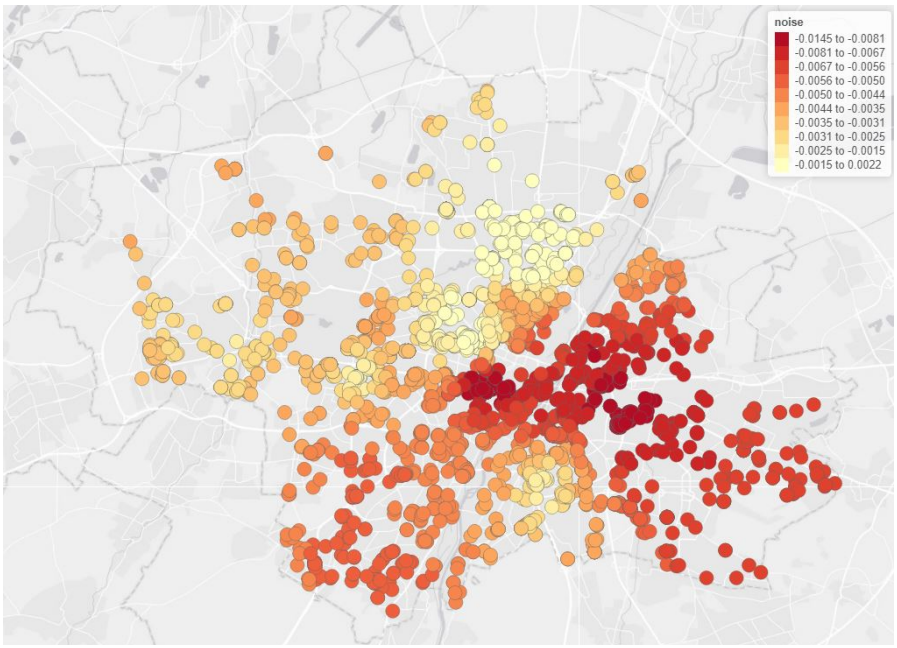

Figure 6.15: Spatial distribution of estimates of the continuous noise variable. Result for the LCR GWR model. Colors based on deciles.

6.6.2 Spatial Econometric Models

Spatial econometric models can take different spatial interactions between neighboring observations into account. Interactions are possible between the dependent and independent variables and the error terms. The so-called 'Manski Model' or General Nesting Spatial (GNS) includes all possibles interactions and is defined as (compare with OLS in eq. 6.2):

$$y = \rho W y + X\beta + WX\Theta + u, \quad \text{with } u = \lambda W u + \epsilon \tag{6.9}$$

here, W is the **spatial weights matrix** that defines neighborhood relations between the different observations and which must be provided as an input. W is a $n \cdot n$ matrix that has all n observations as rows and column indices. The matrix contains a non-zero value whenever two observations are considered as adjacent or neighbors (b, d and b, e in the following example):

$$\mathbf{W} = \begin{array}{c} \begin{matrix} \text{a} & \text{b} & \text{c} & \text{d} & \text{e} \end{matrix} \\ \begin{bmatrix} 0 & 0 & 0 & 0 & 0 \\ 0 & 0 & 0 & 1 & 1 \\ 0 & 0 & 0 & 0 & 0 \\ 0 & 1 & 0 & 0 & 0 \\ 0 & 1 & 0 & 0 & 0 \end{bmatrix} \end{array} \begin{matrix} \text{a} \\ \text{b} \\ \text{c} \\ \text{d} \\ \text{e} \end{matrix} \tag{6.10}$$

As such, the term $\rho W y$ in equation 6.9 describes the spatial lag of the *dependent* variable y, i.e. how strongly do the neighbors' y-values of a given observation impact the y-value of the observation itself. In the context of hedonic pricing estimations, the spatial lag y describes 'to what extend my neighborhood's price defines my price'. The strength of this relationship is defined by ρ, which is an outcome of the estimation. The spatial lag of the dependent variable is 'global', i.e. each observation influences all other observations, as the lag is indirectly propagated to the neighbors of neighbors (and so forth).
The term $WX\Theta$ describes the spatial lag of the *independent* variables X. In other words, it quantifies what impact do the independent variables X of an observation's neighbors have on the observation itself. The strength of this relationship is estimated and given by the vector of lagged coefficients Θ. The spatial lag of independent variables is called 'local'. Here, observations only influence their neighbors' dependent variable and their impact does not propagate to the neighbors of neighbors.
Lastly, the term $u = \lambda W u + \epsilon$ describes that there is a spatial correlation of *error terms* λu among neighbors. This means that residuals may be spatially correlated and capture variance not explained by the given variables. The parameter λ estimates the strength of the correlation.

In general, it is not recommended to apply the full Manski model but instead limit the model specification. The three basic models are:

1. The Spatially Lagged X Model (SLX) only includes the lag of the independent variables (local model), i.e. $\lambda = \rho = 0 \implies y = X\beta + WX\Theta + \epsilon$

2. The spatial lag model or Spatial Auto-Regressive Model (SAR) only includes the lag of the dependent variable (global modal), i.e. $\Theta = \lambda = 0 \Longrightarrow y = \rho Wy + X\beta + \epsilon$

3. The Spatial Error Model (SEM) does not assume any interpretable lag and only accounts for spatially correlated error terms, i.e. $\rho = \Theta = 0 \Longrightarrow y = X\beta + u, \quad \text{with } u = \lambda Wu + \epsilon$

More complex models can be defined, which are combinations of the three basic models, namely:

1. The spatial auto-regressive combined model (SAC) with a lagged dependent variable and a spatial error term, i.e. $Y = \rho WY + X\beta + u, \quad \text{with } u = \lambda Wu + \epsilon$

2. The Spatial Durbin Model (SDM) with both dependent and independent lagged variables, i.e. $Y = \rho WY + X\beta + WX\Theta + \epsilon$

3. The spatial Durbin error model (SDEM) with a lagged independent variable and a spatial error term, i.e. $Y = X\beta + WX\Theta + u, \quad \text{with } u = \lambda Wu + \epsilon$

An overview of spatial econometric models and their nesting structure based on Vega and Elhorst (2015) is shown in figure 6.16. All following analyses and estimations are carried out with the 'spdep'[8] package (Bivand et al., 2013) in *R*.

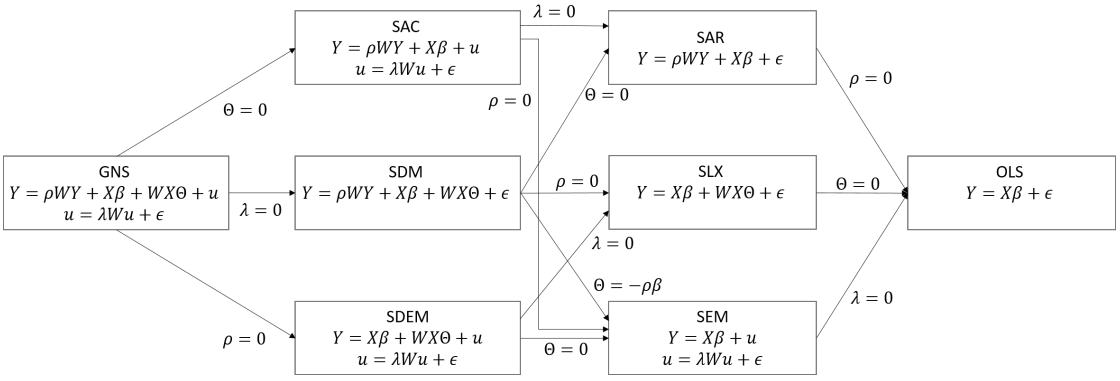

Figure 6.16: Overview of spatial Econometric models. Based on Vega and Elhorst (2015)

The decision for one of the presented types should be primarily driven by theory (Gibbons and Overman, 2012), i.e. whether a local or a global model describes the assumed behavior better or whether the spatial impact should be expressed through error terms. In the present hedonic pricing case, in which the impact of noise is investigated, a spatial lag model is a usual choice. It is a common phenomenon that rent prices are oriented towards average rent prices in a given neighborhood, which is usually reflected in rent indices. Contrarily, it might not be meaningful that individual neighbors' attributes have an impact on their neighbors. For example, the fact that a certain apartment has a low

[8] https://cran.r-project.org/web/packages/spdep/spdep.pdf

interior quality and, thus, a lower rent price, should not have an influence on a nearby apartment. However, local spillovers in the form of spatially lagged X variables could be used to describe (environmental) neighborhood characteristics (Maslianskaïa-Pautrel and Baumont, 2016). For now, only the spatial error model and the spatial lag model will be considered as they seem to be most common in such studies.

Next, the weight matrix W has to be defined. This can be done in multiple ways. One way is to define k nearest neighbors, such that for each observation, the k nearest other observations are defined as neighbors (by having a '1' in the corresponding row-column combination in W). This has the advantage that every observation has the same amount of influencing neighbors and that no observation is isolated without any neighbors. A disadvantage is that some observations in outer/remote areas end up with neighbors that are quite distant and should not have much of an impact. Another option is to define a distance band of distance d which creates a radius around each observation inside which every other observation is marked as a neighbor. In this approach, it is guaranteed that observations that are too distant (i.e. whose distance is larger than d) are not treated as neighbors. However, depending on observation densities in the study area, it may happen that some observations have many neighbors and others have only a few or even none. A combination of the two approaches is to define k nearest neighbors with a distance-based weight. In this case, the k nearest observations are indicated as neighbors. However the weight of the neighbor in W is a value between 0 and 1, depending on the distance such that more distant observations are less influential than close observations (see Tobler's first law of geography above). These weights are called Inverse Distance Weights (IDW).

In the following, the IDW approach is used for creating the weights matrix. The weights are defined using a common exponential distance-decay-function defined as follows (Smith, nd):

$$w_{i,j} = e^{-\alpha \cdot x_{i,j}} \tag{6.11}$$

Here, $w_{i,j}$ is the (non-zero) weight for observation j being a neighbor of observation i. $x_{i,j}$ is the distance between observation i and j. α is a scaling factor. For higher α, the resulting weight decays more quickly and vice versa. The advantage over a linear or power decay function is that distances can be zero, in which case the weight takes the maximum value of 1. This can happen in the present data set, as sometimes multiple apartment advertisements are located at the same address. To reduce the impact of scaling factors such as the unit of distance, the weights of the matrix are normalized by the row-normalization such that the weights of neighbors of each observation i sums up to one, i.e. (Smith, nd):

$$\sum_{j}^{n} w_{i,j} = 1, \quad i = 1, \ldots, n \tag{6.12}$$

After obtaining the weight matrix W, a statistical test on Moran's I can be performed (Moran, 1950). Moran's I can be interpreted as a measure of spatial auto-correlation

and is defined as:

$$I = \frac{N}{\hat{W}} \cdot \frac{\sum_i \sum_j w_{i,j}(x_i - \bar{x}) \cdot (x_j - \bar{x})}{\sum_i (x_i - \bar{x})^2} \tag{6.13}$$

N is the number of spatial units/observations, $\hat{W}$ is the sum of all weights in W, x_i and x_j are the values of the dependent variable of observation i and j, respectively. $\bar{x}$ is the mean value across all observations. I takes values between -1 and 1. If the values of all observations are distributed entirely randomly, I is near 0. If I turns towards -1 or 1, a higher spatial auto-correlation is present. I can be used to test whether spatial auto-correlation is present and significant. Table 6.9 shows I values for different combinations of α and k. All of the given values are highly significant and suggest that spatial auto-correlation is present. However, the magnitude of I seems to decrease with an increasing number of neighbors. This could be interpreted as a 'diffusion' of spatial correlation if too many neighbors are defined.

Table 6.9: Moran's I values for different combinations of k and α. All values are significant at $p < 0.001$.

	k...														
	3			5			10			50			100		
	α...			α...			α...			α...			α...		
	0.5	1	2	0.5	1	2	0.5	1	2	0.5	1	2	0.5	1	2
Moran's I	0.434	0.425	0.434	0.421	0.425	0.434	0.379	0.384	0.394	0.250	0.265	0.297	0.171	0.198	0.250

Figure 6.17 shows a so-called Moran plot for $k = 5$ and $\alpha = 2$, which has been identified as one of the best performing combinations across the different spatial models in terms of model fit. It shows for each observation the observed rent price (x-axis) and the average rent price of its neighbors (='lag', y-axis). Here, the rent prices of most observations are quite close to the respective lag values (i.e. close to the red line). This means that the rent prices of neighbors can be good indicators for rent prices and a spatial relationship exists.

In a next step, the Lagrange multiplier tests presented by Anselin (1988) can be used to check whether a spatial error model or spatial lag model is appropriate or preferably over a simple OLS model. The method which is described in more detail in Anselin (1988), proposes that the statistics returned by the test indicate that a SEM or SAR model is a better fit than the OLS model. In the present case, both statistics are highly significant for all selected combinations of k and α (p-values $< 2.22 \cdot 10^{-26}$ for $k = 5$ and $\alpha = -2$), which means that the null hypotheses, that the simple OLS model is more appropriate, can be withdrawn and either of the two spatial models or even a more complex one, such as the SDM or the Spatial Durbin Error Model (SDEM) can be applied. The simpler SEM and SAR model results will be presented first.

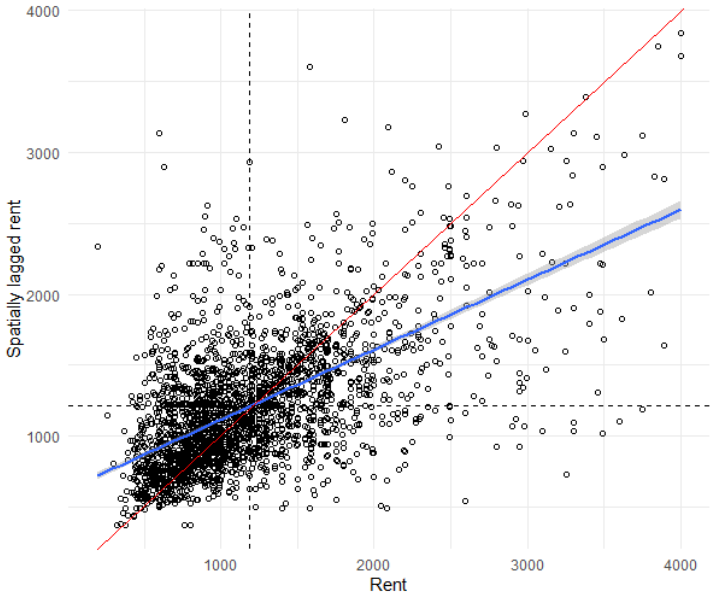

Figure 6.17: Moran plot of rent prices. The x-axis shows observed rent prices, the y-axis depicts the average rent price of each individual's neighbors. Dashed lines dashed lines show mean values; the red line defines y=x; the blue line is a linear fit.

6.6.2.1 Spatial Error Model Results

Estimation results of spatial error models can be interpreted similar to the OLS results. For the sake of brevity only the results of the noise estimates and the spatial variable λ will be discussed here (please see Appendix B for a table with complete results for $k = 5$ and $\alpha = 2$). The results for the noise estimates and λ are presented in tables 6.10 (continuous noise variable) and 6.11 (categorical noise variable) for different k and α. The tables show the percentage impact of noise variables on rent prices (i.e. the estimate multiplied by 100, see equation 6.6), the estimate of λ and the AIC. In both tables one can see that for high k the noise estimates become insignificant with p-values above 0.05. For the categorical noise variables this is also true for small α. For the estimations with significant noise estimates, the values are in similar magnitudes compared to the OLS estimates but consistently lower. The AIC decreases with higher α and is lowest for $k = 10$. In all cases, the AIC is lower than the AIC of the OLS model, which is -2261.1

The consistently lower estimates for the noise impacts compared to the OLS results should be interpreted further. In theory, spatial error model estimates should not be too different from the OLS results, as the OLS estimator should be unbiased compared to the spatial error model and differences should only be reflected in different standard errors and p-values (Anselin, 2001). Any spatial error model should lead to the same estimates as the OLS model (LeSage and Pace, 2009). In fact, there is a spatial Hausman test described by Kelley Pace and LeSage (2008) which tests whether the estimates of a

Table 6.10: Noise estimates for the continuous noise variable (multiplied by 100 to yield NSDI) as well as λ and AIC for different given k and α. Values in highlighted in gray are not significant. All other estimates as well as λ are always significant at $p < 0.001$

	k...														
	3			5			10			50			100		
	α...			α...			α...			α...			α...		
	0.5	1	2	0.5	1	2	0.5	1	2	0.5	1	2	0.5	1	2
noise	-0.31	-0.31	-0.31	-0.32	-0.32	-0.33	0.25	-0.25	-0.25	-0.08	-0.06	-0.07	-0.045338	-0.02	-0.019
λ	0.59	0.59	0.59	0.64	0.64	0.64	0.73	0.73	0.73	0.85	0.86	0.86	0.91	0.92	0.91
AIC	-3424.6	-3433.1	-3445.5	-3369.6	-3387.6	-3416.5	-3420.1	-3443.5	-3483.2	-3153.8	-3235.9	-3361.5	-2956.6	-3088.3	-3288.9

Table 6.11: Noise estimates for the categorical noise variable (multiplied by 100 to yield percentage discounts) as well as ρ and AIC for different given k and α. Note that all impacts as well as ρ are always significant at $p < 0.001$

	k...														
	3			5			10			50			100		
	α...			α...			α...			α...			α...		
	0.5	1	2	0.5	1	2	0.5	1	2	0.5	1	2	0.5	1	2
medium noise	-1.98	-2-00	-2.02	-2.01	-2.13	-2.30	-1.03	-1.15	-1.39	0.22	0.40	0.26	0.52	0.96	0.91
loud noise	-4.51	-4.54	-4.57	-4.93	-5.05	-5.23	-3.23	-3.32	-3.5	-0.51	-0.35	-0.72	0.54	0.86	0.39
very loud noise	-6.43	-6.40	-6.31	-6.26	-6.44	-6.65	-4.91	-5.04	-5.33	-0.43	-0.01	-0.43	-0.34	0.71	0.66
λ	0.59	0.59	0.59	0.64	0.64	0.64	0.73	0.73	0.73	0.85	0.86	0.86	0.91	0.92	0.91
AIC	-3417.7	-3426.2	-3438.8	-3363.9	-3381.8	-3410.6	-3414.8	-3438.3	-3478.2	-3149.4	-3232.2	-3358.3	-2952.6	-3085	-3286

spatial error model are significantly different from the OLS estimation. The authors state that, if the test is significant, it suggests that neither model is 'yielding regression parameter estimates matching the underlying parameters' (Kelley Pace and LeSage, 2008, 283). None of the models fails the Hausman test for the regression results presented here, indicating that all of them should be treated with caution. A possible explanation why the noise estimates are consistently lower might be that the spatial error component and the noise variables explain similar things. Spatial error model assume spatial patterns in omitted variables (Andersson et al., 2010; LeSage and Pace, 2009) and should therefore be chosen to account for the impact of these omitted variables. However, traffic noise itself does follow a spatial pattern as well but is not omitted in the estimation. Neighboring apartments along a busy road will experience similar noise levels and the same is true for quiet neighborhoods in which most of the apartments experience low noise immissions. The spatial component may therefore explain a major share of spatially correlated noise. Noise as a characteristic not exclusive to an individual apartment could be described better in terms of local spatial spillovers, which the SEM cannot represent (Vega and Elhorst, 2015).

LeSage and Pace (2009, p. 61) state that 'presence of omitted variables correlated with the explanatory variable and spatial dependence in the disturbances will lead to a DGP [data generation process] reflecting the SDM model' and that 'passing this test [the Hausman test] would be a good indication that specification problems (such as omitted variables correlated with the explanatory variables) were not present in the SEM model'. In the hedonic model presented here, noise (and accessibility) are likely to be correlated with other omitted spatial variables (e.g. amount of green space, building structure of the neighborhood, income-level of residents, etc.). LeSage and Pace (2009) go on by stating that the model should include a spatial lag of the *dependent* variable (similar to the spatial lag model) and conclude that the SDM should be applied when spatially dependent explanatory (such as noise and accessibility) are included. Even if a SEM would better describe the true underlying data, 'the SDM estimates should still be consistent, but not efficient' (LeSage and Pace, 2009, 68).

Before turning to a more complicated SDM, results for a simple SAR will be presented first.

6.6.2.2 Spatial Auto-Regressive Model Results

Next, the results of the SAR estimations will be presented. In contrast to the OLS and the SEM models, the estimated coefficients are harder to interpret, as a change in an independent variable for a given observation does not only change the rent price of this observation but also the rent price of its neighbors, which in turn impacts the rent prices of neighbors' neighbors and so forth (Golgher and Voss, 2016). The impact on neighbors ultimately spills back to the actual observation. To estimate the influence of independent variables, simulations are used to estimate the direct and the indirect impacts, as the estimated β coefficients and their p-values cannot be interpreted directly due to spillback (the off-diagonal elements of the partial derivative matrix are non-zero, see Golgher and Voss (2016)). In the SAR model, the direct impact is the reaction of the dependent variable of an observation on a change in the given independent variable of the same observation. The indirect impact accounts for the spillback effects of neighboring apartments. The sum of the direct and the indirect impact can be interpreted as the 'total' impact of a change of a dependent variable. Again, for the sake of brevity, only the results of the noise estimates are presented (please see Appendix C for tables with complete results for $k = 5$ and $\alpha = 2$).

Tables 6.12 and 6.6.2.2 summarize impact results of the SAR model for different k and α and for the continuous and the categorical noise variable model formulation, respectively. The tables show the percentage impact of noise variables on rent prices (i.e. the estimate multiplied by 100, see equation 6.6), the estimate of ρ and the AIC. In general, it can be seen that the variation of α barely impacts estimation results. Contrarily, the number of nearest neighbors included shows higher impacts on model results. For higher k, the estimations generally lead to higher estimates for the noise variable, especially for the indirect impact. This can be explained by the fact that more neighbors are included for each observation and, thus, the spillover effect is larger because a change in noise in one place leads to more neighboring places being affected. The resulting estimates are similar to the ones obtained by the OLS regression, confirming the previous results. The estimate of ρ is also increasing for higher k. Since the weight matrices are row-normalized, ρWy can be interpreted as the impact of the weighted average rent price of neighbors (e.g. for $\rho = 0.26$ one term of the estimated rent price is $0.26 \cdot \bar{y}$, where $\bar{y}$ is the weighted average of rent prices of neighbors). As such, this lag is higher when more neighbors are included which can be explained by more information being contained in the neighboring rent prices if many neighbors are included. As ρ is positive, it confirms the theory that there is a positive correlation between rent prices of neighboring apartments, i.e. apartments are expensive if they are located in an expensive neighborhood and vice versa. The AIC is lower than the AIC of the OLS model in every case (AIC = -2440.5 and AIC = -2261.1 for the continuous noise and the categorical noise variable model, respectively), which confirms that these models perform better in terms of model fit. Across different α and k, the AIC is quite similar, however, the AIC is always lowest for $k = 5$ and $\alpha = 2$, i.e. for the models with a moderate number of neighbors and high exponential decay function.

Table 6.12: Direct, indirect and total impacts for the continuous noise variable (multiplied by 100 to yield NSDI) as well as ρ and AIC for different given k and α. Note that all impacts as well as ρ are always significant at $p < 0.001$

	k...														
	3			5			10			50			100		
	α...			α...			α...			α...			α...		
	0.5	1	2	0.5	1	2	0.5	1	2	0.5	1	2	0.5	1	2
direct noise	-0.35	-0.35	-0.35	-0.36	-0.36	-0.36	-0.36	-0.37	-0.37	-0.40	-0.40	-0.40	-0.40	-0.43	-0.41
indirect noise	-0.07	-0.07	-0.07	-0.08	-0.08	-0.08	-0.1	-0.1	-0.1	-0.14	-0.14	-0.14	-0.14	-0.16	-0.16
total noise	-0.42	-0.42	-0.42	-0.45	-0.45	-0.45	-0.46	-0.46	-0.47	-0.54	-0.55	-0.54	-0.54	-0.59	-0.58
ρ	0.17	0.17	0.17	0.19	0.19	0.19	0.21	0.22	0.22	0.26	0.27	0.27	0.26	0.28	0.28
AIC	-2608	-2610	-2614.3	-2615	-2620	-2628	-2607	-2614	-2625	2519	-2538	-2565	2519	-2471	-2523

Table 6.13: Direct, indirect and total impacts for the categorical noise variable (multiplied by 100 to yield percentage discounts) as well as ρ and AIC
for different given k and α. Note that all impacts as well as ρ are always significant at $p < 0.001$

	k...														
	3			5			10			50			100		
	α...			α...			α...			α...			α...		
	0.5	1	2	0.5	1	2	0.5	1	2	0.5	1	2	0.5	1	2
direct medium noise	-3.1	-3.11		-3.01	-3.00	-2.97	-2.37	-2.41	-2.44	-3.10	-3.12	-3.16	-3.19	-3.14	-3.12
indirect medium noise	-0.61	-0.62		-0.69	-0.70	-0.696	-0.65	-0.67	-0.68	-1.11	-1.15	-1.17	-1.10	-1.21	-1.23
total medium noise	-3.73	-3.73		-3.71	-3.70	-3.66	-3.02	-3.08	-3.12	-4.21	-4.28	-4.33	-4.29	-4.34	-4.35
direct loud noise	-4.77	-4.76		-5.06	-5.04	-4.98	-4.62	-4.65	-4.66	-5.61	-5.60	-5.58	-5.74	-5.68	-5.60
indirect loud noise	-0.94	-0.94		-1.17	-1.17	-1.17	-1.26	-1.28	-1.30	-2.01	-2.07	-2.06	-1.98	-2.18	-2.21
total loud noise	-5.72	-5.71		-6.23	-6.21	-6.15	-5.87	-5.93	-5.96	-7.62	-7.68	-7.64	-7.72	-7.87	-7.81
direct very loud noise	-8.22	-8.21		-7.71	-7.69	-7.67	-7.11	-7.18	-7.24	-7.52	-7.56	-7.62	-8.58	-8.26	-7.88
indirect very loud noise	-1.63	-1.63		-1.78	-1.79	-1.80	-1.93	-1.98	-2.03	-2.69	-2.79	-2.81	-2.96	-3.17	-3.11
total very loud noise	-9.85	-9.84		-9.5	-9.48	-9.47	-9.04	-9.17	-9.27	-10.21	-10.34	-10.44	-11.55	-11.43	-10.99
ρ	0.17	0.17		0.19	0.19	0.19	0.22	0.22	0.22	0.26	0.27	0.27	0.26	0.27	0.28
AIC	-2590	-2592.5		-2596	-2601.2	-2608.4	-2585.9	-2593.1	-2604.2	-2495.4	-2514.4	-2541.3	-2404.7	-2443.5	-2497.9

6.6.2.3 Spatial Durbin Model Results

The SDM nests both the SAR and the SEM as a special case and can be defined as:

$$y = \rho W y + X\beta + WX\Theta + \epsilon \tag{6.14}$$

In simple words, it adds a spatial lag on the explanatory X variables such that both the dependent and the independent variables can be spatially correlated. As such, the model allows for local and global spillovers. This way, the indirect impact can be divided into local effects due to the lagged independent variables and the global effects emerging from the lagged dependent variable and its feedback effect (Golgher and Voss, 2016). The SDM model has been applied in numerous hedonic studies and has often proved superior to simpler models (Osland, 2010).

Results for both continuous and categorical noise variable models for different k are shown in table 6.14. The parameter α is always kept at 2, as the results did barely change between different α. For tables with complete results for $k = 5$ and $\alpha = 2$ please see Appendix D. The AIC values of the SDM model results are better than for any of the previously presented models, which suggests better model performance. It becomes clear that here, noise is mostly explained by the *indirect* effect. These effects are similar in magnitude to the estimates of the OLS, GWR and SEM models. Since the indirect impact in the SAR model (which is a global spillover) is smaller than the corresponding direct impact, it may be that the indirect impact is mainly of local nature.

Multiple studies report similar findings for variables that could be characterized as 'local neighborhood' or 'environment' attributes in that they are often characterized by spatial spillovers (i.e., indirect impacts) and that 'this way, SDM impact estimates can explain important characteristics of the close neighborhood' (Herath et al., 2015, p. 19). This is true when most of the indirect impact comes from the local spillover of immediate neighbors (i.e., lagged independent variables). In a study analyzing the impact of natural amenities on housing prices, Izón et al. (2016) find that distance to city parks has a significant negative indirect impact. Maslianskaïa-Pautrel and Baumont (2016) find strong and significant indirect impacts of proximity to the sea, which is shared with neighboring houses. Interestingly, Maslianskaïa-Pautrel and Baumont (2016) also included noise as an explanatory variable which resulted in a significant negative direct impact and a slightly larger (in magnitude) positive significant indirect impact. The authors explain this difference by arguing that the negative direct impact represents the actual disturbance due to noise while the positive direct impact accounts for the accessibility, which they did not control for. The significant positive indirect impact of accessibility is also confirmed in the present thesis. Eilers (2016) applied an SDM model for apartment prices in Hamburg, Germany and, too, found that the variable 'quiet location' was only significant for the indirect impact, although with a negative relationship. The author concludes that such variables reflect the composition of the neighborhood and its quality. The negative association between quiet locations and apartments was explained

Table 6.14: Direct, indirect and total impacts for the continuous/categorical noise variable (multiplied by 100 to yield NSDI/percentage discounts) as well as ρ and AIC for different given k. Note that cells colored in gray are not significant at $p < 0.05$. All other impacts as well as ρ are always significant at this level.

	k...					
	3 α... 2	5 α... 2	10 α... 2	3 α... 2	5 α... 2	10 α... 2
direct noise	-0.07	-0.09	-0.08	-	-	-
indirect noise	-0.62	-0.84	-0.81	-	-	-
total noise	-0.69	-0.93	-0.89	-	-	-
direct medium noise	-	-	-	-0.75	-0.78	-0.11
indirect medium noise	-	-	-	-6.42	-6.79	-5.68
total medium noise	-	-	-	-7.17	-7.57	-5.78
direct loud noise	-	-	-	-2.16	-2.34	-1.17
indirect loud noise	-	-	-	-9.02	-10.69	-8.76
total loud noise	-	-	-	-11.18	-13.04	-9.94
direct very loud noise	-	-	-	-2.72	-2.81	-2.31
indirect very loud noise	-	-	-	-10.37	-14.56	-15.39
total very loud noise	-	-	-	-13.09	-17.36	-17.70
ρ	0.58	0.62	0.70	0.58	0.63	0.70
AIC	-3583.7	-3544	-3569.8	-3565.5	-3521.5	-3554.9

by such apartments usually being in the suburbs. This can be understood by the fact that no kind of accessibility or centrality measure was used to control for the negative aspect of living in more remote places. Dupraz et al. (2018) underline that the indirect impacts of spatially lagged independent variables can explain environment variables (or externalities) that are shared within the same neighborhood.

The idea of appraising the closer neighborhood in terms of noise exposure has also been described in a study by Botteldooren et al. (2011), who find negative relationships between traffic noise and quality of life in residential neighborhoods. Similar findings have been presented by Parkes et al. (2002).

In the presented case, the larger impact of *local* spillovers can be cross-validated when running an SLX model (i.e., spatial lag in the independent variable only), of which the results are not shown here. However, the SLX model confirmed that the negative impact is primarily indirect by local spillover (a summary of noise estimates for the SLX model is included in figures 6.18 and 6.19 of section 6.7).

However, another possible reason why noise mainly has an indirect impact in the estimation could be similar to Herath et al. (2015, p. 19), who state that, in their study, 'distances between neighboring apartments are small [...] Therefore, this outcome reiterates the same [direct] negative relation between distance from the greenbelt and apartment price'. This can be supported by the fact that the mean distance to the nearest neighbor in the given data set is only 44 meters and the median is 0 meters, which is in fact very local. It is therefore very probable that the nearest neighbor of an observation (which also has the highest weight) has a very similar noise value. The short distances to the nearest neighbor can be explained by the fact that, oftentimes, more than one apartment per building was offered. In these cases, the geo-coding would assign the same address to all apartments of the same building. It is, therefore, obvious that the noise estimate is better evaluated at the very local neighborhood. Of course, this also points to a limitation of the collected data, as information on whether an apartment is in the backyard of a building and hence quieter may be obscured when the address is shared across different parts of a building (complex). The observation that the indirect impact increases with increasing k can be explained by the fact that the lagged local spillover can be interpreted as 'how much would the observation's price change when *all* of its neighbors change their independent value by 1 unit'. For higher k, less relative weight is put on very close neighbors as it is split across all neighbors. Thus, the higher estimated impact may compensate for the fact that the weight of the influential closest neighbor is lower for higher k.

To test whether a SDM is more appropriate than an SEM, a simple likelihood ratio test can be employed (Anselin, 2003; Mur and Angulo, 2006). In the presented cases, the test results always suggest that the SDM is preferable.

6.7 Hedonic Pricing Summary

The results of this chapter support the idea of integrating environmental aspects in an ILUT model as traffic noise has a significant negative impact on rent prices. As such, research question 3, whether simulated noise values are able to explain significant rent price discounts, can be answered with 'yes'. Regarding the magnitude of the impact, this chapter showed that this partly depends on the used model. However, all models resulted in reasonable values with most NSDI values in the range of 0.3 and 0.6.

Two simple OLS model formulations were estimated first, differing in the usage of noise as a continuous and a categorical variable. The models show reasonable results in terms of NSDI as compared to existing studies. An important finding of this chapter is that it is important to control as well as possible for the positive aspects of accessibility. Otherwise, the noise estimate will be severely biased. It was shown that modeled noise emissions as part of an ILUT model can be used to identify price discounts in rent prices when evaluated against real-world real estate data. This justifies the implementation of noise exposure into the pricing model of a land use component to create this feedback cycle.

When looking at the models using a spatial component, the negative relationship between noise and rent prices was confirmed. Since the GWR model results should be considered exploratory and a direct application in SILO would be difficult due to the spatially non-stationary coefficients, these are not further considered for application in the ILUT model suite. The spatial econometric models can be used to obtain more 'global' estimates/impacts. However, their application in the land use model is not straightforward either. For any model with a spatially correlated error term or a spatially lagged dependent variable, out-of-sample predictions can become tricky, as the spatial structure of the training dataset is part of the estimation process in the form of the spatial weights matrix. In fact, comparing an OLS model with SAR, SEM and SDM, Bivand (2002) showed that while the spatial models perform better for predictions on the training data set, the simple linear OLS model may outperform spatial models for out-of-sample predictions. In addition, the application of spatial models turned out to be not feasible in terms of runtime. The runtime for a model with a spatially lagged dependent variable (SAR and SDM) for predicting the 3,144 observations of the training dataset takes about 30 seconds. Even if assumed linear, this would require about 6.9 hours of computation time just for predicting the price of all 2.6 million dwellings in SILO for *one year*. Since the weight matrix would also contain more objects, the required computation time would probably be even higher, as the global spillover and feedback effects would ripple through many more observations. Even in the case of the SLX model, which is more 'global' in its assumptions, i.e., the local spillover effect and direct impact are the same anywhere in space), the implementation turned out to be infeasible, as the calculation of the nearest neighbors has a runtime complexity of $O(n^2)$ - where n is the number of objects - and the distances between each of the 2.6 million dwellings would need to be calculated. This is why, finally, the OLS model will be applied in SILO as it is simple enough to be applied

for out-of-sample observations in every year. The underlying assumption here is that the coefficients (especially in regards to noise) are reasonably well captured. Figures 6.18 and 6.19 summarize the estimates/impacts obtained by the different models presented in this chapter. It can be seen that, especially for the categorical noise variable, the OLS estimates do not differ largely from the results obtained by the spatial regression models. The OLS model with a categorical noise variable is thus chosen for implementation in SILO.

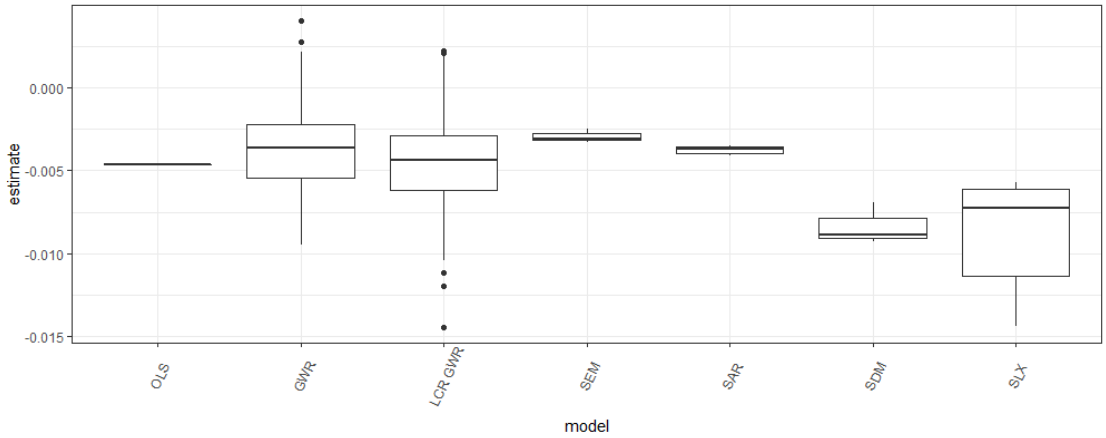

Figure 6.18: Summary of estimates/impacts for the continuous noise variable

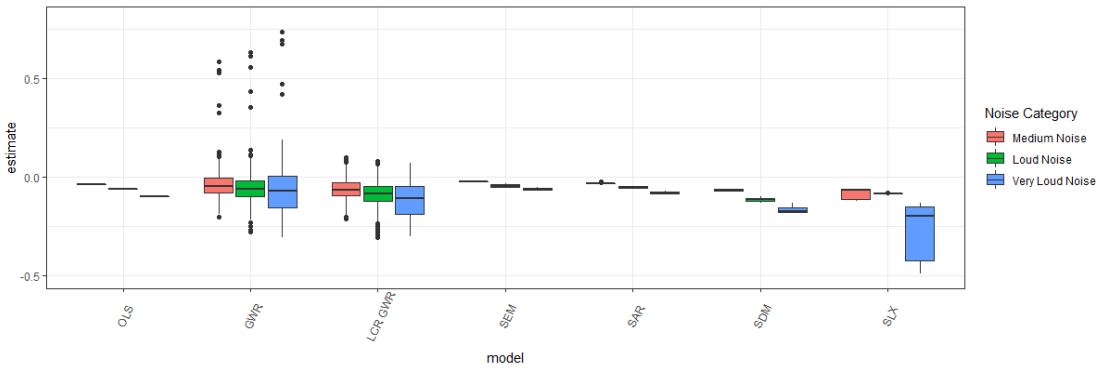

Figure 6.19: Summary of estimates/impacts for the categorical noise variable

7 Towards an Agent-Based Land Use/Transport/Environment Model

> Those who can afford it move away from major roads because of health hazards
>
> Katrin Lompscher, Senator for Health, Environment and Consumer Protection. DER TAGESSPIEGEL, September 2007

This chapter presents the integration of land use, transport and the environment in the form of traffic noise in the FABILUT model. As discussed in chapter 2, a detailed spatial resolution is key for locational attributes. Microscopic agents/households as the central decision unit need accurate information on dwelling attributes if small-scale effects are under investigation. Therefore, as the first step for an integrated model that accounts for the impact of traffic noise, the existing integrated FABILUT modeling suite is enhanced by a microscopic integration with the transport model, including a microscopic representation of travel times. After the microscopic integration, the environmental sub-module will be added to expand the ILUT model to an LTE model.

7.1 Microscopic Integration of Land Use and Transport

Traditional (microscopic) ILUT models usually use zonal indicators for relocation purposes, such as average rent per zone or zone-to-zone travel times for commute trips. Since the environmental impact of noise is expected to be very local, a microscopic integration at the coordinate level is preferable. Since MATSim operates at the coordinate level, it is natural to explore a microscopic integration of the land-use model SILO and the transport model MATSim. Therefore, as a first step, the initial integration described in Ziemke et al. (2016), which was still based on zone-to-zone travel time skims provided by MATSim, was enhanced by a microscopic integration. As such, the travel time feedback from MATSim to SILO was implemented without aggregating travel times on a zone-to-zone basis. Instead, SILO can now 'query' the MATSim router for individual travel time requests made by agents in the synthetic population.

7.1.1 Travel Time Feedback

Travel times in SILO are required for:

- Assessment of current household satisfaction of dwellers and their commute trips to work
- Assessment of possible vacant dwellings and the hypothetical commute trip to work
- Assessment of possible vacant jobs and the hypothetical commute trip from home

Initially, MATSim would create/update skim matrices of size n^2, where n is the number of zones to store zone to zone travel times after each transport model execution. However, this approach has multiple downsides:

- An individual matrix is required for each transport mode m
- An individual matrix is required for each 'time slice' (e.g., peak/off-peak/night hours) t
- Each individual matrix increases by $2n+1$ additional cells for each additional zone
- No individual attributes can be considered (e.g., fuel type of car and permitted routes, income-dependent tolls, different valuation of time vs comfort, acceptable access/egress times, etc...)
- Skims require spatial and temporal aggregation that lead to biases which can be reduced by smaller zones or more time slices but will never vanish completely
- The simulation outcomes depend on the chosen zone system
- Zone systems necessarily lead to intra-zonal trips, which are hard to calibrate and validate

This leads to the issue that the more detailed the matrices become, the more calculations need to be processed, as the number of records depends on $m \cdot t \cdot n^2$. This also means that these matrices take up a large part of the computer's memory. Many (if not most) of the entries are never used throughout the simulation. Therefore, it seems natural to directly query individual travel times instead of preemptively calculating every possible combination.

In the new implementation, agents in SILO create queries that are routed by MATSim router implementations that return individual routes that take into account traffic from the latest MATSim simulation run. Therefore, it is mandatory that dwellings and jobs of the synthetic population are represented as microlocations with an x/y coordinate. Figure 7.1 shows a visualization of a sample of queries registered during household relocation decisions of the first simulation year for the Munich scenario of the FABILUT model. It can be seen that query density is high where population density and job density are high. The implemented query architecture allows agents to query for *expected* individual travel times from and to micro-locations in the form of x/y coordinates at a specific time of day. Whenever SILO requires travel times, MATSim's trip router is

queried. Transit is not explicitly simulated but only routed based on the schedule using the recent implementation of the efficient raptor transit router (Rieser et al., 2018). The router also includes access and egress times as well as transfer times for public transport queries. For car travel time queries, it is assumed that the car is parked very close to origin and destination, resulting in access and egress times that can be neglected.

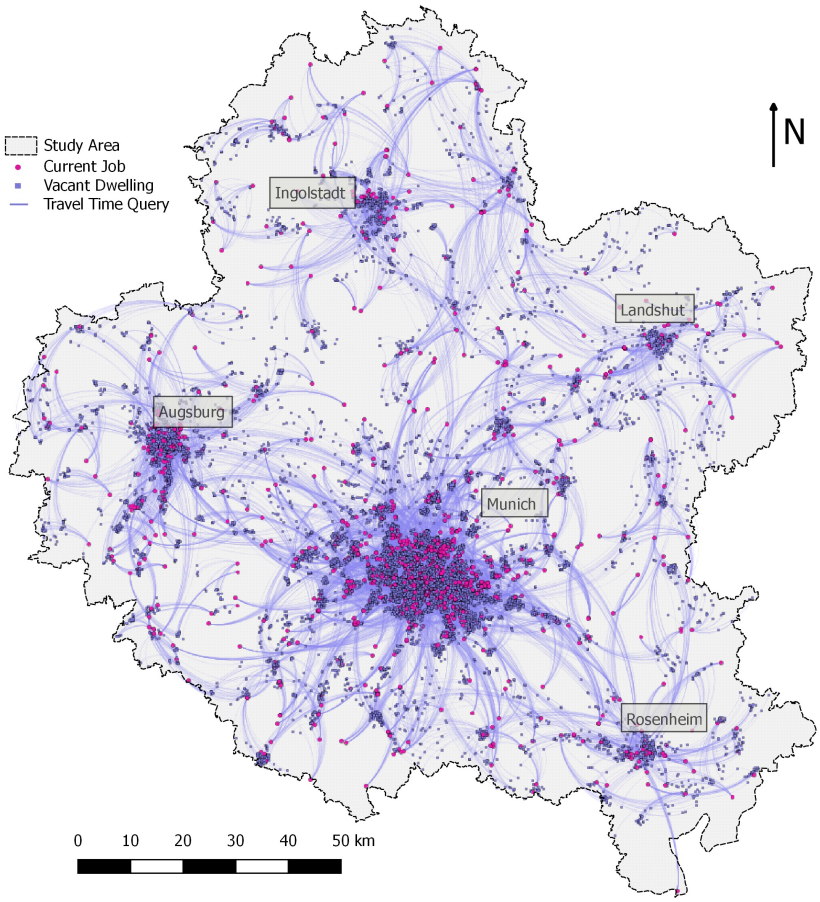

Figure 7.1: Visualization of a sample of 25,000 travel time queries during one SILO simulation year in the Munich study area. Lines depict queries from vacant dwellings (purple) to current job locations (pink) of workers in households looking for a new dwelling.

Previously, skims were calculated for auto and transit travel times by routing between weighted zone centroids of each zone at a defined and fixed peak hour (once for the morning and once for the afternoon peak). For $4,924$ zones in the Munich study area, each skim matrix has $4,924^2 = 24,245,776$ travel time values, of which many entries are never used. Zone centroids are obtained by geographically averaging the micro-coordinates of dwellings, weighted by their residents' household size. This is in line with Stępniak and Jacobs-Crisioni (2017), who report that population-weighted centroids are

to be preferred to reduce uncertainty due to spatial aggregation. For intra-zonal travel times, consider Z as the set of zones that include the n closest neighbors in terms of travel times. The intra-zonal travel time $tt_{i,i}$ of zone i is defined as a given share λ of the average travel time to these closest neighbors:

$$tt_{i,i} = \lambda * \frac{\sum_{j \in Z} t_{i,j}}{n} \tag{7.1}$$

where $t_{i,j}$ is the travel time from zone i to j and λ is a configurable parameter. By trial-and-error, reasonable (i.e., not biased by systematic under- or overestimation) estimates are obtained by setting n to 5 and λ to 0.66. In other words, the intrazonal travel time is set to two-thirds of the average travel time to the next five zones. For individual travel times, all queries ask for the explicit origin and destination x/y coordinates, i.e., no intrazonal travel times need to be calculated.

For transit travel times skims, all stops in a 1,000-meter radius around the weighted centroid of the origin are routed to all stops in the same radius around the centroid of the destination zone. In cases where no stops are found within the 1,000-meter radius, the (single) closest stop to the centroid at any distance is selected. The most optimistic route is then selected and access/egress times by walk are added between the stops of the selected route and the centroids of zones. In a last step, the resulting zone-to-zone travel time by transit is compared to the direct walk travel time. The shorter option is saved in the skim matrix.

Using this, the bias between individual travel times and skims can be measured.

To showcase the problem of spatial aggregation in the case of transit, the implemented model was applied to a simplistic hypothetical study area. Figure 7.2 shows a coarse grid scenario which consists of 5x5 square zones with a side length of 5,000 meters each (i.e., the area of the study area is 25km x 25km). Two U-shaped transit lines connect the corners with the center of the study area. A fixed destination point was picked at the top right corner (blue triangle). Next, the individual and skim travel times to this point were queried in a 100x100 meters resolution. In the case of individual travel times, one can clearly see isochrones around the fixed point that show increasing travel times as distance increases. Here, the router would just return a direct walk trip in the transit case. It is important to see that the isochrones span over the zonal boundaries. In the zone in the second row in the last column, the isochrones have an uneven extension, which is due to the transit stop that is located at the center of the zone and that connects to the upper zone. Every other zone that is connected with the transit system has its own isochrones around stops that stick out from the zones that are not connected. Here, one can see that the size of the isochrones gets smaller as the number of stops to the target zone increases. The isochrones in the top left transit zones are slightly larger than their counterparts in the bottom right, which is due to the fact that the zones in the bottom right are not directly connected and passengers need to transfer to the other line, which

adds waiting time.

In the skim case, every zone consists of one value only. While the overall pattern is similar, one can clearly see the issues that arise due to aggregation. The first issue is that the top-right zone does not show the lowest travel time, which is due to the fact that the intrazonal travel time takes an average to all nearest neighbors, including the zone to the left that is inaccessible by public transport. Secondly, travel times abruptly change when a zone border is crossed. This refers to the partitioning bias of the MAUP. While parts of the fourth zone in the second row have some reasonable travel times in the individual case, it is considered completely inaccessible in the skim case. A third issue is that the skim travel time cannot capture the decreasing isochrone area in more distant zones, as it computes the zonal value for the zone centroid, which is the geographical center in this example. Finally, the skim travel times seem to be biased towards shorter travel times in general. This is due to the fact that the destination, too, is represented by a zonal centroid that is close to the transit stop in the upper right corner. This omits the egress travel time to the actual location.

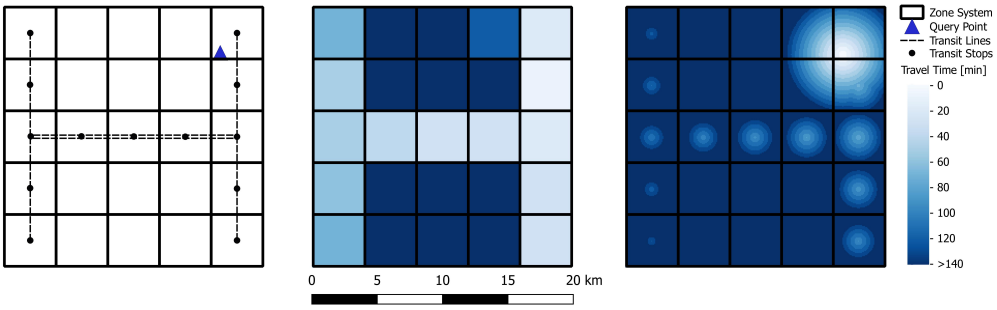

Figure 7.2: A comparison of obtained travel times for a hypothetical scenario. Zone system and transit lines (left), skim zonal travel times to a fixed destination (middle) and the respective individual travel times (right).

Further analyzes showed that time of day as well as network density additionally influenced the introduced bias. In addition, transit-captive relocating agents showed an increased sensitivity to the actual stop location distances when searching for new dwellings (Kuehnel et al., 2020).

The individual travel times add accuracy for the relocation behavior defined by the relocation model presented in the next section. Both car and transit travel times will be part of the decision process of relocating agents.

7.2 Microscopic Integration of the Environment

The next step is to extend the microscopic FABILUT modeling suite to account for environmental feedback using the example of road traffic noise. The modeling suite allows

linking road noise immissions to dwelling locations of residents microscopically at the coordinate level to account for household relocation impacts. The model is thus capable of representing the impacts of land use and transport on the environment and back from the environment to land use. This new fully agent-based approach opens new possibilities to analyze issues of environmental equity with the help of models, as the population that is emitting and the population that is exposed are represented explicitly and can be directly linked throughout the submodels. Complex studies such as location-dependent taxes on environmental externalities and their implications on land use, transport and environment will become possible. The work presented here has first been described in Kuehnel et al. (2021b) which used simple percentage discounts for the price of dwellings. The integration has since been updated to use the full hedonic pricing model.

In an ideal model, agents would derive lower utility from noisy dwellings, thus leading to reduced demand. The real estate market would then react to the lower demand of noisy dwellings and reduce their prices. In the previous chapter 6, the relationship between the simulated noise immission values and their impact on residential rent prices has been confirmed. For the sake of simplification, the integration into the FABILUT modeling suite is twofold:

Relocation of agents is affected by implementing a noise-sensitive choice model. Agents will be less likely to move to noisy places. Different households (or household types) may have different sensitivities to noise.

Prices of dwellings are adjusted by applying the estimated hedonic pricing model presented in chapter 6.

7.2.1 Price Updates

In SILO, the pricing model is run once at the end of each simulation year. Prices of each dwelling type are adjusted according to the current vacancy rate of this housing type in the neighborhood. Prices increase steeply when the vacancy of a dwelling type in a region is low since it means that high demand is present. Higher vacancy rates will cause the dwelling prices to drop - but less steep so as landlords are less willing to accept a decrease in rent revenues. The model does account for a certain structural vacancy rate at which the market is considered to be at equilibrium and prices do not change. However, this model reflects the regional price trends of municipalities or districts in the study area. It does not account for the individual attributes of a dwelling. Therefore, the estimated hedonic pricing model is implemented in SILO. The OLS model with a categorical noise variable was chosen to account for the fact that using a continuous noise variable would also mean that changes in the lower ranges of noise would have a similar impact as changes in noise at higher levels. However, it is assumed that noise will not have a notable effect at lower values below 55 dB(A) as was also confirmed when using different noise categories. To keep the yearly price adjustment rates of SILO's basic pricing model, the predicted prices of the applied hedonic pricing model will be scaled by the yearly adjustment rate. This way, it is ensured that prices do also react to changes

in demand.

For the application of the estimated hedonic pricing model, the variables included need to be present in SILO. The first independent variable is the area of the dwelling. In the Munich use case of SILO, the dwellings of the synthetic population do not have area as an attribute. Instead, the number of rooms per dwelling describes the size of the dwelling. To convert the number of rooms into area, the observed real-world data from chapter 6 are used to estimate dwelling area with a simple linear regression, as shown in table 7.1. As can be seen from the results, each additional room is correlated with an additional area of 26.79 m^2. The intercept/constant is estimated at 6.95 m^2. Both estimators are highly significant and the model shows an R^2 value of 0.74, which is reasonably high. As such, this simple model is considered appropriate to represent areas of dwellings in SILO.

Table 7.1: Estimation results for dwelling area.

	Dependent variable:
	area
intercept	6.9533*** (0.7206)
rooms	26.7960*** (0.2821)
Observations	3,144
R2	0.7417
Adjusted R2	0.7417
Residual Std. Error	16.42
F Statistic	9024

Note: Signif. codes: '***' 0.001 '**' 0.01 '*' 0.05 '.' 0.1 ' ' 1 robust SE in (brackets)

The next variable is the noise variable which is obtained by the MATSim noise extension. Similarly, the microscopic car accessibility is obtained by running MATSim's accessibility extension. The accessibility calculation is only updated after each transport model year and is assumed constant in-between years. In addition, accessibilities are calculated *per zone* and not for each individual dwelling. The reasons are that, for once, accessibility varies rather slowly over space (compare figure 6.8) and, as such, nearby dwellings within a zone should have a similar accessibility value. Secondly, the accessibility calculation is computationally costly, as for each estimation point, the travel times to all opportunities have to be routed. For the roughly 5,000 zones in SILO, the calculation takes around 20 minutes per update year when heavily parallelized. This computation time increases linearly with the number of estimation points and, as such, becomes unfeasible if applied for each of the 2.6 million individual dwellings. It should be noted, however, that this may introduce MAUP issues and abrupt changes across zone boundaries. Given the slow variation over space it is assumed that these problems are minor, especially in populated areas where zones are small.

Table 7.2: Parking availability by dwelling type.

Dwelling Type	Average Number of Parking Spaces
Single-Family Detached House	1.6
Single-Family Attached House	1.3
Multi-Family Apartment (less than 5 units per building)	1
Multi-Family Apartment (5 or more units per building)	0.8

The parking availability per dwelling is determined using the assumptions given in Llorca et al. (nd) where, based on real estate advertisements, each dwelling type is associated with an average number of parking spaces as shown in table 7.2.

Using these average numbers, parking is available for all dwelling types but the multi-family apartment in a building with more than five units, which is common in the large cities. For these dwellings, parking availability was randomly drawn with a probability of 80%.

The quality variable is converted from the quality level in SILO, which is encoded with an integer between 1 and 4 (4 being the highest quality). Here, levels 1 and 2 were set to Average dwelling quality, 3 was set to superior dwelling quality and 4 was set to luxury dwelling quality.

Lastly, the state variable had to be defined in SILO. As this is also not available in the default study area setup, the state is simply based on the distribution of states in the collected real estate data. Figure 7.3 shows the distribution of states based on the age of the building. It can be seen that as age increases, the 'First Time Use' and 'New Building' states decrease in frequency and states such as 'Renovated' or 'Well-Kept' increase in frequency. For the application in SILO, newly constructed dwellings will be assigned 'First Time use' state. Once the dwelling is occupied, the state is changed to 'New Building'. In subsequent years, based on the current age of the dwelling, the state is randomly switched to a different level with a probability based on the frequency of each state for a given age. These updates occur whenever a dwelling enters a new age bracket as defined by the categories seen in figure 7.3. The same distribution is applied to all dwellings in the base year.

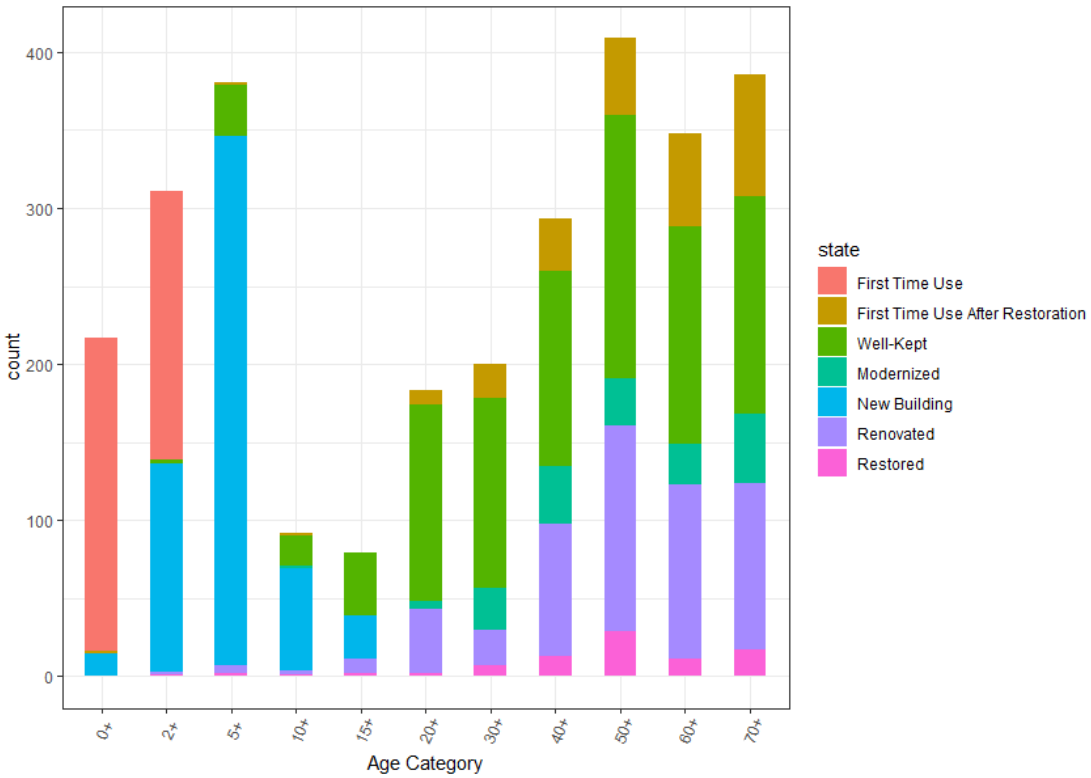

Figure 7.3: Distribution of apartment states depending on the building age.

7.2.2 Relocation Decisions

Due to the lack of available data and existing noise-sensitive relocation choice models for Munich, a model developed by Hunt (2010) is implemented and used. It is based on a stated preference survey in which over 1,200 participants had to choose from dwelling alternatives in Edmonton, Canada. Each respondent was asked to imagine moving to a new home. Multiple hypothetical alternatives were presented, with each of them been described with attributes of different levels of prices, air quality, traffic noise, travel time changes to work, school and shopping, among others. Using the respondent's answers, choice model parameters were estimated. Three versions of the model exist, which were estimated for all households and for two subsamples of high-income and low-income households, respectively. It was shown that high-income households are less sensitive to price but more sensitive to noise and vice versa.

SILO uses a three-step approach for residential relocation. As a first step, every household decides on whether it wants to move at the beginning of each year. The probability for the decision to move is based on a comparative evaluation between the current own housing satisfaction and the average satisfaction in the current region. Once a household decides to move, it will look for a target region in a second step. The region choice is a discrete choice based on average vacancy rates, prices, accessibilities and potential commute travel times of household members. The last step is the selection of a vacant dwelling within the chosen region. Therefore, SILO randomly samples 20 different vacant dwellings and evaluates their utility. The choice follows a multinomial logit model:

$$p(d) = \frac{e^{\beta * u_d}}{\sum_i e^{\beta * u_i}} \tag{7.2}$$

where u_d is the utility of dwelling d and u_i are utilities of all choice alternatives. Utilities in SILO are usually defined in a utility function. The choice model of Hunt works in a similar way and has a linear form:

$$U_i = \beta_1 \cdot x_1 + \beta_2 \cdot x_2 + \ldots + \beta_n \cdot x_n \tag{7.3}$$

where β_n is the utility parameter associated with attribute x_n.

SILO's own utility function has been replaced by the models that were estimated in Hunt's study. Therefore, multiple adjustments and simplifications had to be made. The impact of noise was found to be negative in terms of utility but was classified as a categorical variable that had to be translated into noise levels in SILO. The original noise category 'Sometimes Disturbing' was dropped, as the magnitude of the estimate was considered inconsistent among the models. It was valued less negatively than the 'Constant faint hum' category but is supposed to be worse in terms of noise. Similarly, dwelling types had to be translated between both models. The classifications for low- and high-income households, as well as the utility components, were presented by Canadian Dollars, which were converted into Euro equivalents. Low-income households were de-

Table 7.3: Classifications and relocation variables in the models by Hunt and their representation in SILO

	Hunt (2010)	SILO
Dwelling Type	Single Family	Single Family Detached
	Duplex	Single Family Attached
	Townhouse	Multi-Family (2-4 families)
	Walkup	-
	Highrise	Multi-Family (5+ families)
Traffic Noise	None	L_{DEN} < 30 dB(A)
	Occasionally just noticeable	L_{DEN} 30-50 dB(A)
	Constant faint hum	L_{DEN} 50-60 dB(A)
	Sometimes disturbing	- dropped -
	Frequently disturbing	L_{DEN} < 60 dB(A)
Rent/Tax	CAD 100 per month increase	EUR 68 per month increase
Travel to work	10 min auto drive time increase	10 min auto drive time increase
	10 min transit ride increase	10 min transit ride increase

fined as households with an income below EUR 16,000. High-income households have an income above EUR 68,000. Finally, many variables were not (yet) available in the current SILO model (e.g., air quality, travel time to shopping, car and transit costs). However, the utility components in the original model were based on *comparative measures to the current home* of respondents (e.g., increase of transit costs by $1 compared to current housing) or categorical variables that have a default category which is assigned with a utility of 0. Thus, here, it is assumed that all alternative dwellings are equally good or bad in the utility components that could not be captured in SILO. For instance, the air quality is assumed to never be bad, such that the utility component for all dwellings is 0. Likewise, variables like '1$ transit fare increase to work', which compares fares between current housing and the potential new dwelling, were assumed to yield a difference of zero, i.e., all dwellings would have the same transit fare costs associated with them. It should be noted that ignoring these variables by assuming no differences between dwellings may distort some of the findings. However, the included variables should be able to capture noise sensitivity for a proof-of-concept of an integrated environmental feedback model. Table 7.3 shows the selected variables that are captured in SILO and their representation.

Both sensitivities for relocation and for price had to be included in the model. If only the price was updated, all households would perceive the less expensive dwellings as more attractive even though there is a reason why the dwelling costs less. If only the relocation choice model was adapted, the price discounts found in the hedonic pricing study would not be part of the model and the reduced demand would not lead to differences in the housing market. While one could say that the two effects would 'cancel' each other since the less attractive noisy dwelling is also cheaper, this should still lead to a more distinguished pattern of household distribution. More affluent households are more sensitive to noise and less sensitive to price and will thus afford to move out of noisy places. Less affluent households are much more sensitive to price and are less likely to afford to move

away from noisy places, especially in tight housing markets.

The resulting reactions to noise can be explained by looking at figure 7.4. The utilities of dwellings that only vary in their noise levels are evaluated by the three different household types, compared to a fixed 'current dwelling'. It can be seen that, in general, the higher noise categories are less favorable as they result in less utility. While the high-income households have a high sensitivity to noise and react more and more negatively to higher noise levels, the reaction is less clear in the other two household types. Loud dwellings which exceed the price discount thresholds are rented for a lower amount of rent. Less affluent households are much more sensitive to price, which is why the average household group has a less steep decrease in utility. In the case of low-income households, the potentially high price discounts can actually lead to a better utility when compared to more quiet dwellings, which do not get price discounts. Since the thresholds for the noise categories in the utility function and for the price discounts differ, the two categories 'Constant' and 'Frequent' show some variation in utilities. Two dwellings with noise values of 64 dB(A) and 66 dB(A) will both fall into the 'Frequent' noise category while the first will only qualify for the 55-65 dB(A) discount and the latter experiences the discount for values above 65 dB(A).

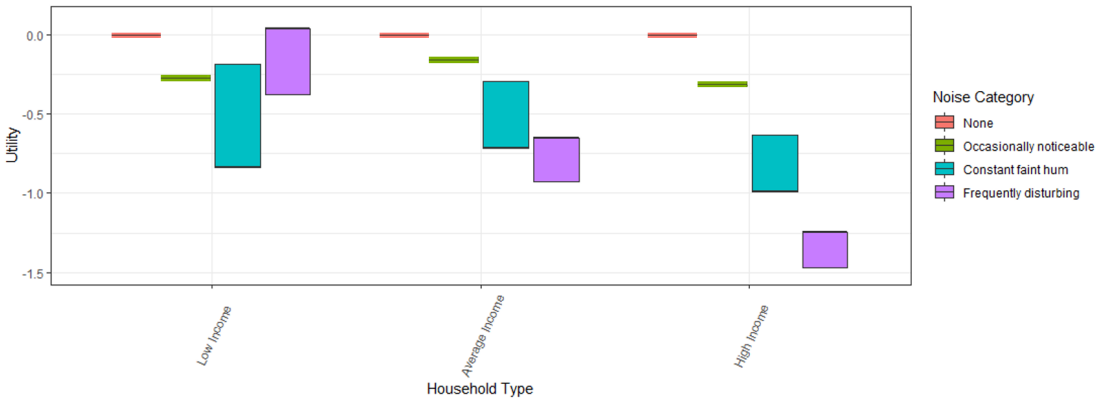

Figure 7.4: Illustrative comparison between noise sensitivities for different household types. The utility is calculated for dwellings with fixed similar attributes, only varying by noise. Because of the price discounts of noisy dwellings, price-sensitive low-income households may even favor the discount and 'accept' the noise exposure.

Referring to figure 2.7, figure 7.5 shows the actual implemented components of the FABILUT modeling suite, including the environmental submodule, which is the noise extension of MATSim. After every transport model execution, noise immission values are updated for *all* dwellings. In between transport model execution years, the traffic state is assumed to be constant. For newly constructed dwellings, the noise submodule will calculate immission values based on the latest traffic conditions at the end of the year.

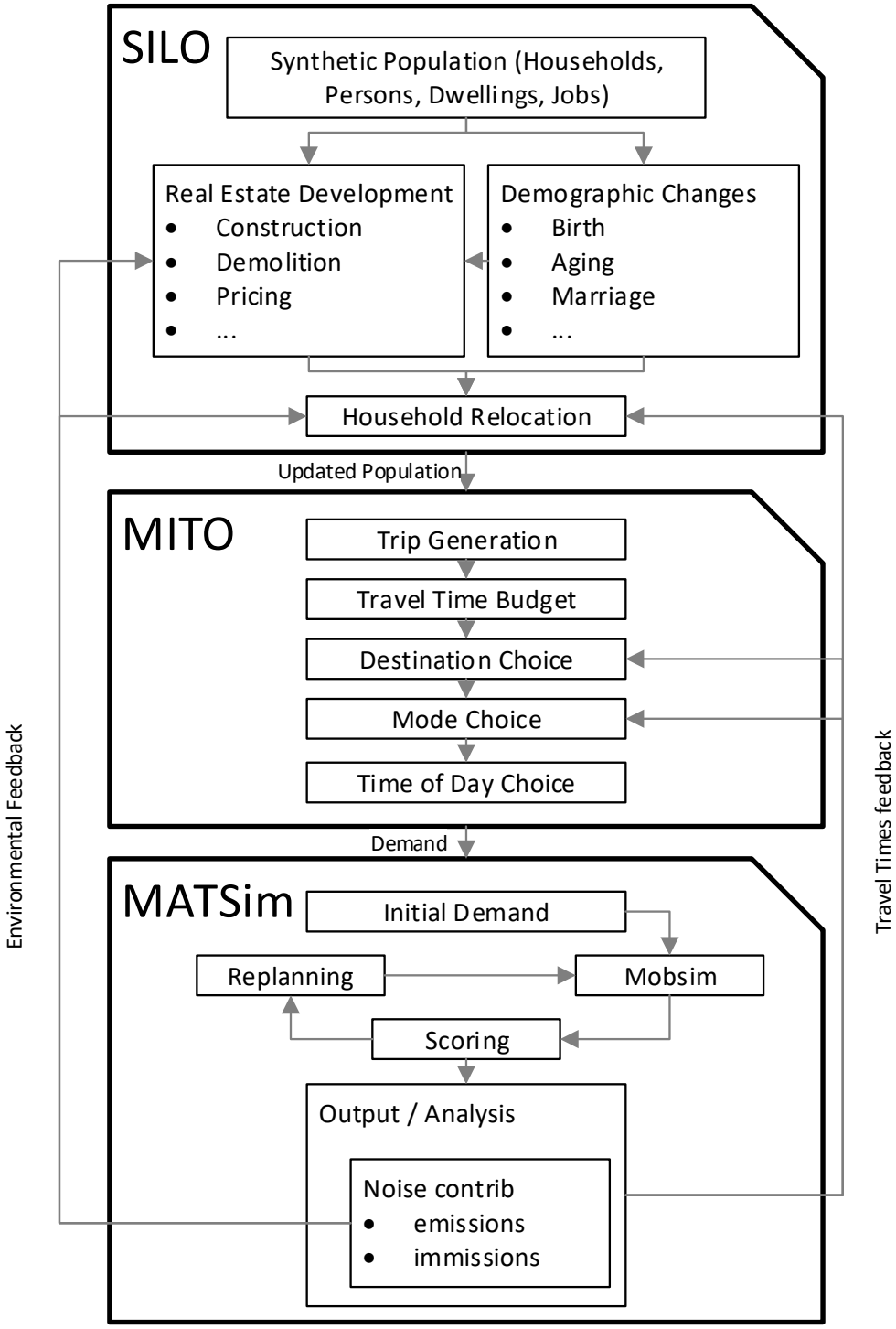

Figure 7.5: Implementation of the presented modeling suite

7.3 Integrated Feedback Model Application

Two setups were run to verify the implementation. In both setups, the model was run between 2011 and 2030 with transport model executions in 2011, 2018, 2024 and 2030. Relocations were microscopically tracked, which allows tracing the movement of households grouped by different socioeconomic traits, especially income. In the first setup, households use the newly implemented relocation strategy based on Hunt, except that *all* dwellings are perceived as *equally (not) noisy*, meaning that all dwellings get assigned the same 'None' noise base category in the utility function. In addition, no price discounts are applied. The second setup uses the actually translated noise category as defined in table 7.3 and applies the presented noise-related price discounts. The hypothesis is that, in the first setup, no significant discrimination by income should be detectable. To verify this, noise levels are still calculated for each dwelling, even though they are not used in the utility function. In the second setup, however, high-income households should tend to move to less noisy places as they are less sensitive to price and more sensitive to noise than low-income households, for which the opposite is true. Next to the hypothesis that the spatial distribution of households will be different between the two setups, it will be examined whether the exposure to traffic noise generally increases as population and its density and thus traffic is increasing in the study area.

Therefore, the average incomes of households living in highly and less exposed dwellings will be compared between the setups. In addition, the average L_{DEN} of dwellings of high- and low-income households will be compared.

As stated earlier, the presented approach tries to overcome issues of aggregated zonal values. To verify that the aggregation of local noise immissions to zonal values indeed is problematic, the standard deviations of L_{DEN} levels have been calculated for every zone and the dwellings contained within. As zones and network differ in size and density, standard deviations have been grouped by locations to distinguish between the five core cities 'Munich', 'Augsburg', 'Rosenheim', Ingolstadt' and 'Landshut' and the remaining zones, here called 'Rural'. Figure 7.6 shows the distribution of standard deviations for each of the defined locations. Note that this figure shows the distribution of standard deviations of noise immissions for multiple zones and not the distribution of noise levels. It becomes clear that standard errors are quite big in rural zones, which is expected as zones are more coarse. With the exception of Rosenheim, the five core cities reveal smaller standard deviations per zone. However, even in Munich, were zones are typically quite small (200x200m), the mean standard deviation of noise levels is around 4.75 dB(A) and the mean range between minimum and maximum noise immission within a zone is 19.5 dB(A). For Rosenheim, the reported values seem to overestimate the variance within zones. This could be due to some network issues as there were some unrealistically high congested links. All in all, the findings support the hypothesis that the aggregation of immission values to zonal indicators is problematic and can cloud local differences.

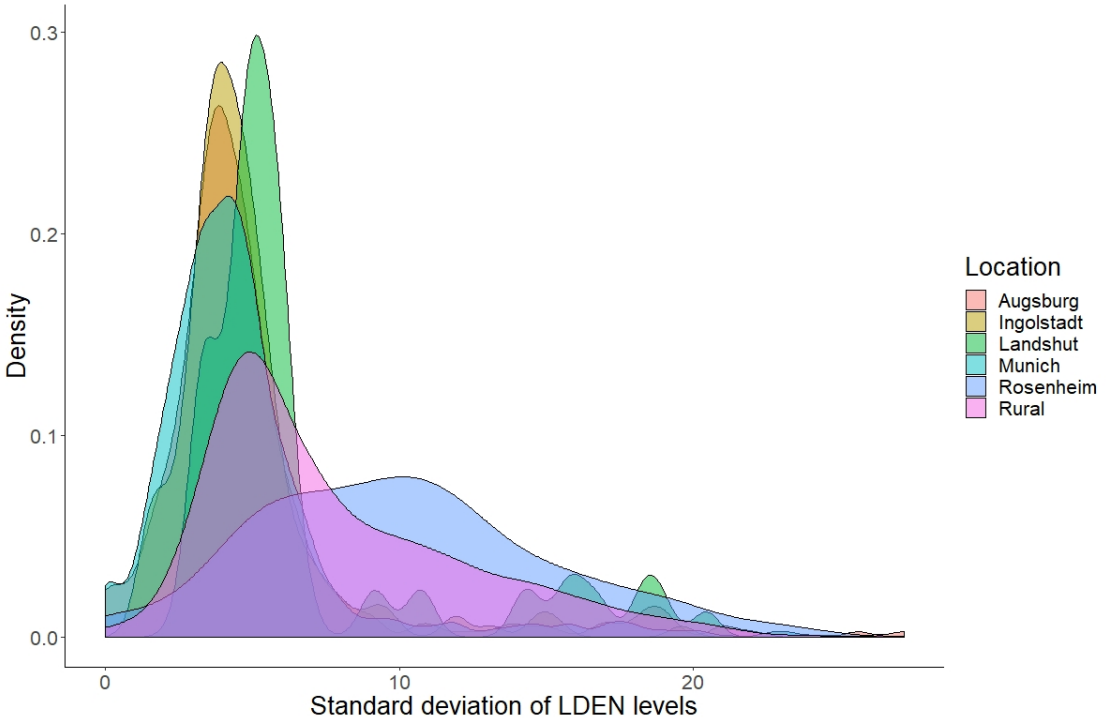

Figure 7.6: Distribution of standard deviations of immission L_{DEN} values *per zone*, grouped by location.

Figure 7.7 shows simulated L_{DEN} values for microscopic apartment locations in the base year as well as the increase of the aggregated indicator throughout 2030 using the noise-sensitive setup. Only dwellings that existed throughout the whole time period are shown, which excludes dwellings that were *built* or *demolished* after 2011. One can see dwellings close to the major motorways in both parts. All dwellings experienced an increase in noise throughout the years. The settlements near major motorways stick out in terms of absolute noise in 2011 and increase of noise until 2030. In addition, as the center of the study area, Munich shows a strongly exposed area with a large number of dwellings. Figure 7.8 shows a close-up of Munich, including the obtained building polygons from OSM used for the shielding correction. It can be seen that the mapped dwelling locations match to the buildings. Loud apartments can be seen along larger roads, while backyards are typically quieter. The larger spots where no noise value is shown include parks like the English Garden, Theresienwiese and the Olympic Village, among others. Those are places without residential buildings.

While for the analyses shown in figures 7.7 and 7.8 the noise-sensitive model was used, table 7.4 shows a comparison between the noise-insensitive model and the noise-sensitive model in which prices and relocations are affected by noise. Average noise exposure by

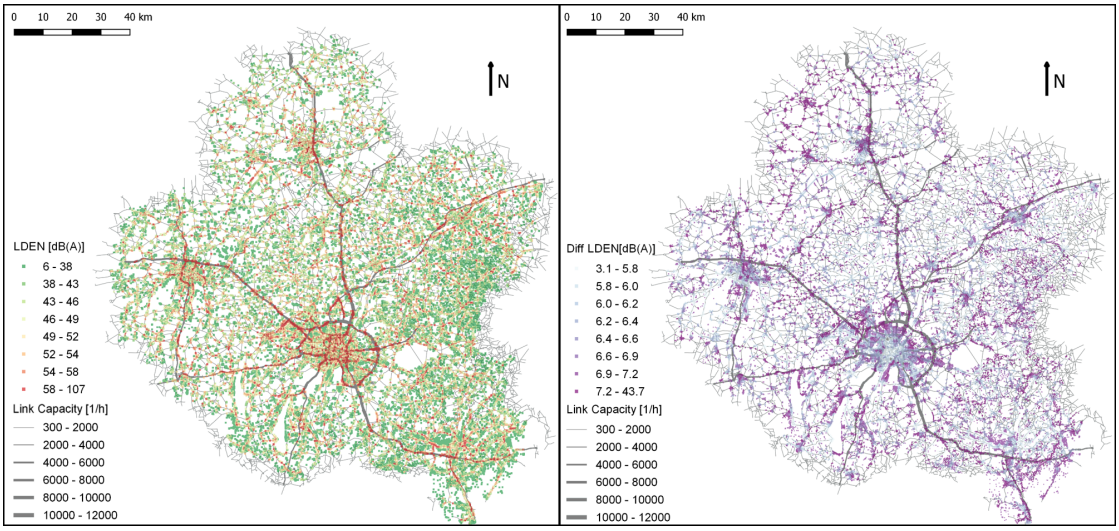

Figure 7.7: Noise levels in 2011 (left) and increase of noise between 2011 and 2030 (right) as well as link capacities per hour. Noise level ranges based on quantiles.

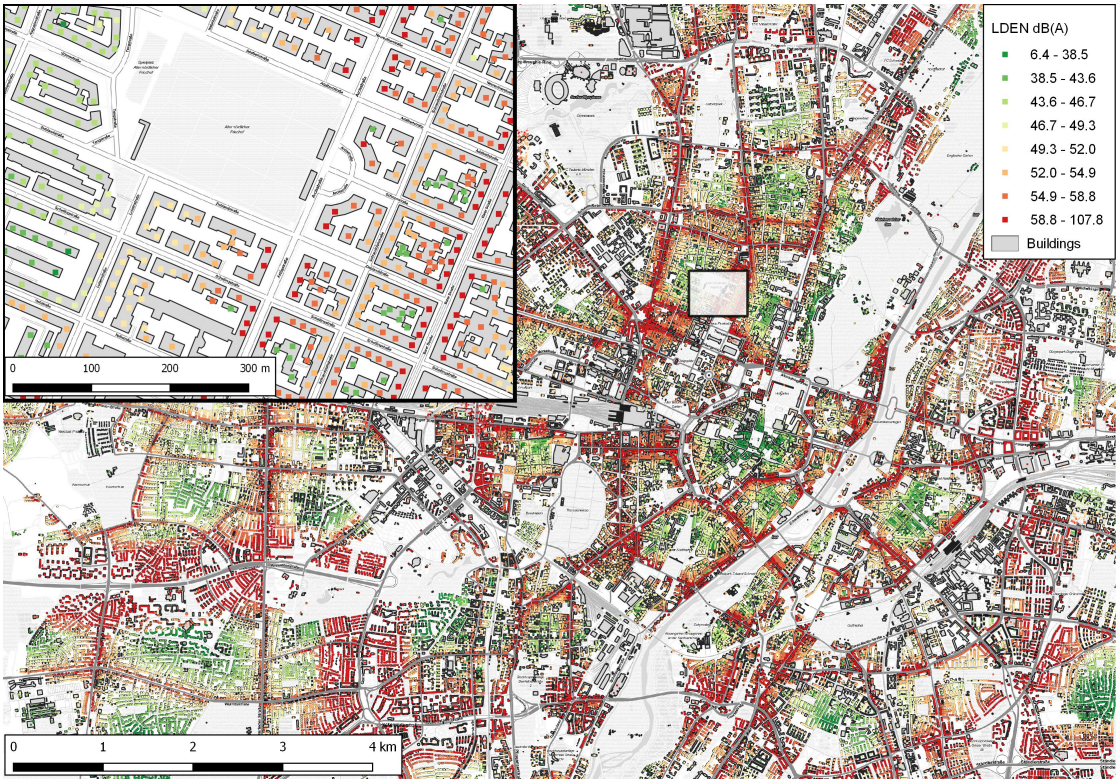

Figure 7.8: Noise levels in 2011 - close up for Munich including building polygons used for the shielding calculations.

income and average income by noise exposure of relocating households are shown for the whole study area and Munich for 2011. Note that these values only include households that actually moved in that simulation year and do not represent values for the whole population. Considering the whole study area, highly-exposed households on average show a considerably lower income than households that moved to more quiet dwellings in both models. However, while the difference in the noise-insensitive model scenario is about 308 €, the difference increases to nearly 2284 € when households and prices react to the noise. Households that move to noisy dwellings thus have around 8% lower income than households that move to quiet dwellings in the noise-sensitive model. A similar direction can be seen when looking at the average noise exposure level. The difference between high- and low-income households is around 0.2 dB(A) in the insensitive model and 1.29 dB(A) in the noise-sensitive model. The latter leads to a 3% higher noise level for low-income households. For Munich, the difference between average incomes is 1877 € and 252 € for the noise-sensitive and the noise-insensitive model, respectively. Average noise levels of relocating households are 1.25 dB(A) less for high-income households in the noise-sensitive model and 0.22 dB(A) in the noise insensitive model. It can be observed that average noise levels are higher in Munich, which is reasonable as the city is much denser and is exposed to more traffic than the rest of the study area. Figure 7.9 summarizes the differences between average incomes of relocations to quiet and noisy dwellings.

Even in the noise-insensitive scenario, high-income households relocate to less noisy dwellings when looking at the whole study area. This can be explained by the fact that high-income households also put high emphasis on the dwelling type and prefer single family houses in Hunt's model (every dwelling type other than 'single family' yields a worse utility penalty than the loudest noise category for high-income households). As single-family homes are more common in more quiet rural sides and suburbs, high-income households will thus still move to more quiet areas even when noise is kept the same for each dwelling. This effect is much smaller when only looking at relocations to Munich. Here, the differences in income between residents of noisy and quiet dwellings are quite small as multi-family houses are the most common dwelling type and noise is ignored. The noise-sensitive model shows considerably higher reactions to noise in the relocation behavior of high- and low-income households in the whole study area as well as in Munich alone. A reason why the differences in average income and noise levels are rather small is that accessibility and travel time to work are also valued highly by households, which causes households to trade off noise versus accessibility and, as such, may cloud some of the negative effects of noise.

7.4 Discussion of the Implemented Feedback

In the presented approach, noise exposures of dwellings/households were successfully traced throughout multiple years in an integrated modeling framework on an individual, microscopic level. Noise exposure levels were calculated for more than two million

Table 7.4: Average income and noise exposure (in L_{DEN}) of households that relocated in 2011. Comparison of the noise-sensitive model ('Sensitive') and the insensitive model ('Insensitive').

		Study Area	Munich
Sensitive	∅ income, noisy (>65 dB(A))	EUR 26,007	EUR 25,793
	∅ income, quiet (<30 dB(A))	EUR 28,291	EUR 27,670
	∅ noise, high inc. (>EUR 68,000)	45.86 dB(A)	49.21 dB(A)
	∅ noise, low inc. (<EUR 15,000)	47.15 dB(A)	50.46 dB(A)
Insensitive	∅ income, noisy (>65 dB(A))	EUR 27,926	EUR 27,530
	∅ income, quiet (<30 dB(A))	EUR 28,234	EUR 27,782
	∅ noise, high inc. (>EUR 68,000)	46.77 dB(A)	49.99 dB(A)
	∅ noise, low inc. (<EUR 15,000)	46.97 dB(A)	50.21 dB(A)

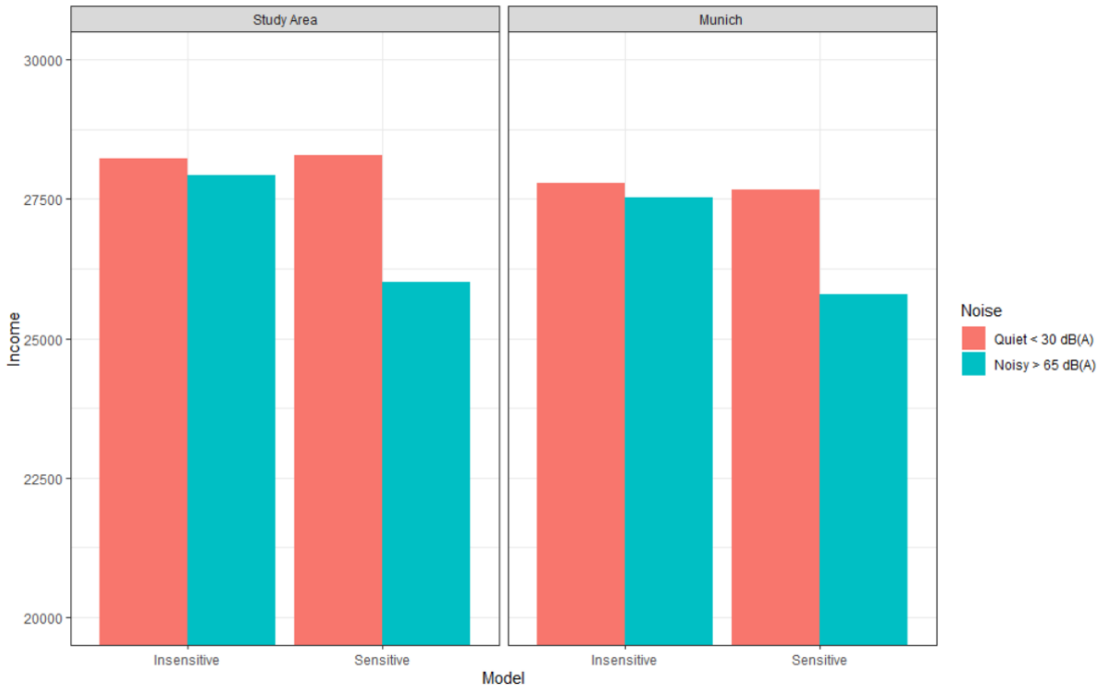

Figure 7.9: Average incomes of households moving to quiet or noisy dwellings, presented for the sensitive and the insensitive model as well as for the whole study area and Munich only.

receiver points that represent dwellings of the land-use model. As shown in previous studies, microscopic noise levels vary on a microscopic scale, especially when the impact of shielding is taken into account. This approach can therefore represent noise exposure better than zonal values could. The results suggest that the various household types react differently to road traffic noise, which verifies the functionality of the implementation.

High-income households -on average- relocated to more quiet dwellings than low-income households that tend to take benefit from the price discounts associated with high noise exposure.

The microscopic, agent-based integration may be valuable

- to identify exposure levels of dwellings and households and project them into future years. MATSim's resolution is capable of simulating noise for a typical 24-hour day in fine-grained time bins, accurately capturing evening and night time levels.
- to simulate changes in noise exposure due to policies on the land use *and* the transport model side and the resulting feedback. This could include time-of-day dependent, individual noise-sensitive taxes on car commutes, causing agents to relocate closer to their workplace.
- to analyze microscopically who is exposed to and who is emitting road traffic noise to understand and simulate issues of environmental equity over the course of multiple years.

The price adjustment model was calibrated specifically for the Munich study area. It is recognized as a limitation that the relocation choice model developed by (Hunt, 2010) was simply transferred to this study area without recalibration. As a proof of concept, however, the approach showed plausible and intuitive results. A large drawback is that the conversion from categorical variables to a continuous immission value is somewhat arbitrary. In addition, Hunt's choice model does not account for the size (in terms of floor space or number of rooms) of a dwelling, which is one of the most important factors for relocation choice. If household relocation survey data were available for the Munich region, a model could be estimated that better represents local conditions.

It is well known that is that exposure to noise is not the same as perceived nuisance (Hamersma et al., 2014). As the framework is agent-based, more complex behavior could be represented. For example, Coensel et al. presented an agent-based approach to explain the perception of environmental stressors (Coensel et al., 2007). Similarly, modeled noise immissions at the building facade do not necessarily reflect the noise annoyance indoors. A surrogate could be the estimated percentage of people that are highly annoyed at specific immission values, an indicator commonly used in the European Union (Council Directive 2002/49/EC, 2002).

The presented framework fills the gap of microscopically integrating noise as a feedback loop in an existing land-use/transport model. The results confirm the setup and open new possibilities of analyzing environmental stressors such as noise in an integrated context. Regarding research question 4, it can be confirmed that the inclusion of model reactions to noise leads to different outcomes in relocation patterns of households. For the whole study area, the difference in average incomes between households moving to quiet or noisy dwellings is roughly 3.6 times higher (2,291 EUR vs 639 EUR) in the noise-sensitive model

when compared to the insensitive model. For Munich, this difference is about 9.2 times higher (1,707 EUR vs 185 EUR) in the noise-sensitive model.

8 Agent-Based Environmental Equity: Who is exposed? Who is responsible?

> In fact, the life expectancy of city dwellers can almost be read on the city map
>
> Lärm, der zum Tode führt. DER SPIEGEL, Juli 1996

This chapter investigates the relationship between individual exposure and causation on the example of traffic noise. While multiple studies investigated the equality of exposure, the author is not aware of studies that linked (individual) exposure and causation of external effects. While the methodology can be applied to analyze exposure-causation by socioeconomic groups, this analysis looks at differences between the spatial location of residents to answer research question 5 and 6.

The results of this chapter have been published in (Kuehnel et al., 2021a).

8.1 Methodology and Scenario Setup

Before comparing exposure and causation by agent, overall distributions are compared by using the Gini index as defined in equation 2.7. Therefore, noise exposure and causation will be monetized. For each time bin (i.e., hour) of the simulation, MATSim throws events for a) agents being exposed in that time bin and b) agents causing noise while driving on a link. The exposure events include the noise damages as defined in equation 3.11. The causation events take into account all receiver points that are affected by the event link and sum up the noise damage introduced by the given agent. Since the relationship between noise level (and, thus, damages) and traffic volumes is non-linear and follows a logarithmic curve, there are two possible options to calculate the noise costs of a single vehicle. The *marginal* cost approach calculates the additional cost of one single vehicle driving on the link (Kaddoura and Nagel, 2016). The resulting cost is also called attributional cost. While the marginal cost explains the individual cost introduced by an additional car using the link, the sum of all marginal costs does not add up to the total costs of the receiver. The *average* takes the total noise damage of a receiver point and divides it evenly between all agents that used link in the given time bin. Here, the resulting cost is also called consequential cost and the sum of costs of all agents add up to the total cost at the receiver. However, in most cases, each vehicle will be charged

more than in the marginal cost approach. For the following analyses, the average cost allocation approach is used such that each agent is held equally responsible when driving on a given link. In addition, the difference of causation subtracted by exposure (δ) is calculated to quantify the net exposure-causation relationship per agent. A positive δ means that agents contribute more to noise damage than they suffer from it, and vice versa.

For area classification, the city and community classification of the Bundesinstitut für Bau-, Stadt- und Raumforschung (BBSR) (Bundesamt für Bauwesen und Raumordnung, 2020) is used. The typology consists of five categories: large city, medium city, small city, small town and rural community. The classification is based on population figures and central location function. Table 8.1 shows the definitions of the different types and the code used throughout the rest of this chapter.

Table 8.1: BBSR type definitions

Code	Type	Definition
BBSR 10	large city	more than 100,000 inhabitants
BBSR 20	medium city	20,000 - 100,000 inhabitants
BBSR 30	small city	10,000 - 20,000 inhabitants
BBSR 40	small town	5,000 - 10,000 inhabitants
BBSR 50	rural community	less than 5,000 inhabitants

As can be seen in figure 4.4 in chapter 4, activity locations of the scenario are distributed randomly across municipalities and are not linked to facility locations. Since noise immissions are very sensitive to actual locations of receiver points, activity locations of all activities were re-located to buildings nearby by using data from OSM. Thereby, the route information of legs was removed while information on selected mode and departure time were kept. Subsequently, the simulation from the relaxed scenario was run again with a re-routing strategy of agents only. Although the relocation of activity locations to building locations is simplistic, receiver point locations and, thus, noise exposure should be more realistic on average. This will not allow for a detailed individual analysis of exposure at the micro-level but should produce reasonable aggregates at larger scales.

After the MATSim assignment, receiver points were defined by creating one receiver per 'home' activity in the output plans of agents to ensure adequate noise cost allocation. For each receiver point, immission values and costs were calculated. Here, the buildings obtained from OSM are also used to account for their noise shielding and reflection effects.

Each receiver point was matched to its BBSR type by spatial location. The BBSR typology in the study area can be seen in figure 8.1. One can see that the large city type is only present in the center and includes the cities of Potsdam and Berlin. Another observation is that, in general, the municipalities become more rural with increasing dis-

tance to the center of the study area.

A total of 491,351 receiver points were obtained from 'home' locations of the 10% population sample in the open Berlin scenario (note that this does not reflect the number of agents, as some agents do not have a home activity at all and agents usually have more than one 'home' activity per day). The estimated noise levels L_{DEN} are shown in the center and on the right of figure 8.1. The noise causation events emitted by MATSim contain the amount of damage induced by an agent driving on a certain link at a certain time bin. Therefore, one can identify the BBSR type of the area where the noise event occurred. Thereby, one can get for each agent the distribution of noise damages imposed on receivers of each BBSR type. Since it is also known where the agents live, the distributions of noise damages can be linked to the BBSR type of causing agents. Agents that do not have a 'home' activity are ignored in the causation analysis, which excludes freight and bus driver agents.

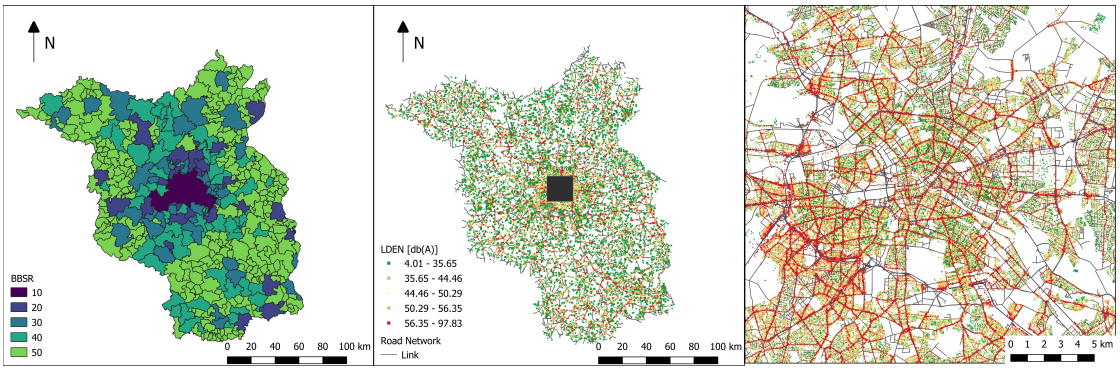

Figure 8.1: Study area and BBSR types (left) and receiver point locations, noise levels and network (center), including a close-up for Berlin (right). Noise levels based on quantile ranges.

8.2 Environmental Equity Analysis Results

First, the Gini indices for exposure and causation were calculated and the respective Lorenz curves are shown in figure 8.2. The Gini index of noise exposure is 0.72, while the Gini index of noise causation is 0.89. This means that both, exposure and causation are distributed quite unequally. By comparing the indices and Lorenz curves, it can be observed that the distribution of noise causation is more unequal than the distribution of exposure, meaning that while around 40% of agents are exposed to most of the damage, only around 20% of agents are actually responsible for the damage.

Figure 8.3 (left) shows the scatter plot of agents' noise exposure and noise causation in monetary terms. This figure shows a logarithmic decreasing trend, which indicates that some agents contribute to much noise but are exposed to less noise and vice versa. That is, not only is the distribution of causation and exposure generally unequal but there is

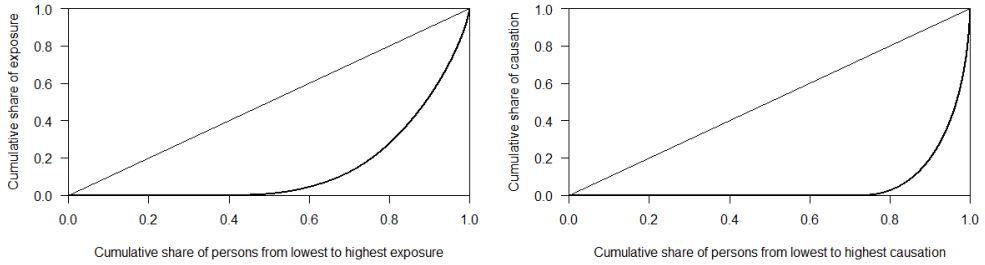

Figure 8.2: Lorenz curves of noise exposure (left) and noise causation (right). Values refer to costs in €.

also a certain inverse relationship in which the very people who suffer the most (least) contribute the least (most) to suffering.

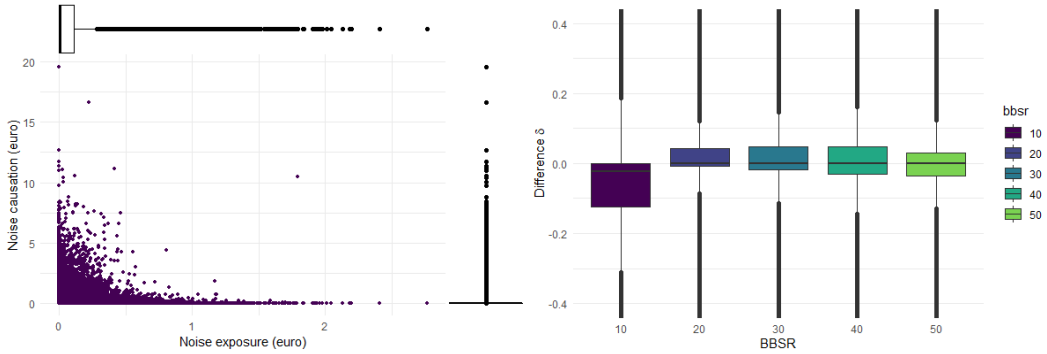

Figure 8.3: Scatter plot of noise exposure and causation per agaent in monetary terms (left) and distribution of the causation to exposure difference δ for each BBSR type (right).

The right part of figure 8.3 shows the distribution of the causation-exposure difference δ by BBSR type. Here, BBSR 10 sticks out clearly, with most of the agents having a negative value, meaning that, on average, agents experience more damage than they cause. This can be explained by the fact that noise levels, in general, are quite high in the large cities and, more importantly, a large share of agents does not cause any noise damage (by private car) at all as agents have more options to travel by other modes. This becomes clearer when looking at table 8.2, which summarizes statistics regarding the spatial distribution of noise causation and exposure. The share of agents that do not cause any noise is highest in BBSR 10 (note that this does not represent the share of non-car modes, as car users may drive on links that do not contribute to receiver points that exceed the immission threshold $L_{\text{eq},t}^{min}$). On the other hand, the share of agents that is not experiencing any noise damage is lowest in BBSR 10 type (32.05%). Still, the mean noise causation for BBSR 10 is very similar to the other community types, which suggests that those agents that actually cause noise damages do so on a high level. This is reasonable because while the per-agent exposure cost is similar in BBSR 10, the population or receiver point density is much higher and, therefore, driving on a link can

affect many more agents. The standard deviations of noise causation in each BBSR type are generally larger than for noise exposure, which again shows that noise causation has a higher variance than noise exposure and is less equally distributed.

Table 8.2: Noise causation and exposure by BBSR type

BBSR	Mean noise causation (standard deviation) [€]	Mean noise exposure (standard deviation) [€]	Mean causation - exposure difference δ [€]	Share of agents without noise causation	Share of agents without noise exposure
BBSR 10	0.07 (0.28)	0.09 (0.12)	-0.02	83.84%	32.05%
BBSR 20	0.08 (0.23)	0.05 (0.11)	0.03	63.11%	65.83%
BBSR 30	0.08 (0.24)	0.05 (0.11)	0.03	60.90%	62.72%
BBSR 40	0.08 (0.21)	0.06 (0.11)	0.02	57.49%	58.92%
BBSR 50	0.06 (0.16)	0.06 (0.11)	0.00	60.10%	59.48%

The Sankey diagram shown in figure 8.4 shows for agents living in each BBSR type (left) the distribution of noise damages caused by these agents in all BBSR types. Note that the shares on the diagram's right cannot be interpreted as distributions of the total noise exposure from different BBSR types, as the share of agents living in each BBSR is quite different. It can be seen that a high share of noise damages stays in each respective BBSR type. However, in BBSR 10, 97.3% of all noise costs are incurred within the same type, while only 38% to 50% of noise costs stay inside other types. In contrast, BBSR types 20, 30 and 40 all have a high share of noise costs caused in BBSR 10 (29%, 41% and 40%), indicating more extensive commute flows from those areas to BBSR 10. For BBSR 50, the noise cost shares split up almost evenly across the other types (between 12% and 19%). A reason for that could be that municipalities of BBSR type 50 are quite distant from Berlin and Potsdam and the respective commute patterns should be relatively small. This can lead to a smaller share of noise pollution-induced in the large cities. In addition, agents that travel from a BBSR 50 to the two cities of BBSR 10 need to pass through communities of other types first, which further smooths the distribution.

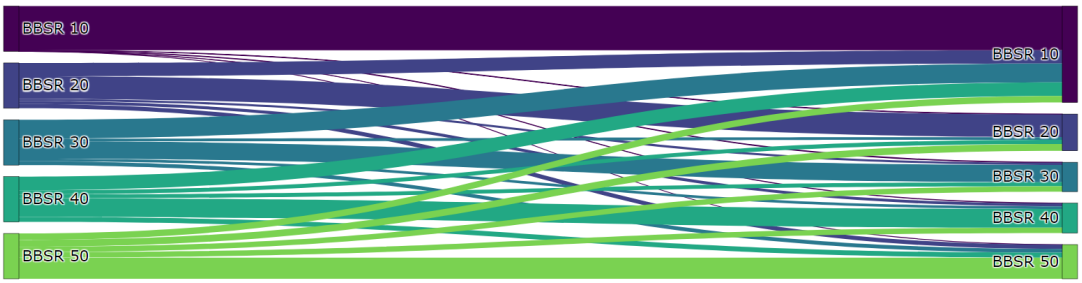

Figure 8.4: Sankey diagram of noise causation distribution by BBSR type

8.3 Discussion of the Equity Analysis

The study presented in this chapter confirmed that agent-based models are suitable tools to analyze equity issues that emerge from individual behavior. Unlike previous studies, individual causation by using social costs as a proxy was analyzed in addition to exposure to environmental stressors. While exposure and causation were both unequally distributed, the inequality of causation is considerably higher. This is partly because only part of the population owns a car and drives, but almost every home is located near roads. As such, everyone benefits (e.g., in the form of accessibility) and suffers (in the form of negative external effects) from shared infrastructure. In addition to these general conclusions, spatial patterns were identified when looking at different city and community classifications and their exposure-causation relationship.

Future studies should look at overcoming limitations introduced by the simplified allocation of residents to buildings. Furthermore, more activity types in addition to being at home should be considered. If more detailed and fine-grained socio-demographic information were available, they should be taken into account by linking exposure and causation to other attributes, such as income, car ownership or education. Other equity analyses could account for the positive aspect of accessibility.

Millimet and Slottje (2002) stressed that the Gini index does not necessarily mean that there is a reason for concerns. The authors, based on Paglin (1975), argue that inequal environmental distribution is not a problem if the inequalities occur between population groups with a similar income and higher polluted groups are compensated by having higher incomes (e.g., people living in large cities having a higher socioeconomic status but also more a higher exposure to pollution). However, they also acknowledge that if different populations cause the unequal distribution of environmental stressors within a given locale, issues of fairness persist and that these questions can only be answered with sufficiently disaggregated data. If more information on sociodemographic traits is available, agent-based simulations could be considered sufficiently disaggregated. Given that the benefits or 'positive' goods such as accessibility or income for each of the BBSR types are not studied here, the findings should not be used for policy implications but are meant to serve as an exploratory analysis using agent-based simulations, including the assessment of individual causation.

As a result of this chapter, research question 5, which asked whether causation of noise is more unequally distributed than exposure thereof, can be answered with 'yes', since the Gini coefficient for causation was found to be higher. In addition, the finding that different BBSR types have different shares of agents with/without noise causation and the fact that almost all BBSR types produce a high share of noise in the BBSR type 10 leads to the conclusion that there is apparently a spatial pattern that shows that dwellers in the large cities are more disproportionally affected by noise caused by agents of surrounding smaller communities. Therefore, research question 6 can be answered affirmatively.

9 Demand Responsive, Autonomous and Electric Transit - The Impacts on Traffic Noise

> [...]we help cities reduce air pollution, congestion, **noise** and space constraints, and achieve their sustainability goals
>
> Part of the ride-pooling provider MOIA's mission

This chapter presents an application of the updated noise model in conjunction with an additional MATSim extension that allows simulating ride-pooling scenarios. This way, the impacts of this new mobility concept on traffic noise are investigated. The application introduces an autonomous on-demand ride-pooling service to the existing transport system in central Munich. Two mode choice scenarios are applied: A draconian one in which the entire car travel demand within the service area is forced to use the new ride-pooling system and a laissez-faire scenario in which all agents are allowed to use the new mode and mode choice decisions are based on an incremental choice model (Koppelman, 1983). For each mode choice scenario, a door-to-door and a stop-based service are introduced and system efficiencies, service levels and noise exposure of residential dwellings are measured. In a stop-based service, passengers are picked up and dropped off at predefined stops and need to walk the first and last part of their journey.

The hypotheses are that a) noise exposure should be reduced by replacing conventional car trips with pooled rides and b) residential exposure should decrease even more in a stop-based service than in a door-to-door service and c) service levels (travel time, wait time) are better in the draconian scenario as the service is not affected by congestion caused by individually driven cars. Lastly, d), a fully electric fleet should lead to a considerably lower noise exposure than a fleet of conventional vehicles. By analyzing these aspects, research questions 2, 7 and 8 will be addressed.

The results presented here have first been published in Zwick et al. (2021).

9.1 Data Preparation and Scenario Setup

MATSim's DRT extension, which has been introduced in section 3.5, will be used for this chapter to investigate the large-scale application of a ride-pooling service. Noise immissions are calculated for each dwelling of the synthetic population in the service area. This allows assessing the environmental impact of noise immissions and how it is affected by the introduction of ride-pooling. The noise analyses in the scenarios are performed once assuming an all-electric fleet and once with a regular combustion fleet to answer research question 2 of this thesis. Thereby, the correction term for electric vehicles presented in section 5.6 will be applied.

The simulation is set up for the Munich metropolitan area as described in chapter 4. The demand of the complete study area is taken as an input, even though the analysis focuses on the core city of Munich. This ensures that in- and outbound traffic is included. The service area for the new ride-pooling system was defined to cover the service area of the former ride-pooling service Clevershuttle[1] in Munich shown in Figure 9.1. It covers roughly 200 km^2 and contains 1,531 public transport stops, provided by OSM, which are used for the stop-based service. Previous studies by Zwick and Axhausen (2020b); Gurumurthy and Kockelman (2020) have shown that the stop network design has a major effect on system efficiency, whereby a thinner stop network enables more efficient pooling, but customers face longer walking distances. More efficient pooling and more distances covered by walking are two reasons why a stop-based service should considerably reduce road traffic noise.

It is assumed that the public transport stop network is already fairly optimized for the current public transport system. Curb space is already used for pick-up and drop-off areas, facilitating the usage of those stops for a ride-pooling system. However, additional curb space would need to be created to account for additional vehicles using the stops.

For the base case, all agents of the greater study area that chose to travel by car are simulated. Next, the resulting vehicle kilometers traveled (VKT) and noise exposure within the service area are measured to obtain the base indicators for comparison in the following scenarios. For ride-pooling scenarios in MATSim it is not feasible to simulate a representative sample of travelers in MATSim to reduce computational runtimes. Sampling would lead to artifacts in the pooling rate that are hard to interpret. If a pooled vehicle can carry four passengers and the sampling rate is 10 %, it becomes impossible to analyze the occupancy rate due to the discrete number of passengers in agent-based modeling. Consequently, 100 % of the car trips are simulated in the base case, which is also used to define the demand of the first ride-pooling scenario.

In all scenarios, the dispatching algorithm is set up with a maximum wait time of 10 minutes and a maximum acceptable travel time of $1.5\,t_{\text{direct}} + 10\,\text{min}$, where t_{direct} is the direct travel time between the origin and destination. This ensures a reasonable balance between service efficiency and service quality (Zwick and Axhausen, 2020b). Re-

[1] Clevershuttle shut down service in Munich in 2020

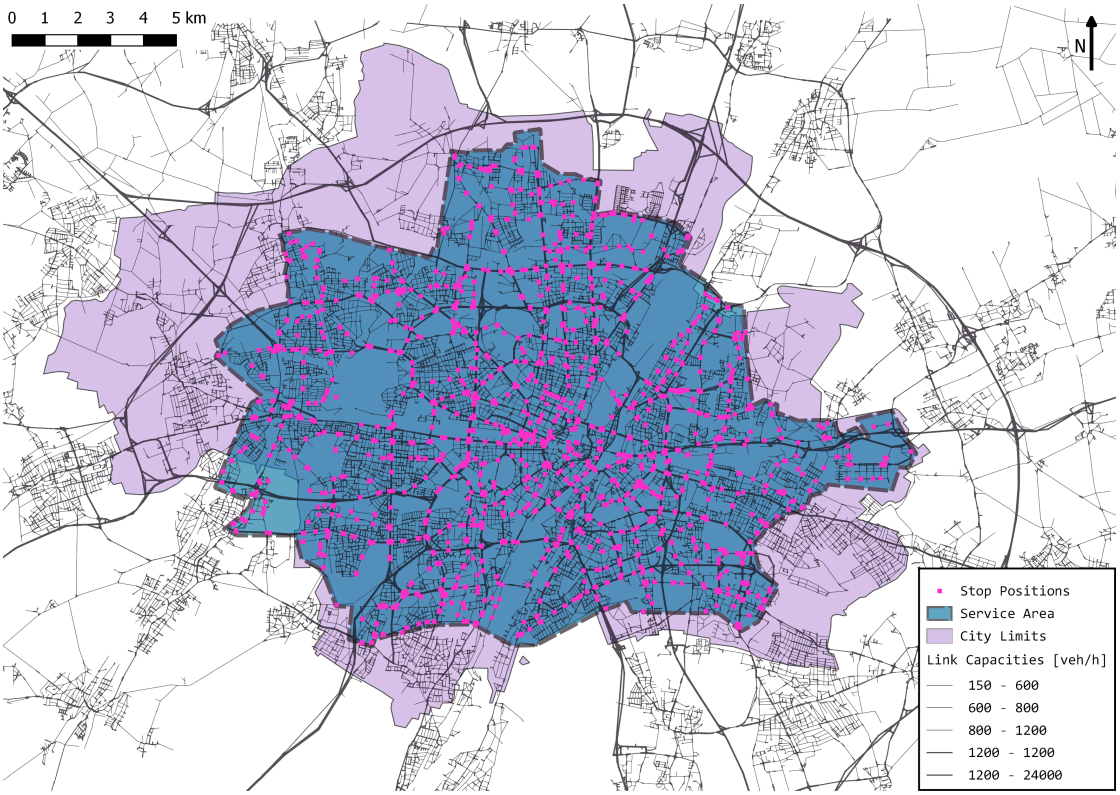

Figure 9.1: Service area and (stop) network.

quests that cannot be served by any vehicle within the given constraints will be rejected and are not further considered within the simulation. The stop time for every pick-up and drop-off is 30 seconds. The vehicles operate 24 hours, without accounting for down-times for charging, maintenance or other operational issues. For both mode choice scenarios, a door-to-door and a stop-based ride-pooling operation system are simulated, which, in combination, leads to four different cases for comparison.

In total, 647,677 dwellings of the synthetic population presented in section 4.2 lie within the service area and will be evaluated to assess noise immissions (see figure 9.1). For each of these dwellings that were matched to OSM buildings, a receiver point is defined. As larger buildings may contain multiple dwellings, the resulting average immission levels will be weighted by household density. Therefore, the spatial location of changes in noise immission levels actually matters, as noise reductions in remote areas will help fewer residents than in crowded areas.

The processes to obtain the demand for the two mode choice scenarios are described in the following two subsections.

9.1.1 Draconian Scenario

In the first mode choice scenario, a radical but straightforward policy is assumed. All existing private car trips that drive within the service area are replaced with ride-pooling trips. Trips that neither start nor end in the service area are cut out to reduce the runtime. External-to-internal trips (E-I) and internal-to-external trips (I-E) are transferred to the ride-pooling system within the service area and are assumed to be transported by an alternative mode outside the service area. Similar to a previous city-wide application of on-demand mobility with un-pooled rides by Bischoff and Maciejewski (2016), travelers using other modes in the base case cannot switch to ride-pooling and are ignored. Through traffic is not taken into account here. This can be justified by the fact that the service area does not include the outer motorway ring commonly used by trips neither starting nor ending within the service area.

The door-to-door service is operated by 18,000 6-seater vehicles. The stop-based service is simulated with 12,000 6-seater vehicles. These numbers have been identified as sufficient to serve at least 99.8 % of all requests without rejections.

9.1.2 Laissez-Faire Scenario

The second setting applies a laissez-faire scenario in which every agent may choose the new ride-pooling mode (among all other existing modes). Therefore, MITO's mode choice model has been extended by a ride-pooling mode to obtain somewhat realistic mode shares. Due to the lack of data for model estimation and calibration, the agents' decisions are based on an existing utility function which is implemented an incremental logit model (Koppelman, 1983). As the original mode choice model does not include a taxi mode, it is assumed that the mode *car passenger* is most similar to ride-pooling. Similar to *car passengers*, agents are not driving themselves and do not need a car or a driver's license. While agents use a third-party service and have to share their trip with strangers, which makes it similar to transit modes, the level of comfort is considered to be more similar to a private car. Agents do not have to rely on connections and transfers, there is no predefined schedule and individual seats are guaranteed without the risk of overcrowding. Lastly, even in the stop-based ride-pooling service, routes, in general, will be more direct than transit routes as any stops can be connected for the start and end of a trip. Utilities for the new mode were calculated by re-using the utility coefficients of the *car passenger* mode. The main difference in utility compared to auto passenger are generalized costs. The generalized costs in MITO include travel time and monetary costs. For the laissez-faire scenario, the generalized costs are adjusted to include wait time, service costs per km and a detour factor for the actual travel time. The simulated service employs an autonomous vehicle fleet. Therefore, a predicted per-kilometer fare for an autonomous service is taken from Bösch et al. (2018) and is set to EUR 0.27. Additionally, a fixed fare of EUR 2 is charged. A previous draconian scenario simulation is used to obtain estimates for the average wait times and detour factors. Figure 9.2 shows that the average wait times in the draconian scenario are constantly around 5 minutes for

most parts of the service area. Thus, the waiting time for ride-pooling is set to 5 minutes for all customers. Travel times are estimated using direct car travel time and multiplying it with the average detour factor taken from a previous simulation. Different from the draconian scenario, only internal-to-internal trips are allowed within the service area to be made by ride-pooling. The assumption is that most people would probably not use another mode from/to the boundary of the study area and change from/to ride-pooling if it is not enforced.

To serve at least 99.8 % of all requests, 8,000 6-seater vehicles are used for the door-to-door service and 5,000 6-seater vehicles for the stop-based service.

9.2 Results of the Large-Scale Ride-Pooling Scenarios

The presented scenarios are analyzed with regard to system efficiency and traffic noise impact within the service area shown in Figure 9.1. After presenting the base case results, the system efficiency is compared to the draconian and the laissez-faire scenarios with the two proposed ride-pooling services. Efficiency and service indicators are important to understand how impacts on resulting noise emerge and whether there are trade-offs between noise exposure levels and transport system efficiency. Finally, the noise impacts are assessed in each scenario.

In the base case, overall VKT within the service area is 9.8 million km, including the VKT by incoming, outgoing and through traffic. The average travel time for internal trips is 13:01 minutes for an average trip length of 6.9 km. Consequently, the average travel speed is 32 km/h, which is in line with values reported by Forbes (2008) and Engelhardt et al. (2019). Access and egress trips for private car trips and parking search traffic are not considered.

9.2.1 Ride-Pooling System Performance

The transport system aims at transporting all agents in the shortest possible time to their destination, including short wait and walk times. Table 9.1 shows performance indicators for the door-to-door ride-pooling service and the stop-based ride-pooling service.

With a door-to-door ride-pooling service and a draconian policy, 18,000 vehicles are used to serve almost 2 million rides that were previously conducted by private vehicles. In total, the ride-pooling system leads to 7.0 million VKT, of which 8 % are driven empty to pick up customers and for reallocation purposes. To facilitate the comparison between the scenarios, the VKT is also measured inside the service area, which is 6.6 million km in this case. In the base case, the VKT is 9.8 million km, which means that a substantial reduction of VKT with the pooling system can be observed. The mean travel time is 15:12 minutes, the agents face an average detour of 40 % and an average wait time of 5:30 minutes. 2,926 requests (0.15 %) could not be served within the maximum wait

Table 9.1: Overview of system performance indicators of the base case system and all ride-pooling (RP) systems within the service area.

	Base case	Draconian scenario		Laissez-faire scenario	
		Door-to-door	Stop-based	Door-to-door	Stop-based
RP vehicles	—	18,000	12,000	8,000	5,000
RP rides	—	1,912,783	1,836,513	503,037	498,529
Rides per RP vehicle	—	106	153	63	100
RP rejections	—	2,926	0	179	132
RP kilometers [km]	—	6.9×10^6	4.5×10^6	1.9×10^6	1.4×10^6
VKT in service area [km]	9.8×10^6	6.6×10^6	4.5×10^6	10.6×10^6	10.1×10^6
Share of empty km [%]	—	8	7	5	6
Avg. travel time [min]	13:01	15:12	14:44	17:01	15:41
Avg. trip length [km]	6.9	9.7	9.6	9.4	9.2
Avg. detour [%]	—	40	41	42	44
Avg. wait time [min]	—	5:30	5:04	5:34	4:56
Median wait time [min]	—	5:37	5:08	5:36	4:43
Avg. walk distance [m]	—	—	271	—	259
Avg. computation time per iteration [h]	1/2	24	16	9	5

Note: Walk distance only includes walk to and from ride-pooling vehicles.

time of 10 minutes or the accepted detour parameter.

Using a stop-based ride-pooling service in the draconian scenario, a small part of the requests are not served by the ride-pooling system. In these cases, the origin and destination stops are the same. The remaining 1.8 million requests can be served by only 12,000 vehicles, leading to more than 150 rides per vehicle. The vehicle kilometers driven are further reduced to 4.5 million km, which is a reduction of 54 % compared to the base case. The average travel time drops to 14:44 minutes and the mean wait time to 5:04 minutes. Additionally, the agents need to walk on average 271 m to and from a stop, or a total of 542 m per trip. None of the requests had to be rejected with the given service constraints.

For the laissez-faire scenarios, MITO's mode choice model predicted a 16 % share for autonomous ride-pooling trips starting and ending in the service area. For the majority of these trips, two rides will be simulated, as these are home-based and include a return trip. Roughly 47 % of the ride-pooling trips were previously made by the modes *car* or *car passenger*, 20 % by *public transport*, 13 % by *bike* and 20 % by *walk*. In total, about half a million ride requests are served by the on-demand system. 8,000 vehicles in the door-to-door system and 5,000 vehicles in the stop-based system are necessary to serve these requests. Similar to the draconian scenario, a small share of requests cannot be served within the given service parameters and is rejected. Fewer kilometers are driven with the ride-pooling system, as fewer rides are served. The total VKT in the service area, however, increases to 10.7 million km for the door-to-door system and to 10.1 million km for the stop-based system. This increase compared to the base case can be explained by

increased number of trips conducted on the road network as the ride-pooling system not only attracts private car users but also agents that previously used the modes transit, walk or bike. With 5% and 6%, the share of empty VKT is slightly lower than in the draconian scenario. Due to the higher traffic volumes, travel times are noticeably higher in the laissez-faire scenario with 17:01 minutes and 15:41 minutes, confirming hypothesis c). Customers also face slightly longer detours.

The number of ride-pooling rides and vehicles highly influence computation times per iteration. In the base case, it only takes half an hour to simulate one iteration. The simulation of the draconian door-to-door system takes roughly 24 hours per iteration. The number of necessary iterations, however, increases with the number of car trips. To reach a system equilibrium, 300 iterations were simulated for the base case, 4 iterations for both draconian scenarios and 10 iterations for both laissez-faire scenarios.

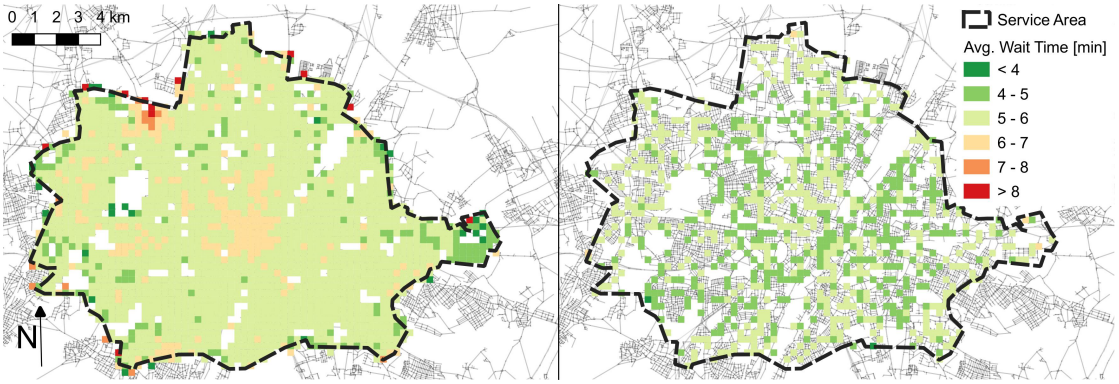

Figure 9.2: Average wait times in minutes per zone for the door-to-door (left) and the stop-based (right) service in the draconian scenario.

Figure 9.2 shows average waiting times per zone for the two ride-pooling systems in the draconian scenario. The waiting times for the door-to-door service predominantly vary between 4 and 7 minutes. Waiting times are slightly higher in the city center, where request density is highest and, consequently, vehicle flow volume increases and causes some congestion in peak times. However, the negative effect on the customer side is rather small. At the border of the service area a high variance of average waiting times can be observed. The number of rides starting in some of the outer cells is very small, which causes a higher variance. Additionally, a cluster of cells in the north-western part of the service area with higher waiting times can be observed. In this area, many rides occur due to an industrial zone with many working places and the location next to a street with incoming and outgoing car traffic that is replaced by the ride-pooling system. The waiting times for the stop-based service vary between 4 and 6 minutes and spread evenly across the service area. As the average waiting times are similar across both draconian scenarios and do not vary drastically across the service area, an average waiting time of 5 minutes for all ride-pooling trips was assumed to calculate possible ride-pooling

shares in the laissez-faire scenario. As stated earlier, the waiting times are part of the generalized costs.

Figure 9.3 shows the vehicle occupancy over time for the two ride-pooling services in both mode choice scenarios. In the draconian scenario, the door-to-door service carries six passengers during 4 % of the covered distance while the stop-based service carries the maximum number of passengers during 25 % of the overall distance, indicating that even larger vehicles than six-seaters could add efficiency.

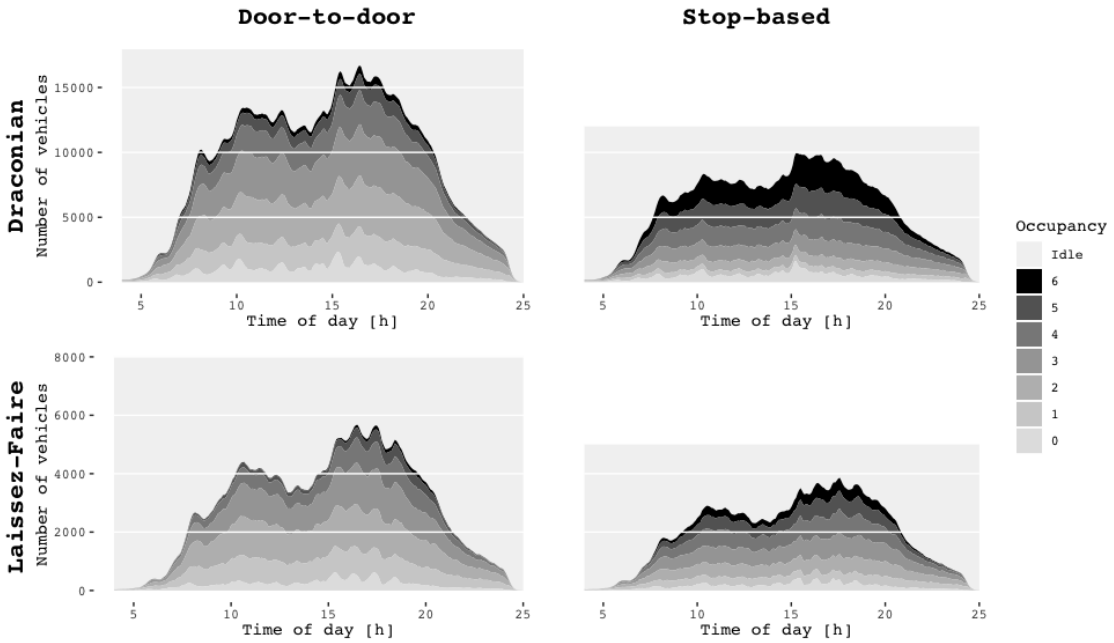

Figure 9.3: Vehicle occupancy for the door-to-door (left) and the stop-based (right) service in the draconian (top) and laissez-faire (bottom) ride-pooling scenario.

The occupancy of the vehicle fleet in the laissez-faire scenario indicates a generally lower occupancy than the draconian scenario. The door-to-door fleet only carries six passengers during 1 % of the distance, whereas the stop-based fleet is fully occupied during 10 % of the total distance. The lower occupancies in the laissez-faire scenarios are caused by a lower request density, lower travel speeds and fewer detour possibilities due to congested roads. Additionally, all incoming and outgoing traffic in the draconian scenario starts or ends at a street accessing the service area from outside, which leads to bundling of requests at those peripheral locations.

9.2.2 Noise Analysis

Figure 9.4 presents the base scenario noise immissions for all receiver points within the service area. While residential areas show noticeable lower noise levels, high noise values

are observed near major roads. Overall, immissions are comparatively high, with about half of urban dwellings experiencing an immission that exceeds 55 dB(A).

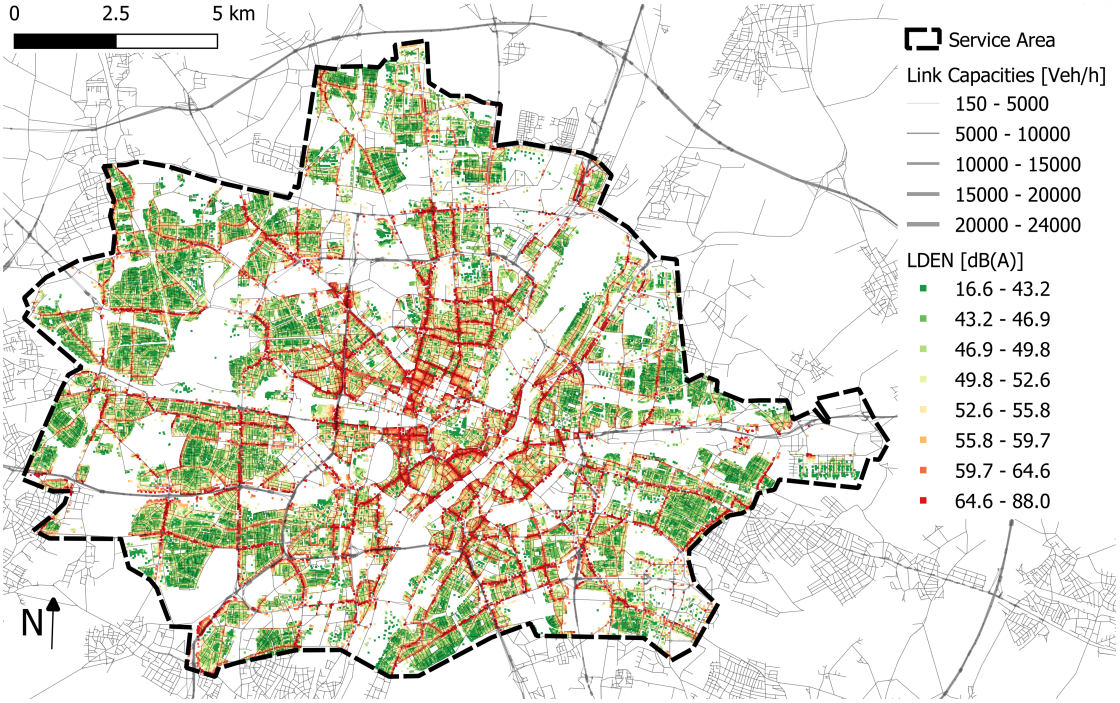

Figure 9.4: Base scenario noise exposure in the given service area in Munich. L_{DEN} values presented in quantile ranges.

Figure 9.5 shows the spatial distribution of *differences* in noise immissions in the ride-pooling scenarios compared to the base case. The results in the maps shown here do not include the electric correction term.

Noise levels –on average– are nearly the same in the base scenario and in the draconian scenario with a door-to-door service. However, when looking at the spatial distribution of differences, it can be seen that major noise reductions are estimated along major roads. Pooling rates along major roads tend to be higher as these are more frequently part of shared routes. Consequently, traffic volumes on major roads are reduced. However, the simulation results show that those reductions are almost fully compensated by increased noise in residential neighborhoods. This can be explained by detours and additional kilometers driven near individual departure/arrival locations to pick up or drop off customers to ensure a door-to-door service. In addition, pooling rates around pick-up/drop-off points in residential areas tend to be lower than at major connecting roads. The logarithmic dose-response relationship between traffic volume and noise leads to relatively high increases in noise in residential areas, where traffic volumes are low and small changes in volume lead to big changes in noise. More consistent and stronger

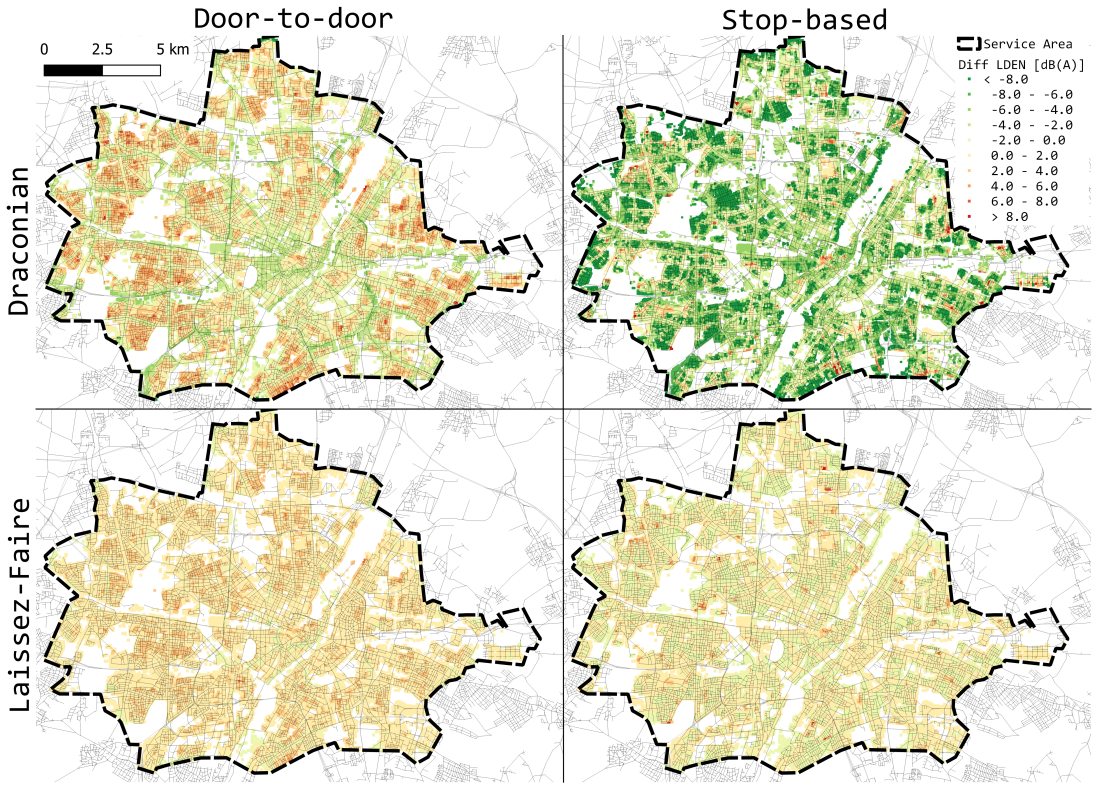

Figure 9.5: Differences in L_{DEN} values for the door-to-door (left) and the stop-based (right) service in the draconian (top) and laissez-faire (bottom) ride-pooling scenario when compared to the base scenario immission values for dwellings inside the study area. Green values indicate a reduction of noise compared to the base case. Red values represent an increase.

reductions in noise can be seen with a stop-based service, due to multiple reasons. First, fewer vehicles are required as the pooling rate is higher, leading overall to lower traffic volumes. Second, a few hundred meters of the trips are done by walking and, lastly, quite a few links do not experience any traffic at all since vehicles only route between stops. This –in contrast to a door-to-door service– leads to some very quiet residential roads and neighborhoods. A few selected sites still experience an increase in noise. These are primarily near stops where traffic volumes can be higher.

The impacts on noise are generally more minor in the laissez-faire scenario, driven by the fact that the fleet sizes are smaller and private car traffic remains the main source of traffic noise. Again, the door-to-door service leads to more noise than the stop-based service. However, since the overall traffic volumes increase in many places, there is almost no compensation at larger roads. With the stop-based service, changes in noise exposure are minimal and happen in either direction with no distinct spatial pattern. This is remarkable in that 53 % of the additional ride-pooling passengers previously used one of the

modes *walk*, *bike* or *public transport* and are now additionally riding on the road network.

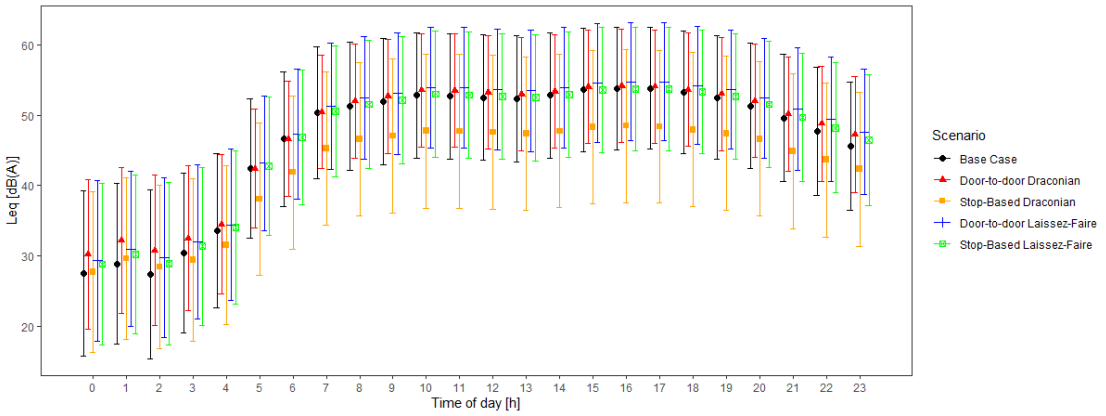

Figure 9.6: Hourly equivalent sound levels L_{eq} across 24 hours for each scenario. Symbols represent the mean across all receiver points, bars delimit standard deviations.

Figure 9.6 shows the temporal variations of the hourly equivalent sound level L_{eq} for each scenario. In general, the variation between scenarios is higher in the morning hours, where traffic volumes are typically low and changes in volume are reflected by greater changes in noise. During the day, the mean hourly sound levels stay very similar across all scenarios, except the draconian stop-based scenario. Here, the mean L_{eq} is constantly significantly lower than in the other scenarios. This indicates that the noise reduction is stable across the day.
The gap between the last and the first hour of the day is a typical limitation of transport models that run for one day only. However, because of its logarithmic nature (see equation 2.5), the L_{DEN} indicator is mainly driven by the maximum levels across a day and therefore robust against inaccuracies in lower noise levels that occur at night.

Table 9.2 shows a comparison of descriptive statistics, while Figure 9.7 shows the overall distributions of L_{DEN} values in the different scenarios and the base case. Note that the figure also shows the results for the draconian scenario with the electric correction term (i.e., under the assumption that fleet is fully electric). In the laissez-faire scenario, the correction term did not lead to any noteworthy changes and is thus not shown here. The depicted threshold of 55 dB(A) was chosen as the target threshold defined by the European Union (2002)

Mean noise immissions increased slightly in the laissez-faire scenario. The overall distribution with a stop-based service looks similar to the base case distribution,. In contrast, a door-to-door service increases the share of highly exposed dwellings by around 5 %. Remarkably, the mean immission value in the draconian scenario with door-to-door service is slightly higher than in the base case, although VKT in the service area are reduced by 33 %. However, when looking at the distribution and standard error, it shows

Table 9.2: Descriptive statistics of noise immission results.

	Base case	Draconian scenario				Laissez-faire scenario	
		Door-to-door	Door-to-door electric	Stop-based	Stop-based electric	Door-to-door	Stop-based
Mean L_{DEN} [dB]	53.17	53.68	51.93	48.41	46.92	54.29	53.37
Median L_{DEN} [dB]	52.57	53.77	51.83	48.31	46.72	54.00	52.85
Min L_{DEN} [dB]	16.64	15.51	13.825	2.75	2.52	16.95	17.04
Max L_{DEN} [dB]	87.99	84.68	83.77	83.84	82.94	88.39	88.37
S.E. L_{DEN} [dB]	8.89	8.04	8.17	10.78	10.82	8.60	8.96
Share > 55dB [%]	40	43	34	30	26	45	41

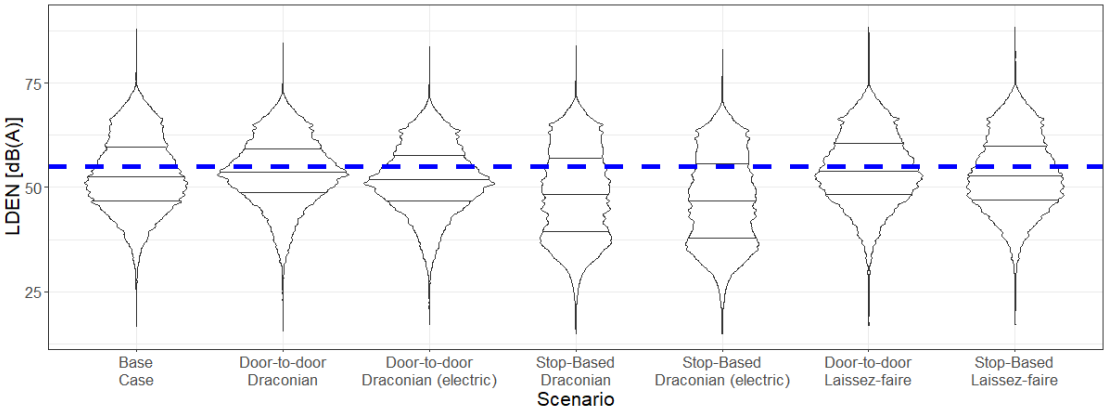

Figure 9.7: Violin plots with quantiles for the distribution of L_{DEN} values of dwellings in the presented scenarios. The dashed line depicts the threshold value of 55 dB(A).

that the immissions are distributed more evenly across all dwellings. One could say that this scenario makes noise exposure more equal. Nonetheless, the share of highly exposed dwellings increases by 3 %. The draconian scenario with a stop-based ride-pooling service, including the correction term for electric vehicles, shows the highest noise reductions, with a mean L_{DEN} of 48.41 dB(A) and only 30 % of the dwellings being exposed to more than 55 dB(A). The stop-based service here leads to higher standard errors and less equally distributed immissions (compare 'quiet' residential neighborhoods in Figure 9.5). Under the given assumptions, noise reductions can be quite significant when a correction is considered for electric vehicles. However, the results suggest that these only become visible once a major share of the vehicles on the road is electric.

Figure 9.8 shows the density distribution of differences in L_{DEN} values. While the overall distribution in Figure 9.7 suggests that, in the draconian door-to-door scenario, the distribution did not change systematically apart from a slight increase, the distribution of differences reveals that noise levels indeed change. However, in line with the spatial distribution in Figure 9.5, changes happen in both directions and therefore 'compensate' to some degree. The draconian stop-based scenarios show a clear trend towards reduced noise levels, while the laissez-faire scenarios barely expose any noteworthy differences. The electric correction term seems to maintain the shape of the distribution while push-

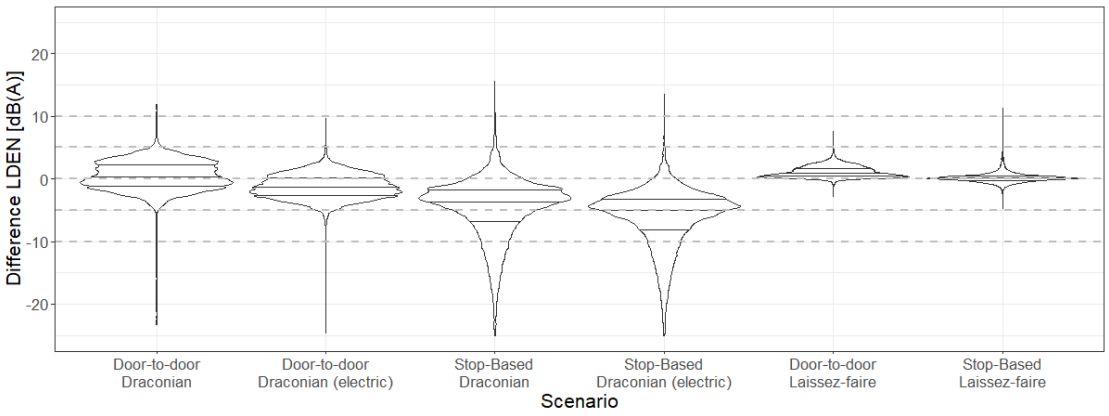

Figure 9.8: Violin plots with quantiles for the distribution of *differences* of L_{DEN} values of dwellings as compared to the base case.

ing it more towards reduced noise levels.

Overall, it can be seen that a reduction of noise can be accomplished by a stop-based ride-pooling service in a draconian scenario. The door-to-door service tends to increase the noise in residential areas, where most people live and where traffic increases because of pick-up and drop-off rides. In general, traffic noise is mainly moderated through traffic volumes and speeds (see equation 5.8). Consequently, noise consistently reduces for the stop-based service in which traffic volumes decreased thoroughly, whereas for the door-to-door service traffic, volumes only decreased on major streets, leading to less clear implications on noise and even louder levels in residential areas.

In the laissez-faire scenario, a stop-based service can keep noise at similar levels as in the base case, even though the amount of road trips increases. Because of the logarithmic dose-response relationship between traffic volume and noise, the impacts on the aggregated L_{DEN} value is small compared to the changes in traffic volumes and VKT. The results confirm that noise exposure is generally further decreased with a stop-based service than with a door-to-door service.

9.3 Discussion of the Ride-Pooling Scenario

The proposed ride-pooling scenarios show the influence of different mode choice settings and service designs on a large scale. A state-of-the-art ride-pooling strategy was employed and the impacts with an updated noise prediction model in MATSim were assessed. However, the investigation has some limitations.

A limitation for the laissez-faire scenario is the difficulty of estimating reasonable mode shares for the ride-pooling system. As observed ride-pooling data are not available for Munich, one could re-estimate a mode choice model with automated ride-pooling based

on stated preference data. However, since most of the current services are relatively new and not autonomous, a survey may only include hypothetical mode choice options. More reliable estimates could be derived by using estimated values of time (VOT) for pooled rides to have a better idea of the impacts of (generalized) costs (see e.g. Alonso-González et al. (2020)). Instead of doing the mode choice in MITO, the mode choice could be included in MATSim, enabling the consideration of the actually experienced service levels for each agent. However, since the simulation of ride-pooling with a 100 % sample runs up to 24 hours per iteration, adding mode choice would require several weeks to run the model, as many more iterations are required to reach an equilibrium. This could be reduced partly by using a discrete mode choice model instead of random mutations in MATSim as described in Hörl et al. (2018). The advantage of simulating mode choice in MATSim would be the feedback loop from actual travel times to the decision making throughout iterations. Nevertheless, even then, utility parameters would be hypothetical.

Another limitation is that both scenarios do not account for induced demand, as the trip generation phase in MITO is not affected by the availability of the ride-pooling system. In reality, however, it could happen that people do additional trips once cheap automated ride-pooling trips become available, as observed by Henao and Marshall (2019) for ride-hailing. This could be especially true for otherwise less mobile persons, i.e. persons without cars/drivers' license, children, persons with disabilities or older people.

The two scenarios presented in this study show possible outcomes under a set of assumptions and after the service is completely introduced/enforced. As pointed out in Basu and Ferreira (2020), it should be acknowledged that exogenous assumptions and the complete replacement assumption limit the use of studies like ours to the identification of long-term possibilities of new technologies. The authors stress the importance of market dynamics, which can impact acceptance and regulations. Haboucha et al. (2017) presented a stated preference study and found quite a reluctance to use shared autonomous vehicles (which were not even defined as a pooled service and just as a replacement to a privately owned vehicle), with 25 % of respondents stating unwillingness to use shared autonomous vehicles even if the service was free. In addition, respondents would instead not use the autonomous service to send children to school, which indicated safety reservations towards automated services. Parents would probably be even more cautious if they had to decide to use a shared service that is pooled with strangers.

While the detours and empty-kilometers of ride-pooling vehicles can lead to increased noise levels in residential areas, the present study does not account for the challenge of parking search for car traffic. A preceding study that included parking search in the simulation found that traffic volumes can be increased by up to 20 % in residential areas when parking search is included (Bischoff and Nagel, 2017). As parking search only applies to personally owned vehicles and not to pooled vehicles, the differences in noise levels between the base scenario and the ride-pooling scenarios would be even more pronounced.

Another limitation of the approach is that commercial vehicles which significantly contribute to noise emission are ignored. The conclusions of this research, however, are likely to hold true. The main limitation can be found on major roads where most commercial vehicle traffic contributes to noise. The impact of these scenarios is expected to be slightly smaller once noise from commercial vehicles is added to the analysis.

The chosen correction term for electric vehicles may reflect noise reductions reasonably well for the applicable speed range of the implemented noise guideline. However, higher reductions should emerge at intersections where acceleration noises of engines make up a large share of the resulting noise immission. Therefore, it is assumed that possible noise reductions at intersections are broadly underestimated since acceleration is not modeled in MATSim and the guideline assumes a minimum speed of 30km/h. This underestimation could be alleviated if s are required to be equipped with an acoustic alerting system at low speeds.

Another limitation is that only one single operator was implemented, which only offers pooled rides. Ruch et al. (2020) showed that it is unclear if the efficiency gains of ride-pooling compensate for the loss of privacy and a lower service level compared to an unpooled system. Private operators may generate higher revenues by offering private rides, which would again lead to more VKT and noise exposure. Thus, from a macroeconomic point of view, it could be beneficial for policymakers to incentivize the supply of pooled on-demand services compared to unpooled services.

Given the current limitations, the present analysis shows results that can be generalized. Major noise reductions can be achieved with a draconian replacement of all private vehicles with electric pooled vehicles and a stop-based service. Although VKT are also reduced with a door-to-door service, average noise exposure increases since more traffic occurs in residential areas. The laissez-faire scenarios indicate that only by implementing the new service, road traffic do not decrease as agents that previously chose other modes than *car* are attracted. A stop-based system is again more efficient than the door-to-door service.

Does a large-scale implementation of a ride-pooling service in a large city lead to reduced noise immissions among residents? How does penetration rate and service design impact potential changes in noise immissions? In conclusion, the first of these research questions (research question 7) can be answered by 'it depends'. In the large-scale draconian scenarios, it is shown that only in the case of a stop-based service consistent reductions among a majority of residents can be achieved. With a door-to-door service, immissions are reduced for some agents but are increased for others. This also partly answers research question (8) regarding the impact of service design. For the penetration rate, it was shown that the laissez-faire scenario did not yield substantial differences in noise immissions. Low penetration rates, therefore, do not seem to lead to noteworthy changes in noise immissions. Lastly, research question 2 'Does the wide usage of electric vehicles lead to considerably lower noise immissions?' can be answered with 'yes, but

on a low level' as the reduction from fully electric fleets indeed reduced noise immissions but only in the draconian scenario and with a reduction of mean L_{DEN} immissions of less than 2 dB(A).

10 Conclusion and Outlook

This thesis presented updates and use cases for an existing noise model in an agent-based transport simulation. The use cases showed different applications that highlight possible noise model applications in the context of agent-based simulations. However, all of the applications shown here still have limitations and lead to possible improvements and more advanced future research, as described in the following paragraphs. These paragraphs will also present the lessons learned in each of the use cases.

The updated noise model now complies with most parts of the official RLS-19 guideline. Except for second-order reflections, all other corrections have been implemented and tested. Nonetheless, more focus could be spent on accurate input data. This is especially true for building data which was shown to be crucial in terms of shielding effects. Therefore, it is essential to improve the quality of building data, especially in terms of correct building heights. This information could then also be used to have more accurate heights of receiver points, which are assumed to be the same for all receivers in this thesis. Similarly, even though the presented study areas are mostly flat, gradients and terrain heights are missing in this thesis and should be taken into account in areas with higher differences in altitude. Another limitation is that the implemented link segmentation approach only accounts for the correct length of segments. It does not check whether conditions relating to the surrounding buildings/obstacles remain constant along segments. However, it is expected that this only slightly influences the results, as segments close to the receiver are quite small. The work done in this part of the thesis included a larger part of active development of source code, which is now hosted in the official MATSim repository[1] and can be accessed freely. As such, this dissertation made use of but also contributed to the concept of open-source models. It underlines the potential of academic collaboration through open-source projects with an active community. On a similar note, many data such as roads and buildings were taken from the volunteered geographic information source OSM. Even though the quality and completeness vary among the different data attributes used in this thesis, the approach taken here presents an example of the usefulness of such data sets for academic projects. The detailed development of the noise model updates show the interdisciplinarity of modern traffic models, where software skills can be beneficial, for example in the application of ray-tracing algorithms to calculate noise reflections.

The rent price analysis showed that it is hard to find a single 'true' coefficient for the impact of traffic noise on prices. Nevertheless, it was one of the first times that a signifi-

[1] https://github.com/matsim-org/matsim-libs/tree/5d4df8361aebf1e2c458e47c95082896f2d362d7/contribs/noise

cant correlation was confirmed for simulated noise values from an agent-based transport simulation. In this thesis, it was not possible to obtain rent price data for the whole study area. For the application in a land-use model that includes multiple municipalities, future studies should identify whether the rent price impact varies substantially *across* municipalities (e.g., with a geographically weighted regression that includes records of multiple municipalities) to assess whether a 'global' relationship between rent and noise is justified. For the actual application of a pricing model in a land-use model, the analyses here concluded that a more simple OLS model that includes an 'implicit spatial variable' in the form of an accessibility indicator is better suited in terms of complexity and run-times. The spatial models can help to better understand local relationships for a given data set but are harder to apply for the prediction of out-of-sample data, as the spatial structure of the training data set is part of the estimation process. In addition, it has been shown that spatial models have a tendency of over-fitting the data. The identification of price impacts of traffic noise has shown to be a great example of a statistic regression in which the impact of confounding variables is very important, as roads can lead to positive (i.e., accessibility) and negative (i.e., noise) impacts. In this regard, the results presented in this thesis also contributed to understanding the combined and individual impacts of accessibility and noise on house prices and thereby hint to preferences of residents. Early attempts of the pricing regression shown here also underlined the importance of a fine resolution of these neighborhood variables that led to better model fits than models that used spatially aggregated zonal variables.

Based on the results of the integration of noise feedback in ILUT models, it can be said that the implementation of such feedback is feasible and leads to plausible results when individual agents can react differently based on their preferences. Based on existing literature, the feedback implemented in this thesis is one of the first-ever reported at such a microscopic scale. Similar to the updated noise model, the feedback implementation is hosted open source[2]. However, the integration shown here can only be viewed as a proof of concept, as the underlying relocation model was not calibrated to the actual study area. Given the complexity of the model and its interactions, it remains questionable if the inclusion of such feedback is justified. A main finding of this part of the thesis was that the technical implementation of such a model is more straightforward than its conceptualization, as ILUT models tend to have many moving parts that may need to be updated and adjusted. While the sensitivity to noise in relocation decisions has been added, the presented scenario did not include an updated initial population, which should already reflect individual preferences towards noise. In contrast to housing prices, data on *observed* residential relocations is very sparse and does not allow to analyze relocation behavior in terms of noise sensitivity as one would require very fine-grained spatial information on individual resident's relocation patterns, which is usually subject to privacy. In the current state, such feedback may be helpful to analyze the mechanism of reported relocation preferences and to conduct sensitivity analyses for policies targeting equity issues in an academic context. The implemented model is a good example for a use case

[2] https://github.com/msmobility/silo/tree/9091a3f67fc067329c69c3a30f304b0b5df57336

in which the complexity of the model probably outweighs the little (and hard to validate) gain in information.

Inequalities in the distributions of exposure and causation of noise have been confirmed with the presented agent-based simulations. In a novel approach, individual noise exposure and contribution at the agent level have been compared. One of the main findings was that, in terms of equity, the causation of noise may be even more of concern than exposure thereof. In addition, exposure and causation clearly show spatial patterns. While the results underline the applicability of agent-based simulations for equity analyses, future research should look at more detailed information of different agent groups. The equity analyses would undoubtedly benefit if more data, such as income or car ownership, were available. As discussed before, equity analyses should probably look at more indicators than noise alone, as agents may trade-off different nuisances according to their preferences (for example, agents living in highly accessible areas with lots of opportunities but also noise, and vice versa). The usage of the open Berlin scenario is another example of opportunities that arise by empowering open data in academic research.

Lastly, the ride-pooling use case showed the capability of large-scale agent-based models to model noise emissions and respective immissions for future transport scenarios. This use case is one of the first in literature that analyzes the impact of ride-pooling on traffic noise and found promising results when a large-scale stop-based service is used. Future research could look into optimizing stop locations to minimize noise exposure of nearby residents by putting these locations along major axes only. This could also be combined with a policy that closes smaller residential roads for ride-pooling vehicles. The results of this chapter showed that noise had to be analyzed explicitly, as the distribution of exposure cannot easily be inferred from aggregated indicators such as the vehicle kilometers traveled. During the simulation studies, it also became clear that there are computational limits that are important to consider when conducting large scenarios. The simulation of 100% of the synthetic population took many hours for just one iteration. If the scenarios had been designed more complex, e.g., by also allowing agents to switch modes between iterations, the studies would have become unfeasible in terms of run-time. The chapter may also serve as an example for results that may come as a surprise if looked at superficially. For one, ride-pooling does not necessarily reduce noise levels, even if such services are usually promoted as environmentally friendly and as a solution to many urban problems. Secondly, the replacement of conventional cars by electric vehicles may not lead to notable reductions in noise, which some readers may not expect.

In a more general view, this thesis confirmed that road traffic noise is a problem that many residents in dense urban settings face. More importantly, noise remains an issue that is hard to tackle, even with radical policies or technical advancements such as electric vehicles. Agent-based approaches may improve the accuracy of identifying problematic exposure and causation of noise at fine spatial and temporal resolutions. The trend towards ever-finer resolution in transport and land-use models offers many opportunities

to investigate new use cases similar to those described here. This gives modelers the chance to understand the systems of transport and environment better. However, this also comes at the cost of increased complexity and runtime and a successful application heavily depends on the availability and quality of large amounts of data.

Bibliography

Acheampong, R. A. and Silva, E. A. (2015). Land use–transport interaction modeling: A review of the literature and future research directions.

Al-harthy, I. and Tamura, A. (1999). Sound environment evaluation and categorization of audible sounds - the first survey of the human response to the sound environment in Muscat city (Oman). *Journal of the Acoustical Society of Japan (E) (English translation of Nippon Onkyo Gakkaishi)*, 20(5):353–364.

Allen, M. T., Austin, G. W., and Swaleheen, M. (2015). Measuring Highway Impacts on House Prices Using Spatial Regression. *Journal of Sustainable Real Estate*, 7(1):83–98.

Alonso-González, M. J., [van Oort], N., Cats, O., Hoogendoorn-Lanser, S., and Hoogendoorn, S. (2020). Value of time and reliability for urban pooled on-demand services. *Transportation Research Part C: Emerging Technologies*, 115:102621.

Alonso-Mora, J., Samaranayake, S., Wallar, A., Frazzoli, E., and Rus, D. (2017). On-demand high-capacity ride-sharing via dynamic trip-vehicle assignment. *Proceedings of the National Academy of Sciences of the United States of America*, 114(3):462–467.

Andersson, H., Jonsson, L., and Ögren, M. (2010). Property prices and exposure to multiple noise sources: Hedonic Regression with road and railway noise. *Environmental and Resource Economics*, 45(1):73–89.

Anselin, L. (1988). Lagrange Multiplier Test Diagnostics for Spatial Dependence and Spatial Heterogeneity. *Geographical Analysis*, 20(1):1–17.

Anselin, L. (2001). Spatial econometrics. *A companion to theoretical econometrics*, 310330.

Anselin, L. (2003). An introduction to spatial regression analysis in r. Technical report, University of Illinois, Urbana-Champaign.

Arbeitsring Lärm der Deutschen Gesellschaft für Akustik (ALD) (2020). Stellungnahme des arbeitsrings lärm der deutschen gesellschaft für akustik (ald) zur änderung der 16. bimschv (rls 19).

Asano, T. (1985). An Efficient Algorithm for Finding the Visibility Polygon for a Polygonal Region with Holes. *IEICE TRANSACTIONS (1976-1990)*, E68-E(9):557–559.

Babisch, W. (2008). Road traffic noise and cardiovascular risk. *Noise and Health*, 10(38):27–33.

Babisch, W. (2014). Updated exposure-response relationship between road traffic noise and coronary heart diseases: A meta-analysis. *Noise and Health*, 16(68):1–9.

Babisch, W., Beule, B., Schust, M., Kersten, N., and Ising, H. (2005). Traffic noise and risk of myocardial infarction. *Epidemiology*, 16(1):33–40.

Baden, B. M., Noonan, D. S., and Turaga, R. M. R. (2007). Scales of Justice: Is There a Geographic Bias in Environmental Equity Analysis? *Journal of Environmental Planning and Management*.

Badoe, D. A. and Miller, E. J. (2000). Transportation-land-use interaction: Empirical findings in North America, and their implications for modeling. *Transportation Research Part D: Transport and Environment*, 5(4):235–263.

Banzhaf, S., Ma, L., and Timmins, C. (2019). Environmental Justice: The Economics of Race, Place, and Pollution. *Journal of Economic Perspectives*.

Baranzini, A. and Ramirez, J. V. (2005). Paying for Quietness: The Impact of Noise on Geneva Rents. *Urban Studies*, 42(4):633–646.

Bartolomaeus, W. and Schade, L. (2006). Testaufgaben für die überprüfungvon Rechenprogrammen nach der 'Vorläufigen Berechnungsmethode für den umgebungslärm an straßen (vbus)'. Technical report, Bundesanstalt für Straßenwesen (BASt)) and Umweltbundesamt (UBA).

Basu, R. and Ferreira, J. (2020). A LUTI microsimulation framework to evaluate long-term impacts of automated mobility on the choice of housing-mobility bundles. *Environment and Planning B: Urban Analytics and City Science*, page 239980832092527.

Bateman, I., Scotland. Development Department., B., Scotland. Scottish Executive., I., University of East Anglia., A., Economic and Social Research Council (Great Britain), and University College, L. (2001). *The effect of road traffic on residential property values : a literature review and hedonic pricing study*. Scottish Executive.

Bauer-Wolf, S., Roth, M. C., Baumfeld, L., and Riesenfelder, A. (2003). Stadt-Umland Migration Wien – Erforschungzielgruppenspezifischer Interventionspotentiale. Endbericht. Technical report, ÖAR Regionalberatung GmbH and LR Sozialforschung OEG.

Becker, N. and Lavee, D. (2002). The Benefits and Costs of Noise Reduction. *MPRA Paper*.

Beckmann, K. J., Brüggemann, U., Gräfe, J., Huber, F., Meiners, H., Mieth, P., et al. (2007). Ilumass-integrated land-use modelling and transportation system simulation. endbericht. hg. v. *Deutsches Zentrum für Luft-und Raumfahrt (DLR). Berlin*.

Bekke, D., Wijnant, Y., Weegerink, T., and De Boer, A. (2013). Tire-road noise: An experimental study of tire and road design parameters. In *42nd International Congress*

and Exposition on Noise Control Engineering 2013, INTER-NOISE 2013: Noise Control for Quality of Life, volume 1, pages 173–180.

Belsley, D. a., Kuh, E., and Welsch, R. E. (1980). *Identifying influential data and sources of collinearity*. Wiley Online Library.

Bendtsen, H., Elleberg Larsen, B., and Mikkelsen, B. (2000). Perceived Annoyance from Road Traffic Noise. *The 29th International Congress and Exhibition on Noise Control Engineering*, (August):1–5.

Bettina Funk (2017). Mieten in München: Die Zahlen für Ihr Viertel. https://www.abendzeitung-muenchen.de/inhalt.preise-heben-weiter-ab-neue-zahlen-die-mieten-fuer-ihr-viertel.6b9ef4c9-15fa-4d7f-abea-18368360667b.html.

BImSchV (1990). Sechzehnte verordnung zur durchführung des bundesimmissionsschutzgesetzes (verkehrslärmschutzverordnung - 16.bimschv). Technical report.

Bischoff, J., Kaddoura, I., Maciejewski, M., and Nagel, K. (2018). Simulation-based optimization of service areas for pooled ride-hailing operators. *Procedia Computer Science*, 130:816–823.

Bischoff, J. and Maciejewski, M. (2016). Simulation of City-wide Replacement of Private Cars with Autonomous Taxis in Berlin. In *Procedia Computer Science*, volume 83, pages 237–244. Elsevier B.V.

Bischoff, J. and Maciejewski, M. (2020). Proactive empty vehicle rebalancing for Demand Responsive Transport services. *Procedia Computer Science*, 170:739–744.

Bischoff, J., Maciejewski, M., and Nagel, K. (2017). City-wide shared taxis: A simulation study in Berlin. *IEEE Conference on Intelligent Transportation Systems, Proceedings, ITSC*.

Bischoff, J. and Nagel, K. (2017). Integrating explicit parking search into a transport simulation. *Procedia Computer Science*, 109:881 – 886. 8th International Conference on Ambient Systems, Networks and Technologies, ANT-2017 and the 7th International Conference on Sustainable Energy Information Technology, SEIT 2017, 16-19 May 2017, Madeira, Portugal.

Bistaffa, F., Blum, C., Cerquides, J., Farinelli, A., and Rodríguez-Aguilar, J. A. (2021). A Computational Approach to Quantify the Benefits of Ridesharing for Policy Makers and Travellers. *IEEE Transactions on Intelligent Transportation Systems*, 22(1):119–130.

Bivand, R. (2002). Spatial econometrics functions in R: Classes and methods. *Journal of Geographical Systems*, 4(4):405–421.

Bivand, R. S., Pebesma, E., and Gomez-Rubio, V. (2013). *Applied spatial data analysis with R, Second edition*. Springer, NY.

Bluhm, G., Nordling, E., and Berglind, N. (2004). Road traffic noise and annoyance-an increasing environmental health problem. *Noise and Health*, 6(24):43–49.

Botteldooren, D., Dekoninck, L., and Gillis, D. (2011). The Influence of Traffic Noise on Appreciation of the Living Quality of a Neighborhood. *International Journal of Environmental Research and Public Health*, 8(3):777–798.

Bradley, J. S. and Jonah, B. A. (1979). The effects of site selected variables on human responses to traffic noise, Part II: Road type by socio-economic status by traffic noise level. *Journal of Sound and Vibration*, 67(3):395–407.

Brians, P. (1996). *Reading about the world*. American Heritage Custom Pub.

Brown, A. L. and Van Kamp, I. (2017). Who environmental noise guidelines for the european region: A systematic review of transport noise interventions and their impacts on health. *International Journal of Environmental Research and Public Health*, 14(8).

Brunsdon, C., Fotheringham, A. S., and Charlton, M. E. (1996). Geographically Weighted Regression: A Method for Exploring Spatial Nonstationarity. *Geographical Analysis*, 28(4):281–298.

Bundesamt für Bauwesen und Raumordnung (2020). Laufende Stadtbeobachtung - Raumabgrenzungen. Stadt- und Gemeindetypen in Deutschland. https://www.bbsr.bund.de/BBSR/DE/forschung/raumbeobachtung/Raumabgrenzungen/deutschland/gemeinden/StadtGemeindetyp/StadtGemeindetyp.html.

Bösch, P. M., Becker, F., Becker, H., and Axhausen, K. W. (2018). Cost-based analysis of autonomous mobility services. *Transport Policy*, 64:76 – 91.

Cammarata, G., Cavalieri, S., and Fichera, A. (1995). A neural network architecture for noise prediction. *Neural Networks*, 8(6):963–973.

Campbell, H. E., Kim, Y., and Eckerd, A. M. (2015). *Rethinking environmental justice in sustainable cities: Insights from agent-based modeling*. Routledge.

Campello-Vicente, H., Peral-Orts, R., Campillo-Davo, N., and Velasco-Sanchez, E. (2017). The effect of electric vehicles on urban noise maps. *Applied Acoustics*, 116:59–64.

Can, A. (2019). *Dynamic approaches for the characterization and mitigation of urban sound environments*. PhD thesis, IFSTTAR, Université du Maine.

Cannelli, G. B., Glück, K., and Santoboni, S. (1983). A Mathematical Model for Evaluation and Prediction of the Mean Energy Level of Traffic Noise in Italian Towns. *Acta Acustica united with Acustica*, 53(1):31–36.

Caponetto, R., Lavorgna, M., Martinez, A., and Occhipinti, L. (1997). Gas for fuzzy modeling of noise pollution. In *Proceedings of 1st International Conference on Conventional and Knowledge Based Intelligent Electronic Systems. KES'97*, volume 1, pages 219–223. IEEE.

Carrier, M., Apparicio, P., and Séguin, A.-M. (2016). Road traffic noise geography during the night in Montreal: An environmental equity assessment. *The Canadian Geographer / Le Géographe canadien*, 60(3):394–405.

Chang Chien, Y.-M., Carver, S., and Comber, A. (2020). Using geographically weighted models to explore how crowdsourced landscape perceptions relate to landscape physical characteristics. *Landscape and Urban Planning*, 203:103904.

Clark, C. and Paunovic, K. (2018). Who environmental noise guidelines for the european region: A systematic review on environmental noise and quality of life, wellbeing and mental health. *International Journal of Environmental Research and Public Health*, 15(11).

Coensel, B. D., Muer, T. D., and Botteldooren, D. (2007). {A}n agent based modeling approach to explain the perception of environmental stressors. In *Proceedings of the 2007 {I}nternational {C}onference on {A}rtificial {I}ntelligence ({ICAI} 2007)*.

Council Directive 2002/49/EC (2002). Directive 2002/49/EC of the European Parliament and of the Council of 25 June 2002 relating to the assessment and management of environmental noise - Declaration by the Commission in the Conciliation Committee on the Directive relating to the assessment a. *Official Journal L 189*, pages 0012 – 0026.

Craney, T. A. and Surles, J. G. (2002). Model-dependent variance inflation factor cutoff values. *Quality Engineering*, 14(3):391–403.

Dale, L. M., Goudreau, S., Perron, S., Ragettli, M. S., Hatzopoulou, M., and Smargiassi, A. (2015). Socioeconomic status and environmental noise exposure in Montreal, Canada. *BMC Public Health*, 15(1):205.

De Coensel, B., Brown, A. L., and Tomerini, D. (2016). A road traffic noise pattern simulation model that includes distributions of vehicle sound power levels. *Applied Acoustics*, 111:170–178.

de Kluizenaar, Y., Janssen, S. A., van Lenthe, F. J., Miedema, H. M. E., and Mackenbach, J. P. (2009). Long-term road traffic noise exposure is associated with an increase in morning tiredness. *The Journal of the Acoustical Society of America*, 126(2):626–633.

de Lisle, S. (2016). Comparison of road traffic noise prediction models: Cortn, tnm, nmpb, asj rtn. *Acoustics Australia*, 44(3):409–413.

Domencich, T. A. and McFadden, D. (1975). *Urban Travel Demand: A Behavioral Analysis*. North-Holland.

Dreger, S., Schüle, S. A., Hilz, L. K., and Bolte, G. (2019). Social Inequalities in Environmental Noise Exposure: A Review of Evidence in the WHO European Region. *International Journal of Environmental Research and Public Health*, 16(6):1011.

Dupraz, P., Osseni, A., and Bareille, F. (2018). Assessing the direct and indirect impacts of breeding activities on residential values: a spatial hedonic approach in Brittany. Technical report, International Association of Agricultural Economists.

Dutilleux, G., Defrance, J., Ecotière, D., Gauvreau, B., Bérengier, M., Besnard, F., and Duc, E. L. (2010). Nmpb-routes-2008: the revision of the french method for road traffic noise prediction. *Acta Acustica united with Acustica*, 96(3):452–462.

Dziauddin, M. F. and Idris, Z. (2017). Use of geographically weighted regression (gwr) method to estimate the effects of location attributes on the residential property values. *Indonesian Journal of Geography*, 49(1).

Eilers, L. (2016). Spatial Dependence in Apartment Offering Prices in Hamburg. Technical report, Verein für Socialpolitik / German Economic Association.

Engelhardt, R., Dandl, F., Bilali, A., and Bogenberger, K. (2019). Quantifying the Benefits of Autonomous On-Demand Ride-Pooling: A Simulation Study for Munich, Germany. In *2019 IEEE Intelligent Transportation Systems Conference (ITSC)*, pages 2992–2997. IEEE.

Estévez-Mauriz, L. and Forssén, J. (2018). Dynamic traffic noise assessment tool: A comparative study between a roundabout and a signalised intersection. *Applied Acoustics*, 130:71–86.

European Environment Agency (2018). Environmental indicator report 2018. https://www.eea.europa.eu/airs/2018.

Fagnant, D. J. and Kockelman, K. M. (2018). Dynamic ride-sharing and fleet sizing for a system of shared autonomous vehicles in Austin, Texas. *Transportation*, 45(1):143–158.

Feldman, O. and Simmonds, D. (2007). Advances in integrated urban/regional land use/transport modelling using the delta package. In *11th World Conference on Transport Research*.

Felix Mildner (2019). Sanieren, renovieren, modernisieren - das sind die Unterschiede.

FGSV (1990). Richtlinien für den Lärmschutz an Straßen (RLS). Technical report.

FGSV (2019). Richtlinien für den Lärmschutz an Straßen (RLS). Technical report.

Fields, J. M. (1993). Effect of personal and situational variables on noise annoyance in residential areas. *The Journal of the Acoustical Society of America*, 93(5):2753–2763.

for Environment Policy, S. (2016). Links between noise and air pollution and socioeconomic status. Technical report, DG Environment by the Science Communication Unit.

Forbes (2008). In depth: Europe's most congested cities. https://www.forbes.com/2008/04/21/europe-commute-congestion-forbeslife-cx_po_0421congestion_slide.html. Last accessed: 2020-08-12.

Forschungsgesellschaft für Straßen- und Verkehrswesen (1997). Empfehlungen für Wirtschaftlichkeitsuntersuchungen an Straßen. Technical report, Forschungsgesellschaft für Straßen- und Verkehrswesen.

Fotheringham, A. S. (1989). Scale-independent spatial analysis. In Goodchild, M. and Gopal, S., editors, *The Accuracy Of Spatial Databases*, chapter 19. Taylor & Francis.

Fotheringham, A. S., Brunsdon, C., and Charlton, M. (2002). Geographically Weighted Regression: The Analysis of Spatially Varying Relationships. *Wiley.com*.

Fotheringham, A. S., Charlton, M., and Brunsdon, C. (1996). The geography of parameter space: an investigation of spatial non-stationarity. *International Journal of Geographical Information Systems*, 10(5):605–627.

Fotheringham, A. S. and Wong, D. W. S. (1991). The Modifiable Areal Unit Problem in Multivariate Statistical Analysis. *Environment and Planning A: Economy and Space*, 23(7):1025–1044.

Fyhri, A. and Aasvang, G. M. (2010). Noise, sleep and poor health: Modeling the relationship between road traffic noise and cardiovascular problems. *Science of The Total Environment*, 408(21):4935 – 4942.

Fyhri, A. and Klæboe, R. (2009). Road traffic noise, sensitivity, annoyance and self-reported health—a structural equation model exercise. *Environment International*, 35(1):91 – 97.

Garg, N. and Maji, S. (2014). A critical review of principal traffic noise models: Strategies and implications. *Environmental Impact Assessment Review*, 46:68–81.

Genaro, N., Torija, A., Ramos-Ridao, A., Requena, I., Ruiz, D., and Zamorano, M. (2010). A neural network based model for urban noise prediction. *The journal of the Acoustical Society of America*, 128(4):1738–1746.

Gibbons, S. and Overman, H. G. (2012). Mostly pointless spatial econometrics?*. *Journal of Regional Science*, 52(2):172–191.

Golgher, A. B. and Voss, P. R. (2016). How to interpret the coefficients of spatial models: Spillovers, direct and indirect effects. *Spatial Demography*, 4(3):175–205.

Gollini, I., Lu, B., Charlton, M., Brunsdon, C., and Harris, P. (2015). GWmodel: An R package for exploring spatial heterogeneity using geographically weighted models. *Journal of Statistical Software*, 63(17):1–50.

Golmohammadi, R., Abbaspour, M., Nassiri, P., and Mahjub, H. (2009). A compact model for predicting road traffic noise. *Journal of Environmental Health Science & Engineering*, 6(3):181–186.

Görgen, T. and Fisch, S. (2013). „lebenswerter öffentlicher raum“ –eine befragung von bürgerinnen und bürgern in heidelberg und ravensburg. Technical report, Deutsche Hochschule der Polizei (Münster).

Greenberg, M. and Cidon, M. (1997). Broadening the definition of environmental equity: A framework for states and local governments. *Population Research and Policy Review*, 16(4):397–413.

Greenblatt, J. B. and Saxena, S. (2015). Autonomous taxis could greatly reduce greenhouse-gas emissions of US light-duty vehicles. *Nature Climate Change*, 5(9):860–863.

Gu, K., Marquez, L., and Smith, N. (2015). An Overview of Contemporary Land Use-Transport-Environment Models. Technical report, CSIRO Building, Construction and Engineering.

Gu, K. and Young, W. (1998). Verifying and validating a land use — transport — environment model. *Transportation Planning and Technology*, 21(3):181–202.

Guarnaccia, C., Bandeira, J., Coelho, M. C., Fernandes, P., Teixeira, J., Ioannidis, G., and Quartieri, J. (2018). Statistical and semi-dynamical road traffic noise models comparison with field measurements. *AIP Conference Proceedings*, 1982(1):020039.

Guarnaccia, C., Lenza, T. L., Mastorakis, N. E., and Quartieri, J. (2011). A comparison between traffic noise experimental data and predictive models results. *International Journal of Mechanics*, 5(3):379–386.

Guarnaccia, C., Quartieri, J., and Tepedino, C. (2017). A hybrid predictive model for acoustic noise in urban areas based on time series analysis and artificial neural network. *AIP Conference Proceedings*, 1836(1):020069.

Gulliver, J., Morley, D., Vienneau, D., Fabbri, F., Bell, M., Goodman, P., Beevers, S., Dajnak, D., J Kelly, F., and Fecht, D. (2015). Development of an open-source road traffic noise model for exposure assessment. *Environmental Modelling & Software*, 74:183–193.

Guo, L., Ma, Z., and Zhang, L. (2008). Comparison of bandwidth selection in application of geographically weighted regression: a case study. *Canadian Journal of Forest Research*, 38(9):2526–2534.

Gurumurthy, K. M. and Kockelman, K. M. (2020). How much does greater trip demand and aggregation at stops improve dynamic ride-sharing in shared autonomous vehicle systems? Preprint at `https://www.researchgate.net/publication/343451580`.

Guski, R., Schreckenberg, D., and Schuemer, R. (2017). Who environmental noise guidelines for the european region: A systematic review on environmental noise and annoyance. *International Journal of Environmental Research and Public Health*, 14(12).

Haboucha, C. J., Ishaq, R., and Shiftan, Y. (2017). User preferences regarding autonomous vehicles. *Transportation Research Part C: Emerging Technologies*, 78:37–49.

Hamersma, M., Tillema, T., Sussman, J., and Arts, J. (2014). Residential satisfaction close to highways: The impact of accessibility, nuisances and highway adjustment projects. *Transportation Research Part A: Policy and Practice*, 59:106–121.

Han, Z. X., Lei, Z. H., Zhang, C. L., Xiong, W., Gan, Z. L., Hu, P., and Zhang, Q. B. (2015). Noise monitoring and adverse health effects in residents in different functional areas of Luzhou, China. *Asia-Pacific Journal of Public Health*, 27(2S):93S–99S.

Hanák, T., Marović, I., and Aigela, P. (2015). Perception of residential environment in cities: A comparative study. In *Procedia Engineering*, volume 117, pages 495–501. Elsevier Ltd.

Hansen, W. G. (1959). How Accessibility Shapes Land Use. *Journal of the American Institute of Planners*, 25(2):73–76.

Hartig, T. (2007). Congruence and conflict between car transportation and psychological restoration. In Gärling, T. and Steg, L., editors, *Threats From Car Traffic to the Quality of Urban Life : Problems, Causes, and Solutions*, chapter 6, pages 103–122. Elsevier, 1 edition.

Havard, S., Reich, B. J., Bean, K., and Chaix, B. (2011). Social inequalities in residential exposure to road traffic noise: An environmental justice analysis based on the RECORD Cohort Study. *Occupational and Environmental Medicine*, 68(5):366–374.

Henao, A. and Marshall, W. E. (2019). The impact of ride-hailing on vehicle miles traveled. *Transportation*, 46(6):2173–2194.

Herath, S., Choumert, J., and Maier, G. (2015). The value of the greenbelt in vienna: a spatial hedonic analysis. *The Annals of Regional Science*, 54(2):349–374.

Herridge, C. and Low-Beer, L. (1973). Observations of the effects of aircraft noise near heathrow airport on mental health. *Proceedings of the International Congress on Noise as a Public Health Problem.*

Heutschi, K. (2004). *SonRoad – Berechnungsmodell fürStrassenlärm.* Bundesamt für Umwelt, Wald und Landschaft (BUWAL), Bern.

Hiebert, J. and Allen, K. (2019). Valuing environmental amenities across space: A geographically weighted regression of housing preferences in greenville county, sc. *Land*, 8(10):147.

Homer, M. W. and Murray, A. T. (2002). Excess Commuting and the Modifiable Areal Unit Problem. *Urban Studies*, 39:131–139.

Hörl, S. (2017). Agent-based simulation of autonomous taxi services with dynamic demand responses. In *Procedia Computer Science*, volume 109, pages 899–904.

Hörl, S., Balac, M., and Axhausen, K. W. (2018). A first look at bridging discrete choice modeling and agent-based microsimulation in MATSim. In *Procedia Computer Science*, volume 130, pages 900–907. Elsevier B.V.

Horni, A., Nagel, K., and Axhausen, K. W., editors (2016). *The Multi-Agent Transport Simulation MATSim*. Ubiquity Press, London.

Hunt, J., Kriger, D. S., and Miller, E. J. (2005). Current operational urban land-use–transport modelling frameworks: A review. *Transport Reviews*, 25(3):329–376.

Hunt, J. D. (2010). Stated Preference Examination of Factors Influencing Residential Attraction. In Pagliara, F., Preston, J., and Simmonds, D., editors, *Residential Location Choice: Models and Applications*, pages 21–59. Springer Berlin Heidelberg, Berlin, Heidelberg.

Infas and DLR (2010). Mobilität in Deutschland 2008. Technical report, infas Institut für angewandte Sozialwissenschaft GmbH and Deutschles Zentrum für Luft- und Raumfahrt e.v., Bonn and Berlin.

Iversen, L. M., Marbjerg, G., and Bendtsen, H. (2013). Noise from electric vehicles-'state-of-the-art' literature survey. In *INTER-NOISE*, Innsbruck.

Izón, G. M., Hand, M. S., Mccollum, D. W., Thacher, J. A., and Berrens, R. P. (2016). Proximity to Natural Amenities: A Seemingly Unrelated Hedonic Regression Model with Spatial Durbin and Spatial Error Processes. *Growth and Change*, 47(4):461–480.

Jabben, J., Verheijen, E., and Potma, C. (2012). Noise reduction by electric vehicles in the Netherlands. In *INTER-NOISE and NOISE-CON Congress and Conference Proceedings*, volume 2012, pages 6958–6965. Institute of Noise Control Engineering.

Jarvis, R. (1973). On the identification of the convex hull of a finite set of points in the plane. *Information Processing Letters*, 2(1):18–21.

Jing, P., Hu, H., Zhan, F., Chen, Y., and Shi, Y. (2020). Agent-Based Simulation of Autonomous Vehicles: A Systematic Literature Review. *IEEE Access*, 8:79089–79103.

Jonasson, H. G. and Storeheier, S. (2001). Nord 2000. new nordic prediction method for road traffic noise.

Jones, J. (2016). *Spatial bias in LUTI models*. PhD thesis.

Kaddoura, I. (2019). *Simulated Dynamic Pricing for Transport System Optimization*. PhD thesis, Technische Universität Berlin.

Kaddoura, I., Bischoff, J., and Nagel, K. (2020). Towards welfare optimal operation of innovative mobility concepts: External cost pricing in a world of shared autonomous vehicles. *Transportation Research Part A: Policy and Practice*, 136:48–63.

Kaddoura, I., Kröger, L., and Nagel, K. (2017). An activity-based and dynamic approach to calculate road traffic noise damages. *Transportation Research Part D: Transport and Environment*, 54:335–347.

Kaddoura, I. and Nagel, K. (2016). Activity-based computation of marginal noise exposure costs: Implications for traffic management. *Transportation Research Record*, 2597(1):116–122.

Kelley Pace, R. and LeSage, J. P. (2008). A spatial Hausman test. *Economics Letters*, 101(3):282–284.

Kephalopoulos, S., Paviotti, M., and Anfosso-Lédée, F. (2012). Common noise assessment methods in europe (cnossos-eu).

Khan, J., Ketzel, M., Jensen, S. S., Gulliver, J., Thysell, E., and Hertel, O. (2020). Comparison of Road Traffic Noise Prediction Models: CNOSSOS-EU, Nord2000 and TRANEX. *Environmental Pollution*, page 116240.

Kim, K. S., Park, S. J., and Kweon, Y. J. (2007). Highway traffic noise effects on land price in an urban area. *Transportation Research Part D: Transport and Environment*, 12(4):275–280.

Kistler, E., Holler, M., Wiegel, C., Schiller, O., Jovcic, V., and Faik, J. (2017). Expertise III zum Münchner Armutsbericht 2017. Technical report, Internationales Institut für Empirische Sozialökonomie, INIFES gGmbH, Stadtbergen.

Koppelman, F. S. (1983). Predicting transit ridership in response to transit service changes. *Journal of Transportation Engineering*, 109(4):548–564.

Krapf, K.-G. and Ibbeken, S. (2012). Lärmkartierung 2012 für den ballungsraum berlin. Technical report, Wölfel Beratende Ingenieure GmbH und Co. KG in cooperation with Lärmkontor GmbH.

Kruize, H., Driessen, P. P. J., Glasbergen, P., and van Egmond, K. N. D. (2007). Environmental Equity and the Role of Public Policy: Experiences in the Rijnmond Region. *Environmental Management*, 40(4):578–595.

Kuehnel, N., Huang, W.-C., and Moeckel, R. (2021a). Environmental equity analysis in agent-based transport simulations: A study on causation and exposure. *Procedia Computer Science (in press)*.

Kuehnel, N., Kaddoura, I., and Moeckel, R. (2019). Noise shielding in an agent-based transport model using volunteered geographic data. In *Procedia Computer Science*, volume 151, pages 808–813. Elsevier.

Kuehnel, N. and Moeckel, R. (2020). Impact of simulation-based traffic noise on rent prices. *Transportation Research Part D: Transport and Environment*, 78:102191.

Kuehnel, N., Ziemke, D., and Moeckel, R. (2021b). Traffic noise feedback in agent-based Integrated Land-Use/Transport Models. *Journal of Transport and Land Use*, 14(1):325–344–325–344.

Kuehnel, N., Ziemke, D., Moeckel, R., and Nagel, K. (2020). The end of travel time matrices: Individual travel times in integrated land use/transport models. *Journal of Transport Geography*, 88:102862.

Kumar, K., Parida, M., and Katiyar, V. K. (2011). Road traffic noise prediction with neural networks-a review. *An International Journal Of Optimization And Control: Theories & Applications (IJOCTA)*, 2(1):29–37.

Lambert, J., Simonnet, F., and Vallet, M. (1984). Patterns of behaviour in dwellings exposed to road traffic noise. *Journal of Sound and Vibration*, 92(2):159 – 172.

Landeshauptstadt Muenchen (2020). Bevoelkerung.

Landeshauptstadt München (2015). Münchner Stadtteilstudie. Fortschreibung 2015. Technical report, Referat für Stadtplanung und Bauordnung, Munich.

Laußmann, D., Haftenberger, M., Lampert, T., and Scheidt-Nave, C. (2013). Soziale ungleichheit von lärmbelästigung und straßenverkehrsbelastung. *Bundesgesundheitsblatt - Gesundheitsforschung - Gesundheitsschutz*, 56(5-6):822–831.

Leich, G. and Bischoff, J. (2019). Should autonomous shared taxis replace buses? A simulation study. *Transportation Research Procedia*, 41:450–460.

Leon Bluhm, G., Berglind, N., Nordling, E., and Rosenlund, M. (2007). Road traffic noise and hypertension. *Occupational and Environmental Medicine*, 64(2):122–126.

Lercher, P. and Kofler, W. W. (1996). Behavioral and health responses associated with road traffic noise exposure along alpine through-traffic routes. In *Science of the Total Environment*, volume 189-190, pages 85–89. Elsevier B.V.

LeSage, J. and Pace, R. K. (2009). *Introduction to Spatial Econometrics*. Chapman and Hall/CRC.

Llorca, C. and Moeckel, R. (2019). Effects of scaling down the population for agent-based traffic simulations. *Procedia Computer Science*, 151:782–787.

Llorca, C., Moreno, A., Ammar, G., and Moeckel, R. (n.d.). Impact of autonomous vehicles on household relocation: An agent-based simulation. *under review*.

Lowry, I. (1964). A model of Metropolis. Technical report, Rand Corporation.

Lu, B., Harris, P., Charlton, M., and Brunsdon, C. (2014). The GWmodel R package: further topics for exploring spatial heterogeneity using geographically weighted models. *Geo-spatial Information Science*, 17(2):85–101.

Löchl, M. and Axhausen, K. W. (2010). Modelling hedonic residential rents for land use and transport simulation while considering spatial effects. *Journal of Transport and Land Use*, 3(2).

Ma, J., Li, H., Yuan, F., and Bauer, T. (2013). Deriving Operational Origin-Destination Matrices From Large Scale Mobile Phone Data.

Maciejewski, M. (2016). Dynamic Transport Services. In *The Multi-Agent Transport Simulation MATSim*, chapter 23, pages 145–152. Andreas Horni, Kai Nagel and Kay W. Axhausen.

Maguire, K. and Sheriff, G. (2011). Quantifying the distribution of environmental outcomes for regulatory environmental justice analysis. Technical report.

Maloir, C., Tillema, T., and Arts, J. (2009). Residential location preferences , accessibility and road proximity : towards a better or more inclusive infrastructure planning ? In *Colloquium Vervoersplanologisch Speurwerk*, page 15, Antwerp.

Mansourkhaki, A., Berangi, M., Haghiri, M., and Haghani, M. (2018). A neural network noise prediction model for Tehran urban roads. *Journal of Environmental Engineering and Landscape Management*, 26(2):88–97.

Martinez, L. M. and Viegas, J. M. (2017). Assessing the impacts of deploying a shared self-driving urban mobility system: An agent-based model applied to the city of Lisbon, Portugal. *International Journal of Transportation Science and Technology*, 6(1):13–27.

Maslianskaïa-Pautrel, M. and Baumont, C. (2016). Environmental Spillovers and their Impacts on Housing Prices: A Spatial Hedonic Analysis. *Revue d'economie politique*, Vol. 126(5):921–945.

Matsumura, Y. and Rylander, R. (1991). Noise sensitivity and road traffic annoyance in a population sample. *Journal of Sound and Vibration*, 151(3):415 – 419.

Mendez, V. M., Monje, C. A., and White, V. (2017). Beyond Traffic: Trends and Choices 2045—A National Dialogue About Future Transportation Opportunities and Challenges. Lecture Notes in Mobility, pages 3–20. Springer International Publishing, Cham.

Miedema, H. M. and Vos, H. (1998). Exposure-response relationships for transportation noise. *The Journal of the Acoustical Society of America*, 104(6):3432–45.

Miedema, H. M. E. and Vos, H. (2003). Noise sensitivity and reactions to noise and other environmental conditions. *The Journal of the Acoustical Society of America*, 113(3):1492–1504.

Millimet, D. L. and Slottje, D. (2002). An environmental Paglin-Gini. *Applied Economics Letters*, 9(4):271–274.

Moeckel, R. (2016). Constraints in household relocation: Modeling land-use/transport interactions that respect time and monetary budgets. *Journal of Transport and Land Use*, 10(2):1–18.

Moeckel, R., Kuehnel, N., Llorca, C., Moreno, A. T., and Rayaprolu, H. (2020). Agent-Based Simulation to Improve Policy Sensitivity of Trip-Based Models. *Journal of Advanced Transportation*, 2020:1902162.

Moeckel, R., Llorca Garcia, C., Moreno Chou, A. T., and Okrah, M. B. (2018). Trends in integrated land use/transport modeling: An evaluation of the state of the art. *Journal of Transport and Land Use*, 11(1).

Moeckel, R., Spiekermann, K., Schurmann, C., and Wegener, M. (2003). Microsimulation of land use. *International Journal of Urban Sciences*, 7(1):14–31.

Molloy, J. and Moeckel, R. (2017). Automated design of gradual zone systems. *Open Geospatial Data, Software and Standards*, 2(1):19.

Moran, P. A. P. (1950). Notes on continuous stochastic phenomena. *Biometrika*, 37(1/2):17–23.

Moreno, A. and Moeckel, R. (2018). Population Synthesis Handling Three Geographical Resolutions. *ISPRS International Journal of Geo-Information*, 7(5):174.

Moreno, A. T. and Moeckel, R. (2016). Microscopic Destination Choice: Incorporating Travel Time Budgets as Constraints. In *World Conference on Transport Research-WCTR 2016*.

Müller, J. (2014). Analyse der vorgesehenen eu-bewertungsmethode für den straßenverkehrslärm. Technical report, Umweltbundesamt.

Mur, J. and Angulo, A. (2006). The Spatial Durbin Model and the Common Factor Tests. *Spatial Economic Analysis*, 1(2):207–226.

Murphy, E. and King, E. A. (2010). Strategic environmental noise mapping: Methodological issues concerning the implementation of the eu environmental noise directive and their policy implications. *Environment international*, 36(3):290–298.

Naumov, S., Keith, D. R., and Fine, C. H. (2020). Unintended Consequences of Automated Vehicles and Pooling for Urban Transportation Systems. *Production and Operations Management*, 29(5):1354–1371.

Nega, T. H., Chihara, L., Smith, K., and Jayaraman, M. (2013). Traffic Noise and Inequality in the Twin Cities, Minnesota. *Human and Ecological Risk Assessment: An International Journal*, 19(3):601–619.

Nelson, J. P. (1982). Highway noise and property values - a survey of recent evidence. *Journal of Transport Economics and Policy*, 16(2):117–138.

Nexiga GmbH (n.d.). Etagen, stockwerke pro gebäude. https://www.nexiga.com/news/etagen-in-gebaeuden/.

Nielsen, H. L. (1997). *Road traffic noise: Nordic prediction method*. Number 525. Nordic Council of Ministers.

Niemann, H. and Maschke, C. (2004). WHO LARES noise effects and morbidity final report.

Nijland, H. A., Hartemink, S., Van Kamp, I., and Van Wee, B. (2009). The influence of sensitivity for road traffic noise on residential location: does It trigger a process of spatial selection? *Noise and Vibration Worldwide*, 40(3):17–26.

Openshaw, S. (1977). A Geographical Solution to Scale and Aggregation Problems in Region-Building, Partitioning and Spatial Modelling. *Transactions of the Institute of British Geographers*, 2(4):459.

Openshaw, S. (1984). Ecological Fallacies and the Analysis of Areal Census Data:. *Environment and Planning A*.

OpenStreetMap Contributors (2018). OpenStreetMap.

Osada, Y. (1991). Comparison of community reactions to traffic noise. *Journal of Sound and Vibration*, 151(3):479 – 486.

Osada, Y., Yoshida, T., Yoshida, K., Kawaguchi, T., Hoshiyama, Y., and Yamamoto, K. (1997). Path analysis of the community response to road traffic noise. *Journal of Sound and Vibration*, 205(4):493–498.

Osland, L. (2010). An Application of Spatial Econometrics in Relation to Hedonic House Price Modeling. *Journal of Real Estate Research*, 32(3):289–320.

Ouis, D. (2001). Annoyance from Road Traffic Noise: A Review. *Journal of Environmental Psychology*, 21(1):101–120.

Ow, L. F. and Ghosh, S. (2017). Urban cities and road traffic noise: Reduction through vegetation. *Applied Acoustics*, 120:15–20.

Paglin, M. (1975). The Measurement and Trend of Inequality: A Basic Revision. *The American Economic Review*, 65(4):598–609.

Parkes, A., Kearns, A., and Atkinson, R. (2002). What Makes People Dissatisfied with their Neighbourhoods? *Urban Studies*, 39(13):2413–2438.

Pernestål, A. and Kristoffersson, I. (2019). Effects of driverless vehicles : Comparing simulations to get a broader picture. *European Journal of Transport and Infrastructure Research*, 1(19):1–23.

Potvin, S., Apparicio, P., and Séguin, A.-M. (2019). The spatial distribution of noise barriers in Montreal: A barrier to achieve environmental equity. *Transportation Research Part D: Transport and Environment*, 72:83–97.

Putman, S. H. and Chung, S.-H. (1989). Effects of Spatial System Design on Spatial Interaction Models. 1: The Spatial System Definition Problem:. *Environment and Planning A*.

Páez, A., Farber, S., and Wheeler, D. (2011). A Simulation-Based Study of Geographically Weighted Regression as a Method for Investigating Spatially Varying Relationships. *Environment and Planning A: Economy and Space*, 43(12):2992–3010.

Quartieri, J., Iannone, G., Guarnaccia, C., D'Ambrosio, S., Troisi, A., and Lenza, T. (2009). A review of traffic noise predictive models. In *Recent Advances in Applied and Theoretical Mechanics*.

Rayaprolu, H. S., Llorca, C., and Moeckel, R. (2018). Impact of bicycle highways on commuter mode choice: A scenario analysis. *Environment and Planning B: Urban Analytics and City Science*, page 239980831879733.

Rickborn, R. (2012). *VISUM 12 Grundlagen*. epubli.

Rieser, M., Métrailler, D., and Lieberherr, J. (2018). Adding Realism and Efficiency to Public Transportation in MATSim. In *18th Swiss Transport Research Conference*, pages 1—-21.

Rodrigue, J.-P. (2016). *The Geography of Transport Systems*. Routledge.

Rodrigue, J.-P. (n.d.). Noise Levels from Different Sources. https://transportgeography.org/contents/chapter4/transportation-and-environment/noise-levels/. date accessed: 02/15/2021.

Rosen, S. (1974). Hedonic Prices and Implicit Markets: Product Differentiation in Pure Competition. *Journal of Political Economy*, 82(1):34–55.

Rosenbaum, A. S. and Koenig, B. E. (1997). Evaluation of Modeling Tools for Assessing Land Use Policies and Strategies. Technical Report 97-007, U.S. Environmental Protection Agency, San Rafael.

Ruch, C., Horl, S., and Frazzoli, E. (2018). AMoDeus, a Simulation-Based Testbed for Autonomous Mobility-on-Demand Systems. In *2018 21st International Conference on Intelligent Transportation Systems (ITSC)*, volume 2018-Novem, pages 3639–3644. IEEE.

Ruch, C., Lu, C., Sieber, L., and Frazzoli, E. (2020). Quantifying the Efficiency of Ride Sharing. *IEEE Transactions on Intelligent Transportation Systems*, pages 1–6.

Rückert-John, J., Bormann, I., and John, R. (2013). Umweltbewusstsein in Deutschland 2012. Technical report.

Sakamoto, S. (2015). Road traffic noise prediction model "asj rtn-model 2013": Report of the research committee on road traffic noise. *Acoustical Science and Technology*, 36(2):49–108.

Samara, T. and Tsitsoni, T. (2011). The effects of vegetation on reducing traffic noise from a city ring road. *Noise Control Engineering Journal*, 59(1):68–74.

Schirmer, P. M., Eggermond, M. A. B. v., and Axhausen, K. W. (2014). The role of location in residential location choice models: a review of literature. *Journal of Transport and Land Use*, 7(2):3–21.

Sen, A., Foster, J. E., et al. (1973). *On economic inequality*. Oxford university press.

Shepherd, D., Welch, D., Dirks, K. N., and McBride, D. (2013). Do Quiet Areas Afford Greater Health-Related Quality of Life than Noisy Areas? *International Journal of Environmental Research and Public Health*, 10(4):1284–1303.

Simmonds, D. (2010). The DELTA residential location model. In *Advances in Spatial Science*, volume 65, pages 77–97. Springer International Publishing.

Simmonds, D. C. (1999). The Design of the Delta Land-Use Modelling Package. *Environment and Planning B: Planning and Design*, 26(5):665–684.

Smith, T. E. (n.d.). Spatial weight matrices. https://www.seas.upenn.edu/~ese502/lab-content/extra_materials/SPATIAL%20WEIGHT%20MATRICES.pdf.

Spiekermann, K. and Wegener, M. (2008). Environmental feedback in Urban models. *International Journal of Sustainable Transportation*, 2(1):41–57.

Stanek, J. (2021). Taugen Deutschlands neue Wolkenkratzer als Wahrzeichen? *Der Spiegel*.

Steele, C. (2001). A critical review of some traffic noise prediction models. *Applied acoustics*, 62(3):271–287.

Stępniak, M. and Jacobs-Crisioni, C. (2017). Reducing the uncertainty induced by spatial aggregation in accessibility and spatial interaction applications. *Journal of transport geography*, 61:17–29.

Sygna, K., Aasvang, G. M., Aamodt, G., Oftedal, B., and Krog, N. H. (2014). Road traffic noise, sleep and mental health. *Environmental Research*, 131:17 – 24.

Szczepańska, A., Senetra, A., and Wasilewicz, M. (2014). Traffic Noise as a Factor Influencing Apartment Prices in Large Cities. *Real Estate Management and Valuation*, 22(3):37–44.

Theebe, M. A. J. (2004). Planes, Trains, and Automobiles: The Impact of Traffic Noise on House Prices. *The Journal of Real Estate Finance and Economics*, 28(2/3):209–234.

Thomas, I., Cotteels, C., Jones, J., Bala, A. P., and Peeters, D. (2015). Spatial challenges in the estimations of LUTI models: some lessons from the SustainCity project. In Bierlaire, M., de Palma, A., Hurtubia, R., and Waddell, P., editors, *Integrated Transport & Land Use Modeling for Sustainable Cities*, chapter 4, pages 55–74. EPFL Press, Lausanne.

Thomas, I., Jones, J., Caruso, G., and Gerber, P. (2018). City delineation in European applications of LUTI models: review and tests. *Transport Reviews*, 38(1):6–32.

Tobler, W. R. (1970). A Computer Movie Simulating Urban Growth in the Detroit Region. *Economic Geography*, 46:234–240.

Tobías, A., Recio, A., Díaz, J., and Linares, C. (2015). Health impact assessment of traffic noise in madrid (spain). *Environmental Research*, 137:136 – 140.

Tomal, M. (2020). Modelling Housing Rents Using Spatial Autoregressive Geographically Weighted Regression: A Case Study in Cracow, Poland. *ISPRS International Journal of Geo-Information*, 9(6):346.

Umweltbundesamt (2012). Traffic noise. https://www.umweltbundesamt.de/en/topics/transport-noise/traffic-noise.

United Kingdom Department of the Environment (1988). Calculation of road traffic noise. Technical report.

US Federal Highway Administration (2004). Traffic noise modelversion 2.5. Technical report.

van Blokland, G. and Peeters, B. (2007). The noise emission model for european road traffic. deliverable 11 of the imagine project. Technical report, MP consulting engineers.

Van Wee, B. (2007). Environmental effects of urban traffic. In Gärling, T. and Steg, L., editors, *Threats From Car Traffic to the Quality of Urban Life : Problems, Causes, and Solutions*, chapter 2, pages 11–32. Elsevier, 1 edition.

Vega, S. H. and Elhorst, J. P. (2015). The SLX Model. *Journal of Regional Science*, 55(3):339–363.

Verheijen, E. and Jabben, J. (2010). Effect of electric cars on traffic noise and safety.

Viegas, J. M., Martinez, L. M., and Silva, E. A. (2009). Effects of the Modifiable Areal Unit Problem on the Delineation of Traffic Analysis Zones. *Environment and Planning B: Planning and Design*, 36(4):625–643.

von Auer, L. (2016). *Ökonometrie : eine Einführung*. Springer Gabler.

Vosooghi, R., Puchinger, J., Jankovic, M., and Vouillon, A. (2019). Shared autonomous vehicle simulation and service design. *Transportation Research Part C: Emerging Technologies*, 107:15–33.

Wagner, P. and Wegener, M. (2012). Urban Land Use, Transport and Environment Models. *disP - The Planning Review*, 43(170):45–56.

Wang, B., Ordonez Medina, S. A., and Fourie, P. (2018). Simulation of Autonomous Transit On Demand for Fleet Size and Deployment Strategy Optimization. *Procedia Computer Science*, 130:797–802.

Wardman, M. and Bristow, A. L. (2004). Traffic related noise and air quality valuations: Evidence from stated preference residential choice models. *Transportation Research Part D: Transport and Environment*, 9(1):1–27.

Wäscher, A. (2018). Die auswirkungen von lärm auf den immobilienwert. https://www.immoverkauf24.de/services/expertenrat/welche-auswirkungen-hat-laerm-auf-den-wert-einer-immobilie/.

Wegener, M. (2021). *Land-Use Transport Interaction Models*, pages 229–246. Springer Berlin Heidelberg, Berlin, Heidelberg.

Wegener, M. and Fürst, F. (1999). Land-use transport interaction: State of the art. Technical report, Institut für Raumplanung TU Dortmund.

Weinhold, D. (2008). How big a problem is noise pollution? A brief happiness analysis by a perturbable economist. MPRA Paper 9885, University Library of Munich, Germany.

Weinstein, N. D. (1982). Community noise problems: Evidence against adaptation. *Journal of Environmental Psychology*, 2(2):87–97.

Wheeler, D. C. (2007). Diagnostic Tools and a Remedial Method for Collinearity in Geographically Weighted Regression. *Environment and Planning A: Economy and Space*, 39(10):2464–2481.

WHO (2009). Night Noise Guidelines for Europe. Technical report, world Health Organization.

Wilhelmsson, M. (2000). The Impact of Traffic Noise on the Values of Single-family Houses. *Journal of Environmental Planning and Management*, 43(6):799–815.

Wolde, T. (2003). The eu noise policy and the related research needs. *Acta Acustica united with Acustica*, 89:735–742.

Wolfram Bartolomaeus (2019). Richtlinien für den Lärmschutz an Straßen RLS19.

Word Health Organization (2018). Environmental noise guidelines for the european region. Technical report.

Wu, S. and Heberling, M. T. (2013). The distribution of pollution and environmental justice in Puerto Rico: a quantitative analysis. *Population and Environment*, 35(2):113–132.

Xiao Y (2017). Hedonic Housing Price Theory Review 2.1 Introduction 2.2 Hedonic Model. pages 11–40.

Zahavi, Y. (1974). Traveltime Budgets and Mobility in Urban Areas. Technical report, United States. Federal Highway Administration.

Zhang, S. and Zhou, W. (2018). Recreational visits to urban parks and factors affecting park visits: Evidence from geotagged social media data. *Landscape and Urban Planning*, 180(18):27–35.

Zhang, Y., Zhang, D., and Miller, E. J. (2021). Spatial Autoregressive Analysis and Modeling of Housing Prices in City of Toronto. *Journal of Urban Planning and Development*, 147(1):05021003.

Ziemke, D., Joubert, J. W., and Nagel, K. (2018). Accessibility in a Post-Apartheid City: Comparison of Two Approaches for Accessibility Computations. *Networks and Spatial Economics*, 18(2):241–271.

Ziemke, D., Kaddoura, I., and Nagel, K. (2019). The MATSim Open Berlin Scenario: A multimodal agent-based transport simulation scenario based on synthetic demand modeling and open data. *Procedia Computer Science*, 151:870–877.

Ziemke, D., Nagel, K., and Moeckel, R. (2016). Towards an Agent-based, Integrated Land-use Transport Modeling System. In *Procedia Computer Science*, volume 83, pages 958–963.

Źróbek, S., Trojanek, M., Źróbek-Sokolnik, A., and Trojanek, R. (2015). The influence of environmental factors on property buyers' choice of residential location in Poland. *Journal of International Studies*, 8(3):164–174.

Zwick, F. and Axhausen, K. W. (2020a). Analysis of ridepooling strategies with MATSim. In *20th Swiss Transport Research Conference*.

Zwick, F. and Axhausen, K. W. (2020b). Impact of Service Design on Urban Ridepooling Systems. In *2020 IEEE Intelligent Transportation Systems Conference (ITSC)*.

Zwick, F., Kuehnel, N., Moeckel, R., and Axhausen, K. W. (2021). Agent-based simulation of city-wide autonomous ride-pooling and the impact on traffic noise. *Transportation Research Part D: Transport and Environment*, 90:102673.

A Appendix: Derivation of Immission Calculation to Allow Pre-processing of Correction Terms

We start from equation 5.20:

$$L_{\mathrm{W},k_j,i,t}(v_{k_j,m,t}) = L_{\mathrm{W0},m,t}(v_{k_j,m,t}) + D_{\mathrm{surf}_{k_j},k}(v_{k_j,m,t}) + D_{\mathrm{grad}_{k_j},m}(g_{k_j}, v_{k_j,m,t}) + D_{\mathrm{inter}}(x_{k_j}) + D_{\mathrm{electric}}(v_{k_j,m,t})$$

We assume that velocity, surface and gradient stay constant across all segments k_j of a link j:

$$\begin{aligned} v_{k_j,m,t} &\stackrel{\mathrm{def}}{=} v_{j,m,t}, && \forall k_j \in j, \forall j \\ D_{\mathrm{surf}_{k_j},m}(v_{k_j,m,t}) &\stackrel{\mathrm{def}}{=} D_{\mathrm{surf}_j,m}(v_{j,m,t}), && \forall k_j \in j, \forall j \\ D_{\mathrm{grad}_{k_j},k}(g_{k_j}, v_{k_j,m,t}) &\stackrel{\mathrm{def}}{=} D_{\mathrm{grad}_j,m}(g_j, v_{j,m,t}), && \forall k_j \in j, \forall j \end{aligned}$$

Now only the intersection term $D_{\mathrm{inter}}(x_{k_j})$ still depends on the actual segment. We separate the intersection term and define:

$$\begin{aligned} L_{\mathrm{W},k_j,m,t}(v_{j,m,t}) &= L_{\mathrm{W},j,m,t}(v_{j,m,t}) + D_{\mathrm{inter}}(x_{k_j}), \text{ with} \\ L_{\mathrm{W},j,m,t}(v_{j,m,t}) &= L_{\mathrm{W0},m,t}(v_{j,m,t}) + D_{\mathrm{surf},m}(v_{j,m,t}) + D_{\mathrm{grad},m}(g, v_{j,m,t}) + D_{\mathrm{electric}}(v_{j,m,t}) \end{aligned}$$

Using this, we update equation 5.8:

$$L_{\mathrm{W},k_j,t} = 10 \cdot \log_{10}[M_{k_j,t}] + 10 \cdot \log_{10}\left[\sum_m \lambda_{k_j,m,t} \cdot \frac{10^{0.1 \cdot (L_{\mathrm{W},j,m,t}(v_{m,t}) + D_{\mathrm{inter}}(x_{k_j}))}}{v_{j,m,t}}\right] - 30$$

$$L_{\mathrm{W},k_i,t} = 10 \cdot \log_{10}[M_{k_i,t}] + 10 \cdot \log_{10}\left[\sum_m \lambda_{k_j,m,t} \cdot \frac{10^{0.1 \cdot L_{\mathrm{W},j,m,t}(v_{j,m,t}) + 0.1 \cdot D_{\mathrm{inter}}(x_{k_j})}}{v_{j,m,t}}\right] - 30$$

$$L_{\mathrm{W},k_j,t} = 10 \cdot \log_{10}[M_{k_j,t}] + 10 \cdot \log_{10}\left[\sum_m \lambda_{k_j,m,t} \cdot \frac{10^{0.1 \cdot L_{\mathrm{W},k,m,t}(v_{j,m,t})} \cdot 10^{0.1 \cdot D_{\mathrm{inter}}(x_{k_j})}}{v_{j,m,t}}\right] - 30$$

$$L_{\mathrm{W},k_j,t} = 10 \cdot \log_{10}[M_{k_j,t}] + 10 \cdot \log_{10}\left[10^{0.1 \cdot D_{\mathrm{inter}}(x_{k_j})} \cdot \sum_m \lambda_{k_j,m,t} \cdot \frac{10^{0.1 \cdot L_{\mathrm{W},j,m,t}(v_{m,t})}}{v_{j,m,t}}\right] - 30$$

$$L_{\mathrm{W},k_j,t} = 10 \cdot \log_{10}[M_{k_j,t}] + 10 \cdot \left\{\log_{10}\left[10^{0.1 \cdot D_{\mathrm{inter}}(x_{k_j})}\right] + \log_{10}\left[\sum_m \lambda_{k_j,m,t} \cdot \frac{10^{0.1 \cdot L_{\mathrm{W},j,m,t}(v_{m,t})}}{v_{j,m,t}}\right]\right\} - 30$$

$$L_{\mathrm{W},k_j,t} = 10 \cdot \log_{10}[M_{k_j,t}] + D_{\mathrm{inter}}(x_{k_j}) + 10 \cdot \log_{10}\left[\sum_m \lambda_{k_j,m,t} \cdot \frac{10^{0.1 \cdot L_{\mathrm{W},j,m,t}(v_{m,t})}}{v_{j,m,t}}\right] - 30$$

Next, we also assume that traffic volumes M_{k_j}, and vehicle type shares λ_{k_j} stay constant across all segments k_j of a link j:

$$M_{k_j} \overset{\text{def}}{=} M_j, \qquad \forall k_j \in j, \forall j$$
$$\lambda_{k_j} \overset{\text{def}}{=} \lambda_j, \qquad \forall k_j \in j, \forall j$$

Now we can separate the segment-dependent intersection term again:

$$L_{\mathrm{W},k_j,t} = L_{\mathrm{W},j,t} + D_{\mathrm{inter}}(x_{k_j}), \text{ with}$$
$$L_{\mathrm{W},j,t} = L_{\mathrm{W0},m,t}(v_{m,t}) + 10 \cdot \log_{10}[M_{j,t}] + 10 \cdot \log_{10}\left[\sum_m \lambda_{j,m,t} \cdot \frac{10^{0.1 \cdot L_{\mathrm{W},j,m,t}(v_{m,t})}}{v_{j,m,t}}\right] - 30$$

We can now update the immission calculation shown in equation 5.7:

$$L_{\mathrm{eq},i,t} = 10 \cdot \log_{10} \sum_j \sum_{k_j} 10^{0.1 \cdot (L_{\mathrm{W},j,t} + D_{\mathrm{inter}}(x_{k_j}) + 10 \cdot \log_{10}[l_{k_j}] - D_{\mathrm{A},i,k_j} - D_{\mathrm{RV1},k_j} - D_{\mathrm{RV2},k_j})}$$

We now separate time- from segment-dependent terms:

$$L_{\mathrm{eq},i,t} = 10 \cdot \log_{10}\left[\sum_j \sum_{k_j} 10^{0.1 \cdot (L_{\mathrm{W},j,t} + D_{\mathrm{inter}}(x_{k_j}) + 10 \cdot \log_{10}[l_{k_j}] - D_{\mathrm{A},k_j} - D_{\mathrm{RV1},k_j} - D_{\mathrm{RV2},k_j})}\right]$$
$$L_{\mathrm{eq},i,t} = 10 \cdot \log_{10}\left[\sum_j \sum_{k_j} 10^{0.1 \cdot L_{\mathrm{W},j,t} + 0.1 \cdot (D_{\mathrm{inter}}(x_{k_j}) + 10 \cdot \log_{10}[l_{k_j}] - D_{\mathrm{A},k_j} - D_{\mathrm{RV1},k_j} - D_{\mathrm{RV2},k_j})}\right]$$
$$L_{\mathrm{eq},i,t} = 10 \cdot \log_{10}\left[\sum_j \sum_{k_j} 10^{0.1 \cdot L_{\mathrm{W},j,t}} \cdot 10^{0.1 \cdot (D_{\mathrm{inter}}(x_{k_j}) + 10 \cdot \log_{10}[l_{k_j}] - D_{\mathrm{A},k_j} - D_{\mathrm{RV1},k_j} - D_{\mathrm{RV2},k_j})}\right]$$
$$L_{\mathrm{eq},i,t} = 10 \cdot \log_{10}\left[\sum_j 10^{0.1 \cdot L_{\mathrm{W},j,t}} \cdot \sum_{k_j} 10^{0.1 \cdot (D_{\mathrm{inter}}(x_{k_j}) + 10 \cdot \log_{10}[l_{k_j}] - D_{\mathrm{A},k_j} - D_{\mathrm{RV1},k_j} - D_{\mathrm{RV2},k_j})}\right]$$

Now, only the first part of the equation depends on t. The second part basically sums up all correction terms for the respective link segments and can be summarized as c_i :

$$L_{\mathrm{eq},i,t} = 10 \cdot \log_{10}\left[\sum_j \left(10^{0.1 \cdot L_{\mathrm{W},j,t}} \cdot c_j\right)\right], \text{ with}$$
$$c_j = \sum_{k_j} 10^{0.1 \cdot (D_{\mathrm{inter}}(x_{k_j}) + 10 \cdot \log_{10}[l_{k_j}] - D_{\mathrm{A},k_j} - D_{\mathrm{RV1},k_j} - D_{\mathrm{RV2},k_j})}$$

B Appendix: Spatial Error Model Results

Table B.1: Estimation results for the spatial error model (SEM) with $k = 5$ and $\alpha = 2$.

	Dependent variable: log(rent)	
	continuous noise variable	categorical noise variable
log(area)	0.7864*** (0.0062)	0.7865*** (0.0062)
noise	-0.0030*** (0.0007)	
low noise		0 (Base)
moderate noise		-0.0202 . (0.0123)
loud noise		-0.0457*** (0.0146)
very loud noise		-0.0631*** (0.0227)
microscopic car accessibilities	0.2139*** (0.0153)	0.2072*** (0.0153)
Parking available	0.0122 . (0.0064)	0.0120 . (0.0044)
Quality: Luxury	0.1200*** (0.0109)	0.1210*** (0.0109)
Quality: Superior	0 (Base)	0 (Base)
Quality: Average	-0.1256*** (0.0073)	-0.1256*** (0.0073)
State: First time use	0 (Base)	0 (Base)
State: New Building	-0.0199. (0.0111)	-0.0194 (0.0111)
State: First time use after restoration	-0.0803*** (0.0135)	-0.0802*** (0.0135)
State: Restored	-0.0816*** (0.0177)	-0.0806*** (0.0177)
State: Modernized	-0.1150*** (0.0147)	-0.1145*** (0.0147)
State: Well-kept	-0.1166*** (0.0116)	-0.1152*** (0.0117)
State: Renovated	-0.1249*** (0.0125)	-0.1235*** (0.0125)
constant	2.3292*** (0.1154)	2.2158*** (0.1223)
Observations	3,144	3,144
λ	0.5956***	0.5992***
AIC	-3445	-3438

Note:Signif. codes: '***' 0.001 '**' 0.01 '*' 0.05 '.' 0.1 ' ' 1 robust SE in (brackets)

C Appendix: Spatial Auto-regressive Model Results

Table C.1: Estimation results for the spatial auto-regressive (SAR) model with $k = 5$ and $\alpha = 2$: estimated coefficients.

	Dependent variable: log(rent)	
	continuous noise variable	categorical noise variable
log(area)	0.7248*** (0.0071)	0.7241*** (0.0071)
noise	-0.0035*** (0.0005)	
low noise		0 (Base)
moderate noise		-0.0294 . (0.0108)
loud noise		-0.0495*** (0.0125)
very loud noise		-0.076*** (0.0202)
microscopic car accessibilities	0.2016*** (0.0089)	0.1942*** (0.0090)
Parking available	0.0113 . (0.0062)	0.0110 . (0.0062)
Quality: Luxury	0.1554*** (0.0107)	0.1563*** (0.0108)
Quality: Superior	0 (Base)	0 (Base)
Quality: Average	-0.1236*** (0.0075)	-0.1231*** (0.0075)
State: First time use	0 (Base)	0 (Base)
State: New Building	-0.0183. (0.0100)	-0.0152 (0.0101)
State: First time use after restoration	-0.0649*** (0.0129)	-0.0646*** (0.0130)
State: Restored	-0.0720*** (0.0194)	-0.0712*** (0.0177)
State: Modernized	-0.1031*** (0.0151)	-0.1026*** (0.0152)
State: Well-kept	-0.1284*** (0.0108)	-0.1274*** (0.0109)
State: Renovated	-0.1226*** (0.0113)	-0.1218*** (0.0114)
constant	1.3628*** (0.0858)	1.2114*** (0.0884)
Observations	3,144	3,144
ρ	0.1919***	0.19499***
AIC	-2628	-2608

Note:Signif. codes: '***' 0.001 '**' 0.01 '*' 0.05 '.' 0.1 ' ' 1 robust SE in (brackets)

Table C.2: Estimation results for the spatial autoregressive (SAR) model with $k = 5$ and $\alpha = 2$: direct, indirect and total impacts.

	continuous			categorical		
	direct	indirect	total	direct	indirect	total
log(area)	0.7291***	0.1678***	0.8969***	0.7286***	0.1709***	0.8995***
noise	-0.0036***	-0.0008***	-0.0044***			
low noise		0 (Base)				
moderate noise				-0.0296**	-0.0069***	-0.0366***
loud noise				-0.0498***	-0.0116	-0.0615***
very loud noise				-0.0767***	-0.0179***	-0.0947***
microscopic car accessibilities	0.2028***	0.0466***	0.2495***	0.1954***	0.045***	0.2412***
Parking available	0.0114	0.0026	0.0140	0.0110 .	0.0025 .	0.0136 .
Quality: Luxury	0.1564***	0.0359***	0.1924***	0.1573****	0.0369***	0.1942***
Quality: Superior	0 (Base)	0 (Base)				
Quality: Average	-0.1244***	-0.0286***	-0.1530***	-0.1239***	-0.0290***	-0.1529***
State: First time use	0 (Base)	0 (Base)				
State: New Building	-0.0184*	-0.0042*	-0.0226*	-0.0153	-0.0036	-0.0189
State: First time use after restoration	-0.065***	-0.0150***	-0.0803***	-0.0650***	-0.0152***	-0.0803***
State: Restored	-0.0724*	-0.0166*	-0.0891*	-0.0717***	-0.0168***	-0.0885***
State: Modernized	-0.1037***	-0.0238***	-0.1276***	-0.1032***	-0.0242***	-0.1274***
State: Well-kept	-0.1292***	-0.0297***	-0.1589***	-0.1282***	-0.0300***	-0.1583***
State: Renovated	-0.1234***	-0.0284***	-0.1518***	-0.1226***	-0.0287***	-0.1514***

D Appendix: Spatial Durbin Model Results

Table D.1: Estimation Results for the spatial Durbin model (SDM) with $k = 5$ and $\alpha = 2$: Estimated coefficients.

Dependent variable:		
	log(rent)	
	continuous noise variable	categorical noise variable
log(area)	0.7910*** (0.0063)	0.7902*** (0.0063)
noise	-0.0003 (0.0007)	
low noise		0 (Base)
moderate noise		-0.0029 (0.0125)
loud noise		-0.0158 (0.0154)
very loud noise		-0.0177 (0.0233)
microscopic car accessibilities	0.0207 (0.0364)	0.0337 (0.0354)
Parking available	0.0101 (0.0064)	0.0096 (0.0064)
Quality: Luxury	0.1197*** (0.0107)	0.1197*** (0.0107)
Quality: Superior	0 (Base)	0 (Base)
Quality: Average	-0.1242*** (0.0074)	-0.1244*** (0.0074)
State: First time use	0 (Base)	0 (Base)
State: New Building	-0.0223 . (0.0116)	-0.0212 . (0.0116)
State: First time use after restoration	-0.0719*** (0.0139)	-0.0715*** (0.0139)
State: Restored	-0.0784*** (0.0182)	-0.0778*** (0.0183)
State: Modernized	-0.1087*** (0.0151)	-0.1077*** (0.0151)
State: Well-kept	-0.1091*** (0.0122)	-0.1084*** (0.0122)
State: Renovated	-0.1095*** (0.0132)	-0.1091*** (0.0132)
constant	0.9638*** (0.0780)	0.8175*** (0.0790)
lag: log(area)	-0.5062*** (0.0143)	-0.5070*** (0.0142)
lag: noise	-0.0031*** (0.0009)	
lag: low noise		0 (Base)
lag: moderate noise		-0.0250 (0.0161)
lag: loud noise		-0.0324 . (0.0194)
lag: very loud noise		-0.0466 . (0.0291)
lag: microscopic car accessibilities	0.0757* (0.0371)	0.0550 (0.0362)

lag: Parking available	-0.0266*** (0.0085)	-0.0275*** (0.0085)
lag: Quality: Luxury	-0.0539*** (0.0151)	-0.0540*** (0.0151)
lag: Quality: Superior	0 (Base)	0 (Base)
lag: Quality: Average	0.0711*** (0.0107)	0.0733*** (0.0107)
lag: State: First time use	0 (Base)	0 (Base)
lag: State: New Building	0.0248 . (0.0146)	0.0284* (0.0146)
lag: State: First time use after restoration	0.0272 (0.0187)	0.0275 (0.0188)
lag: State: Restored	-0.0071 (0.0296)	-0.0059 (0.0297)
lag: State: Modernized	0.0615 . (0.0231)	0.0625 (0.0232)
lag: State: Well-kept	0.0097 (0.0161)	0.0100 . (0.0162)
lag: State: Renovated	0.0200 (0.0168)	0.0192 (0.0169)
Observations	3,144	3,144
ρ	0.62511***	0.62912***
AIC	-3544	-3521

Note:Signif. codes: '***' 0.001 '**' 0.01 '*' 0.05 '.' 0.1 ' ' 1 robust SE in (brackets)

Table D.2: Estimation Results for the Spatial Durbin Model with $k = 5$ and $\alpha = 2$: Direct, indirect and total impacts.

	continuous			categorical		
	direct	indirect	total	direct	indirect	total
log(area)	0.7889***	-0.0292***	0.7597***	0.7884***	-0.0249	0.7635***
noise	-0.0008	-0.0084***	-0.0093***			
low noise		0 (Base)				
moderate noise				-0.0078	-0.0678**	-0.0756*
loud noise				-0.0234	-0.1069***	-0.1303***
very loud noise				-0.0280	-0.1455***	-0.1736***
microscopic car accessibilities	0.0364	0.2211***	0.2575***	0.0473	0.1920***	0.2394***
Parking available	0.0065 .	-0.0505***	-0.0439**	0.0058	-0.0539*	-0.0480 .
Quality: Luxury	0.1233***	0.05198 .	0.1753***	0.1236***	0.0537	0.1773***
Quality: Superior	0 (Base)	0 (Base)				
Quality: Average	-0.1254***	-0.0162	-0.1417***	-0.1253***	-0.0124	-0.1377***
State: First time use	0 (Base)	0 (Base)				
State: New Building	-0.0204**	0.0271 .	0.0066	-0.0185	0.0379 .	0.0193
State: First time use after restoration	-0.0750***	-0.0440	-0.1190*	-0.0746***	-0.0439.	-0.1186***
State: Restored	-0.0883***	-0.1400	-0.2284**	-0.0876***	-0.1382***	-0.2259***
State: Modernized	-0.1098***	-0.0160	-0.1259 .	-0.1086***	-0.0132	-0.1219***
State: Well-kept	-0.1193***	-0.1455***	-0.2649***	-0.1188***	-0.1465***	-0.265***
State: Renovated	-0.1181***	-0.1206***	-0.2387***	-0.1180***	-0.1246***	-0.2426*